Identification, screening and exploring potentials of PKC directed molecules in anti-cancer drug development

A thesis submitted in partial fulfilment of the requirement for the degree of

Doctor of Philosophy

by

Suman Jyoti Deka

Department of Biosciences and Bioengineering,
Indian Institute of Technology Guwahati
Guwahati-781039, Assam, India

Dedicated to my Parents, Brother and all of my Teachers & Mentors who have always encouraged, motivated and stood beside me with full faith in all of my journeys and ventures towards success…

Suman Jyoti Deka

Indian Institute of Technology Guwahati.
Department of Biosciences and Bioengineering.

Statement

I hereby declare that the matter embodied in this thesis entitled **"Identification, screening and exploring potentials of PKC directed molecules in anti-cancer drug development"** is a cumulative account of the results of investigations carried out in the Department of Biosciences & Bioengineering, Indian Institute of Technology, Guwahati, India, under the joint supervision of **Dr. Vishal Trivedi and Professor Rakhi Chaturvedi.**

In keeping with the general practice of reporting scientific observations, due acknowledgements have been made wherever the work of other investigators are referred.

Suman Jyoti Deka

February 2017 Roll no: 11610611

Indian Institute of Technology Guwahati.
Department of Biosciences and Bioengineering.

Certificate

It is certified that the work described in this thesis entitled, **"Identification, screening and exploring potentials of PKC directed molecules in anti-cancer drug development",** by **Mr. Suman Jyoti Deka** (Roll no: 11610611), submitted to Indian Institute of Technology, Guwahati, India, for the award of the degree of Doctor of Philosophy, is an authentic record of results obtained from the research work carried out under our joint supervision at the Department of Biosciences & Bioengineering, Indian Institute of Technology, Guwahati, Assam, India. This work has not been submitted elsewhere for a degree.

Dr. Vishal Trivedi
(Supervisor 1)

Prof. Rakhi Chaturvedi
(Supervisor 2)

Acknowledgements

It is a great pleasure to acknowledge whoever is involved and supported me to complete my research work in time.

I would like to thank Dr. **Vishal Trivedi** and Professor **Rakhi Chaturvedi** for their support and trust in my abilities, and the chance to do this project in Malaria Research Group. Nothing of this would have been possible without their support and I am thankful to their nearly endless patience and guidance.

I would also like to thank my doctoral committee members Dr. **Nitin Chaudhary**, Dr. **Sanjukta Patra** and Dr. **Shrikrishna N Joshi** for their cyclic evaluation and valuable suggestions for this work.

I am also thankful to Dr. **Vibin Ramakrishnan**, who provided me important guidance to carry out part of my research work.

I would like to thank all my Malaria Research Group colleagues Dr. Rohitas Deshmukh, Dr. Kimjolly Lhouvum, Mr S.N.Balaji, Mr. Ankur Mishra, Mr. Kankgan Kalita, Mr. Sooram Banesh, Mr. Anil Kumar, Ms. Vimee Raturi, Mr. Sushant Kumar, Ms**.** Ankita Hazarika, Mr. Anish Jain, Mr. Sourav Layek, Mr. KMN Prasad, Mrs. Swagata Nag, Mrs. Ananya Bhowmick and Ms. Pallavi for their support**.**

I would like to thank all research scholars from Department of Biosciences & Bioengineering and specifically members belonging to Dr. Vibin Ramakrishnan's Lab, Dr. Rakhi Chaturvedi's Lab, Dr. V.K Dubey's lab, Dr. A.M. Limaye's Lab and Dr. B. Anand's lab who have helped me in my research.

I would like to thank the Department of Biosciences & Bioengineering, IIT Guwahati for giving me an opportunity for the PhD Program as well as providing descent infrastructure and good research environment for my work.

I would like to thank NTRF and DAE-BRNS for providing financial support to carry out my research work.

I would also like to thank Indian Institute of Technology, Guwahati, for providing financial assistantship.

Finally, I would like to thank my lovable family members and my dear friends, who gave immense care and support for my career growth.

-Suman Jyoti Deka

Table of Contents

List of Figures

List of Tables

Abbreviations

Akt/PKB	Protein kinase B
ATP	Adenosine triphosphate
β-Gly	β-Glycyrrhetinic acid
BRCA1	Breast cancer 1
BSA	Bovine serum albumin
CGA	Chlorogenic acid
DAG	Diacylglycerol
DAPI	4',6-Diamidino-2-phenylindole
DCFH-DA	2',7'-Dichlorofluorescin diacetate
DMEM:F12	Dulbecco's modified eagle's medium:F12
DMSO	Dimethyl sulfoxide
DNPH	Dinitrophenylhydrazine
EDTA	Ethylene diacetate tetra acetic acid
EGCG	Epigallocatechin gallate
EGF	Epidermal growth factor
EGFR	Epidermal growth factor receptor
EML4-ALK	Echinoderm microtubule-associated protein-like 4- Anaplastic lymphoma kinase
ERK	Extracellular signal–regulated kinase
Et-Br	Ethidium bromide
FBS	Fetal bovine serum
FITC	Fluorescein isothiocyanate
GA	Gallic acid
GSK-3β	Glycogen synthase kinase-3 beta
HEPES	(4-(2-hydroxyethyl)-1-piperazineethanesulfonic acid
HGF	Hepatocyte growth factor
IC_{50}	50 % inhibitory concentration
IFN-γ	Interferon gamma
IGF1	Insulin-like growth factor 1
IKK	Inhibitor of nuclear factor kappa kinase
IL	Interleukin
IP_3	Inositol 1,4,5-trisphosphate
JAK	Janus kinase
MAPK	Mitogen-activated protein kinase
MDA	Malondialdehyde
MEK-1	Dual specificity mitogen-activated protein kinase kinase 1
MMP	Matrix metalloproteinase
MTT	3-(4,5-dimethyl thiazol-2- yl)-2,5-diphenyl tetrazolium bromide
NAC	N-Acetyl cysteine
NADH	Nicotinamide adenine dinucleotide
NFAT	Nuclear factor of activated T-cells
NF-κB	Nuclear factor- kappa-light-chain-enhancer of activated B cells
PAGE	Polyacrylamide gel electrophoresis
PBS	Phosphate buffered saline
PDB	Protein Data Bank
PDGF	Platelet-derived growth factor
PDK-1	3-Phosphoinositide-dependent protein kinase-1
PDT	Photodynamic therapy
PI-3K	Phosphatidylinositol-4,5-bisphosphate 3-kinase
PIP_2	Phosphatidylinositol 4,5-bisphosphate
PKA	Protein kinase A
PKC	Protein Kinase C
PKD	Protein Kinase D
PMA	Phorbol 12-myristate 13-acetate
PS	Photosystems
PVDF	Polyvinylidene fluoride
ROS	Reactive oxygen species
SDS	Sodium dodecyl sulfate
STAT	Signal transducer and activator of transcription
TBARS	Thiobarbituric acid reactive substances
TCA	Trichloro acetic acid
TEMED	Tetramethylethylenediamine
TGF-β	Transforming growth factor-β
TNF-α	Tumor necrosis factor-α
Tris	Tris(hydroxymethyl)aminomethane
VEGFR2	Vascular endothelial growth factor receptor2

Units

°C	Degree Celcius
gm	Gram
gm/dl	Gram per deciLitre
gm/ml	Gram per milliLitre
hr	Hour
mg/ml	Milligram per milliLitre
min	Minute
mM	Milli Molar
xg	Times the unit of gravitational force
rpm	Revolution per minute
v/v	Volume per volume
w/v	Weight per volume
µg	Microgram
µg/ml	Microgram per milliLitre
µl	MicroLitre
µm	Micrometer
µM	Micro Molar

Chapter 1

Potentials of PKC in cancer development and therapeutic outcomes.

1.1 Introduction

Individual cells constitute the fundamental units of life in human body. More than 200 different types of cells are found in the human body with a specific physiological purpose in different organs and organ systems (GM., 2000). Maintenance of a homeostatic environment in the body is achieved by suitable coordination between different cellular and organ systems. This homeostatic environment ensures smooth functioning of all the organs and organ-systems that carry out diverse functions in the body (Keesey and Powley, 2008). Thus, under normal circumstances, cells would divide in a controlled process, which is just sufficient to replenish the old and dead cells that are regularly lost from the body. However, this usually uninterrupted coordinated replenishment of cells can be lost at certain times in the lifetime of an individual (Hanahan and Weinberg, 2011). In such a scenario, some specific cell-types under the influence of genetic mutations can become unresponsive to the cell-division regulatory signals and start to proliferate aberrantly (Figure 1.1). This clinical situation is termed as cancer, which is characterized by uncontrolled proliferation of cells (Hanahan and Weinberg, 2011).

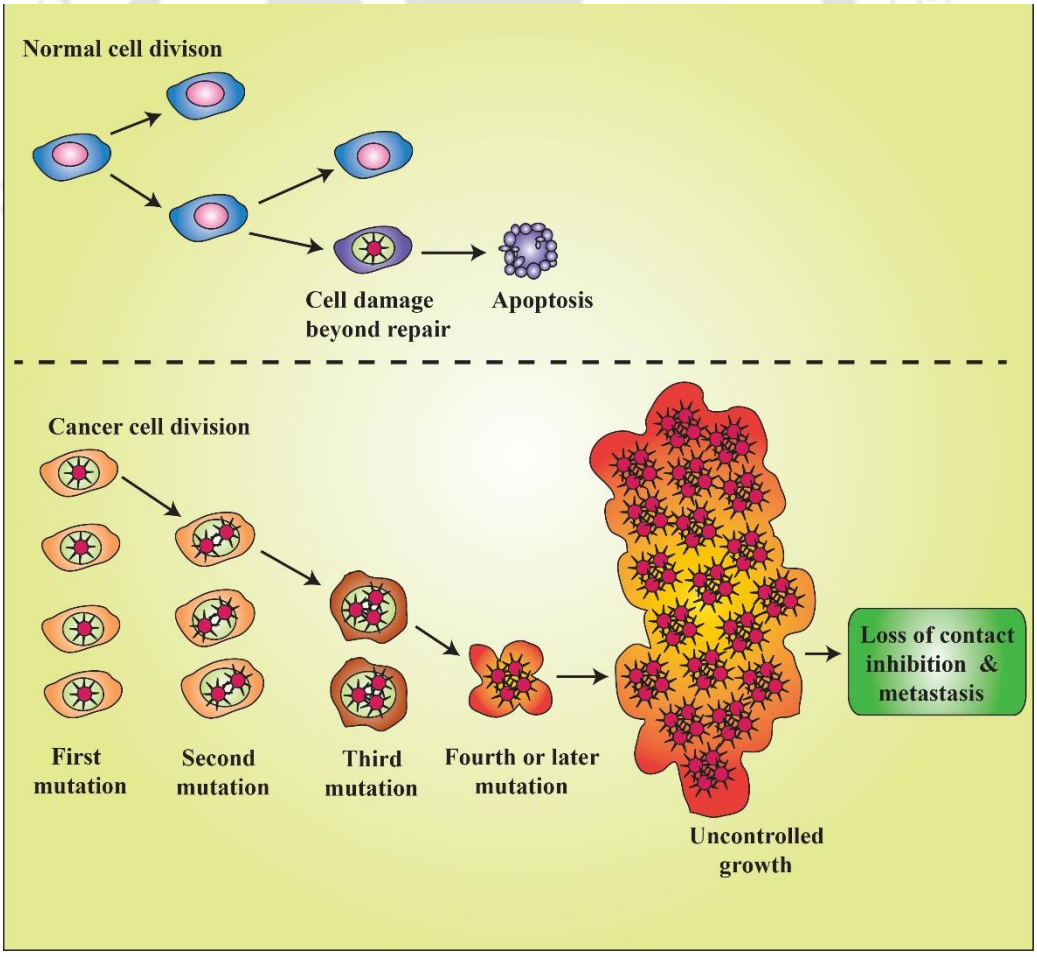

Figure 1.1: Schematic illustration of tumor formation. In an event of cell damage beyond repair, normal cells proceed for apoptosis. However, cancer cells accumulate mutations over the course of generations and finally attain a stage of unlimited cellular proliferation. Ultimately, cancer cells display loss of contact inhibition and subsequently metastasize to distant sites to establish secondary cancer.

1.2 Cancer facts and statistics

1.2.1 Global scenario: Cancer has been the forerunner amongst maladies that claim millions of lives every year. According to WHO, cancer as a group account for approximately 13% of all deaths occuring annually in the world. In the developed countries, it is the leading cause of death. In U.S.A cancer is accountable for 25% of all death every year. Lung, stomach, liver, colon and breast related cancer is responsible for most deaths each year (Global Burden of Disease Cancer, 2015). Cancer is also seen to be more prevalent among certain genetic populations. African-American men have the highest incidence and mortality rates compared to white, asian and hispanic men (Albain et al., 2009). Generally, poorer and less educated communities have higher mortality rates compared to rich and highly-educated families (Albano et al., 2007). Thus, nations from all around the world invest a significant proportion of their annual GDP to combat cancer or related disorders. In few instances these expenditure ranges 1-4% of total GDP of the country. Cancer types vary in orders of magnitude between different populations around the world (Doll and Peto, 1981). The most frequent cancer type associated with a particular sex varies considerably among different countries. Lung cancer is the most common in men of Eastern Europe and Asia (Ferlay et al., 2010). Prostate cancer is most common in North America, Australia, Western & Northern Europe and South America (Ferlay et al., 2010). Liver cancer and Kaposi sarcoma is most common in African countries. Breast cancer is the most common type of cancer diagnosed among women in Australia, Western Asia, North Africa, North America and parts of South America (Ferlay et al., 2010). Cervical cancer is common in Central America, parts of South America, Sub-Saharan Africa and India (Ferlay et al., 2010).

1.2.2 Indian scenario: India contains around 17% of the world's total population. Among the total 14 million new cancer cases diagnosed world-wide in 2012, 1 million cases were reported from India. The recorded incidence for India is 94 per 10^5 people which is roughly half of the world average of 182 per 10^5 people. Compared to these figures, the recorded incidence in the developed countries stands at 268 per 10^5 people. Oral, lung, stomach and colorectal cancer are the most reported in Indian men while breast and cervical cancers are the most reported in Indian women (Figure 1.2). Statistical evidence indicates that cancer incidences vary greatly between different regions of India which may reflect role of food habits, lifestyle and geographical aspects in causing cancer (Forman D, 2014). The north-eastern state of Mizoram has been recorded for the highest incidence rates of cancer while Barshi, a small city at the state of Maharashtra has been recorded with the lowest rates of cancer incidence in India (Figure 1.2-B). Thus, there is considerable variation in cancer incidence across different regions of India (Forman D, 2014). As India's population expands, the total number of incidence per year is expected to increase to 1.7 million in 2035 from the current figure of 1 million in 2012.

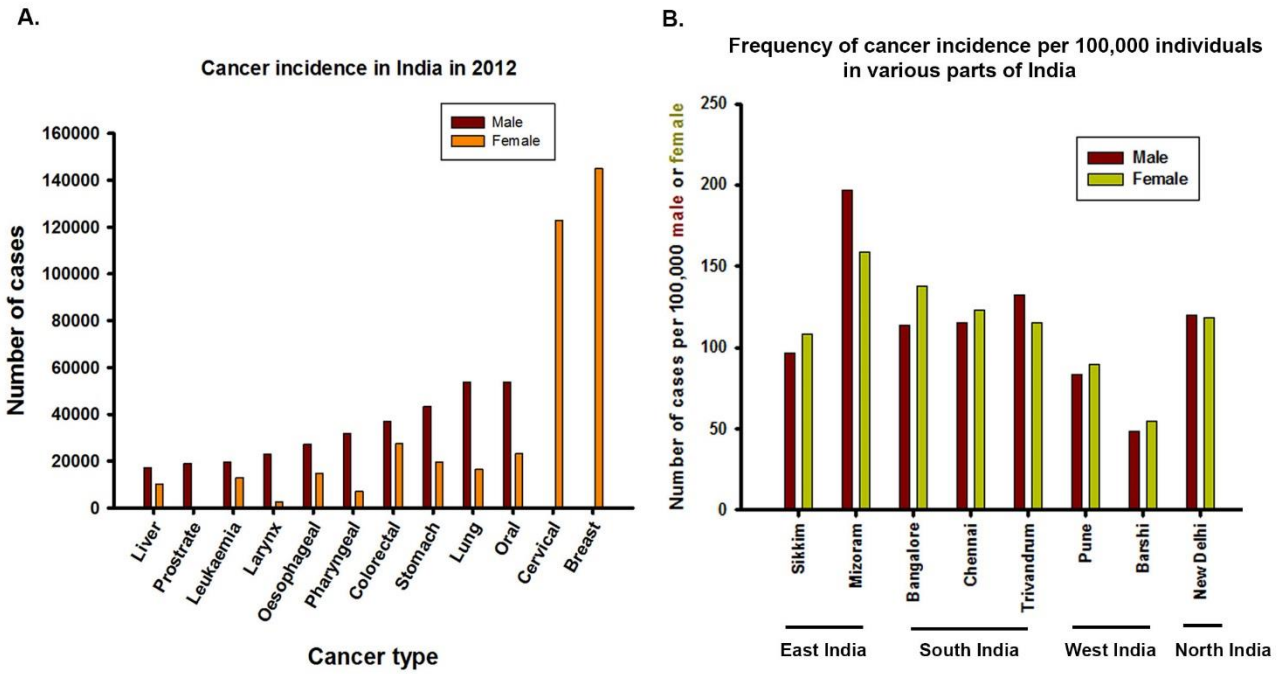

Figure 1.2: Cancer incidence rates in India. (A)Frequency of different cancer type during 2012 in India (Globocan data).(B) Regional variations in cancer rates in India among males and females. Data is shown in number of cases of all cancer types in a population of 100,000 males or 100,000 females (Forman D, 2014).

1.3 Cancer development and progression

Cancer can occur at many sites in the human body although some sites are more susceptible than others. The most prominent sites include lungs, breast, prostate, colon, liver, cervix and skin (Figure 1.3). Generally, these abnormal cells form a solid mass and are called tumors. However, the different types of blood cancers don't form solid mass.

1.3.1 Lung Cancer: Lung cancer is the leading cause of death in men and the second highest cause of death in women. In men, African-American have the highest incidence of lung cancer in U.S.A. In Europe, lung cancer has the highest incidence rate in Africa, Central & South America and South Central Asia (Ferlay et al., 2010). Lung cancer is also highly prevalent among women in North America and parts of Europe, including the United Kingdom and Denmark (Ferlay et al., 2010). Tobacco has been identified as the most common reason behind lung cancer. Smoking is accounted for about 80% of global lung cancer associated deaths in men and 50% of the deaths in women (Ezzati et al., 2005; Ezzati and Lopez, 2003). However, environmental exposures other than tobacco have also been reported to act as inducers of lung cancer. These include some organic chemicals, radiation, air pollution, coal-smoke, radon & asbestos, certain types of metals (chromium, cadmium, arsenic) and indoor emissions from burning other fuels. Lung cancer arise from epithelial cells and, hence, are termed as carcinomas. Mutations in KRAS proto-oncogene (Herbst et al., 2008), EML4-ALK tyrosine kinase gene and EGFR receptor (Herbst et al., 2008) are found in common lung cancer. Recent studies

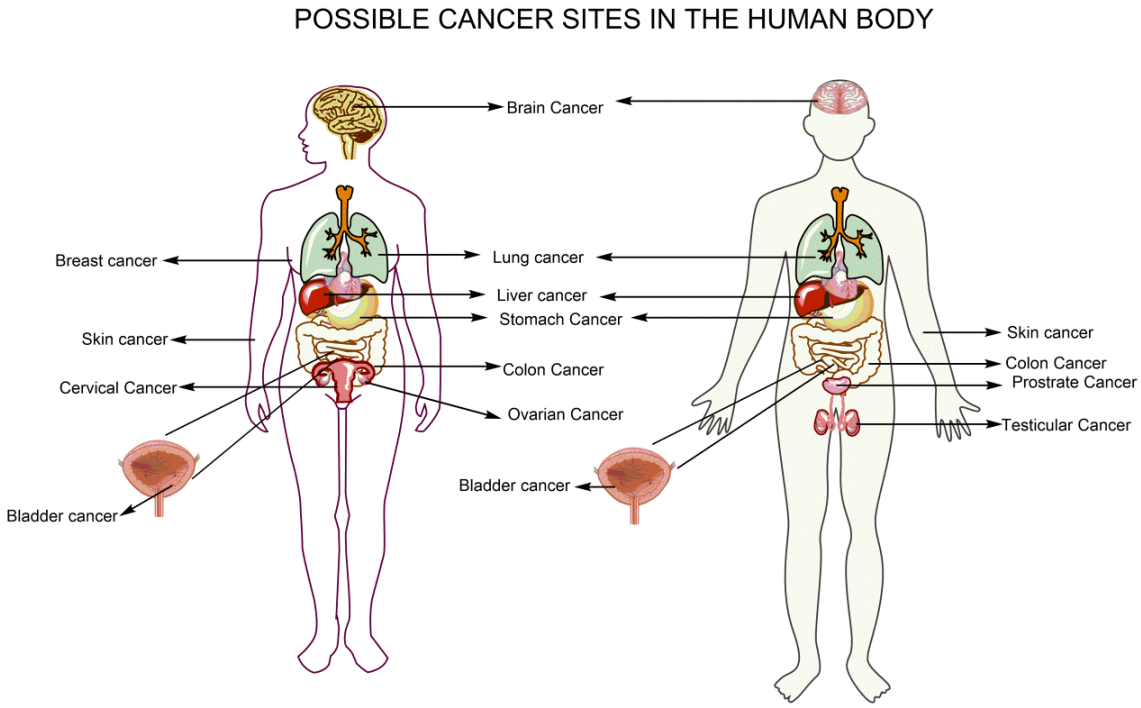

Figure 1.3: Frequent cancer induction sites in the human body.

have revealed active participation of PKC isozymes in lung cancer development (Fan et al., 2013). Like other prominent cancer, lung cancer is also highly metastatic and has been known to metastasize to liver, brain, bones and adrenal glands. Hence, different clinical therapeutic intervention has been developed to treat lung cancer. Surgery is generally used in case of lung tumors which are relatively smaller in size. However, advanced tumors are treated with chemotherapy or a combined treatment of chemotherapy and radiotherapy. Currently used drugs for chemotherapy include capecitabine, carboplatin, cyclophosphamide, docetaxel, doxorubicin, epirubicin, cisplatin, etoposide, fluorouracil, gemcitabine, paclitexal, vinorelbine etc.

1.3.2 Colon/Rectal cancer: Colon cancer is the second most common cancer in women and third in men. People of Eastern European countries (Czech Republic and Slovakia), Japan (Miyagi), New Zealand, Australia, Germany, and U.S.A. have reported highest rates of colon cancer in the world (Ferlay et al., 2010). The lowest rates are found in South-East Asia (India & Pakistan) and Central & Southern America. However, in recent times, there is an increase in colorectal cancer cases in low-risk countries. This is reflected in the gradual embracement of western lifestyle, such as smoking, increase in junk food in diet and obesity (Center et al., 2009). The epithelial cells lining the colon or rectum of the gastrointestinal tract give rise to colon cancer (Fleming et al., 2012). The genetic risks are almost negligible in the formation of colon cancer. This brings our attention towards other causes; such as alcohol, smoking, sex, old age, no or low physical exercises, diet comprising of red meat and processed meat. Persons suffering from inflammatory bowel diseases are also considered at high risk. Mutational inactivation of the Adenomatous polyposis coli (APC) gene, a key component of the

classical Wnt signalling pathway leads to high levels of β-catenin levels in cancer cells. This is conducive to colorectal cancer (Fodde, 2002). However, activation of PKC-α has been linked with suppression of β-catenin levels in colorectal cancer cells. PKC-α can serve as a major therapeutic target in colorectal cancer (Gwak et al., 2009). Other deactivated genes in colorectal cancer include TGF-β and SMADs. On the contrary, KRAS, RAF and PI-3K kinases are over expressed (Markowitz and Bertagnolli, 2009) in colorectal cancer. Studies have identified a gene Metastasis-associated in colon cancer-1 (MACC1), which is highly expressed in colon cancer specimens. MACC1 drives the transcription of hepatocyte growth factor that promotes colon cancer cell proliferation (Stein et al., 2009). The mortality due to colorectal cancer is gradually decreasing in developed countries due to improved treatment along with increased awareness and early detection (Chu et al., 1994; Edwards et al., 2010; Sant et al., 2001). Early stages of colon cancer are dealt with surgical removal of the tumor. Chemotherapy drugs include capecitabine, fluorouracil, irinotecan, oxaliplatin, trifluridine/tipiracil. Target therapy drugs include bevacizumab, regorafenib, ziv-aflibercept (Zaltrap) and ramucirumab (Cyramza), cetuximab (Erbitux), panitumumab (Vectibix) etc.

1.3.3 Breast cancer: It is one of the most prevalent cancer among women causing death (Du et al., 2008). Although the death rates vary from country to country, the highest incidence rates are reported in Switzerland, USA, whereas low incidence rates are found in Africa, Asia and South America (Ferlay et al., 2010). Reproductive factors, such as early menarche, late child bearing and fewer pregnancies, use of menopausal hormone therapy are thought to be largely associated with breast cancer (McPherson et al., 2000). Common metastatic sites of breast cancer are bones, lung, liver and brain. Genetic factors play a prominent role in the risk of breast cancer. Women with BRCA1 or BRCA2 mutations (both are tumor suppressor genes) have ~50% probability to get breast cancer in their lifetime (Antoniou et al., 2003). Mutations in oncogenes as Human epidermal growth factor receptor-2 (HER2/erbB-2) play a crucial role in breast cancer induction and progression (Yarden, 2001). These mutations are further aggravated by overexpression of other signalling kinases. PKC isozymes have been recognized as signalling kinases intrinsically involved in breast cancer progression (Urtreger et al., 2012). Early detection through mammography and improved treatment have contributed to the stability or decreased rates in modern times in the developed world (Althuis et al., 2005; Sant et al., 2006). Surgery options include lumpectomy (removal of the small tumors from the breast) and mastectomy (surgical removal of entire breast in extreme cases). Radiation therapy routines include 5 times a week for 5 to 6 weeks. Chemotherapy drugs include capecitabine, carboplatin, cisplatin, cyclophosphamide, docetaxel, doxorubicin, epirubicin, fluorouracil, gemcitabine (Gemzar), methotrexate, paclitaxel, vinorelbine, eribulin and ixabepilone. Hormonal therapeutic agents include tamoxifen and aromatase inhibitors (drugs that reduce production of estrogen).

1.3.4 Prostate cancer: Among men, prostate cancer is the second most frequently diagnosed cancer. It is the sixth leading cause of 'cancer-associated death' worldwide (Ferlay et al., 2010). Individuals harbouring malignant cancer cells in their prostate secrete a specific protein known as prostate specific antigen (PSA). The PSA is detected to ascertain prostate cancer in a person. Advanced prostate cancer is metastatic and can spread to the bones of spine, ribs and pelvis. Many different genes have been implicated in the development of prostate cancer. These include mutations in BRCA1 and BRCA2 genes (Struewing et al., 1997), Hereditary Prostate cancer gene 1 (HPC1) (Gallagher and Fleshner, 1998) and Trans-membrane protease, serine 2 (TMPRSS2) genes (Beuzeboc et al., 2009). Prostate cancer is treated according to the different stages of cancer progression. At early stages, various form of radiation therapy, like X-rays, proton beams and radium-223, are given to the patient. However, surgical removal of the prostate is recommended in severe cases. Prostate cancer is driven by male sex hormones (androgens) and, hence, androgen deprivation therapy (ADT) is used. Chemotherapeutic drugs include docetaxel combined with a steroid called prednisone, mitoxantrone and cabazitaxel. Studies have revealed that different signalling kinases, like PKC can be a target for prostrate cancer therapy (Xiao et al., 2009).

1.3.5 Liver Cancer: Liver cancer is also known as hepatocellular carcinoma. Liver cancer is the third leading cancer causing death worldwide. However, it is mainly confined to asian countries, such as China and Hong Kong which account for about 50% of the total incidence reported (Ferlay et al., 2010). The western countries of Europe and North America have 20-40 fold lower incidence of liver cancer compared to asian countries. Liver cancer is to a large extent caused by virus infections (78%). The most prominent among them are chronic hepatitis B virus (HBV) and hepatitis C virus (HCV) infections (Bosch et al., 2004). The HBV infections are prevalent in regions, such as Asia and Sub-Saharan Africa whereas the HCV strain is dominant in North America and most parts of Europe. Other known risk factors include dietary exposure to aflatoxins in poor countries, alcohol-related cirrhosis, smoking and non-alcoholic fatty liver disease (Bosch et al., 2004; Seeff and Hoofnagle, 2006). However, many signalling kinases are also involved in hepatocellular carcinoma whose expression levels are significantly altered after integration of viral DNA. Many isozymes of PKC have shown very less activity in the plasma membrane in hepatocellular carcinoma cells (Chang et al., 1996; Tsai et al., 2000). Liver cancer is known to metastasize to lungs and the hepatic portal veins. Therapeutic treatment involves surgery to remove a portion of the liver (hepatectomy) and liver transplantation in severe cases. Percutaneous ethanol injection involves direct injection of ethanol to kill liver tumor cells (Livraghi, 2001). Radiation therapy is used with caution not to damage healthy liver cells. Conventional chemotherapeutics are not routinely used in treatment but chemo-embolization technique is used. Chemo-embolization involves injection of drugs in hepatic artery and stopping the flow of blood for short time. Development of a vaccine against HBV has reduced the incidence of

liver cancer around the world but a vaccine against the HCV strain still needs to be developed as of yet.

1.3.6 Cervical cancer: Cervical cancer is the third leading cause of cancer-associated death in women all over the world. The incidence rate varies substantially worldwide. Low incidences (5 cases per 10^5) are found in women from countries like Egypt, China and many European countries (Ferlay et al., 2010). High incidences (45 cases per 10^5) are found in African countries, South America, the Caribbean and Southern Asia (Yang et al., 2004). The global variation in cervical cancer rate is attributed to the distribution of different sub-types of human papilloma virus (HPV), of which there are 15 high-risk human sub-types. HPV-16 and HPV-18 infections accounts for about 70% of the total cases (Castellsague et al., 2006). Smoking and long term oral contraceptive use is also associated with cervical cancer. Metastasis of cervical cancer is normally restricted to adjacent organs around the cervix such as pelvis, rectum and bladder. However, reports of metastasis to distant organs such as bones, lungs and liver are also found (Friedlander and Grogan, 2002). Therapeutic procedures include surgical removal of the tumor and surrounding healthy tissue. Radiation therapy is mainly used along with chemotherapy. Drugs routinely used include bevacizumab, hycamtin and cisplatin.

1.4 Mechanism of tumor formation

Cancer is caused by mutations in genes that control the proliferation of mammalian cells (Pedraza-Fariña, 2006). Some of the genetic changes are hereditary that makes an individual more susceptible to cancer. Environmental factors such as UV radiation, certain chemicals like formaldehyde, heavy metals (Hg), plant derived alkaloids (nicotine) and pathogenic virus (HPV) can induce cancer development in vertebrates (Alberts B, 2002). The key genetic changes in cancer are attributed to mutations in three sets of genes: proto-oncogenes, tumor-suppressor genes and DNA repair genes (Lee and Muller, 2010). Proto-oncogenes have the potential to act as oncogenes. Oncogenes are genetically mutated versions of proto-oncogenes that become more active to provide cell-proliferation signals resulting in uncontrolled cell-division (Anderson et al., 1992b). Examples of proto-oncogenes include receptor tyrosine kinases, H/K-Ras, NF-κβ, TNF-α, Wnts, cyclins and cyclin dependent kinases (CDKs). Tumor-suppressor genes inactivation by mutation removes the checkpoints for unregulated cell proliferation. Examples of tumor-suppression genes include p21, p27, master transcription factor p53, pRb, enzymes such as GSK-3β, caspases, PKC-δ, PKC-α and cytokines like TGF-β (Anderson et al., 1992b). The DNA repair genes are considered as part of the tumor suppressor genes. Some viral infection also leads to cancer. Chronic infection of the liver by HBV sometimes leads to the integration of HBV DNA into the chromosomal DNA of hepatocytes (Matsubara and Tokino, 1990). This leads to secondary rearrangements of chromosomes, such as

translocations, inversions, deletions and (possibly) amplifications. This ultimately results in uncontrolled proliferation of hepatocytes forming a malignant tumor.

1.5 Different factors contributing to cancer development

Every cancer type is exclusive to some part of the world. Many cancer epidemiologists have concluded that most of the cancers are result of mostly lifestyle habits and can be avoided by following recommended guidelines (Anand et al., 2008). Smoking, obesity and a few oncogenic viruses are some of the notable causes found responsible for development of cancer while exact reasons behind a particular cancer type is not conclusive.

1.5.1 Lifestyle: The lifestyle of a person has a profound influence on the development of cancer. Erratic unhealthy lifestyles such as lack of exercise, improper sleep, high intake of junk food and social habits such as smoking has been linked to cancer (Anand et al., 2008). Tobacco which is the main ingredient associated with smoking, is directly linked to lung cancer (Doll, 1978). Individuals who start smoking at an early age are at the greatest risk of developing lung cancer. The habit of smoking was acquired in western countries during the First World War which saw an unprecedented rise in lung cancer cases till 1955. Since then, due to increased awareness, the rates of lung cancer are steadily on the decline in the western world (Peto et al., 2000; Wynder and Graham, 1950). The carcinogenic effects of tobacco is not only restricted to the lungs and the adjoining areas (the larynx, mouth, pharynx, the pancreas, kidney and bladder), it also aggravates cancer of the liver, stomach and cervix (Doll, 1996; Liu et al., 1998).

Food habits play an important role in developing cancer in a person's life. A diet rich in green vegetables, pulses and cereals is thought to be cancer preventive whereas a diet rich in red-meat and fats is thought to contribute to cancer (Liu et al., 1998). However, it is generally agreed that cancer is more common in people who are overweight (Josefson, 2001). A person's Body Mass Index (BMI) provides evidence that obesity is conducive to cancer (Josefson, 2001). Newer studies support that a diet rich in nutrients, such as aspirin and folate supplements might reduce the chance of developing cancer in a person (Jänne and Mayer 2000).

Hormonal factors also do play a role in developing cancer, especially in women. The probability of breast cancer is transiently increased in pregnant women (Martin and Weber, 2000). Hormone replacement therapy is known to increase the probability of endometrial cancer. However, ovarian and endometrial cancers seem to decrease with increasing parity (Casagrande et al., 1979). The higher rate of breast cancer in the western countries is due to the result of western diet which induces early menarche and early menopause together with post-menopausal obesity (Newcomb et al., 1994; Pike et al., 1983).

1.5.2 Environmental agents: The environment around a person decides whether he is being regularly exposed to toxic hazardous material as it play an important role in the development of cancer (Parsa, 2012). Industrial workers have exposure to several composite mixtures and heavy organo-metallic complexes. Many such mixtures such as combustion products of fossil fuels can pose as risk factors of lung cancer (Cohen and Pope, 1995). Asbestos is a mineral which is widespread in construction industries and give rise to mesothelioma in many workers (Peto et al., 1999; Wagner et al., 1960). However, many environmental carcinogens might have latent effect for many years until it begins to show its effect at old-age. Ionizing radiation has increased the frequency of germ-cell mutation in humans (Xu et al., 2012). After the Second World War, radioactive material was gradually distributed as a result of testing of nuclear explosives by several countries. In Japan, leukaemia has been linked to the radiation after-effects of the nuclear explosion during second world war (Doll, 1995). Malignant carcinomas began to develop in the hands of workers exposed to X-rays. There have been many cases of radiologists developing leukaemia. Radium is another element that has been recognized to induce sarcomas, most particularly bone sarcoma in luminal dial painters. In the 1920s, there was an instance of 18 deaths from a disease among 800 young women who had been employed in the factory. Later it was revealed that 5 of these young women had developed bone sarcoma and significant amount of radium was present in their bones (Martland, 1931). Irradiation therapy for tuberculosis affecting the skin, bones and cervical glands can also result in cancer of the lip, larynx, pharynx, thyroid and connective tissue after a few decades of latency. Radon escape from construction sites can also compound the lung cancer of smokers (Dockery et al., 1993). In recent times, nations have put efforts to switch on to green energy resources that can significantly curtail environmental hazards.

1.5.3 Hereditary factors: Development of cancer is linked to polymorphisms in tumor-suppressor genes, oncogenes, genes involved in the metabolism of endogenous or exogenous mutagens (Osborne et al., 2004). Also, genes associated with production, processing of sex hormones are also been linked to the prevalence of cancer (Osborne et al., 2004). There is an increased risk of bladder cancer on polymorphisms of the *N*-acetyltransferase 2 (NAT2) (Hein et al., 2000). About 1 in 20 Ashkenazi Jews have a SNP mutation in the Adenomatous polyposis coli (APC) gene which doubles their colon cancer risk (Woodage et al., 1998). Similarly, 5% of the population carry mutation in the HRAS1 gene, which increases the risk by a factor of 1.5 to 2 to many common cancer types (Krontiris et al., 1993). Women who are deficient for the Glutathione S-transferase mu 1 **(**GSTM1) gene have a much greater risk to lung cancer (Woodage et al., 1998). Some women have alleles of the NAT2 gene which results in decreased capacity to detoxify carcinogenic aromatic amines in cigarette smoke. These women have a greater risk for breast cancer especially during the post-menopausal phase (Ambrosone et al., 1996). Polymorphisms in the methylene-tetrahydrofolate reductase (MTHFR) gene is largely associated with colorectal cancer (Chen et al., 1999). Perhaps, the most profounding effect is seen in breast cancer

among family lineage in that twin and sibling risks can be estimated very precisely. Susceptible mothers contribute a significant high risk factor for her daughters (Peto and Mack, 2000). Breast cancer that runs hereditarily in families is due to the prevalence of mutations in the BRCA1 or BRCA2 genes. However, the degree of contribution of penetrant genes to many common cancer types remains yet to be determined. Sometimes, many genes may contribute together to a large genetic effect that may result in cancer. In those cases, attributing polymorphisms to a single gene is not possible.

1.5.4 Pathogens: During the later part of the 20th century, it was begun to be increasingly recognized the contribution of different pathogens in the induction of carcinogenesis in humans (Vandeven and Nghiem, 2014). Human papillomavirus (HPV) is a major pathogen in women and 15 strains are reported to induce cervical cancer in women. Especially the strains HPV16, HPV18, and HPV45, are virtually detectable in all cervical cancer cases worldwide (Walboomers et al., 1999). HPV strains are normally sexually transmitted and can cause cancer at other sites such as skin, oesophagus, head, and neck. In the same way, liver cancer is induced by infection with hepatitis B virus (HBV) and its counterpart strain hepatitis C virus (HCV) (Lim and Torresi, 2014). Their actions are synergistically enhanced by damaging liver from cigarette smoking and alcohol consumption. Many other pathogens also contribute to depose a person to high risk of cancer. The Epstein–Barr virus (EBV) is associated with nasopharyngeal cancer and various B-cell malignancies (Song et al., 2016). Human T-cell lymphotropic virus1 is associated with T-cell leukaemia and lymphomas; plasmodium induced malaria acts as a co-factor for EBV-induced Burkitt's lymphoma; human herpesvirus causes Kaposi sarcoma, and liver flukes cause cholangio-sarcoma (Anwar et al., 1994). The SV-40 virus which is found to be involved in many cancer types is known to inactivate the tumor suppressor gene p53 through SV40 large T-antigen and SV40 small T-antigen. Infection-mediated cancers pose a significant health burden globally (Parkin, 2006). A significant proportion of cancers can be prevented if these pathogens or their infections could be eradicated.

1.6 How cancer spreads to different parts of the body?

What makes cancer very dangerous is that they can break off from the original tumor site and can spread to other areas of the body. This phenomenon is termed as metastasis(Chaffer and Weinberg, 2011). Approximately 90% of deaths in cancer is attributed to metastasis (Spano et al., 2012). Metastasis is a coordinated sets of events involving angiogenesis, epithelial-mesenchymal transition (EMT) and activation of MMPs to evade tissue (Valastyan and Weinberg, 2011). During an EMT, benign cancer cells of epithelial morphology downregulate epithelial markers such as E-cadherin, upregulate mesenchymal markers like N-cadherin & vimentin and starts secretion of fibronectin (Chiang and Massagué, 2008). EMT is triggered by key signalling cytokines TGF-β (Akhurst and Balmain, 1999; Heldin et al., 2009), TNF-α, canonical Wnts, EGF, HGF, IGF1 and Prostraglandin E2

etc. which are actively secreted by reactive stromal cells in proximity to the tumor (Berx et al., 2007). These cytokines initiate signalling cascades activating key transcription factors (TFs) such as NF-κβ, snail, slug, twist etc. in benign cancer cells (Valastyan and Weinberg, 2011). These TFs in turn actively promotes transcription of cytokines such as canonical and non-canonical Wnts, TGF-β as well as snail, slug, twist and NF-κβ themselves. These key molecules initiate autocrine signalling loops that drive the EMT progression successfully and maintain the mesenchymal state henceforth (Huber et al., 2005). However, the extracellular matrix (ECM) acts as an obstacle before the transformed cancer cells from gaining access to the circulatory systems. To tackle this problem, transformed cells actively secrete various matrix metallo-proteases (MMPs) that degrade all the components of the ECM one by one (Valastyan and Weinberg, 2011). Slowly, the transformed cells gain access to the circulatory systems and travel to newer destinations at different organ sites (Figure 1.4). At new locations, these runaway cancer cells revert back to epithelial state and start new colonies (Valastyan and Weinberg, 2011). Metastasis can impair the function of important organ and organ-systems with life threatening consequences for the patient. For instance, malignant breast cancers frequently metastasize to lung, liver, brain and bone.

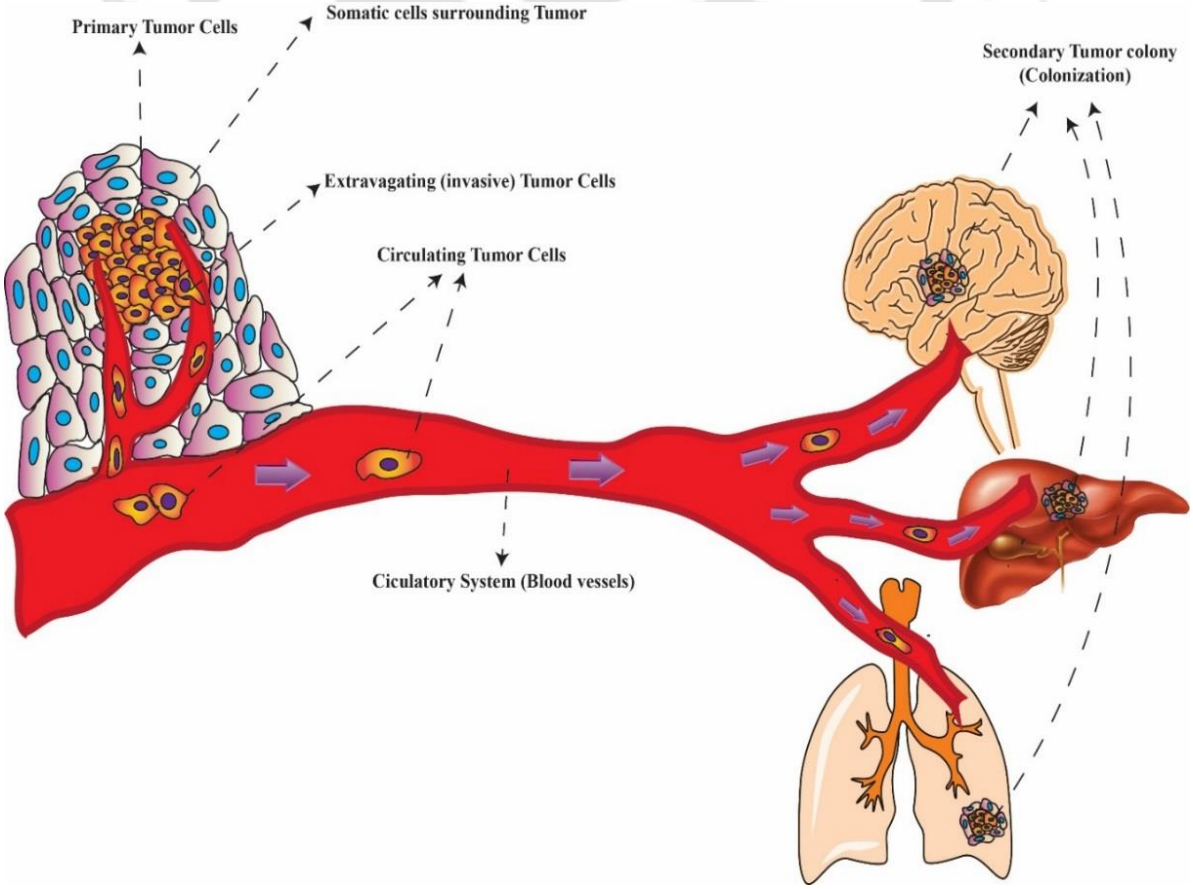

Figure 1.4: Schematic diagram to explain the process of cancer spread from their site of origin to the other parts of the body. In general, most of the primary tumors are of epithelial origin. When a primary tumor transforms itself into malignant type, some of the cancer cells acquire mesenchymal morphology and invade nearby circulatory systems to migrate to distant organs. They revert back to epithelial phenotype and establish secondary colonies at new site.

Doctors have devised TNM (Tumor, Node, Metastasis) system to describe and asses the severity of cancer in human body (Brierley, 2006; Sellers, 1971). In this system, "T" describes the size of tumor and refer to the spread of cancer from the site of origin. It can have values between 1 to 4. Lymph nodes are present in the vicinity of every organ and organ systems in the body. So, "N" describes whether the cancer has spread to nearby lymph nodes. It can have values between 0 (cancer has not reached any lymph node) to 3 (cancer has spread to lots of nearby lymph nodes). Similarly, "M" (metastasis) describes whether the cancer has metastasized (value= 1) or not (value=0).

Thus, cancer occurs at many sites in the human body although some sites are more frequent than others. Also different cancers metastasize to different locations in the body (Figure 1.5). A closer look into the most common sites of cancer metastasis can help us realize the severity of the disease in more detail.

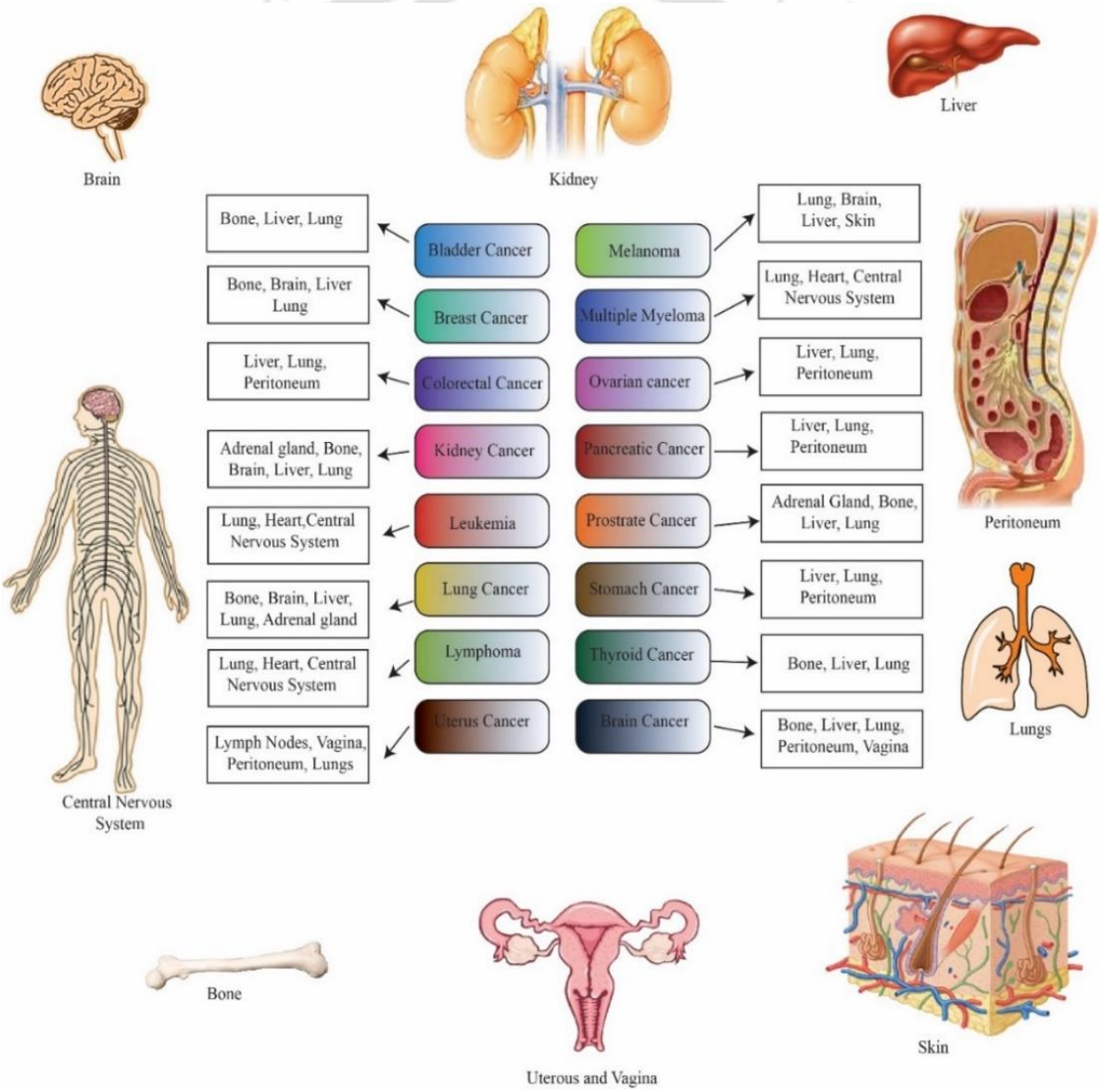

Figure 1.5: Frequent preferred metastatic destination of common cancer types in humans. This figure has been derived and reconstructed from (Martin TA, 2013).

1.7 Different therapeutic approaches to treat cancer

There has been an upsurge in cancer research in the latter half of the 20th century. Recent research efforts has led to a better understanding of the cellular and molecular biology aspect of cancer. This has provided the impetuous for designing newer generation of drugs with the potential of targeted cancer-cell therapy (Perez-Herrero and Fernandez-Medarde, 2015). These drugs have broad spectrum activity against several types of cancer cells from different origins. Today, surgery, chemotherapy, radiation therapy, hormonal therapy (a part of chemotherapy), photodynamic therapy and stem- cell therapy are the major therapeutic approaches to treat cancer (Figure 1.6).

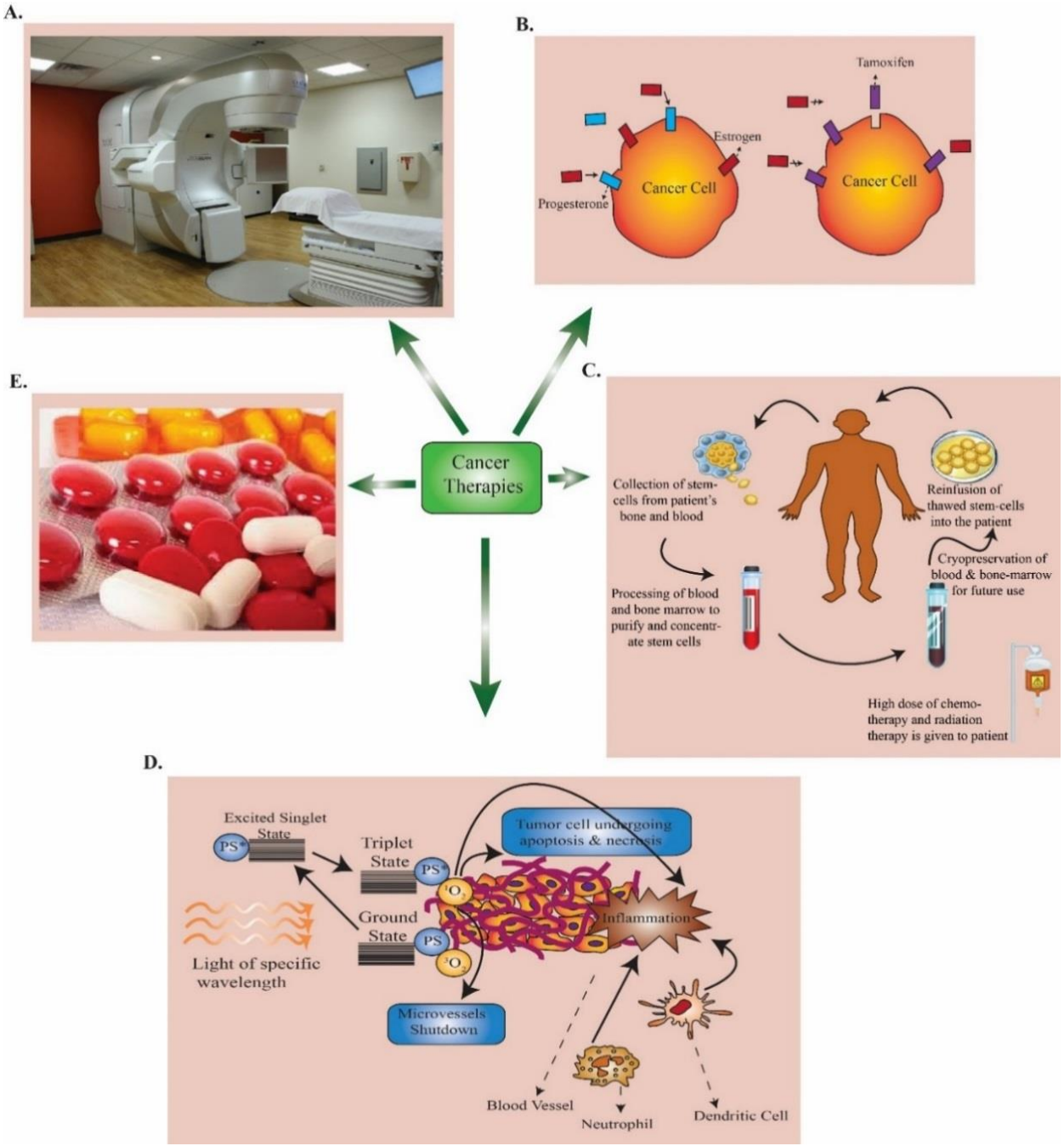

Figure 1.6: Different available therapies to treat cancer in patients.(A) Radiation therapy, **(B)** Hormonal Therapy, **(C)** Bone marrow stem-cell replacement therapy, **(D)** Photodynamic therapy **(E)** Chemotherapy.

1.7.1 Chemotherapy: Chemotherapy is the use of chemical compounds (drugs) to treat cancer. Different classes of chemotherapeutic drugs (Table 1.1) are available with different mechanisms to kill cancer cells. Some of them are depicted in Figure 1.7.

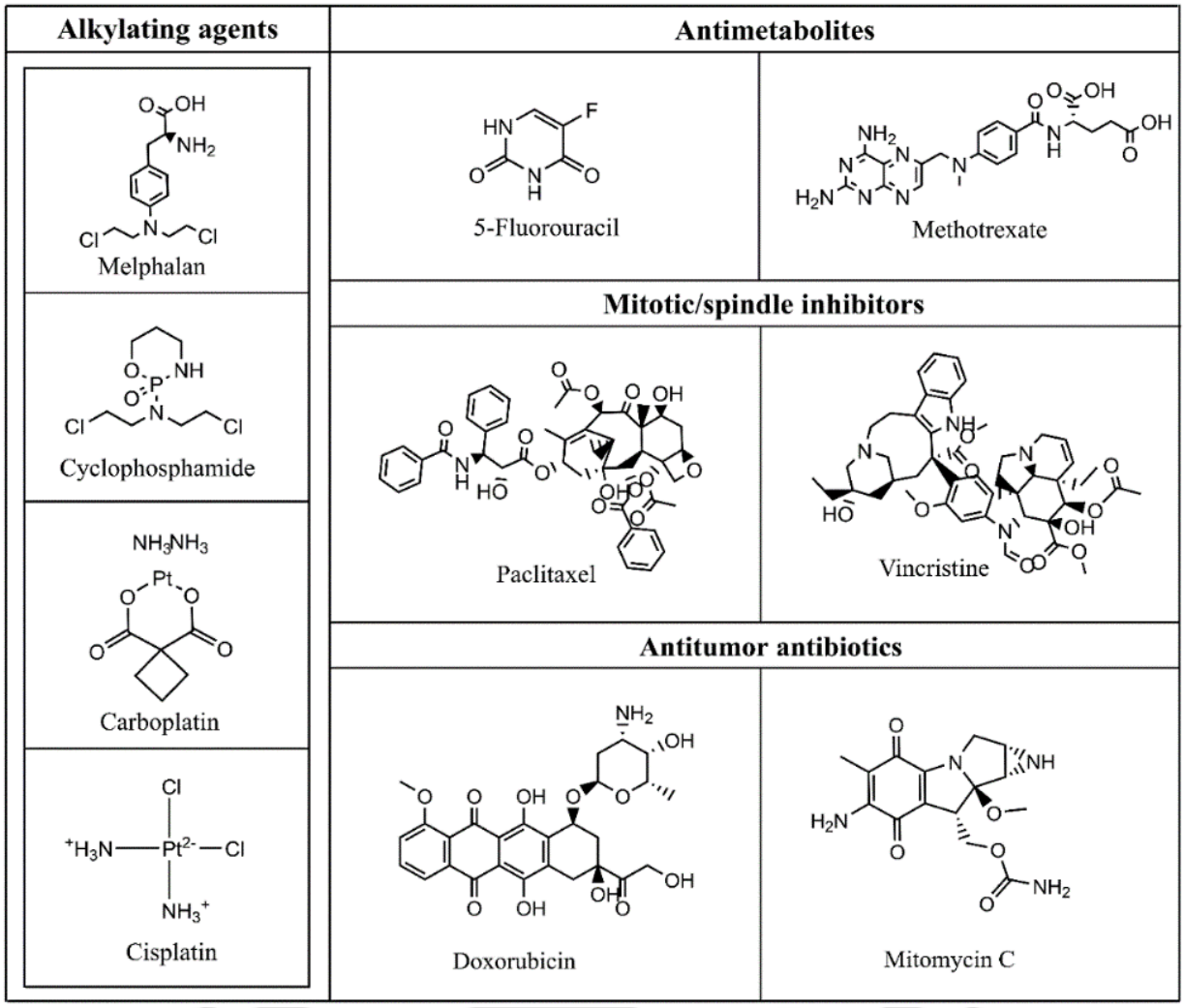

Figure 1.7: Some of the classes of popular chemotherapeutic drugs

A) Alkylating agents: The nitrogen mustard derivatives (e.g., mechlorethamine, melphalan, cyclophosphamide), nitrosoureas (e.g., carmustine) and the heavy metal alkylators (e.g., cisplatin, carboplatin) are collectively termed as alkylating agents (Figure 1.7). The alkylating agents attach an alkyl group (C_nH_{2n+1}) to DNA (Rappeneau et al., 2000). The resulting alkylated bases prevent DNA synthesis and RNA transcription. The attached alkyl group can also form cross-bridges, i.e., covalent bonds between atoms in DNA (Figure 1.8). Bridges can form within a single molecule of DNA (intra-molecular), or a cross-bridge may connect two different DNA molecules (inter-molecular). Subsequently, this cross-linking prevents DNA from separation which is required for DNA synthesis or RNA transcription (Apps et al., 2015; Ewend et al., 2007). These agents induce mispairing of the nucleotides during DNA replication leading to permanent mutations in the subsequent generations.

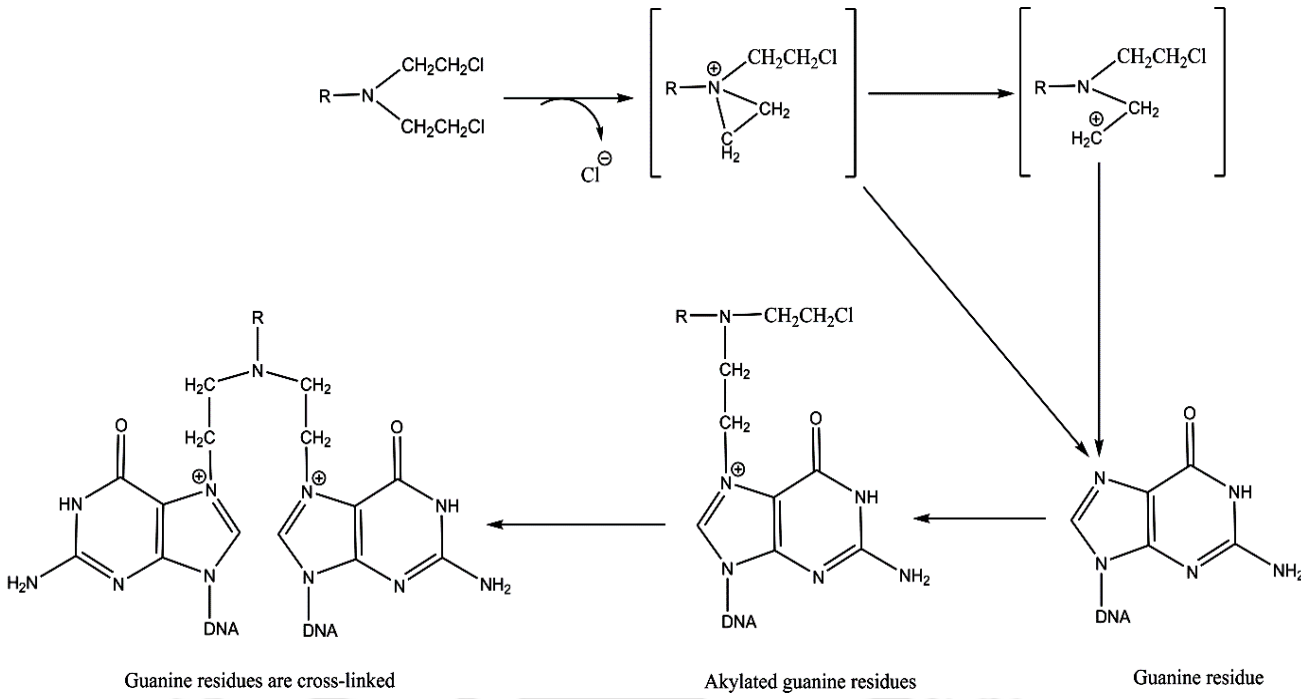

Figure 1.8: Schematic diagram to explain the mechanism of action of alkylating agents as anti-cancer molecules.

B) Antimetabolites: Antimetabolites consist of purine analogues (e.g., mercaptopurine), pyrimidine analogues (e.g., 5-fluorouracil, gemcitabine) and folic acid antagonists (e.g., methotrexate). Structures of different antimetabolites are shown in Figure 1.7. These drugs are designed to interfere with nucleotide metabolism. They interfere with the synthesis of purines and pyrimidines and block their synthesis(Longley et al., 2003). The cancer cell is thus deprived of deoxy-ribo and ribo nucleotides which blocks DNA replication and RNA transcription (Sahasranaman et al., 2008; Weinblatt, 2013).

C) Mitotic/spindle inhibitors and plant alkaloids: These anticancer drugs hyper stabilize the microtubule assembly and prevent its breakdown. This destroys the dynamism of microtubule structure. This process destroys the cell's ability to use its cytoskeleton in a flexible manner (Peltier et al., 2006). For example, the well-known drug paclitaxel is known to bind to the β subunit of tubulin, the 'building block' of microtubules (Figure 1.9). This locks these building blocks in place preventing the disassembly of microtubule/paclitaxel complex. This limitation halts cellular transport as well as locks down the mitotic spindle during metaphase. Other drugs in this category act in a reverse way. They bind tubulin but inhibit the assembly of microtubules. The disruption of microtubules arrests mitosis in the metaphase as the spindle fibers which are normally made up of microtubules can't form in the presence of the drug.

D) Topoisomerase inhibitors: These drugs or their active metabolite cause the direct inhibition of topoisomerase I or topoisomerase II enzymes which are essential for DNA replication. This eventually leads to inhibition of DNA replication and induction of apoptosis in cancer cells (Pommier et al., 2010).

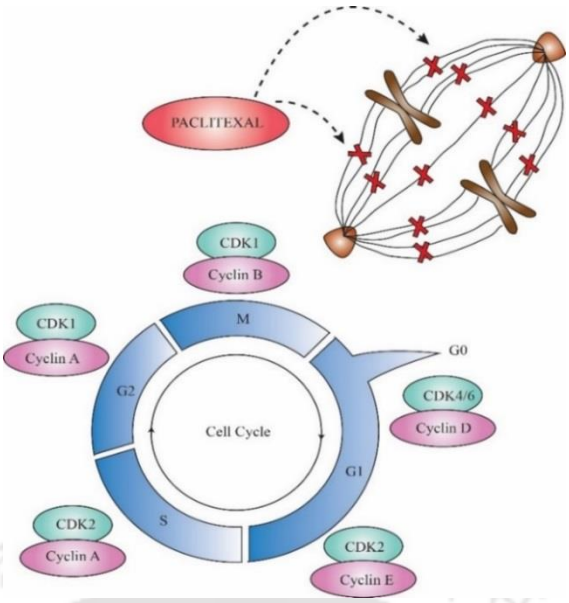

Figure 1.9: Schematic diagram to explain the mechanism of action of paclitexal as anti-cancer agents.

E) Antitumor antibiotics: These agents prevent separation of DNA during replication which eventually results in prevention of cell-division (Rao and Lown, 1990). Antitumor antibiotics also bind to RNA and inhibit enzyme/protein synthesis (Goldberg, 1974). These can be done by several elegant ways. Mitoxantrone and dactinomycin intercalate between base pairs via non-intercalative electrostatic interaction which results in inhibition of DNA replication, RNA transcription and protein synthesis (Figure 1.9). On the other hand, doxorubicin intercalates between the strands of DNA (Kaczmarek et al., 2012). This intercalation inhibits the progression of the enzyme topoisomerase II. Doxorubicin thus stabilizes the topoisomerase II complex after it has broken the DNA chain with the intention of uncoiling. This process prevents the DNA double helix from re-sealing, thereby stopping the process of DNA replication.

F) Signal transduction inhibitors: Most of the new generation of drugs fall into this category. Some notable examples include cetuximab (Erbitux) which binds specifically to the extracellular domain of the human epidermal growth factor receptor (EGFR) (Ng and Cunningham, 2004). The binding to the receptor blocks receptor phosphorylation to prevent signalling and activation of down-stream kinases. It results in inhibition of cell growth and induction of apoptosis. Another well-known drug, trastuzumab (Herceptin) binds to domain IV of the extracellular segment of the HER2 (human epidermal growth factor receptor2)/neu oncogenic receptor (Figure 1.10) (Hudis, 2007). This binding prevents receptor dimerization and inhibits further signalling through the downstream PI3-K cascade. Bevacizumab binds to VEGF and prevents the interaction of the VEGF ligands to its receptors (FLT-1 and KDR) on the surfaces of endothelial cells, thus, inhibiting angiogenesis (Shih and Lindley, 2006). The renowned drug imatinib (Gleevec) binds to the tyrosine kinase active site of the Bcr-Abl tyrosine kinase which is a constitutive abnormal tyrosine kinase (Hernandez-Boluda and Cervantes, 2002). This binding inhibits activity of Bcr-Abl kinase.

Table 1.1: Common class of anti-cancer drugs based on their mechanism of action.				
S No.	**Class of Drugs**	**Mechanism of action**	**Examples**	**References**
1.	Alkylating agents	Attach alkyl groups to DNA which prevents DNA synthesis and RNA transcription	mechlorethamine, melphalan, ifosfamide, cyclophosphamide, carmustine (BiCNU), cisplatin, carboplatin, oxyplatin	(Ewend et al., 2007),(Apps et al., 2015)
2.	Antimetabolites	Block the synthesis of purines and pyrimidines.	gemcitabine, 5-Fluorouracil, cytarabine, capecitabine, mercaptopurine (6-MP), methotrexate (MTX)	(Longley et al., 2003), (Sahasranaman et al., 2008), (Weinblatt, 2013)
3.	Mitotic/spindle inhibitors and plant alkaloids	These drugs hyperstabilize the microtubule assembly and prevents its breakdown.	Paclitaxel, docetaxel, ixabepilone, vinblastine, vincristine, vinorelbine,	(Peltier et al., 2006)
4.	Topoisomerase inhibitors	Direct inhibition of topoisomerase I or topoisomerase II enzymes.	irinotecan (CPT-11), topotecan, etoposide	(Pommier et al., 2010)
5.	Antitumor antibiotics	They prevent separation of DNA by binding to DNA.	mitoxantrone, dactinomycin, doxorubicin, epirubicin, bleomycin, mitomycin	(Kaczmarek et al., 2012)
6.	Signal transduction inhibitors	They prevent signalling through the receptor tyrosine kinases by binding to them.	cetuximab, trastuzumab, erlotinib, bevacizumab, sorafenib, imatinib, dasatinib, temsirolimus	(Hudis, 2007)
7.	Hormonal agents	These compete with natural ligands to bind to nuclear receptors and affect signaling.	tamoxifen	(Jordan, 2006)
8.	Epigenetic agents	They effect chromatin modification of oncogenes.	vorinostat, azacitidine	(Lee et al., 2013)
9.	Immuno-modulators	Modulate activation of the immune system.	Interferon α-2a and α-2b, rituximab	(Spiegel, 1986), (Edwards et al., 2004)
10.	Miscellaneous agents	Mechanism of action is not clearly understood.	lenalidomide, bexarotene, tretinoin, arsenic trioxide, asparaginase, bortezomib	(Cruz, 2016), (Dragnev et al., 2007), (Douer et al., 2003), (Chen et al., 2011)

Different classes of chemotherapeutic drugs act via different mechanisms of action. Some act by binding to DNA whereas others act by acting on the microtubule assembly. Still others act by affecting chromatin modifications. Renowned examples of each class is mentioned in the table.

G) Hormonal agents: This kind of drugs is mainly targeted for cancers originating in hormonally responsive tissues such as the breasts, prostate, endometrium and adrenal cortex. Tamoxifen is one of

the most familiar examples of hormone therapy given for cancer treatment (Jordan, 2006). Tamoxifen is a prodrug and its active metabolite competitively binds to estrogen receptors on tumors, producing a complex that translocates to the nucleus. The new estrogen receptor/tamoxifen complex does not respond to estrogen and binds to those estrogen-responsive promoters. But instead of activation, this complex binds to these stretches of DNA elements as a repressor where it recruits co-repressors to stop genes that were earlier being switched "on" by estrogen.

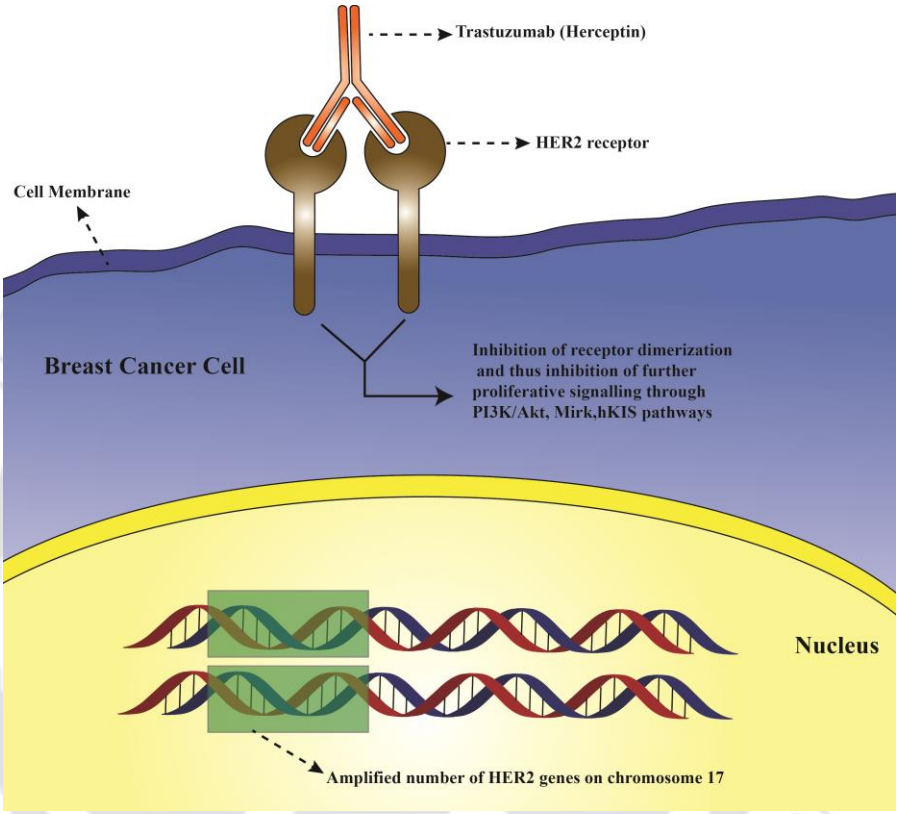

Figure 1.10: Mechanism of action of Herceptin. Herceptin inhibits signaling through HER2 receptor.

H) Epigenetic agents: These drugs are designed to effect chromatin modification of tumor suppressor genes or oncogenes. Vorinostat is known to inhibit the enzymatic activity of histone deacetylases namely HDAC1, HDAC2, and HDAC3 and HDAC6 (Lee et al., 2013). This inhibition allows for the accumulation of acetyl groups on the N-terminal tails of histone lysine residues resulting in an open chromatin structure (Lee et al., 2013). This leads to heightened transcriptional activation and subsequent expression of tumor suppressor genes.

I) Immunomodulatory agents: These agents boost the ability of the immune system to fight cancer. Most of them include recombinant cytokines like interferon α-2a (Roferon-A) & interferon α-2b (Intron-A). They also include antibodies like rituximab sold under the trade name Rituxan. (Bekisz et al., 2010). Interferons binds to their respective receptors on the cell-membrane and initiate crucial signaling networks that halt cancer-cell proliferation (Spiegel, 1986). While acting on immune cells, they augment the phagocytic activity of macrophages and specific cytotoxicity of lymphocytes for

target cells. Interferons also inhibit virus replication in virally infected cells (Spiegel, 1986). Rituximab binds to CD20 molecules expressed in mature B-cells to augment antibody-dependent cellular cytotoxicity (ADCC) and complement-dependent cytotoxicity (CDC) mechanisms (Edwards et al., 2004). It also mediates apoptosis of older B-cells, allowing a newer generation of B-cells to develop from lymphoid stem cells.

J) Miscellaneous agents: The agents included in this category have either multiple or unknown mechanism of to kill tumor cells. Lenalidomide (Revlimid) effects antitumor activity by affecting the micro-environment support for tumor cells and boosting the immune response (Cruz, 2016). Bexarotene (Targretin) binds and activates retinoid X receptor subtypes (Dragnev et al., 2007). However, it is unclear how these activated X receptors halt the proliferation of cancer cells. Arsenic trioxide (Trisenox) is seen to induce morphological changes and DNA fragmentation in cancer cells (Douer et al., 2003). However, its detail mechanism of action is unclear. Bortezomib (Velcade) binds reversibly to 26S proteasome of mammalian cells to inhibit it. This inhibition results in disruption of numerous cellular processes that are required for the growth and survival of cancer cells (Chen et al., 2011). However, other mechanisms are also proposed that are not clearly elucidated as of yet.

1.7.2 Radiation therapy for cancer: Radiation therapy involves the use of high-energy radiation(X-rays, gamma rays, and charged particles) to shrink tumors and kill cancer cells (Klein and Dawson, 2013). There are three modes of radiation therapy: i) External radiation therapy where the radiation is delivered by a machine from outside the body (Sadeghi et al., 2010), ii) Internal radiation therapy where a radioactive material is placed in the body near cancer cells (Sadeghi et al., 2010), iii) Systematic eradication therapy which involves use of radioactive substances that travel through the bloodstream to the targeted cancer site. Radiation therapy damages DNA directly or indirectly, creating free radicals/charged particles within the cancer cells. This process creates a state in cancer cells where the DNA damage is beyond repair due to which they die to be eventually broken down and eliminated by the body's natural processes (Brown et al., 2015). However, radiation therapy is a non-selective process in that it can also damage healthy cells, leading to side effects (Brown et al., 2015). The amount of radiation that can be received safely by healthy tissue is known for every part of the body. This information is helpful to the doctors to decide where to aim radiation during treatment.

1.7.3 Photodynamic therapy for cancer: Photodynamic therapy (PDT) for cancer takes advantage of substances called photosensitizers (PS) which can harvest the energy of a particular wavelength of light and in turn can initiate a reaction that can kill cancer cells (Wainwright, 2008). The principle of a photosystem is illustrated in Figure 1.11.

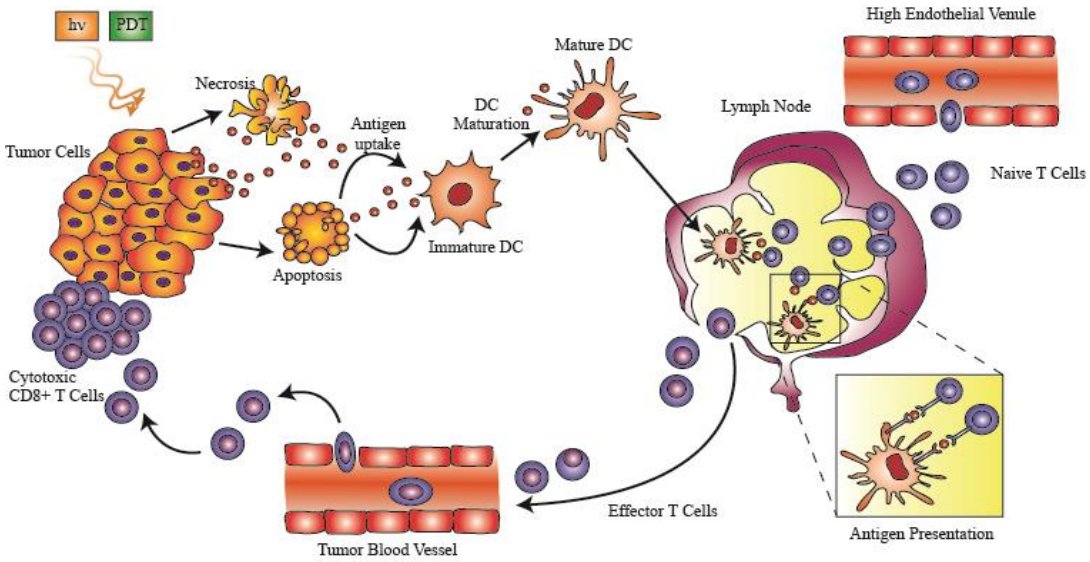

Figure 1.11: Schematic illustration of photodynamic therapy. In photodynamic therapy, light of specific wavelengths activates photosystems which produce free radicals to kill cancer cells. Cancer cell death release antigens which are processed by the immune cells to mount a heightened immune response to the tumor.

Photodynamic therapy is directed mainly at oncologic targets and their vascular supply. Based on the target, PDT can be performed as a single intensely illuminated therapy session or as a series of intensely illuminated therapy sessions.

When the light of an appropriate wavelength/energy is introduced to a particular PS, there are generally three reactions (PDR) that can be initiated by the photosystem (O'Connor et al., 2009). The reaction termed as Type II redox reaction takes place in the presence of oxygen and there is the generation of a triplet oxygen species. Afterwards, this triplet oxygen is degraded into singlet oxygen species which is extremely toxic to cancer cells and has a relatively long half-life (Gorman et al., 2004). Many photosystems are designed to achieve a high activity of this pathway. The type I redox reaction takes place in the absence of oxygen and leads to the generation of many other reactive species rather than triplet oxygen production (Dolmans et al., 2003). If water is the target, then this reaction would lead to the generation of hydroxyl radicals and superoxide ions which are very toxic to cancer cells. Another oxygen-independent pathway termed as the type III redox reaction exists where the activated PS directly destroys the target. Many tumors have internal regions which are devoid of oxygen supply known as hypoxia regions (Clapp et al., 1965). To kill those parts, the type III aspect of PDR is very efficient since it is an oxygen-independent system.

Generally, wavelengths above 600 nm and below 800 nm are used in PDT (Castano et al., 2004). Wavelengths approaching 700-800 nm will penetrate tissue about 1 cm and wavelength closer to 600 nm will penetrate tissue by 0.5 cm (Plaetzer et al., 2009). Most of the PS concentrates in cell and sub-cellular membranes, and the PDR reactions occur there. A successful PS must have hydrophilic properties to travel through the bloodstream to its target site. As cancer cells express higher receptors for lipophilic compounds, so a PS should also be lipophilic (Henderson and Dougherty,

1992). Photodynamic therapy is known to activate the immune system to promote tumor cell further killing (Castano et al., 2006).

1.7.4 Bone marrow stem-cell transplantation therapy for cancer: Bone marrow stem-cell transplantation is a technical application of immunological principles as therapy for the treatment of certain inherited blood diseases, some diseases of the immune system and most importantly in the treatment of cancer (Corsten and Shah, 2008). High doses of chemotherapy along with radiation therapy are administered to a patient suffering from highly resistant blood-borne cancers such as leukaemia, multiple myelomas. This process also kills the malignant bone marrow stem-cells which are the source of cancers. Stem-cells from a syngeneic (cells from identical twin or triplet) donor or an allogeneic (cells from a related or an unrelated person) donor (Ringden, 2007) are transplanted to the patients. The transplanted cells repopulate the bone marrow and new batch of blood cells are formed in the body. The transplanted stem-cells can make their own immune cells which could kill any new cancer cells in case of a possible relapse (Ringden, 2007).

1.8 Emergence of PKC as a master regulator in carcinogenesis

1.8.1 PKC regulates important signalling pathways crucial for cancer cells: Protein Kinase C (PKC) was first discovered by Nishizuka et. al (Takai et al., 1977) as a proteolytically activated protein kinase. Subsequently, many isoforms of the enzyme were discovered. All the isoforms are serine-threonine kinases. Intracellular calcium and membrane anionic phospholipids (most notably PS and PIP_2), as well as unsaturated diacylglycerols (DAGs), were found to be essential regulators of PKC activity.

Signalling networks play crucial roles in tumor growth and development. Important signal transduction pathways regulating cancer cell proliferation are the MAPK/ERK pathway, the JNK pathway, the NF-κβ pathway, the Wnt signalling pathway, TGF-β pathway, the Hedgehog pathways and the JAK-STAT pathways (Dhillon et al., 2007). The connection of PKC with tumorigenesis came into existence when PKC was recognized as the receptor of the tumor promoting phorbol esters (Castagna et al., 1982). This led to considerable interests to reveal the contribution of PKC in tumorigenesis. Recent studies have recognized Protein Kinase C as a key player regulating the signal transduction pathways as mentioned (Figure 1.12). By regulating these signalling pathways, PKC acts on numerous substrates like transcription factors, enzymes and histone remodelers to effect important cellular functions (Antal and Newton, 2014; Kang, 2014; Tan and Parker, 2003). NFAT are a series of transcription factors which are implicated in many cancers and immune responses. PKC family members have been discovered as key regulators of NFAT activation (Grumont et al., 2004; Pfeifhofer et al., 2003). PKC isozymes are intrinsically involved in the MAPK pathway. Conventional, novel and atypical PKC isozymes are known to phosphorylate and activate MEK-1 (Schönwasser et al., 1998).

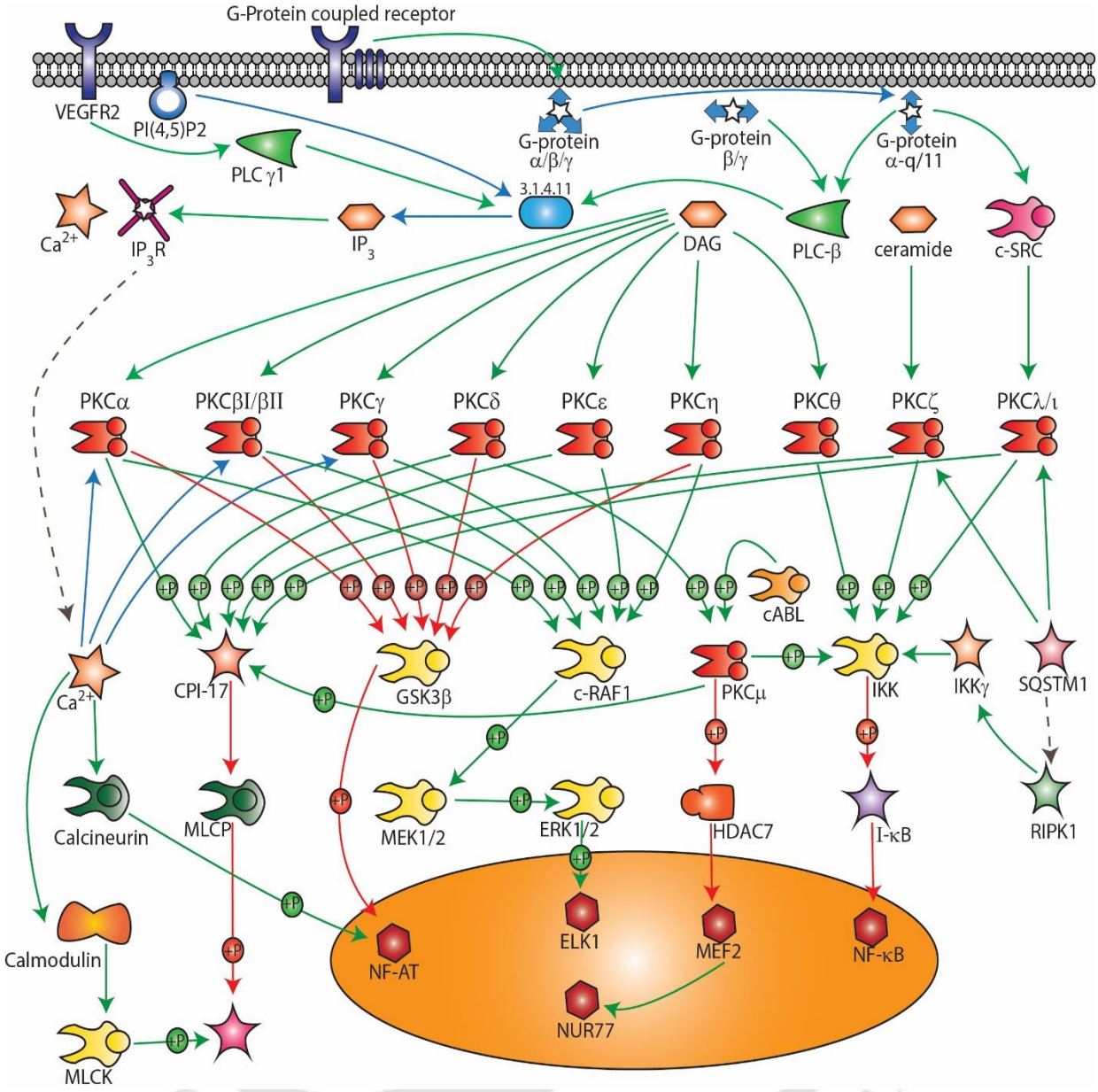

Figure 1.12: PKC isozymes regulating important signalling pathways

However, only conventional and novel PKCs are known to phosphorylate and activate c-Raf-1, the upstream activator of MEK-1 (Schönwasser et al., 1998). Conventional and novel PKC isozymes phosphorylate GSK-3β kinase which is a negative regulator of β-catenin to retard cell proliferation (Goode et al., 1992). NF-κβ is an important transcription factor for proliferating cancer cells. Novel PKC isozyme PKC-θ (Lin et al., 2000) and the atypical PKC isozyme PKC-ι are involved in the activation of NF-κβ by phosphorylation of its activator IKK kinase (Lu et al., 2001). Activation of PKC leads to stimulation of apoptosis in many cancer cells, and as a result, it is much sought for cancer therapy (Santiago-Walker et al., 2005). Also, PKC is known to have pronounced effect in cancer stem cell (CSC) formation and metastasis. However, it is found that PKC isozymes display overlapping, different and opposite biological functions (Mackay and Twelves, 2007b). This is due to the engagement of PKC isozymes with a myriad of regulatory proteins and signalling pathways. It makes

difficult to interpret the function of an individual isoform in context to biological outcomes (Mackay and Twelves, 2007a). PKC-α is credited as an initiator of anti-proliferative signaling in cancer associated with breast (Sun and Rotenberg, 1999), pancreas (Detjen et al., 2000) and the intestine (Frey et al., 2000). However, PKC-α is also involved in the promotion of proliferative signalling in gastric cancer (Jiang et al., 2004) and malignant hepatocellular carcinoma (Wu et al., 2008). Whereas, PKC-δ is more linked to anti-proliferative and pro-apoptotic responses in the majority of cancer types (Nakagawa et al., 2005; Yoshida, 2007). Overall, the expression profile of various PKC isozymes is altered in particular cancer to realize the importance of PKC isozymes in cancer biology (Griner and Kazanietz, 2007). Hence, the pivotal role of PKC isozymes in cancer biology is undisputed.

1.8.2 Potentials of PKC in cancer induction, progression (growth and invasion) and spread (metastasis): Formation of a malignant, invasive tumor is a long process which is often supported by different signalling molecules and their associated pathways. PKC isozymes have been one of the most studied kinases since their discovery. PKC isozymes regulate important genes involved in cellular proliferation that supports initiation of carcinogenesis (Grossoni et al., 2007). Later studies revealed active role of PKC in various stages of progression of cancer (Garg et al., 2014). Extensive efforts to study the role of PKC isozymes in carcinogenesis have identified its critical roles in different sub-stages of cancer progression.

A) PKC in cancer induction: Cancer induction is a complex process. Carcinogenesis is a result of the mutation of genomic DNA and propagation of mutated cells in an uncontrolled manner. (Sarasin, 2003). The mutation may be brought about by three processes: i) Error during DNA replication by DNA polymerases, ii) spontaneous chemical changes (depurination & depyrimidation) of nucleotides present in DNA, and iii) attacks from various endogenous and exogenous mutagenic agents on DNA (Gates, 2009; Liu et al., 2016). The DNA repair machinery is usually successful in repairing various DNA damages but few damages may not get repaired properly and eventually pass on to daughter cells (Gates, 2009). It is believed that the stem-cells underlying every tissue-types are the most affected with such mutations. This is because stem-cells are the only ones accredited with replicative potential rather than terminally differentiated somatic cells. DNA mutations might critically over-activate proto-oncogenes (i.e proto-oncogene mutate to oncogene) such as receptor tyrosine kinases or signalling kinases (Anderson et al., 1992a). Mutations might also inactivate crucial tumor-suppressor genes. This process gives rise to unresponsiveness of cell towards cell-cycle check-points, which is the hallmark of a new-born cancer cell. This summarizes the mechanistic steps involved in cancer induction. Different molecules like PKC isozymes play crucial roles in the induction of carcinogenesis (Garg et al., 2014). PKC may serve as an oncogene as its overexpression might constitutively activate the cell-cycle (Black and Black, 2012). Thus, PKC has been found responsible for neoplastic transformation induced by chemical and UV (Reddig et al., 2000; Wheeler et al., 2004). Cell-cycle promoting cyclins

and cyclin dependent kinases (CDKs) are regulated by PKC mediated signalling pathways. PKC activates PKD kinase which in turn activates Raf/MEK1/ERK1/2 signalling (Hausser et al., 2001) and Akt signalling (Chen et al., 2008). The ERK and the Akt pathways are strong survival and cell-proliferating signals to a healthy cell. In addition to that, PKC activation suppresses apoptotic signalling. JNK kinase, an important enzyme that activates apoptotic signalling is actively inhibited by PKD kinase. The PKD kinase, in turn, is activated by PKC, creating a platform for induction of carcinogenesis (Hurd and Rozengurt, 2001; Waldron et al., 2007). Apart from regulating cyclin and CDK expression, PKC-mediated signalling also regulates key-transcription factors involved in cell-cycle proliferation. During UV induced carcinogenesis, PKC phosphorylate the transcription factor STAT3 for EGFR signalling (Aziz et al., 2007). Similarly, elevated levels of transcription factor phospho c-jun & cyclin D1 levels is accomplished by coordination between the isozyme PKC-α and & RACK1 scaffold protein, which results in melanoma induction.(Lopez-Bergami et al., 2005; Lopez-Bergami et al., 2007). Likewise, elevated ERK signalling mediated by another isozyme PKC-β has been discovered to be a potent inducer of both triple negative and positive breast cancer (Cruz-Correa et al., 2006).

B) PKC in cancer progression (growth, invasion and metastasis): In the early phase of tumor progression, the induced cancer cells slowly begin to proliferate and form a primary tumor mass. The tumor increases to a considerable size of 100 billion to 1 trillion cells before it starts facing oxygen crisis for further proliferation. Since vasculature is only present around the tumor, the diffusion of oxygen is insufficient to meet the growing oxygen demands of all tumor cells, especially cells at the center of the tumor mass. Thus, tumor cells seek to obtain new vasculature within the tumor. These cells condition the stromal cells around them by secretion of PDGF and recruit cancer associated fibroblasts (CAFs). These two cells, in turn, help to recruit endothelial cell precursors to the tumor site and start the building of neo-vasculature around and within the tumor. Under stress (low oxygen conditions), PKC is activated in CAFs which upregulates hypoxia-inducible factor-1 (HIF-1) (Lee et al., 2007). HIF-1 is a transcription factor which upregulates production of vascular endothelial growth factor (VEGF) by CAFs. The CAFs secreted VEGF induce activation of PKCs in endothelial cell precursors. PKC activation leads to Akt-mediated signalling that promotes angiogenesis (Gliki et al., 2002). Other studies have implicated specifically the active role played by PKC-β in angiogenesis (Yoshiji et al., 1999).

After the tumor has sufficiently grown in size, some of the cancer cells begins to undergo an epithelial to mesenchymal transition (EMT). This complex molecular process produces some very aggressive cancer cells within the tumor that prepare themselves to leave the parent tumor site. PKC play a crucial role in EMT by stabilizing the important transcription factor snail (Liu et al., 2014). PKC also translocate to the nucleus to activate genes involved in EMT (Zafar et al., 2015).But the

extracellular matrix with its numerous components pose a big hurdle for cancer cell movement. Degradation of the basement membrane is necessary for primary tumors to invade and gain access to the circulatory system. Invading cancer cells accomplish this by the secretion of metallo-protease enzymes (MMPs) which serve to degrade the basement membrane (BM) and extracellular matrix (ECM) proteins. These cleavage process serve to liberate and mobilize various growth factors that remain tethered in inactive form in the ECM. Invasive carcinomas recruit a variety of stromal cells that also secrete different MMPs (Vong and Kalluri, 2011). The recruited stromal cells consists of macrophages, fibroblasts and mast cells. An important metallo-protease, MTI-MMP is directly tethered to the plasma membrane of cancer cells (Yao et al., 2006). MTI-MMP is extensively used by invading cancer cells like a scissor to cleave critical ECM components as they slowly move through the ECM. Again, PKC has been found to stimulate MMPs through EGFR signalling in breast cancer cells (Lin et al., 2008; Soto-Guzman et al., 2010). After, gaining access to the lumen of blood vessels, invading cancer cells migrate for newer locations to establish colonies in a chemotaxis driven process. During metastasis, stimuli such as growth factors, cytokines, etc. play a vital role in the induction of chemotaxis of malignant tumor cells. Activation of PKC has been found to activate components of the chemotactic pathways in MDAMB-231, T47-D, and MCF-7 breast cancer cells. (Sun et al., 2005; Wang et al., 2008). Thus, PKC plays important roles in the invasion and metastasis of cancer cells. Carcinogens catechol and hydroquinone promotes tumor metastasis via activation of PKC in lung carcinoma cells (Gopalakrishna et al., 1994). PKC is found to affect at the level of chromatin modulation to activate metastasis in cancer cells (Lin et al., 2012). PKC can also serve as a therapeutic target to halt metastasis as suppression of PKC-α halts metastasis in ovarian cancer cells (Jiang et al., 2005). Hence, understanding the crucial role of PKC in cancer induction and metastasis opens up avenues for drug development.

1.9 Structural and Biochemical Details of PKC

1.9.1 Structure of Protein kinase C: The PKC family consists of several isozymes which share a common 3-Dimensional fold: a kinase domain present on the C-terminal and a flexible hinge segment links it to the regulatory domains present in the N-terminal region (Figure 1.13). The regulatory domains are further divided into the C1 domain (Figure 1.14-B) and the C2 domain (Figure 1.14-C). The C1 domain binds to the natural ligand diacylglycerols while the C2 domain binds to anionic lipids on the plasma membrane in the presence of Ca^{2+}. PKC isozymes also have a pseudo-substrate region attached in tandem to the C1 domain which occupies the substrate binding site of the kinase domain in the absence of agonist (Figure 1.15). The Kinase domain (Figure 1.13 and 1.14-D) has bilobed structure and has the substrate and ATP binding sites. It also has important motifs, like the PxxP clamp where chaperone HSP90 and the co-chaperone Cdc37 binds. These two chaperones aid in the

phosphorylation of another motif in the kinase domain, the activation loop (shown in purple in Figure 1.14-D) by the PDK-1 kinase. The V5 region present at the carboxy-terminal region is the site for important phosphorylations by the mTORC2 complex. These phosphorylation events are crucial for the development of the final mature & functionally active form of the PKC.

The pseudo-substrate region forms the extreme end of the N-terminal region. It occupies the substrate binding site of the Kinase domain in the absence of any agonist/ligand of the C1 domains. Presence of agonists of the C1 domains direct the C1 regions away from the kinase domain towards the cellular membranes. As a result, the substrate binding site of the kinase domain is relieved of the pseudo-substrate region. Perhaps, the early region (residues 619-633 in PKC-βII) of carboxy tail known as the NFD-helix region (shown in red in Figure 1.13) is a very interesting regulatory element of PKC activation. The NFD-helix has an important amino acid residue, Phe 629 (in PKC-βII) that is important to provide stability to ATP at the ATP binding site. In the absence of any agonist, the NFD-helix remains bound to the C1 domain in the agonist binding site, and the Phe 629 is prevented from contacting the ATP binding site. However, agonist binding to C1 domain releases the NFD-helix which is now in an elongated state. In this state, the Phe 629 residue is able to contact the ATP binding

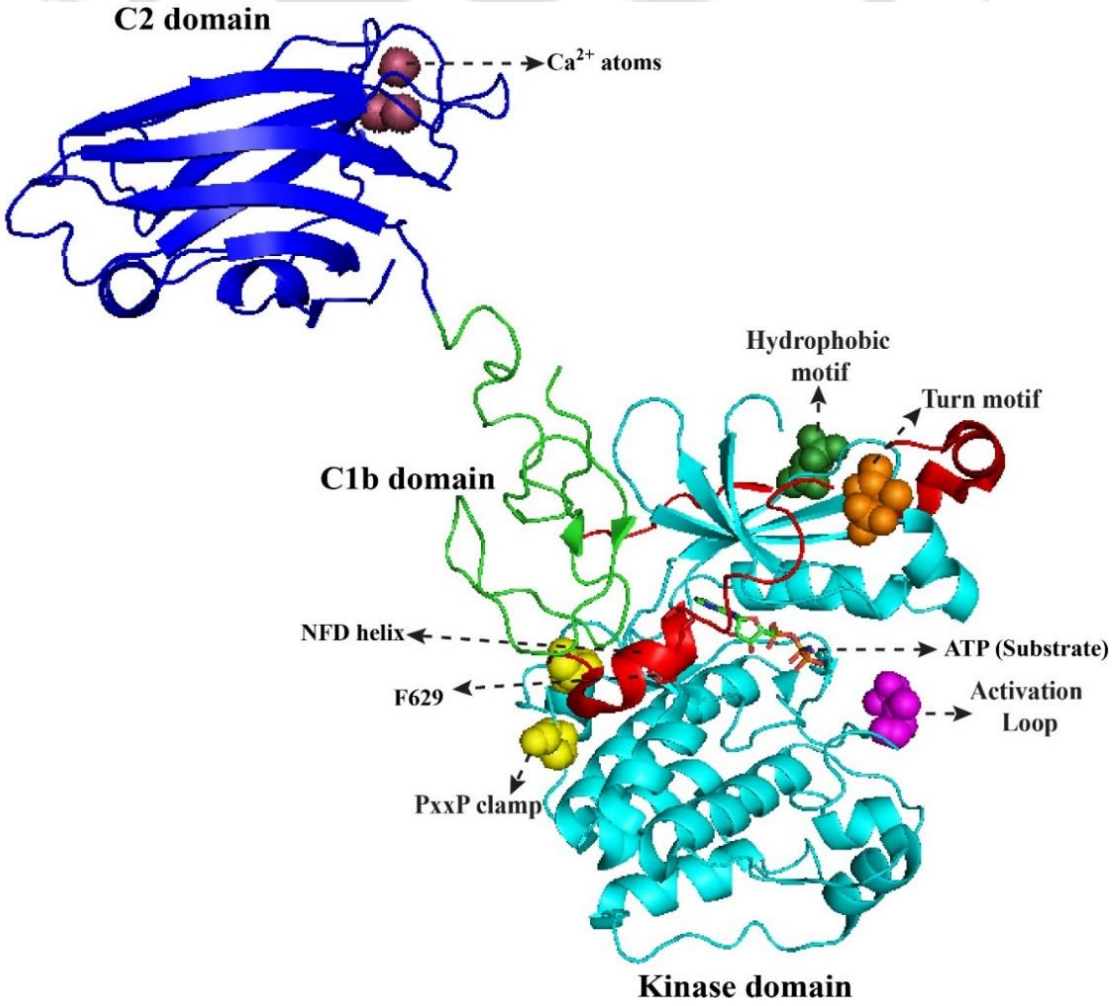

Figure 1.13: Structure of PKC-βII (PDB ID: 3PFQ). Kinase domain is shown in cyan along with C1b domain (green) and C2 domain (blue).

site and promote ATP binding. Although, this model is described for PKC-βII, this is similar for other PKC isozymes as well.

1.9.2 Protein Kinase C and its different isoforms: Protein Kinase C (PKC) are serine-threonine kinases that exists as a family of isozymes consisting of 10 members discovered till date in mammalian cells and belong to the family of AGC kinases (Pearce et al., 2010). The 10 members are grouped into 3 classes based on their domain composition and order of individual domains (Figure 1.15). The first class are the conventional PKCs (cPKCs) comprising of PKC-α, PKC-βI, PKC-βII and PKC-γ.(Nishizuka, 1995). Amongst the cPKCs, PKC-βI and PKC-βII are the alternatively spliced versions of the same gene. The second class are the novel PKCs (nPKCs) which comprise of PKC-δ, PKC-ε, PKC-η and PKC-θ. The final classes are called as atypical PKCs (aPKCs) and they have two family members PKC-ζ and PKC-ι/λ. The C1 domain is an important constituent of protein structure for both cPKCs and nPKCs as it is an important regulatory domain. Likewise, the C2 domain is also a regulatory domain but is functionally active only for cPKCs. A functionally redundant form of C2 domain is present in nPKCs which is altogether absent in the atypical isozymes. Instead, aPKCs

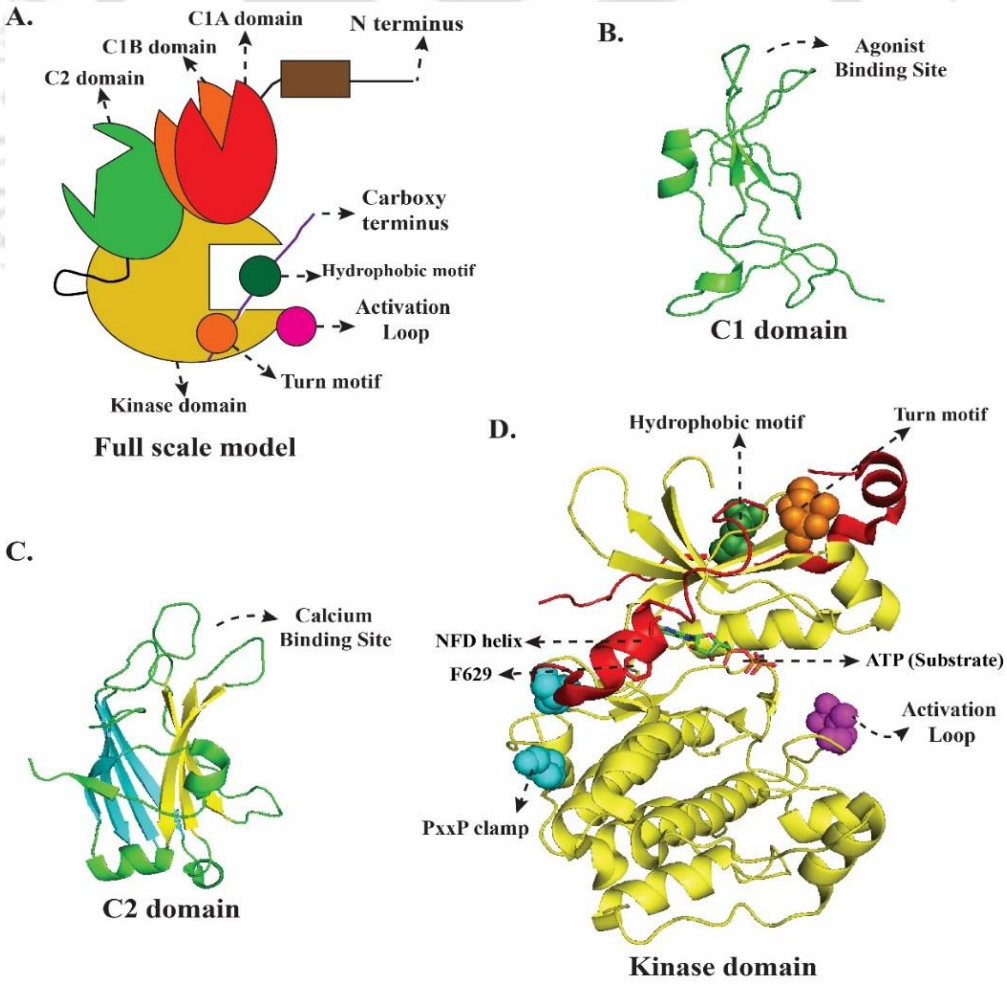

Figure 1.14: General Structure of PKC (A) Illustration of full structure of **PKCα (B)** C1 domain of **PKC-α (C)** C2 domain of **PKC-α (D)** Kinase domain of **PKC-βII (PDB ID: 3PFQ).**

contain a unique domain, the PB1 domain which serves to provide regulatory function. All PKC isozymes have a central hinge region (Figure 1.15) which works as a connector to the regulatory subunits towards the N- terminal side and the kinase subunit towards the C-terminal side.

PKC isozymes activation is regulated by various ligand-protein and protein-protein interactions. Early studies indicated that after activation, much of the active enzyme was present in the particulate fraction rather than the cell soluble fraction (Takai et al., 1979). The C1 domain of cPKCs and nPKCs were later found to bind to lipid messengers which speculated their translocation primarily to plasma membranes. Later, it was revealed that many of these isozymes translocate to many different sub-cellular organelle membranes such as the mitochondrial membrane (Churchill et al., 2005), the Golgi apparatus (Lehel et al., 1995), the endoplasmic reticulum (Qi and Mochly-Rosen, 2008), on cell-cell contacts (Vallentin et al., 2001), contractile elements and even inside the nucleus (Disatnik et al., 1994). Receptor for active C Kinases (RACKs) are a class of scaffold proteins that are known to interact actively to different PKC isozymes (Mochly-Rosen et al., 1991).

Thus, different PKC isozymes are localized to a subset of substrates in different cell-types and under different physiological conditions which results in differential isozyme-selective functions. A detailed review of the individual domains will further clarify the functional attributes of each class of PKC isozymes in the cellular microenvironment.

1.9.3 C1 domain: The C1 domain is the principal regulatory domain of cPKCs and nPKCs as it binds efficiently secondary messenger diacylglycerol (DAG). It is comprised of a tandem repeat of two cysteine rich motifs. The C1 domain was discovered to be the binding site for potent tumor promoting phorbol esters (Zhang et al., 1995). There are two C1 domains in a PKC molecule, C1a and C1b of which the C1b domain binds to agonists with relatively higher efficiency. Besides, the C1b domain of nPKCs has a substitution of tryptophan for tryosine which increase their affinity for agonists many folds than the C1b domains of cPKCs. The C1b domain also binds anionic phospholipids at the cellular membranes, most notably phosphatidylserine (PS) in a stereospecific manner (Johnson et al., 2000). DAGs generated during signal transduction pathways in cells bind to the C1 domains and translocate PKCs to various cellular membranes for the participation of active signalling. Although the primary role of the C1 domain is to interact with agonist molecules, this domain also has sequences that participate in protein-protein interactions. Recent studies have discovered that the C1 domain aids in localization to the Golgi apparatus (Schultz et al., 2003). The C1 domain also interacts with actin (Prekeris et al., 1996) and G proteins (Ghosh et al., 1994). The C1 domain of aPKCs doesn't bind to any agonist or phospholipid and is thought to be non-functional.

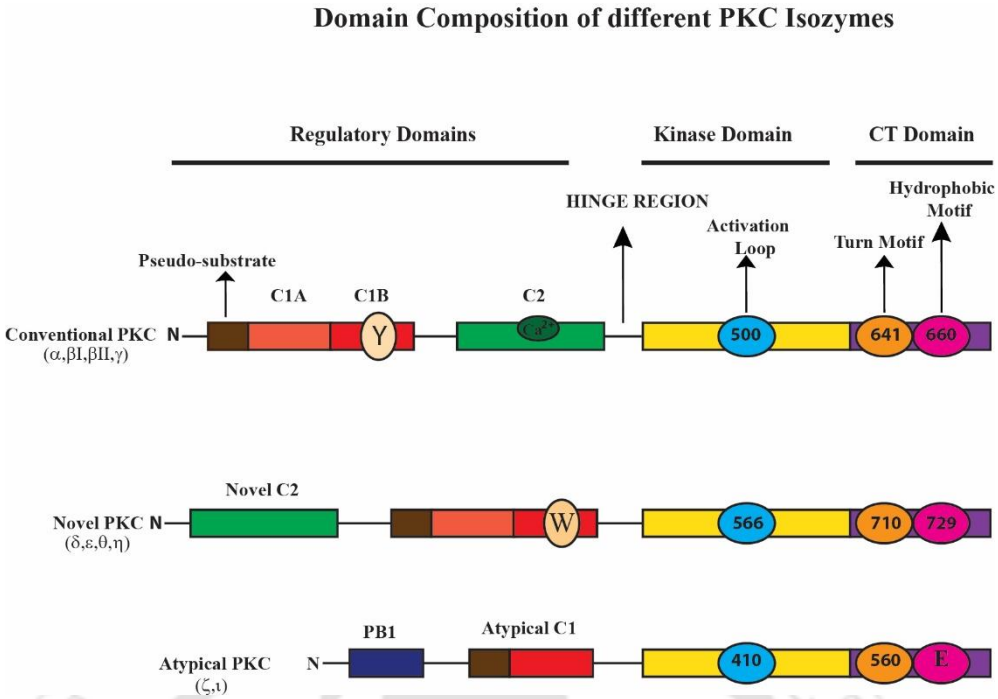

Figure 1.15: Different PKC isozymes with diverse building blocks.

1.9.4 C2 domain: The C2 domain is a very important regulatory subunit as this domain binds mainly to anionic phospholipids at various organelle membranes and the plasma membrane (Figure 1.14-C). This domain has a strong affinity for the phospholipid phosphatidylinositol (PIP_2) and also binds to intracellular Ca^{2+} released from internal stores. Thus, the C2 domain of cPKCs serves as a sensor of increased Ca^{2+} levels in the cytosol generated as a result of important signal transduction pathways. On agonist presence, the C1 and C2 domains together help to anchor the PKCs to various cellular membranes and bring out the functionally active form of the enzyme. Novel PKCs contain a variant of the C2 domain that is mutated at key amino acid residues which render it incapable of binding to Ca^{2+} binding or any anionic phospholipid. Thus, nPKCs have a functionally redundant C2 domain (Figure 1.15). To compensate for that, nPKCs' C1b domain binds to agonist with many fold higher affinity than cPKCs. The atypical PKCs (aPKCs) lack a C2 domain altogether. The C2 domain of aPKCs is also actively involved in protein-protein interactions, most notably with many members of the RACK family (Mochly-Rosen et al., 1992).

1.9.5 Catalytic/Kinase domain: The kinase/catalytic domain of PKC is folded into the classical bilobal fold (Grodsky et al., 2006) as seen with other kinases (Figure 1.14-D). In PKC-βII, the kinase domain comprises of residues 321-673 and is roughly of 40.7 kDa. The positions of the phosphorylation sites are: Thr-500 (activation loop), Thr-641 (turn motif) and Ser-660 (hydrophobic motif). The turn and hydrophobic motifs are present in the V5 domain of carboxy terminal region. Residues 339-421 comprises the N-terminal lobe of the PKC-βII kinase domain. It contains five β sheets (β1-β5) and two α helices (αB & αC), (Grodsky et al., 2006). The N-terminal lobe is connected

to the C-terminal lobe via residues 422-425. The C-terminal lobe consists of residues 426-620. It contains eight α helices. Residues Lys-371, Asp-466, Asp-484 and Asn-471 are the key catalytic residues. Asp-466 is a conserved residue amongst all PKC isozymes and forms the active part of the catalytic loop emanating from the base of the catalytic site. Asp-466 interacts with the hydroxyl site of the substrate and the other catalytic residue Asn-471 (Grodsky et al., 2006). The substrate binding sub-domain of PKC is also termed as C4 domain and the ATP binding sub-domain is termed as C3 domain (House and Kemp, 1987). Further, a special class of substrate proteins collectively termed STICKs (substrates that interact with C-kinases) interact with PKC via binding to special sequences in the kinase domain (Jaken and Parker, 2000). A variety of inhibitors have been designed as potential drugs that target the kinase domain of PKC. Bisindolylmaleimides (Goekjian and Jirousek, 1999) are such a class of inhibitors that competitively inhibit binding of ATP at the ATP binding site.

1.9.6 Maturation of protein kinase C: Newly synthesized (naïve) Protein Kinase C undergoes a series of ordered phosphorylation events before it is competent enough to respond to agonists or lipophilic secondary messengers. These phosphorylation events are crucial to convert the naïve enzyme into a catalytically competent form and also to prevent the naïve enzyme from degradation (Newton, 2003). That is why these events are known as the priming phosphorylations reactions. It is noteworthy that PKC also undergoes phosphorylations at other serine, threonine and tyrosine residues. These phosphorylations refine the functioning of specific isozymes, but these are not necessary for maturity of the enzyme or preventing it from degradation (Gould and Newton, 2008).

The activation loop is a sub-domain in the substrate binding domain of PKCs. It contains a conserved threonine residue (Thr 500 for cPKCs, Thr 566 for nPKCs and Thr 410 for aPKCs). This threonine is the first of the ordered priming phosphorylation series. This threonine residue is subjected to phosphorylation by a coordinated effort between the chaperone HSP90 and the kinase PDK-1. During the first step, newly synthesized PKC attaches to the membrane fraction (Figure 1.16). It allows the auto-inhibitory pseudo-substrate region to be removed from the substrate binding cavity which exposes the activation loop for phosphorylation. Then, HSP90 binds to a conserved sequence known as the PXXP clamp/motif where P is proline and X stands for any amino acid residue. The integrity of this motif is very essential for HSP90 binding. The binding of HSP90 to a newly synthesized PKC allows the PDK-1 kinase to dock to the carboxyl-terminal tail of PKC and phosphorylate the Thr residue in the activation loop. Any naïve PKC which is unphosphorylated at the activation loop is unstable and subsequently degraded (Balendran et al., 2000). The immediate consequence of the phosphorylation of the activation loop is the tightly coupled phosphorylation of the turn motif which is carried out by the mTORC2 complex (Facchinetti et al., 2008). This is followed by the subsequent auto-phosphorylation of the hydrophobic motif.

These priming phosphorylation reactions are carried out in a constitutive manner for cPKCs. But in case of nPKCs, the priming phosphorylations seem basal but are directly proportional at higher agonist concentrations. Atypical PKCs seem to display a proportional increase in phosphorylation at the activation loop with agonist concentrations. Recent studies indicate that after phosphorylation at the turn motif and the hydrophobic motif, the phosphorylation at the activation loop becomes dispensable (Keranen et al., 1995).

1.9.7 Signalling of conventional PKCs: After maturation of PKCs at the membrane, the matured PKC is released into the cytosol where it awaits for secondary messengers and remains bound to scaffold proteins (most notably RACKs). In this conformation, the auto-inhibitory pseudo-substrate region reoccupies the catalytic substrate-binding cleft. Few reports suggest that sometime in the absence of secondary messengers, the PKCs bounces on and off the membrane by diffusion-controlled mechanism due to their lower affinity with the membrane. Signalling pathways activating phospholipase C enzymes generate DAGs and IP_3 from the cleavage of PIP_2 at the plasma membranes. IP_3 generation leads to the release of Ca^{2+} from the endoplasmic reticulum which leads to elevated levels of Ca^{2+} at the membranes. The C2 domain binds to Ca^{2+} and is recruited to the plasma membranes. There it binds to PIP_2 and the interaction between PKC and membrane is slightly strengthened (Oancea and Meyer, 1998). This allows the PKC to search for its ligand DAGs which are embedded in the plasma membrane. The C1 domain subsequently binds to DAGs and subsequently also to PS which completes the anchorage of the enzyme at the plasma membrane (Johnson et al., 2000). Thus, membrane lipids PS and PIP_2 plays a vital role in the translocation of cPKCs to the plasma membrane. Firm anchorage of the C1 domain to the plasma membrane results in the release of the pseudo-substrate region from the substrate binding pocket, allowing the complete catalytic activity of cPKCs.

Although the individual binding activity of the C1 or the C2 domains to the membrane ligands is not sufficient enough to release the pseudo-substrate region from the catalytic pocket, combined engagement of both the C1 and C2 domains is sufficient to do so. But the binding affinity of some foreign agonists such as phorbol esters to the C1 domain is much higher than that of DAGs. In such scenario, alone phorbol ester binding to the C1 domain is sufficient enough to release the pseudo-substrate region (Mosior and Newton, 1996). The cPKCs are translocated primarily to the plasma membrane because the two lipids PIP_2 and PS are found primarily on the plasma membrane.

1.9.8 Signalling in novel PKCs: As the C2 domain of nPKCs is not capable of binding to Ca^{2+} or any membrane phospholipid, the translocation of nPKCs to any membrane is directed by the C1 domain. The C1b domain of nPKCs have a tryptophan residue at position 22 instead of a tyrosine residue in conventional isozymes. The result of this mutation is that the C1b domain of nPKCs have a two order

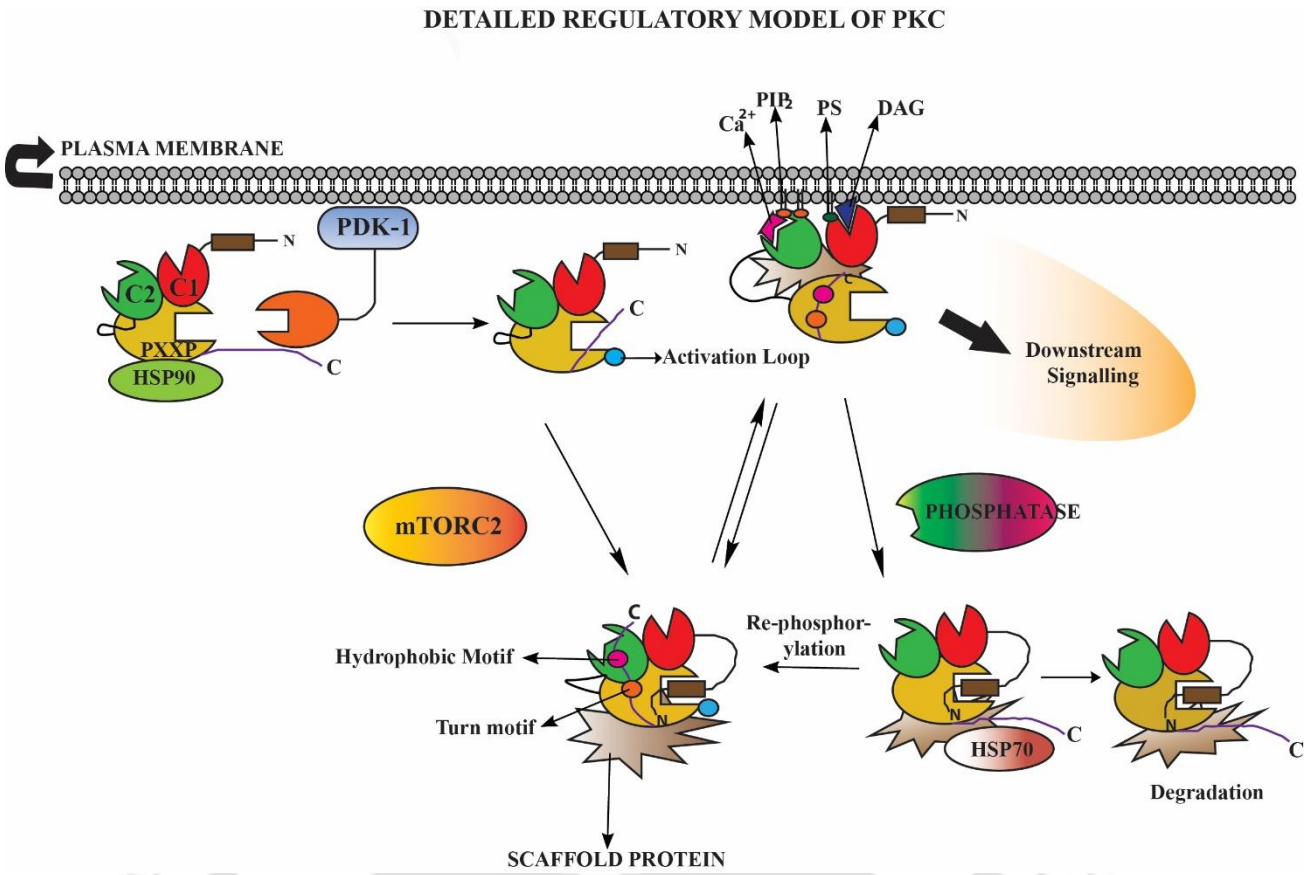

Figure 1.16: A schematic model to depict PKC maturation, signalling and degradation.

of higher affinity for DAGs than the C1b domain of cPKCs (Dries et al., 2007). Thus, the nPKCs are mainly recruited to membranes where there is an increase in the levels of DAGs only which is dictated by the C1b domain. The novel isozymes are also highly sensitive to slight increment in DAG levels in any membranes within the cell. The basal levels of DAGs are relatively quite high in the Golgi than in the plasma membrane. Hence, the novel isozymes are generally actively translocated to the Golgi apparatus than the plasma membrane (Gallegos et al., 2006).

1.9.9 Interaction of PKC with scaffold proteins: Recently, scaffold proteins have been recognized as important regulators of PKC signalling (Mochly-Rosen and Gordon, 1998). The most prominent amongst them are RACK proteins (Mochly-Rosen et al., 1991). PKC isozymes have many sites within their domain structure that bind to specific scaffold proteins when they (PKC) are in active phosphorylated form. The C2 domain has been recognized to contain regions that bind to RACK proteins (Chen et al., 2001). Inactive PKCs (unphosphorylated) don't interact with the RACKs or any scaffold proteins. So, the RACK binding region in the C2 domain of inactive PKC bind to an intra-molecular sequence (pseudo-RACK sequence) of a different domain within that PKC that mimics the PKC binding site/motif in the corresponding RACK protein. Different isozymes have different specificities for a subset of scaffold proteins which impart isozyme specific function to individual PKC isoforms. In the absence of lipid secondary messengers or other agonists, PKC isozymes maintain internal basal level of signalling via interaction with specific scaffold proteins depending on the

availability of these scaffold proteins. Most of the signalling via scaffold proteins may be involved in housekeeping functions which depict the crucial role played by PKC isozymes. The binding of PKC to scaffold proteins have the potential to maintain sustained PKC signalling in the absence of secondary messenger.

1.9.10 Termination of PKC signalling: Any signalling pathway cannot be carried out for sustained periods of time in a cellular system. Likewise, PKC signalling is also kept in check by cellular systems. Membrane bound active PKC adopts a conformation which exposes the already phosphorylated sites to cellular phosphatases. The phosphatase 'PH domain Leucine-rich repeat Protein Phosphatase (PHLPP)' has been identified as the first one to cleave the phosphate group (Figure 1.16) from the hydrophobic motif (Gao et al., 2005). This event detaches PKC from the membrane, subsequently it is further de-phosphorylated at the activation loop and at the turn motif by other phosphatases. The phosphatases of the PP2A-type have been recognized to be involved in these downstream events (Hansra et al., 1996). At this stage, the de-phosphorylated PKC is generally channelled away for degradation by ubiquitinylation. However, in certain scenarios, the de-phosphorylated PKC is rescued from degradation by the chaperone HSP70 which binds to the de-phosphorylated turn motif of PKC. This event stabilizes PKC and allows the phosphorylations to take place again at the priming phosphorylation sites (Gao and Newton, 2006).

1.10 Targeting of PKC for anti-cancer drug development

Having recognized that PKC isozymes play a vital role in cancer biology, researchers have identified and designed many molecules that can modulate specific PKC isoform activity in a hope to control and eradicate cancer.

1.10.1 PKC-directed agonist molecules: PKC agonists are those molecules that bind to the C1b domain and induce translocation of PKCs from the cytosol to the different cellular membranes. This event results in firm anchorage of PKC to the inner leaflet of the plasma membrane or other membranes which reveals the functionally active conformation of the kinase domain. Functionally active PKC starts phosphorylating substrates according to the nature of specific substrates present in the micro-environment, giving rise to signal transduction pathways (Caponigro et al., 1997). The initiated signalling pathways can either be apoptotic or cell-proliferative according to the nature of ligands. Natural ligands such as DAGs provide sufficient controlled activation (for a shorter duration) of PKC as a cell proliferation signal. Plant derived phorbol esters such as PMA provide extensive (much longer duration) activation of PKC leading to unregulated cell division. However, sometimes phorbol esters or other agonists cause extensive sustained over-activation of PKC which is thought to generate cellular stress, cell-cycle arrest (Yoshida et al., 1998) and ultimately induce apoptosis. Below is a list of specific PKC agonists.

(A) Bryostatins (agonist of cPKCs and nPKCs): The structure of bryostatins is given in Figure 1.17-A. Bryostatins constitute a family of 20 macrocyclic lactones that are derived from the marine bryozoan *Bulgula neritina* (Schaufelberger et al., 1991). Bryostatins mimic the binding of DAG to the C1 domain of PKC isoforms and act as regulators of conventional and novel PKCs. They are also known for suppression or activation of PKC isoform responses. Bryostatin I is one of the most studied bryostatin molecules. Short term exposure of bryostatin I results in activation and nuclear translocation of cPKCs and nPKCs. However, long term exposure of bryostatin I results in decreased PKC activity due to depletion of PKC levels in the membrane (Hennings et al., 1987). Bryostatin showed promising anti-cancer activity in phase I clinical trials but showed low anti-cancer activity against melanoma, colorectal and gastric cancer in phase II clinical trials. However, in phase II clinical trials, bryostatin showed good anti-cancer activity when used in conjunction with standard anticancer drugs such as paclitaxel, cisplatin and vincristine (Ajani et al., 2006; Barr et al., 2009).

(B) Ingenol-3-angelate (PEP005) : Ingenol-3-angelate also known as ingenol mebutate (Figure 1.17-B) is a novel compound extracted from the plant *Euphorbia peplus*. The structure of Ingenol-3-angelate is similar to phorbol esters and it mimics the binding of phorbol esters to the C1 domain of PKC isozymes. Ingenol-3-angelate is a potent modulator of PKC isozymes (Kedei et al., 2004). It is known to induce apoptosis in myeloid leukaemia and colon cancer cell lines by the activation of PKC-δ (Hampson et al., 2005). It is also known to inhibit the Akt signalling pathway and induce apoptosis in other cancer models. The activation of PKC-δ in cancer cell lines by PEP005 is due to the halting of cells at the G1 phase of cell-cycle. Ingenol-3-angelate when used in conjunction with other chemotherapeutic agents in appropriate concentrations can be a potent apoptosis inducer in many cancer types such as highly malignant skin cancer (Ogbourne et al., 2004). It is worth mentioning that ingenol-3-angelate has a novel immunostimulatory effect. Thus, it is a novel immunostimulatory chemotherapeutic phytochemical that has been demonstrated to generate anti-cancer CD8 T-cells. These CD8 T-cells can synergize with anti-carcinogenic activity of PEP005 or other chemotherapeutic drugs to regress distant secondary tumors (Le et al., 2009).

(C) Phorbol Esters: Phorbol 12-myristate 13-acetate (PMA) is an extensively used phorbol ester activator of protein kinase C (Figure 1.17-C). It is a tumor promoter and was first isolated from the oil of the seeds of *Croton tiglium L*. PMA binds to PKC with a K_D value of 2.6 nM as measured by displacement of [^{3}H] phorbol 12,13-dibutyrate binding in rat cortex synaptosomal membranes. Like all phorbol esters, PMA binds to the C1b domain of PKCs and induce translocation to the plasma membrane. It is primarily implicated in the activation of cPKCs. Although labelled as a potent tumor promoter, PMA has also been recognized as inducer of apoptosis in several cell lines including gastric (Park et al., 2001) and prostate cancer cell lines (Itsumi et al., 2014).

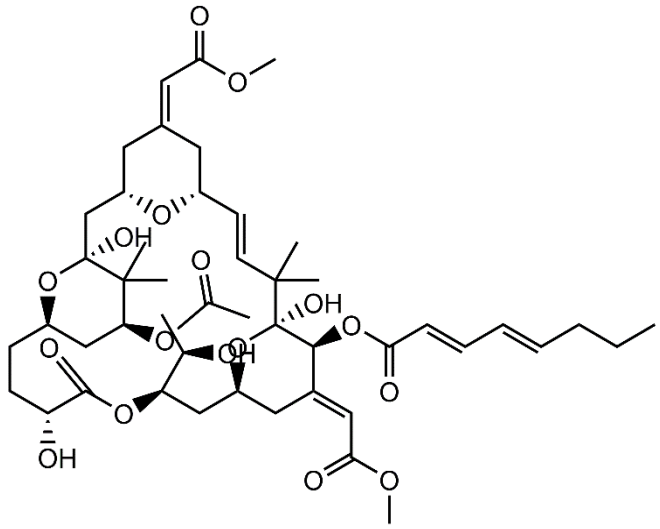

(A) Bryostatin 1

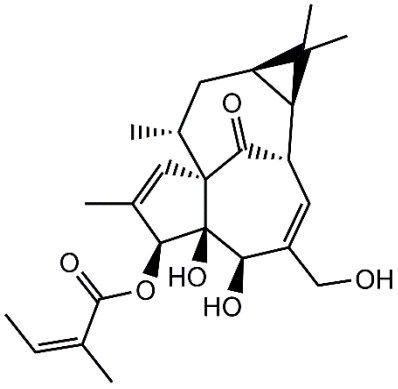

(B) Ingenol-3-angelate

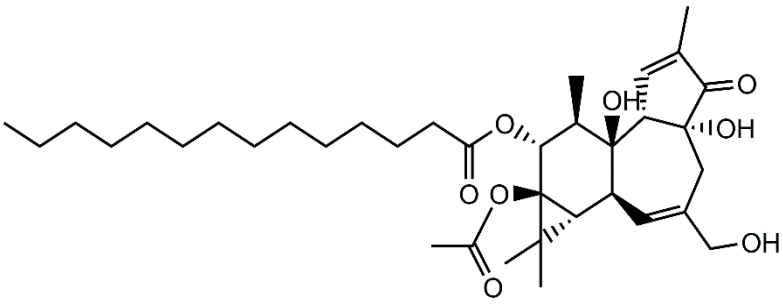

(C) Phorbol 12-myristate 13-acetate (PMA)

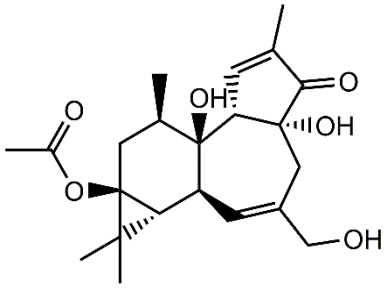

(D) Prostratin

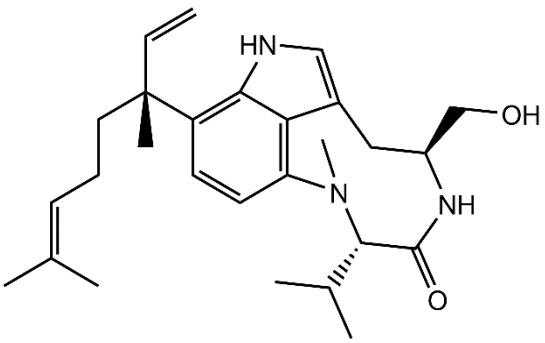

(E) Teleocidin

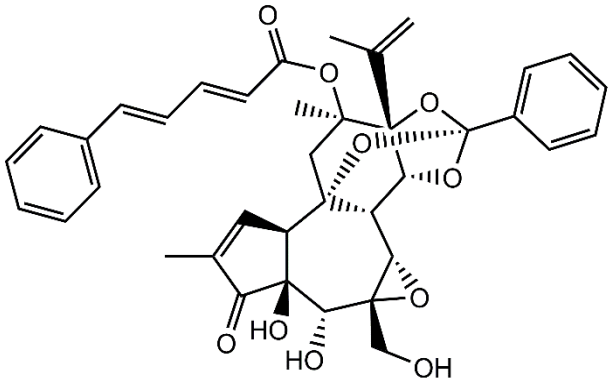

(F) Mezerein

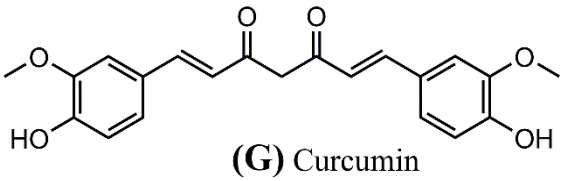

(G) Curcumin

Figure 1.17: Chemical Structures of few selected PKC agonists.

(D) Prostratin: The structure of prostratin is given in Figure 1.17-D. Prostratin is an unusual phorbol ester which doesn't induce tumor formation. It is a non-tumorogenic phorbol ester. It is a potent activator of PKC. It is obtained from the bark of the mamala tree of Samoa, *Homalanthus nutans*. Prostratin inhibits growth and induces differentiation of AML cell lines (Shen et al., 2015). It also inhibits tumorigenesis in *KRAS* mutant pancreatic cancer cells and reduces tumor growth in mouse pancreatic tumor models (Wang et al., 2015). Prostratin inhibits induction of edema and hyperplasia by PMA in mouse skin (Szallasi and Blumberg, 1991).With this view, many prostratin analogues have been synthesized that are up to 100-fold more potent than the preclinical lead (prostratin) in binding to cell-free PKC.

(E) Teleocidin: Teleocidin is an indole alkaloid which is obtained from the bacteria Streptomyces spp (Figure 1.17-E). It was discovered as a PKC agonist and tried for possible anti-cancer activity by researchers. However, it was discovered to be a potent tumor promoter that binds to the C1b domain. It has two other indole alkaloid relatives, lyngbyatoxin A and debromoaplysiatoxin which are obtained from the marine blue-green alga *Lyngbya majuscule.* Dihydroteleocidin B is a hydrogenated derivative of teleocidin and is the most potent tumor promoter amongst the teleocidins, having a tumor promoting ability as close as PMA (Fujiki et al., 1981). Further studies showed that teleocidins activate PKC by binding to the C1b domain and inducing membrane translocation of PKCs (Arcoleo and Weinstein, 1985; Gaveriaux et al., 1988). So far, no therapeutic potential of teleocidin has been reported.

(F) Mezerein: Mezerein is a non-phorbol ester diterpene (Figure 1.17-F). Earlier studies discovered mezerien to be a weak promoter of Stage 1 tumorogenesis. However, it is as potent as phorbol esters in stage 2 tumorogenesis (Jaken et al., 1983).Thus, it is considered as a moderate activator of PKC. Later, mezerein was recognized as an activator of PKC and that it bound to the C1b domain as that of phorbol esters (Nishio et al., 1994). Although tried as a possible anti-cancer compound, no anti-cancer activity of mezerein has been reported yet.

(G) Curcumin: Curcumin is a natural polyphenol which is obtained from the plant *Curcuma longa* (Figure 1.17-G). Curcumin binds to the C1b domain of PKC (Majhi et al., 2010), can effect translocation of PKCs and serves as an activator of PKC in cells (Mahmmoud, 2007). However, it does so only at moderate or higher concentrations of Ca^{2+} and in the presence of cellular membranes as in biological systems (Mahmmoud, 2007). Studies have revealed that curcumin also has a low affinity for the Ca^{2+} binding site of the C2 domain. In the absence of cellular membranes, curcumin can bind to the C2 domain by competing with Ca^{2+} ions, but the concentration of Ca^{2+} should be low (Mahmmoud, 2007). Still, curcumin can't bind to the C2 domain in the presence of cellular membranes. This inhibition of PKC by curcumin binding to C2 domain is readily lost once the

concentration of Ca^{2+} increases or in the presence of membranes. Thus, in biological systems, at cellular Ca^{2+} concentrations, curcumin generally serves as an activator of PKC. Regardless of serving as an activator or a mild inhibitor, curcumin mediated signalling is always pro-apoptotic in cancer cells. Curcumin is a very safe and found effective in inducing apoptosis in several cancer types (Aoki et al., 2007; Bachmeier et al., 2007; Li et al., 2007). However, it is also very effective in patients with familial adenomatous polyposis (Cruz-Correa et al., 2006). By acting upon PKC as well as other kinases, curcumin exerts its regulatory effect on various signalling networks at multiple levels. This regulatory power enables curcumin to induce apoptosis in cancer cells. It can mediate cell-cycle arrest in actively proliferating cancer cells (Choudhuri et al., 2005). It promotes caspase-3 mediated cleavage of the transcription factor β-catenin to reduce cyclin D1 levels (Jaiswal et al., 2002). It can downregulate the pro-proliferative transcription factor NF-κβ (Bharti et al., 2003). Curcumin is also reported to active the JNK dependent pathways of apoptosis in cancer cells (Collett and Campbell, 2004). Thus, the therapeutic potential of curcumin is mainly mediated through PKC.

1.10.2 PKC directed antagonist molecules: PKC antagonists are classified as molecules that bind to the C1b domain irreversibly to render PKC inactive to stimulate apoptotic signal (Gray et al., 1997). However, other molecules that bind to ATP binding site or substrate binding site to impair its kinase activity are also known as PKC antagonists. Some of the PKC antagonist are being actively pursued by researchers worldwide for the development of anti-cancer drugs.

(A) Balanol: Balanol is a fungal metabolite (Figure 1.18-A) which was isolated in 1993 from the fungus *Verticillium balanoides* (Hu et al., 1997). This compound is a potent inhibitor of all the conventional and novel isozymes of PKC and PKA. It is capable of inhibiting PKC at low nanomolar concentrations. Balanol is distinct in structure amongst all known PKC inhibitors. Balanol mimics ATP and binds to the ATP binding site in the kinase domain. As, the natural molecule is inhibitory to both PKC and PKA, synthetic acylic balanol analogues have been prepared that are highly selective to only cPKCs and nPKCs over any other enzymes such as PKA (Defauw et al., 1996). Because of the structural novelty and low availability of natural resources, balanol has received considerable attention for development as potent PKC inhibiting drug for cancer and other diseases involving PKC.

(B) Calphostins (UCN-1028): Calphostin is another class of novel fungal metabolite (Figure 1.18-B) which was discovered in 1989. It is produced by the fungus *Cladosporium cladosporioides.* Further studies identified five types of calphostin, calphostin A, calphostin B, calphostin C, calphostin D and calphostin I. Calphostin C has the lowest IC_{50} at around 50 nM against all PKC isozymes (Kobayashi et al., 1989). All the calphostins were able to induce apoptosis in cervical and breast cancer cell lines.

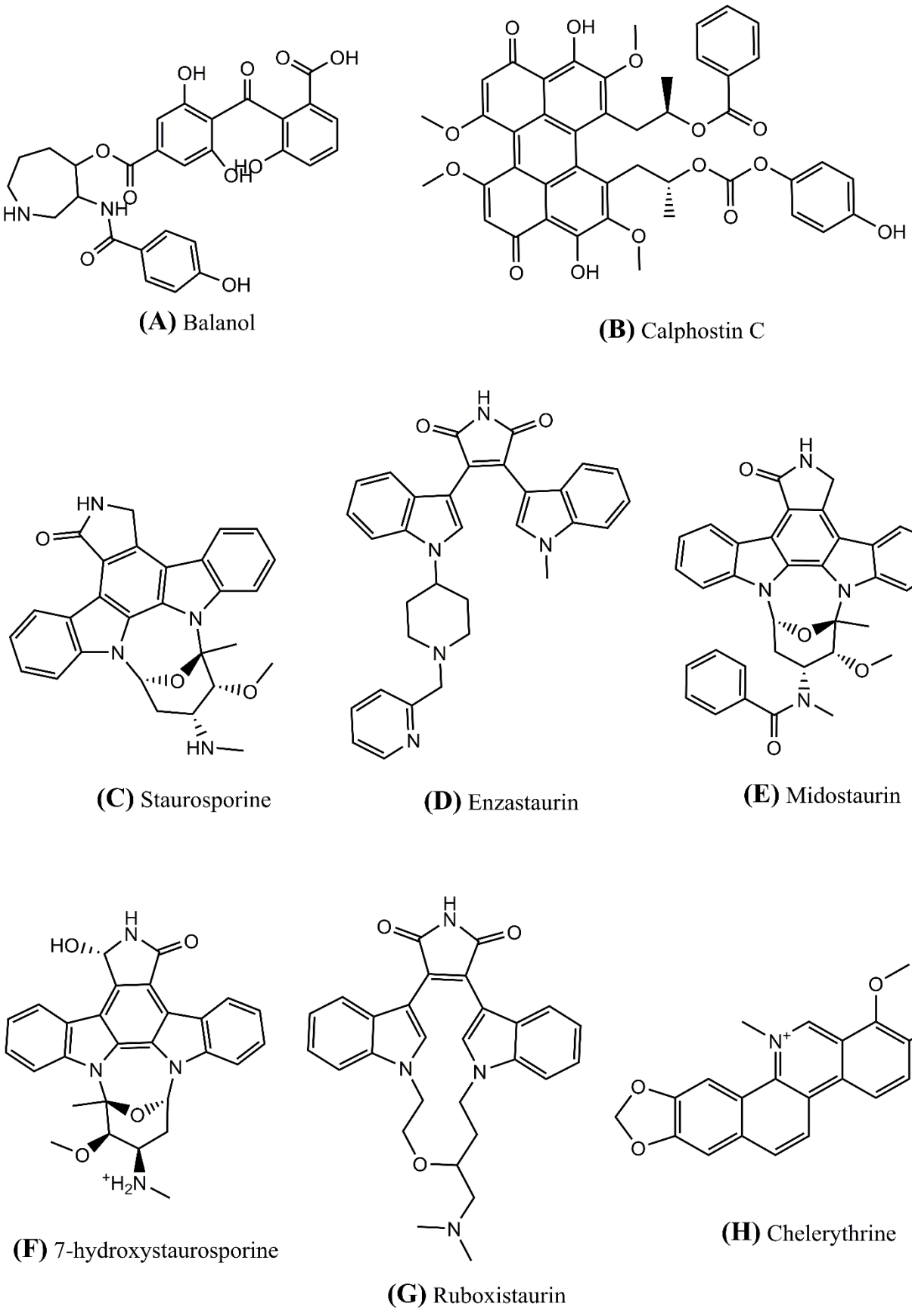

Figure 1.18: Structures of selected PKC antagonists.

An IC_{50} concentration of 180 nM was achieved for calphostin C against MCF-7 breast cancer cells (Kobayashi et al., 1989). Later studies revealed that calphostins bound to the C1b domain of PKCs and affects the translocation of cPKCs and nPKCs (Rotenberg et al., 1995). Further, PKC-α and PKC-ε appear to be the primary targets of calphostin C.

(C) Staurosporine: Staurosporine is a competitive inhibitor (Figure 1.18-C) of ATP and is produced naturally by Streptomyces spp (Takahashi et al., 1987). This is a member of the bisindolylmaleimide family. This compound has anti-proliferative action in many cell lines but lacks the specificity for PKC isoforms. Thus, this compound has served as a lead compound for the development of other PKC inhibitors such as enzastaurin and midostaurin which are described below.

(D) Enzastaurin (LY317615): Enzastaurin interferes with the phosphor-transferase activity of PKC-β by acting as a competitive inhibitor at the ATP binding site (Figure 1.18-D). At lower concentration, enzastaurin is specific for PKC-β but at higher concentrations it is targeting other PKC isoforms. Enzastaurin induces apoptosis in various cancer cell lines including non–small-cell lung cancer (NSCLC) and small-cell lung cancer (SCLC) cell lines by inhibiting the phosphorylation of GSK-3β (Hanauske et al., 2007). It also shows antitumor and anti-angiogenic activities in lung cancer in mice and human Calu-6 NSCLC xenografts. When enzastaurin is used in a combination with other chemotherapeutic drugs, there is heightened apoptotic activity in NSCLC cells.

(E) Midostaurin (PKC412): Midostaurin is the analogue of n-benzylated staurosporine (Figure 1.18-E) which was developed as a PKC inhibitor but was later found to inhibit tyrosine kinases as well. Midostaurin sensitized cancer cells to radiation therapy through the phosphoinositide-3-kinase/Akt pathway (Tenzer et al., 2001). Midostaurin display anti-metastatic activity against murine melanoma cells and is cytotoxic towards B cell chronic lymphocytic leukemia than towards healthy B cells. Midostaurin inhibits the Akt pathway and induces apoptosis in human melanoma cells. Midostaurin has been successfully used in conjunction with standard anticancer drugs such as Gleevec, rapamycin and histone deacetylase inhibitors.

(F) UCN-01 (7-hydroxystaurosporine): UCN-01 is an analogue of staurosporine which was also isolated from the Streptomyces species of bacteria (Figure 1.18-F). It is an inhibitor of conventional and novel PKC isoforms (Mizuno et al., 1993). UCN-01 has synergistic action along with a number of other anti-cancer drugs probably because of its longer half-life in the body (Monks et al., 2000). This molecule has been in clinical trials for the treatment for leukemia, non-small cell lung cancer (NSCLC) and lymphoma.

(G) Ruboxistaurin: Ruboxistaurin is a potential drug which is in the final stages of development (Figure 1.19-G). It is a selective inhibitor of PKC-β (IC_{50} of ~5nM) and inhibits these two isozymes at 250-fold lower concentrations than other PKC isozymes (Jirousek et al., 1996). Thus, this molecule is intended to use against cancer where PKC-βI and PKC-βII isozymes are heavily involved including other important diseases such as Diabetic Retinopathy. The product intended to be sold in the market is ruboxistaurin mesylate under the trade name LY333531. After administration in the body, ruboxistaurin mesylate is rapidly converted to its main equipotent metabolite, N-desmethyl ruboxistaurin by the cytochrome P_{450} enzyme CYP3A4. The half-life of ruboxistaurin is 9 hrs whereas the half-life its metabolite is 16 hrs which allows once in a day dosing (Deissler and Lang, 2016).

(H) Chelerythrine: Chelerythrine is a potent, selective inhibitor of PKC isozymes (Figure 1.18-H). Chelerythrine is a competitive inhibitor for the catalytic site of PKC. It is a benzophenanthridine alkaloid and is obtained from the plant *Chelidonium majus*. It is also present in other plant species such as *Zanthoxylum clava-herculis* and *Zanthoxylum rhoifolium*. Compared to other PKC inhibitors such as staurosporine, chelerythrine is 100 times more selective for PKC isozymes in respect to other kinases such as PKA, PKG, etc. Chelerythrine inhibits PKC translocation to the plasma membrane in poly-morphonuclear macrophages and thereby inhibits their oxidative burst (Siomboing et al., 2001). This compound has potent anti-tumor properties as it exhibited cytotoxicity against nine human tumor cell lines. These tumor cell lines included the highly radio-resistive and chemo-resistive head and neck squamous cell carcinoma line (HNSCC) (Chmura et al., 2000).

(I) Aurothiomalate (ATM) and (J) Aurothioglucose (ATG): The structure of ATM and ATG is given in Figure 1.19-I. Aurothiomalate (ATM) and aurothioglucose (ATG) are related compounds that acts as potent inhibitors for PB1 domain-mediated interaction between PKC-ι and Par6 scaffold protein (Stallings-Mann et al., 2006). Both the drugs target the unique cysteine residue 69 (cys 69) of PKC-ι located at the binding interface between PKC-ι and Par6. Thus, the interaction of PKC-ι with the Par6 protein is disrupted very specifically without disturbing the interaction of other atypical isozymes with Par6. In this way, only the PKC-ι dependent oncogenic signalling is blocked. Both drugs are known to inhibit the growth of NSCLC cells and tumors in mice by blocking PKC-ι mediated signalling to Rac1 protein. ATM is also known to inhibit the ERK/MEK signalling pathway which results in inhibition of cellular proliferation in NSCLC xenografts (Regala et al., 2005).

(K) Disulfiram: Disulfiram (1,1',1",1'"-[disulfanediylbis(carbonothioylnitrilo)]tetraethane) is a new FDA approved drug (Figure 1.19-K). It regulates PKC isozyme activity by S-thiolation mechanism (Chu and O'Brian, 2005). S-thiolation is a post-translational modification entailing disulfide linkage of low-molecular-weight species to selected protein sulfhydryls. PKC S-thiolation by disulfiram

induces differential regulatory effects on PKC isozymes which has the ultimate result of cancer preventive activity of disulfiram. The role of disulfiram as a redox chemotherapeutic agent in metastatic melanoma has also been demonstrated (Fruehauf and Trapp, 2008).

(L) Tamoxifen: Tamoxifen was primarily designed as an antagonist to estrogen receptors for the treatment of breast cancers (Figure 1.19-L). Its active metabolites 4-hydroxytamoxifen and N-desmethyl-4-hydroxytamoxifen have high affinity for estrogen receptors to block transcription of estrogen-responsive genes. However, studies have also found that tamoxifen inhibits PKC when the enzyme is activated in a Ca^{2+}, phospholipid and DAG/phorbol ester dependent manner (O'Brian et al., 1985). However, tamoxifen fails to inhibit PKC that are independent of Ca^{2+} and DAG/phorbol ester signalling suggesting that tamoxifen has specificity for classical PKC isoforms. Similarly, oxygen consumption and reactive oxygen metabolite production in neutrophils that is stimulated by phorbol ester treatment is directly inhibited by tamoxifen (Horgan et al., 1986).

(M) Bisindolylmaleimide I, (N) Gö 6983 and (O) Gö 6976: Bisindolylmaleimide I, Gö 6983, Gö 6976 (Figure 1.19-M,N,O) are derivatives of the parent compound staurosporine that have higher selectivity and lower IC_{50} of inhibition towards PKC isozymes. For instance, Gö 6983 have 7 nM as IC_{50} values of inhibition against both PKC-α and PKC-β while Gö 6976 has IC_{50} of inhibition of 2 nM and 6 nM against PKC-α and PKC-β respectively (Young et al., 2005). Bisindolylmaleimide I has IC_{50} of inhibition of 8 nM and 18 nM against PKC-α and PKC-β. All of these inhibitors bind in ATP binding site and inhibit PKC. Activation of PKC is associated with ROS production from neutrophils which is responsible for inflammation during acute ischemia/reperfusion processes in clinical situations. Treatment with these inhibitors have shown successful results in clinical trials, particularly in the restoration of cardiac contractile function within 5 min of reperfusion. These inhibitors can also attenuate neutrophil generated responses in the setting of ischemia-reperfusion. Studies are undergoing to determine the therapeutic potential of these compounds in various cancer types.

(P) Peptide drugs: Peptide drugs are a new generation of chemotherapeutic agents that function to regulate the activity of specific PKC isoforms. The peptide drugs work by disrupting the crucial interaction between a specific PKC isoform and its corresponding scaffold protein. These peptides are designed to mimic the amino acid sequence of a specific region of particular PKC isoform that is involved in the interaction with a scaffold protein. Thus, they block the interaction of the PKC isozyme with the scaffold protein and inhibit its function. εV1-2 peptide with amino acid sequence 'EAVSLKPT'is a specific inhibitor of PKCε. NSCLC cell growth was completely blocked by εV1-2 peptide and it was previously known that NSCLC cells require PKC-ε for survival (Caino et al., 2012).

Similarly, αV5-3, a novel peptide inhibitor with amino acid sequence 'QLVIAN' is selective for PKC-α, and actively inhibited metastasis of breast cancer cells in a mouse model (Kim et al., 2011).

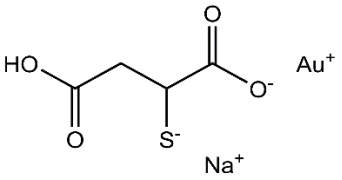

(I) Aurothiomalate (Sodium salt)

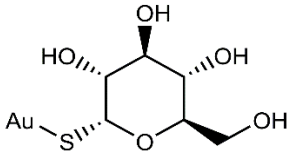

(J) Aurothioglucose

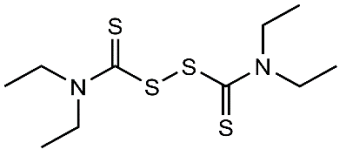

(K) Disulfiram

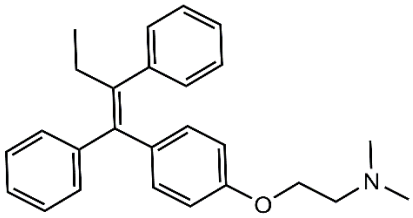

(L) Tamoxifen

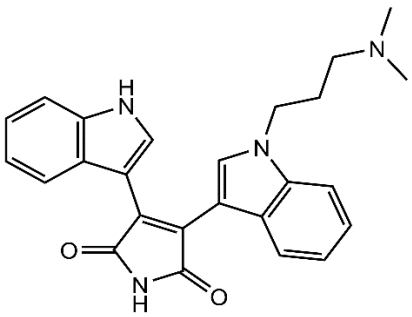

(M) Bisindolylmaleimide I

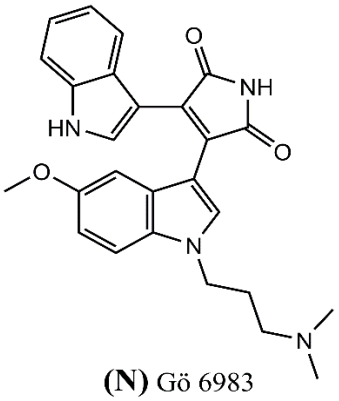

(N) Gö 6983

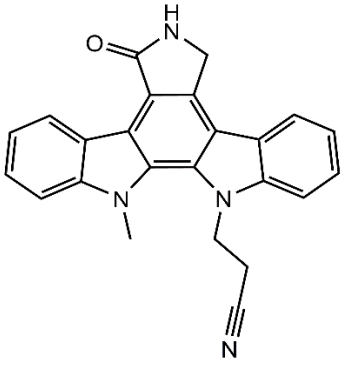

(O) Gö 6976

Figure 1.19: Structures of selected PKC antagonists (continued).

1.11 Aim and scope of the proposed work

Based on the literature search and the potentials of PKC in cancer induction, growth and metastasis, we would like to propose the following objectives:

1) Identification of novel PKC-directed molecules from heterocyclic libraries, clinically approved drug-databank and phytochemical reservoir to develop potential anti-cancer drug: In this objective, we want to identify novel PKC directed molecules that can efficiently function as potential anti-cancer drug. Ligands from three different sources (drug library, phytochemical reservoir and de-novo synthesized molecules) are used for the study.

2) Screening of identified molecules as potential ligands for PKC: After collecting the molecules, next, it was necessary to screen all the molecules, and to select only those that can serve as proper ligands of PKC. An in-silico screening approach was to be chosen that can effectively identify only those molecules that bind to the regulatory C1b domain of PKC with good efficiency. After selection of the best compounds, it was also necessary to characterize the molecular interactions between the molecules (ligands) and the C1b domain (receptor). Interaction analysis helps us to decipher the basis of differences in binding of stronger and weaker ligands to the receptor. Finally, the in-silico studies were complimented with in-vitro binding assays of the best ligands to the C1b domain.

3) Validation and understanding the mechanism of action of PKC directed molecules in breast cancer cells: After selection of the best ligand molecules, it is time to explore the physiological changes in cancer cells that can be potentially brought about by candidate PKC directed molecule treatment. Even subtle changes in cancer cell physiology upon candidate molecule treatment would validate the ability of these molecules to exhibit anti-cancer action. Then it would be scientifically intriguing to explore the mechanism of action of candidate molecules behind the effects on the physiological aspects of cancer cells.

4) To establish the potentials of PKC-directed molecules in anti-cancer drug-discovery programme: The final objective is to prove that the identified PKC-directed molecules have great therapeutic potential to be considered as suitable candidates in anti-cancer drug discovery programme. A clear understanding of anti-cancer mechanism of action of PKC-directed molecules along with a consideration of future experimental platforms will only strengthen the claims for these molecules to be taken up for drug discovery programme.

The proposed study has following scope:

1) Potentials of heterocyclic compounds, exploitation of drugs present in drug database as anti-cancer molecules: A vast repository of heterocyclic compounds exists in different chemical databases and libraries. Heterocyclic compounds have diverse range of structures with different chemical properties. Thus, this makes them attractive candidates for any in-silico drug screening programs. The current study has actively pursued to discover potential heterocyclic compounds that can act as strong ligands to PKC regulatory C1b domain. Heterocyclic molecules discovered to be strong candidates as PKC ligands as well as those obtained from a collaborator lab have been explored for anti-cancer potential. Thus, this study shows that heterocyclic compounds utilize PKC as the molecule to exert their anti-cancer effects. **The findings makes one realize that candidates can be found among heterocyclic compounds that act through PKC and have the potential to be developed as future**

anti-cancer drugs. Hence, the current study depicts the importance of heterocyclic compounds in anti-cancer drug therapy.

2) To reveal the importance of natural molecules as modulators of PKC: The study also explores if popular beverages such as tea have the potential to act as adjuvants mainly as immune therapy for cancer. Beverages are enriched in exotic phytochemicals and regular intake of beverage is beneficial to the health of the individual. The study explored the possible role of phytochemicals as probable mediator of PKC activity. It was also intended to decipher and comprehend any possible mechanistic details of PKC-directed anti-cancer activity of phytochemicals **which can fortify the notion of incorporating herbal beverages in daily life and especially as additional immune therapy during the treatment of cancer by radiation or immunotherapy practices.**

3) Exploitation of clinically approved pharmaceutical drugs for cancer treatment: Another important aspect of this study is that **it intends to uncover the potential use of drugs for other diseases as anti-cancer compounds with a potential emphasis on their relation to PKC**. These trial includes drugs that are already in use for treatment in other ailments, or drugs that are in circulation as clinical trials or passed the clinical trials, as possessing the potential to be tested as anti-cancer drugs. We believe that there is enormous scope in this regard to uncover many drugs as having anti-cancer potential since already prevailing clinical drugs have negligible toxicity concerns as compared to a newly discovered novel molecule.

1.12 References

- Ajani, J.A., Jiang, Y., Faust, J., Chang, B.B., Ho, L., Yao, J.C., Rousey, S., Dakhil, S., Cherny, R.C., Craig, C., *et al.* (2006). A multi-center phase II study of sequential paclitaxel and bryostatin-1 (NSC 339555) in patients with untreated, advanced gastric or gastroesophageal junction adenocarcinoma. Investigational New Drugs *24*, 353-357.
- Akhurst, R.J., and Balmain, A. (1999). Genetic events and the role of TGF beta in epithelial tumour progression. The Journal of Pathology *187*, 82-90.
- Albain, K.S., Unger, J.M., Crowley, J.J., Coltman, C.A., Jr., and Hershman, D.L. (2009). Racial disparities in cancer survival among randomized clinical trials patients of the Southwest Oncology Group. Journal of the National Cancer Institute *101*, 984-992.
- Albano, J.D., Ward, E., Jemal, A., Anderson, R., Cokkinides, V.E., Murray, T., Henley, J., Liff, J., and Thun, M.J. (2007). Cancer mortality in the United States by education level and race. Journal of the National Cancer Institute *99*, 1384-1394.
- Alberts B, J.A., Lewis J, et al. (2002). The Preventable Causes of Cancer. Molecular Biology of the Cell. 4th edition. Garland Science.
- Althuis, M.D., Dozier, J.M., Anderson, W.F., Devesa, S.S., and Brinton, L.A. (2005). Global trends in breast cancer incidence and mortality 1973-1997. International Journal of Epidemiology *34*, 405-412.

- Ambrosone, C.B., Freudenheim, J.L., Graham, S., Marshall, J.R., Vena, J.E., Brasure, J.R., Michalek, A.M., Laughlin, R., Nemoto, T., Gillenwater, K.A., *et al.* (1996). Cigarette smoking, N-acetyltransferase 2 genetic polymorphisms, and breast cancer risk. Jama *276*, 1494-1501.
- Anand, P., Kunnumakara, A.B., Sundaram, C., Harikumar, K.B., Tharakan, S.T., Lai, O.S., Sung, B., and Aggarwal, B.B. (2008). Cancer is a Preventable Disease that Requires Major Lifestyle Changes. Pharmaceutical Research *25*, 2097-2116.
- Anderson, M.W., Reynolds, S.H., You, M., and Maronpot, R.M. (1992a). Role of proto-oncogene activation in carcinogenesis. Environmental Health Perspectives *98*, 13-24.
- Anderson, M.W., Reynolds, S.H., You, M., and Maronpot, R.M. (1992b). Role of proto-oncogene activation in carcinogenesis. Environmental Health Perspectives *98*, 13-24.
- Antal, C.E., and Newton, A.C. (2014). Tuning the signalling output of protein kinase C. Biochemical Society Transactions *42*, 1477-1483.
- Antoniou, A., Pharoah, P.D., Narod, S., Risch, H.A., Eyfjord, J.E., Hopper, J.L., Loman, N., Olsson, H., Johannsson, O., Borg, A., *et al.* (2003). Average risks of breast and ovarian cancer associated with BRCA1 or BRCA2 mutations detected in case Series unselected for family history: a combined analysis of 22 studies. American Journal of Human Genetics *72*, 1117-1130.
- Anwar, W., Armstrong, B.K., Correa, P., Forman, D., Gentile, J.M., Haswell-Elkin, M., Ishi, A., Kaufman, D.G., Kuipers, E.J., Lee, A., *et al.* (1994). Schistosomes, liver flukes and Helicobacter pylori. IARC Working Group on the Evaluation of Carcinogenic Risks to Humans. Lyon, 7-14 June 1994. IARC Monographs on the Evaluation of Carcinogenic Risks to Humans *61*, 1-241.
- Aoki, H., Takada, Y., Kondo, S., Sawaya, R., Aggarwal, B.B., and Kondo, Y. (2007). Evidence that curcumin suppresses the growth of malignant gliomas in vitro and in vivo through induction of autophagy: role of Akt and extracellular signal-regulated kinase signaling pathways. Molecular Pharmacology *72*, 29-39.
- Apps, M.G., Choi, E.H.Y., and Wheate, N.J. (2015). The state-of-play and future of platinum drugs. Endocrine-Related Cancer *22*, R219-R233.
- Arcoleo, J.P., and Weinstein, I.B. (1985). Activation of protein kinase C by tumor promoting phorbol esters, teleocidin and aplysiatoxin in the absence of added calcium. Carcinogenesis *6*, 213-217.
- Aziz, M.H., Manoharan, H.T., and Verma, A.K. (2007). Protein kinase C epsilon, which sensitizes skin to sun's UV radiation-induced cutaneous damage and development of squamous cell carcinomas, associates with Stat3. Cancer Research *67*, 1385-1394.
- Bachmeier, B., Nerlich, A.G., Iancu, C.M., Cilli, M., Schleicher, E., Vene, R., Dell'Eva, R., Jochum, M., Albini, A., and Pfeffer, U. (2007). The chemopreventive polyphenol Curcumin prevents hematogenous breast cancer metastases in immunodeficient mice. Cellular physiology and Biochemistry *19*, 137-152.
- Balendran, A., Hare, G.R., Kieloch, A., Williams, M.R., and Alessi, D.R. (2000). Further evidence that 3-phosphoinositide-dependent protein kinase-1 (PDK1) is required for the stability and phosphorylation of protein kinase C (PKC) isoforms. FEBS Letters *484*, 217-223.
- Barr, P.M., Lazarus, H.M., Cooper, B.W., Schluchter, M.D., Panneerselvam, A., Jacobberger, J.W., Hsu, J.W., Janakiraman, N., Simic, A., Dowlati, A., *et al.* (2009). Phase II study of bryostatin 1 and vincristine for aggressive non-Hodgkin lymphoma relapsing after an autologous stem cell transplant. American Journal of Hematology *84*, 484-487.
- Bekisz, J., Baron, S., Balinsky, C., Morrow, A., and Zoon, K.C. (2010). Antiproliferative Properties of Type I and Type II Interferon. Pharmaceuticals *3*, 994-1015.
- Berx, G., Raspe, E., Christofori, G., Thiery, J.P., and Sleeman, J.P. (2007). Pre-EMTing metastasis? Recapitulation of morphogenetic processes in cancer. Clinical & Experimental Metastasis *24*, 587-597.

- Beuzeboc, P., Soulie, M., Richaud, P., Salomon, L., Staerman, F., Peyromaure, M., Mongiat-Artus, P., Cornud, F., Paparel, P., Davin, J.L., *et al.* (2009). Fusion genes and prostate cancer. From discovery to prognosis and therapeutic perspectives. Progres en Urologie *19*, 819-824.
- Bharti, A.C., Donato, N., Singh, S., and Aggarwal, B.B. (2003). Curcumin (diferuloylmethane) down-regulates the constitutive activation of nuclear factor-kappa B and IkappaBalpha kinase in human multiple myeloma cells, leading to suppression of proliferation and induction of apoptosis. Blood *101*, 1053-1062.
- Black, A.R., and Black, J.D. (2012). Protein kinase C signaling and cell cycle regulation. Frontiers in Immunology *3*, 423.
- Bosch, F.X., Ribes, J., Diaz, M., and Cleries, R. (2004). Primary liver cancer: worldwide incidence and trends. Gastroenterology *127*, S5-S16.
- Brierley, J. (2006). The evolving TNM cancer staging system: an essential component of cancer care. CMAJ : Canadian Medical Association Journal *174*, 155-156.
- Brown, L.C., Mutter, R.W., and Halyard, M.Y. (2015). Benefits, risks, and safety of external beam radiation therapy for breast cancer. International Journal of Women's Health *7*, 449-458.
- Caino, M.C., Lopez-Haber, C., Kim, J., Mochly-Rosen, D., and Kazanietz, M.G. (2012). Proteins kinase Cvarepsilon is required for non-small cell lung carcinoma growth and regulates the expression of apoptotic genes. Oncogene *31*, 2593-2600.
- Caponigro, F., French, R.C., and Kaye, S.B. (1997). Protein kinase C: a worthwhile target for anticancer drugs? Anti-cancer Drugs *8*, 26-33.
- Casagrande, J.T., Pike, M.C., Ross, R.K., Louie, E.W., Roy, S., and Henderson, B.E. (1979). "Incessant ovulation" and ovarian cancer. The Lancet *314*, 170-173.
- Castagna, M., Takai, Y., Kaibuchi, K., Sano, K., Kikkawa, U., and Nishizuka, Y. (1982). Direct activation of calcium-activated, phospholipid-dependent protein kinase by tumor-promoting phorbol esters. The Journal of Biological Chemistry *257*, 7847-7851.
- Castano, A.P., Demidova, T.N., and Hamblin, M.R. (2004). Mechanisms in photodynamic therapy: part one-photosensitizers, photochemistry and cellular localization. Photodiagnosis and Photodynamic Therapy *1*, 279-293.
- Castano, A.P., Mroz, P., and Hamblin, M.R. (2006). Photodynamic therapy and anti-tumour immunity. Nat Rev Cancer *6*, 535-545.
- Castellsague, X., Diaz, M., de Sanjose, S., Munoz, N., Herrero, R., Franceschi, S., Peeling, R.W., Ashley, R., Smith, J.S., Snijders, P.J., *et al.* (2006). Worldwide human papillomavirus etiology of cervical adenocarcinoma and its cofactors: implications for screening and prevention. Journal of the National Cancer Institute *98*, 303-315.
- Center, M.M., Jemal, A., Smith, R.A., and Ward, E. (2009). Worldwide variations in colorectal cancer. CA: A Cancer Journal for Clinicians *59*, 366-378.
- Chaffer, C.L., and Weinberg, R.A. (2011). A Perspective on Cancer Cell Metastasis. Science *331*, 1559-1564.
- Chang, K.J., Lin, J.K., Lee, P.H., Hsieh, Y.S., Cheng, C.K., and Liu, J.Y. (1996). The altered activity of membrane-bound protein kinase C in human liver cancer. Cancer Letters *105*, 211-215.
- Chen, D., Frezza, M., Schmitt, S., Kanwar, J., and Dou, Q.P. (2011). Bortezomib as the First Proteasome Inhibitor Anticancer Drug: Current Status and Future Perspectives. Current Cancer Drug Targets *11*, 239-253.
- Chen, J., Deng, F., Singh, S.V., and Wang, Q.J. (2008). Protein kinase D3 (PKD3) contributes to prostate cancer cell growth and survival through a PKC epsilon/PKD3 pathway downstream of Akt and ERK 1/2. Cancer Research *68*, 3844-3853.

- Chen, J., Giovannucci, E.L., and Hunter, D.J. (1999). MTHFR polymorphism, methyl-replete diets and the risk of colorectal carcinoma and adenoma among U.S. men and women: an example of gene-environment interactions in colorectal tumorigenesis. The Journal of Nutrition *129*, 560S-564S.
- Chen, L., Hahn, H., Wu, G., Chen, C.H., Liron, T., Schechtman, D., Cavallaro, G., Banci, L., Guo, Y., Bolli, R., *et al.* (2001). Opposing cardioprotective actions and parallel hypertrophic effects of delta PKC and epsilon PKC. Proceedings of the National Academy of Sciences of the United States of America *98*, 11114-11119.
- Chiang, A.C., and Massagué, J. (2008). Molecular Basis of Metastasis. New England Journal of Medicine *359*, 2814-2823.
- Chmura, S.J., Dolan, M.E., Cha, A., Mauceri, H.J., Kufe, D.W., and Weichselbaum, R.R. (2000). In vitro and in vivo activity of protein kinase C inhibitor chelerythrine chloride induces tumor cell toxicity and growth delay in vivo. Clinical Cancer Research *6*, 737-742.
- Choudhuri, T., Pal, S., Das, T., and Sa, G. (2005). Curcumin selectively induces apoptosis in deregulated cyclin D1-expressed cells at G2 phase of cell cycle in a p53-dependent manner. The Journal of biological chemistry *280*, 20059-20068.
- Chu, F., and O'Brian, C.A. (2005). PKC sulfhydryl targeting by disulfiram produces divergent isozymic regulatory responses that accord with the cancer preventive activity of the thiuram disulfide. Antioxidants & Redox Signaling *7*, 855-862.
- Chu, K.C., Tarone, R.E., Chow, W.H., Hankey, B.F., and Ries, L.A. (1994). Temporal patterns in colorectal cancer incidence, survival, and mortality from 1950 through 1990. Journal of the National Cancer Institute *86*, 997-1006.
- Churchill, E.N., Murriel, C.L., Chen, C.H., Mochly-Rosen, D., and Szweda, L.I. (2005). Reperfusion-induced translocation of deltaPKC to cardiac mitochondria prevents pyruvate dehydrogenase reactivation. Circulation Research *97*, 78-85.
- Clapp, P., Charyulu, K.K., Tayao, M.S., Tyree, E.B., Nickson, J.J., and Lawrence, W., Jr. (1965). Regional oxygenation and therapeutic response to irradiation; an experimental study. Cancer *18*, 927-936.
- Cohen, A.J., and Pope, C.A., 3rd (1995). Lung cancer and air pollution. Environmental Health Perspectives *103 Suppl 8*, 219-224.
- Collett, G.P., and Campbell, F.C. (2004). Curcumin induces c-jun N-terminal kinase-dependent apoptosis in HCT116 human colon cancer cells. Carcinogenesis *25*, 2183-2189.
- Corsten, M.F., and Shah, K. (2008). Therapeutic stem-cells for cancer treatment: hopes and hurdles in tactical warfare. The Lancet Oncology *9*, 376-384.
- Cruz-Correa, M., Shoskes, D.A., Sanchez, P., Zhao, R., Hylind, L.M., Wexner, S.D., and Giardiello, F.M. (2006). Combination treatment with curcumin and quercetin of adenomas in familial adenomatous polyposis. Clinical gastroenterology and hepatology : the official clinical practice journal of the American Gastroenterological Association *4*, 1035-1038.
- Cruz, M.P. (2016). Lenalidomide (Revlimid): A Thalidomide Analogue in Combination With Dexamethasone For the Treatment of All Patients With Multiple Myeloma. Pharmacy and Therapeutics *41*, 308-313.
- Defauw, J.M., Murphy, M.M., Jagdmann, G.E., Hu, H., Lampe, J.W., Hollinshead, S.P., Mitchell, T.J., Crane, H.M., Heerding, J.M., Mendoza, J.S., *et al.* (1996). Synthesis and Protein Kinase C Inhibitory Activities of Acyclic Balanol Analogs That Are Highly Selective for Protein Kinase C over Protein Kinase A. Journal of Medicinal Chemistry *39*, 5215-5227.
- Deissler, H.L., and Lang, G.E. (2016). The Protein Kinase C Inhibitor: Ruboxistaurin. Developments in Ophthalmology *55*, 295-301.

- Detjen, K.M., Brembeck, F.H., Welzel, M., Kaiser, A., Haller, H., Wiedenmann, B., and Rosewicz, S. (2000). Activation of protein kinase Calpha inhibits growth of pancreatic cancer cells via p21(cip)-mediated G(1) arrest. Journal of Cell Science *113 (Pt 17)*, 3025-3035.
- Dhillon, A.S., Hagan, S., Rath, O., and Kolch, W. (2007). MAP kinase signalling pathways in cancer. Oncogene *26*, 3279-3290.
- Disatnik, M.H., Buraggi, G., and Mochly-Rosen, D. (1994). Localization of protein kinase C isozymes in cardiac myocytes. Experimental Cell Research *210*, 287-297.
- Dockery , D.W., Pope , C.A., Xu , X., Spengler , J.D., Ware , J.H., Fay , M.E., Ferris , B.G.J., and Speizer , F.E. (1993). An Association between Air Pollution and Mortality in Six U.S. Cities. New England Journal of Medicine *329*, 1753-1759.
- Doll, R. (1978). An epidemiological perspective of the biology of cancer. Cancer Research *38*, 3573-3583.
- Doll, R. (1995). Hazards of ionising radiation: 100 years of observations on man. British Journal of Cancer *72*, 1339-1349.
- Doll, R. (1996). Cancers weakly related to smoking. British Medical Bulletin *52*, 35-49.
- Doll, R., and Peto, R. (1981). The causes of cancer: quantitative estimates of avoidable risks of cancer in the United States today. Journal of the National Cancer Institute *66*, 1191-1308.
- Dolmans, D.E.J.G.J., Fukumura, D., and Jain, R.K. (2003). Photodynamic therapy for cancer. Nat Rev Cancer *3*, 380-387.
- Douer, D., Hu, W., Giralt, S., Lill, M., and DiPersio, J. (2003). Arsenic trioxide (trisenox) therapy for acute promyelocytic leukemia in the setting of hematopoietic stem cell transplantation. Oncologist *8*, 132-140.
- Dragnev, K.H., Petty, W.J., Shah, S.J., Lewis, L.D., Black, C.C., Memoli, V., Nugent, W.C., Hermann, T., Negro-Vilar, A., Rigas, J.R., *et al.* (2007). A proof-of-principle clinical trial of bexarotene in patients with non-small cell lung cancer. Clinical Cancer Research *13*, 1794-1800.
- Dries, D.R., Gallegos, L.L., and Newton, A.C. (2007). A single residue in the C1 domain sensitizes novel protein kinase C isoforms to cellular diacylglycerol production. The Journal of Biological Chemistry *282*, 826-830.
- Du, X.L., Fox, E.E., and Lai, D. (2008). Competing Causes of Death for Women With Breast Cancer and Change Over Time From 1975 to 2003. American Journal of Clinical Oncology *31*, 105-116.
- Edwards, B.K., Ward, E., Kohler, B.A., Eheman, C., Zauber, A.G., Anderson, R.N., Jemal, A., Schymura, M.J., Lansdorp-Vogelaar, I., Seeff, L.C., *et al.* (2010). Annual report to the nation on the status of cancer, 1975-2006, featuring colorectal cancer trends and impact of interventions (risk factors, screening, and treatment) to reduce future rates. Cancer *116*, 544-573.
- Edwards , J.C.W., Szczepański , L., Szechiński , J., Filipowicz-Sosnowska , A., Emery , P., Close , D.R., Stevens , R.M., and Shaw , T. (2004). Efficacy of B-Cell–Targeted Therapy with Rituximab in Patients with Rheumatoid Arthritis. New England Journal of Medicine *350*, 2572-2581.
- Ewend, M.G., Brem, S., Gilbert, M., Goodkin, R., Penar, P.L., Varia, M., Cush, S., and Carey, L.A. (2007). Treatment of Single Brain Metastasis with Resection, Intracavity Carmustine Polymer Wafers, and Radiation Therapy Is Safe and Provides Excellent Local Control. Clinical Cancer Research *13*, 3637-3641.
- Ezzati, M., Henley, S.J., Lopez, A.D., and Thun, M.J. (2005). Role of smoking in global and regional cancer epidemiology: current patterns and data needs. International Journal of Cancer *116*, 963-971.
- Ezzati, M., and Lopez, A.D. (2003). Estimates of global mortality attributable to smoking in 2000. Lancet *362*, 847-852.

- Facchinetti, V., Ouyang, W., Wei, H., Soto, N., Lazorchak, A., Gould, C., Lowry, C., Newton, A.C., Mao, Y., Miao, R.Q., *et al.* (2008). The mammalian target of rapamycin complex 2 controls folding and stability of Akt and protein kinase C. The EMBO Journal *27*, 1932-1943.
- Fan, C., Li, Y., and Jia, J. (2013). Protein kinase Cs in lung cancer: A promising target for therapies. Journal of Cancer Research and Therapeutics *9*, 74-79.
- Ferlay, J., Shin, H.R., Bray, F., Forman, D., Mathers, C., and Parkin, D.M. (2010). Estimates of worldwide burden of cancer in 2008: GLOBOCAN 2008. International Journal of Cancer *127*, 2893-2917.
- Fleming, M., Ravula, S., Tatishchev, S.F., and Wang, H.L. (2012). Colorectal carcinoma: Pathologic aspects. Journal of Gastrointestinal Oncology *3*, 153-173.
- Fodde, R. (2002). The APC gene in colorectal cancer. European Journal of Cancer *38*, 867-871.
- Forman D, B.F., Brewster DH. In: Gombe Mbalawa C, Kohler B, Piñeros M, Steliarova-Foucher E, Swaminathan R, Ferlay J, eds (2014). Cancer incidence in five continents, Vol X (electronic version). IARC Publications *164*.
- Frey, M.R., Clark, J.A., Leontieva, O., Uronis, J.M., Black, A.R., and Black, J.D. (2000). Protein kinase C signaling mediates a program of cell cycle withdrawal in the intestinal epithelium. The Journal of cell biology *151*, 763-778.
- Friedlander, M., and Grogan, M. (2002). Guidelines for the Treatment of Recurrent and Metastatic Cervical Cancer. The Oncologist *7*, 342-347.
- Fruehauf, J.P., and Trapp, V. (2008). Reactive oxygen species: an Achilles' heel of melanoma? Expert Review of Anticancer Therapy *8*, 1751-1757.
- Fujiki, H., Mori, M., Nakayasu, M., Terada, M., Sugimura, T., and Moore, R.E. (1981). Indole alkaloids: dihydroteleocidin B, teleocidin, and lyngbyatoxin A as members of a new class of tumor promoters. Proceedings of the National Academy of Sciences of the United States of America *78*, 3872-3876.
- Gallagher, R.P., and Fleshner, N. (1998). Prostate cancer: 3. Individual risk factors. Canadian Medical Association Journal *159*, 807-813.
- Gallegos, L.L., Kunkel, M.T., and Newton, A.C. (2006). Targeting protein kinase C activity reporter to discrete intracellular regions reveals spatiotemporal differences in agonist-dependent signaling. The Journal of Biological Chemistry *281*, 30947-30956.
- Gao, T., Furnari, F., and Newton, A.C. (2005). PHLPP: a phosphatase that directly dephosphorylates Akt, promotes apoptosis, and suppresses tumor growth. Molecular Cell *18*, 13-24.
- Gao, T., and Newton, A.C. (2006). Invariant Leu preceding turn motif phosphorylation site controls the interaction of protein kinase C with Hsp70. The Journal of Biological Chemistry *281*, 32461-32468.
- Garg, R., Benedetti, L.G., Abera, M.B., Wang, H., Abba, M., and Kazanietz, M.G. (2014). Protein kinase C and cancer: what we know and what we do not. Oncogene *33*, 5225-5237.
- Gates, K.S. (2009). An Overview of Chemical Processes That Damage Cellular DNA: Spontaneous Hydrolysis, Alkylation, and Reactions with Radicals. Chemical Research in Toxicology *22*, 1747-1760.
- Gaveriaux, C., Fehr, T., Montecino-Rodriguez, E., Sanglier, J.J., and Loor, F. (1988). Protein kinase C activators of the teleocidin family decrease the IgE-binding capacity of rat basophilic leukemia cells. International Archives of Allergy and Applied Immunology *86*, 465-471.
- Ghosh, S., Xie, W.Q., Quest, A.F., Mabrouk, G.M., Strum, J.C., and Bell, R.M. (1994). The cysteine-rich region of raf-1 kinase contains zinc, translocates to liposomes, and is adjacent to a segment that binds GTP-ras. The Journal of Biological Chemistry *269*, 10000-10007.

- Gliki, G., Wheeler-Jones, C., and Zachary, I. (2002). Vascular endothelial growth factor induces protein kinase C (PKC)-dependent Akt/PKB activation and phosphatidylinositol 3'-kinase-mediates PKC delta phosphorylation: role of PKC in angiogenesis. Cell Biology International *26*, 751-759.
- Global Burden of Disease Cancer, C. (2015). The Global Burden of Cancer 2013. JAMA Oncology *1*, 505-527.
- GM., C. (2000). Cells As Experimental Models. In The Cell: A Molecular Approach 2nd edition Sinauer Associates.
- Goekjian, P.G., and Jirousek, M.R. (1999). Protein kinase C in the treatment of disease: signal transduction pathways, inhibitors, and agents in development. Current Medicinal Chemistry *6*, 877-903.
- Goldberg, I.H. (1974). Mechanisms of action of antitumor antibiotic inhibitors of protein synthesis. Cancer Chemotherapy Reports *58*, 479-489.
- Goode, N., Hughes, K., Woodgett, J.R., and Parker, P.J. (1992). Differential regulation of glycogen synthase kinase-3 beta by protein kinase C isotypes. The Journal of Biological Chemistry *267*, 16878-16882.
- Gopalakrishna, R., Chen, Z.H., and Gundimeda, U. (1994). Tobacco smoke tumor promoters, catechol and hydroquinone, induce oxidative regulation of protein kinase C and influence invasion and metastasis of lung carcinoma cells. Proceedings of the National Academy of Sciences of the United States of America *91*, 12233-12237.
- Gorman, A., Killoran, J., O'Shea, C., Kenna, T., Gallagher, W.M., and O'Shea, D.F. (2004). In vitro demonstration of the heavy-atom effect for photodynamic therapy. Journal of the American Chemical Society *126*, 10619-10631.
- Gould, C.M., and Newton, A.C. (2008). The life and death of protein kinase C. Current Drug Targets *9*, 614-625.
- Gray, M.O., Karliner, J.S., and Mochly-Rosen, D. (1997). A selective epsilon-protein kinase C antagonist inhibits protection of cardiac myocytes from hypoxia-induced cell death. The Journal of Biological Chemistry *272*, 30945-30951.
- Griner, E.M., and Kazanietz, M.G. (2007). Protein kinase C and other diacylglycerol effectors in cancer. Nat Rev Cancer *7*, 281-294.
- Grodsky, N., Li, Y., Bouzida, D., Love, R., Jensen, J., Nodes, B., Nonomiya, J., and Grant, S. (2006). Structure of the catalytic domain of human protein kinase C beta II complexed with a bisindolylmaleimide inhibitor. Biochemistry *45*, 13970-13981.
- Grossoni, V.C., Falbo, K.B., Kazanietz, M.G., de Kier Joffe, E.D., and Urtreger, A.J. (2007). Protein kinase C delta enhances proliferation and survival of murine mammary cells. Molecular Carcinogenesis *46*, 381-390.
- Grumont, R., Lock, P., Mollinari, M., Shannon, F.M., Moore, A., and Gerondakis, S. (2004). The mitogen-induced increase in T cell size involves PKC and NFAT activation of Rel/NF-kappaB-dependent c-myc expression. Immunity *21*, 19-30.
- Gwak, J., Jung, S.J., Kang, D.I., Kim, E.Y., Kim, D.E., Chung, Y.H., Shin, J.G., and Oh, S. (2009). Stimulation of protein kinase C-alpha suppresses colon cancer cell proliferation by down-regulation of beta-catenin. Journal of Cellular and Molecular Medicine *13*, 2171-2180.
- Hampson, P., Chahal, H., Khanim, F., Hayden, R., Mulder, A., Assi, L.K., Bunce, C.M., and Lord, J.M. (2005). PEP005, a selective small-molecule activator of protein kinase C, has potent antileukemic activity mediated via the delta isoform of PKC. Blood *106*, 1362-1368.
- Hanahan, D., and Weinberg, Robert A. (2011). Hallmarks of Cancer: The Next Generation. Cell *144*, 646-674.

- Hanauske, A.R., Oberschmidt, O., Hanauske-Abel, H., Lahn, M.M., and Eismann, U. (2007). Antitumor activity of enzastaurin (LY317615.HCl) against human cancer cell lines and freshly explanted tumors investigated in in-vitro [corrected] soft-agar cloning experiments. Investigational New Drugs *25*, 205-210.
- Hansra, G., Bornancin, F., Whelan, R., Hemmings, B.A., and Parker, P.J. (1996). 12-O-Tetradecanoylphorbol-13-acetate-induced dephosphorylation of protein kinase Calpha correlates with the presence of a membrane-associated protein phosphatase 2A heterotrimer. The Journal of Biological Chemistry *271*, 32785-32788.
- Hausser, A., Storz, P., Hubner, S., Braendlin, I., Martinez-Moya, M., Link, G., and Johannes, F.J. (2001). Protein kinase C mu selectively activates the mitogen-activated protein kinase (MAPK) p42 pathway. FEBS Letters *492*, 39-44.
- Hein, D.W., Doll, M.A., Fretland, A.J., Leff, M.A., Webb, S.J., Xiao, G.H., Devanaboyina, U.S., Nangju, N.A., and Feng, Y. (2000). Molecular genetics and epidemiology of the NAT1 and NAT2 acetylation polymorphisms. Cancer Epidemiology, Biomarkers & Prevention *9*, 29-42.
- Heldin, C.H., Landstrom, M., and Moustakas, A. (2009). Mechanism of TGF-beta signaling to growth arrest, apoptosis, and epithelial-mesenchymal transition. Current Opinion in Cell Biology *21*, 166-176.
- Henderson, B.W., and Dougherty, T.J. (1992). How does photodynamic therapy work? Photochemistry and Photobiology *55*, 145-157.
- Hennings, H., Blumberg, P.M., Pettit, G.R., Herald, C.L., Shores, R., and Yuspa, S.H. (1987). Bryostatin 1, an activator of protein kinase C, inhibits tumor promotion by phorbol esters in SENCAR mouse skin. Carcinogenesis *8*, 1343-1346.
- Herbst, R.S., Heymach, J.V., and Lippman, S.M. (2008). Lung cancer. The New England Journal of Medicine *359*, 1367-1380.
- Hernandez-Boluda, J.C., and Cervantes, F. (2002). Imatinib mesylate (Gleevec, Glivec): a new therapy for chronic myeloid leukemia and other malignancies. Drugs of Today *38*, 601-613.
- Horgan, K., Cooke, E., Hallett, M.B., and Mansel, R.E. (1986). Inhibition of protein kinase C mediated signal transduction by tamoxifen. Importance for antitumour activity. Biochemical Pharmacology *35*, 4463-4465.
- House, C., and Kemp, B.E. (1987). Protein kinase C contains a pseudosubstrate prototope in its regulatory domain. Science *238*, 1726-1728.
- Hu, H., Mendoza, J.S., Lowden, C.T., Ballas, L.M., and Janzen, W.P. (1997). Synthesis and protein kinase C inhibitory activities of balanol analogues with modification of 4-hydroxybenzamido moiety. Bioorganic & Medicinal Chemistry *5*, 1873-1882.
- Huber, M.A., Kraut, N., and Beug, H. (2005). Molecular requirements for epithelial-mesenchymal transition during tumor progression. Current Opinion in Cell Biology *17*, 548-558.
- Hudis, C.A. (2007). Trastuzumab--mechanism of action and use in clinical practice. The New England Journal of Medicine *357*, 39-51.
- Hurd, C., and Rozengurt, E. (2001). Protein kinase D is sufficient to suppress EGF-induced c-Jun Ser 63 phosphorylation. Biochemical and Biophysical Research Communications *282*, 404-408.
- Itsumi, M., Shiota, M., Yokomizo, A., Takeuchi, A., Kashiwagi, E., Dejima, T., Inokuchi, J., Tatsugami, K., Uchiumi, T., and Naito, S. (2014). PMA induces androgen receptor downregulation and cellular apoptosis in prostate cancer cells. Journal of Molecular Endocrinology *53*, 31-41.
- Jaiswal, A.S., Marlow, B.P., Gupta, N., and Narayan, S. (2002). Beta-catenin-mediated transactivation and cell-cell adhesion pathways are important in curcumin (diferuylmethane)-induced growth arrest and apoptosis in colon cancer cells. Oncogene *21*, 8414-8427.
- Jaken, S., and Parker, P.J. (2000). Protein kinase C binding partners. BioEssays *22*, 245-254.

- Jaken, S., Shupnik, M.A., Blumberg, P.M., and Tashjian, A.H., Jr. (1983). Relationship between mezerein-mediated biological responses and phorbol ester receptor occupancy. Cancer Research *43*, 11-14.
- Jänne , P.A., and Mayer , R.J. (2000). Chemoprevention of Colorectal Cancer. New England Journal of Medicine *342*, 1960-1968.
- Jiang, X.H., Tu, S.P., Cui, J.T., Lin, M.C., Xia, H.H., Wong, W.M., Chan, A.O., Yuen, M.F., Jiang, S.H., Lam, S.K., *et al.* (2004). Antisense targeting protein kinase C alpha and beta1 inhibits gastric carcinogenesis. Cancer Research *64*, 5787-5794.
- Jiang, Y., Berk, M., Singh, L.S., Tan, H., Yin, L., Powell, C.T., and Xu, Y. (2005). KiSS1 suppresses metastasis in human ovarian cancer via inhibition of protein kinase C alpha. Clinical & Experimental Metastasis *22*, 369-376.
- Jirousek, M.R., Gillig, J.R., Gonzalez, C.M., Heath, W.F., McDonald, J.H., 3rd, Neel, D.A., Rito, C.J., Singh, U., Stramm, L.E., Melikian-Badalian, A., *et al.* (1996). (S)-13-[(dimethylamino)methyl]-10,11,14,15-tetrahydro-4,9:16, 21-dimetheno-1H, 13H-dibenzo[e,k]pyrrolo[3,4-h][1,4,13]oxadiazacyclohexadecene-1,3(2H)-d ione (LY333531) and related analogues: isozyme selective inhibitors of protein kinase C beta. J Med Chem *39*, 2664-2671.
- Johnson, J.E., Giorgione, J., and Newton, A.C. (2000). The C1 and C2 domains of protein kinase C are independent membrane targeting modules, with specificity for phosphatidylserine conferred by the C1 domain. Biochemistry *39*, 11360-11369.
- Jordan, V.C. (2006). Tamoxifen (ICI46,474) as a targeted therapy to treat and prevent breast cancer. British Journal of Pharmacology *147*, S269-S276.
- Josefson, D. (2001). Obesity and inactivity fuel global cancer epidemic. BMJ (Clinical Research Ed) *322*, 945.
- Kaczmarek, A., Brinkman, B.M., Heyndrickx, L., Vandenabeele, P., and Krysko, D.V. (2012). Severity of doxorubicin-induced small intestinal mucositis is regulated by the TLR-2 and TLR-9 pathways. The Journal of Pathology *226*, 598-608.
- Kang, J.-H. (2014). Protein Kinase C (PKC) Isozymes and Cancer. New Journal of Science *2014*, 36.
- Kedei, N., Lundberg, D.J., Toth, A., Welburn, P., Garfield, S.H., and Blumberg, P.M. (2004). Characterization of the interaction of ingenol 3-angelate with protein kinase C. Cancer Research *64*, 3243-3255.
- Keesey, R.E., and Powley, T.L. (2008). Body Energy Homeostasis Appetite *51*, 442-445.
- Keranen, L.M., Dutil, E.M., and Newton, A.C. (1995). Protein kinase C is regulated in vivo by three functionally distinct phosphorylations. Current Biology : CB *5*, 1394-1403.
- Kim, J., Thorne, S.H., Sun, L., Huang, B., and Mochly-Rosen, D. (2011). Sustained inhibition of PKCalpha reduces intravasation and lung seeding during mammary tumor metastasis in an in vivo mouse model. Oncogene *30*, 323-333.
- Klein, J., and Dawson, L.A. (2013). Hepatocellular Carcinoma Radiation Therapy: Review of Evidence and Future Opportunities. International Journal of Radiation Oncology Biology Physics *87*, 22-32.
- Kobayashi, E., Ando, K., Nakano, H., Iida, T., Ohno, H., Morimoto, M., and Tamaoki, T. (1989). Calphostins (UCN-1028), novel and specific inhibitors of protein kinase C. I. Fermentation, isolation, physico-chemical properties and biological activities. The Journal of Antibiotics *42*, 1470-1474.
- Krontiris, T.G., Devlin, B., Karp, D.D., Robert, N.J., and Risch, N. (1993). An association between the risk of cancer and mutations in the HRAS1 minisatellite locus. The New England Journal of Medicine *329*, 517-523.

- Le, T.T., Gardner, J., Hoang-Le, D., Schmidt, C.W., MacDonald, K.P., Lambley, E., Schroder, W.A., Ogbourne, S.M., and Suhrbier, A. (2009). Immunostimulatory cancer chemotherapy using local ingenol-3-angelate and synergy with immunotherapies. Vaccine *27*, 3053-3062.
- Lee, E.Y.H.P., and Muller, W.J. (2010). Oncogenes and Tumor Suppressor Genes. Cold Spring Harbor Perspectives in Biology *2*, a003236.
- Lee, J.-H., Mahendran, A., Yao, Y., Ngo, L., Venta-Perez, G., Choy, M.L., Kim, N., Ham, W.-S., Breslow, R., and Marks, P.A. (2013). Development of a histone deacetylase 6 inhibitor and its biological effects. Proceedings of the National Academy of Sciences *110*, 15704-15709.
- Lee, J.W., Park, J.A., Kim, S.H., Seo, J.H., Lim, K.J., Jeong, J.W., Jeong, C.H., Chun, K.H., Lee, S.K., Kwon, Y.G., *et al.* (2007). Protein kinase C-delta regulates the stability of hypoxia-inducible factor-1 alpha under hypoxia. Cancer Science *98*, 1476-1481.
- Lehel, C., Olah, Z., Jakab, G., and Anderson, W.B. (1995). Protein kinase C epsilon is localized to the Golgi via its zinc-finger domain and modulates Golgi function. Proceedings of the National Academy of Sciences of the United States of America *92*, 1406-1410.
- Li, L., Ahmed, B., Mehta, K., and Kurzrock, R. (2007). Liposomal curcumin with and without oxaliplatin: effects on cell growth, apoptosis, and angiogenesis in colorectal cancer. Molecular Cancer therapeutics *6*, 1276-1282.
- Lim, E.J., and Torresi, J. (2014). Prevention of hepatitis C virus infection and liver cancer. Recent Results in Cancer Research *193*, 113-133.
- Lin, C.W., Hou, W.C., Shen, S.C., Juan, S.H., Ko, C.H., Wang, L.M., and Chen, Y.C. (2008). Quercetin inhibition of tumor invasion via suppressing PKC delta/ERK/AP-1-dependent matrix metalloproteinase-9 activation in breast carcinoma cells. Carcinogenesis *29*, 1807-1815.
- Lin, K.T., Wang, Y.W., Chen, C.T., Ho, C.M., Su, W.H., and Jou, Y.S. (2012). HDAC inhibitors augmented cell migration and metastasis through induction of PKCs leading to identification of low toxicity modalities for combination cancer therapy. Clinical Cancer Research *18*, 4691-4701.
- Lin, X., O'Mahony, A., Mu, Y., Geleziunas, R., and Greene, W.C. (2000). Protein kinase C-theta participates in NF-kappaB activation induced by CD3-CD28 costimulation through selective activation of IkappaB kinase beta. Mol Cell Biol *20*, 2933-2940.
- Liu, B., Xue, Q., Tang, Y., Cao, J., Guengerich, F.P., and Zhang, H. (2016). Mechanisms of mutagenesis: DNA replication in the presence of DNA damage. Mutation Research Reviews in Mutation Research *768*, 53-67.
- Liu, B.Q., Peto, R., Chen, Z.M., Boreham, J., Wu, Y.P., Li, J.Y., Campbell, T.C., and Chen, J.S. (1998). Emerging tobacco hazards in China: 1. Retrospective proportional mortality study of one million deaths. BMJ (Clinical Research Ed) *317*, 1411-1422.
- Liu, Z.C., Chen, X.H., Song, H.X., Wang, H.S., Zhang, G., Wang, H., Chen, D.Y., Fang, R., Liu, H., Cai, S.H., *et al.* (2014). Snail regulated by PKC/GSK-3beta pathway is crucial for EGF-induced epithelial-mesenchymal transition (EMT) of cancer cells. Cell and Tissue Research *358*, 491-502.
- Livraghi, T. (2001). Guidelines for treatment of liver cancer. European journal of ultrasound *13*, 167-176.
- Longley, D.B., Harkin, D.P., and Johnston, P.G. (2003). 5-Fluorouracil: mechanisms of action and clinical strategies. Nat Rev Cancer *3*, 330-338.
- Lopez-Bergami, P., Habelhah, H., Bhoumik, A., Zhang, W., Wang, L.H., and Ronai, Z. (2005). RACK1 mediates activation of JNK by protein kinase C [corrected]. Molecular Cell *19*, 309-320.
- Lopez-Bergami, P., Huang, C., Goydos, J.S., Yip, D., Bar-Eli, M., Herlyn, M., Smalley, K.S., Mahale, A., Eroshkin, A., Aaronson, S., *et al.* (2007). Rewired ERK-JNK signaling pathways in melanoma. Cancer Cell *11*, 447-460.

- Lu, Y., Jamieson, L., Brasier, A.R., and Fields, A.P. (2001). NF-kappaB/RelA transactivation is required for atypical protein kinase C iota-mediated cell survival. Oncogene *20*, 4777-4792.
- Mackay, H.J., and Twelves, C.J. (2007a). Targeting the protein kinase C family: are we there yet? Nat Rev Cancer *7*, 554-562.
- Mackay, H.J., and Twelves, C.J. (2007b). Targeting the protein kinase C family: are we there yet? Nat Rev Cancer *7*, 554-562.
- Mahmmoud, Y.A. (2007). Modulation of protein kinase C by curcumin; inhibition and activation switched by calcium ions. British Journal of Pharmacology *150*, 200-208.
- Majhi, A., Rahman, G.M., Panchal, S., and Das, J. (2010). Binding of curcumin and its long chain derivatives to the activator binding domain of novel protein kinase C. Bioorganic & Medicinal Chemistry *18*, 1591-1598.
- Markowitz, S.D., and Bertagnolli, M.M. (2009). Molecular origins of cancer: Molecular basis of colorectal cancer. The New England Journal of Medicine *361*, 2449-2460.
- Martin, A.M., and Weber, B.L. (2000). Genetic and hormonal risk factors in breast cancer. Journal of the National Cancer Institute *92*, 1126-1135.
- Martin TA, Y.L., Sanders AJ (2013). Cancer Invasion and Metastasis: Molecular and Cellular Perspective. Landes Bioscience, 2000-2013. .
- Martland, H.S. (1931). The Occurrence of Malignancy in Radio-Active Persons: A General Review of Data Gathered in the Study of the Radium Dial Painters, with Special Reference to the Occurrence of Osteogenic Sarcoma and the Inter-Relationship of Certain Blood Diseases. The American Journal of Cancer *15*, 2435-2516.
- Matsubara, K., and Tokino, T. (1990). Integration of hepatitis B virus DNA and its implications for hepatocarcinogenesis. Molecular Biology & Medicine *7*, 243-260.
- McPherson, K., Steel, C.M., and Dixon, J.M. (2000). Breast cancer—epidemiology, risk factors, and genetics. BMJ : British Medical Journal *321*, 624-628.
- Mizuno, K., Saido, T.C., Ohno, S., Tamaoki, T., and Suzuki, K. (1993). Staurosporine-related compounds, K252a and UCN-01, inhibit both cPKC and nPKC. FEBS Letters *330*, 114-116.
- Mochly-Rosen, D., and Gordon, A.S. (1998). Anchoring proteins for protein kinase C: a means for isozyme selectivity. FASEB journal : official publication of the Federation of American Societies for Experimental Biology *12*, 35-42.
- Mochly-Rosen, D., Khaner, H., and Lopez, J. (1991). Identification of intracellular receptor proteins for activated protein kinase C. Proceedings of the National Academy of Sciences of the United States of America *88*, 3997-4000.
- Mochly-Rosen, D., Miller, K.G., Scheller, R.H., Khaner, H., Lopez, J., and Smith, B.L. (1992). p65 fragments, homologous to the C2 region of protein kinase C, bind to the intracellular receptors for protein kinase C. Biochemistry *31*, 8120-8124.
- Monks, A., Harris, E.D., Vaigro-Wolff, A., Hose, C.D., Connelly, J.W., and Sausville, E.A. (2000). UCN-01 enhances the in vitro toxicity of clinical agents in human tumor cell lines. Investigational New Drugs *18*, 95-107.
- Mosior, M., and Newton, A.C. (1996). Calcium-independent binding to interfacial phorbol esters causes protein kinase C to associate with membranes in the absence of acidic lipids. Biochemistry *35*, 1612-1623.
- Nakagawa, M., Oliva, J.L., Kothapalli, D., Fournier, A., Assoian, R.K., and Kazanietz, M.G. (2005). Phorbol ester-induced G1 phase arrest selectively mediated by protein kinase Cdelta-dependent induction of p21. The Journal of Biological Chemistry *280*, 33926-33934.

- Newcomb, P.A., Storer, B.E., Longnecker, M.P., Mittendorf, R., Greenberg, E.R., Clapp, R.W., Burke, K.P., Willett, W.C., and MacMahon, B. (1994). Lactation and a reduced risk of premenopausal breast cancer. The New England Journal of Medicine *330*, 81-87.
- Newton, A.C. (2003). Regulation of the ABC kinases by phosphorylation: protein kinase C as a paradigm. The Biochemical Journal *370*, 361-371.
- Ng, M., and Cunningham, D. (2004). Cetuximab (Erbitux)--an emerging targeted therapy for epidermal growth factor receptor-expressing tumours. International Journal of Clinical Practice *58*, 970-976.
- Nishio, H., Ikegami, Y., Segawa, T., and Nakata, Y. (1994). Stimulation of calcium sequestration by mezerein, a protein kinase C activator, in saponized rabbit platelets. General Pharmacology *25*, 413-416.
- Nishizuka, Y. (1995). Protein kinase C and lipid signaling for sustained cellular responses. FASEB Journal *9*, 484-496.
- O'Brian, C.A., Liskamp, R.M., Solomon, D.H., and Weinstein, I.B. (1985). Inhibition of protein kinase C by tamoxifen. Cancer Research *45*, 2462-2465.
- O'Connor, A.E., Gallagher, W.M., and Byrne, A.T. (2009). Porphyrin and nonporphyrin photosensitizers in oncology: preclinical and clinical advances in photodynamic therapy. Photochemistry and Photobiology *85*, 1053-1074.
- Oancea, E., and Meyer, T. (1998). Protein kinase C as a molecular machine for decoding calcium and diacylglycerol signals. Cell *95*, 307-318.
- Ogbourne, S.M., Suhrbier, A., Jones, B., Cozzi, S.J., Boyle, G.M., Morris, M., McAlpine, D., Johns, J., Scott, T.M., Sutherland, K.P., *et al.* (2004). Antitumor activity of 3-ingenyl angelate: plasma membrane and mitochondrial disruption and necrotic cell death. Cancer Research *64*, 2833-2839.
- Osborne, C., Wilson, P., and Tripathy, D. (2004). Oncogenes and Tumor Suppressor Genes in Breast Cancer: Potential Diagnostic and Therapeutic Applications. The Oncologist *9*, 361-377.
- Park, I.C., Park, M.J., Rhee, C.H., Lee, J.I., Choe, T.B., Jang, J.J., Lee, S.H., and Hong, S.I. (2001). Protein kinase C activation by PMA rapidly induces apoptosis through caspase-3/CPP32 and serine protease(s) in a gastric cancer cell line. International Journal of Oncology *18*, 1077-1083.
- Parkin, D.M. (2006). The global health burden of infection-associated cancers in the year 2002. International Journal of Cancer *118*, 3030-3044.
- Parsa, N. (2012). Environmental Factors Inducing Human Cancers. Iranian Journal of Public Health *41*, 1-9.
- Pearce, L.R., Komander, D., and Alessi, D.R. (2010). The nuts and bolts of AGC protein kinases. Nat Rev Mol Cell Biol *11*, 9-22.
- Pedraza-Fariña, L.G. (2006). Mechanisms of Oncogenic Cooperation in Cancer Initiation and Metastasis. The Yale Journal of Biology and Medicine *79*, 95-103.
- Peltier, S., Oger, J.M., Lagarce, F., Couet, W., and Benoit, J.P. (2006). Enhanced oral paclitaxel bioavailability after administration of paclitaxel-loaded lipid nanocapsules. Pharm Res *23*, 1243-1250.
- Perez-Herrero, E., and Fernandez-Medarde, A. (2015). Advanced targeted therapies in cancer: Drug nanocarriers, the future of chemotherapy. European Journal of Pharmaceutics and Biopharmaceutics : eV *93*, 52-79.
- Peto, J., Decarli, A., La Vecchia, C., Levi, F., and Negri, E. (1999). The European mesothelioma epidemic. British Journal of Cancer *79*, 666-672.
- Peto, J., and Mack, T.M. (2000). High constant incidence in twins and other relatives of women with breast cancer. Nature Genetics *26*, 411-414.

- Peto, R., Darby, S., Deo, H., Silcocks, P., Whitley, E., and Doll, R. (2000). Smoking, smoking cessation, and lung cancer in the UK since 1950: combination of national statistics with two case-control studies. BMJ (Clinical Research Ed) *321*, 323-329.
- Pfeifhofer, C., Kofler, K., Gruber, T., Tabrizi, N.G., Lutz, C., Maly, K., Leitges, M., and Baier, G. (2003). Protein kinase C theta affects Ca2+ mobilization and NFAT cell activation in primary mouse T cells. The Journal of Experimental Medicine *197*, 1525-1535.
- Pike, M.C., Krailo, M.D., Henderson, B.E., Casagrande, J.T., and Hoel, D.G. (1983). 'Hormonal' risk factors, 'breast tissue age' and the age-incidence of breast cancer. Nature *303*, 767-770.
- Plaetzer, K., Krammer, B., Berlanda, J., Berr, F., and Kiesslich, T. (2009). Photophysics and photochemistry of photodynamic therapy: fundamental aspects. Lasers in Medical Science *24*, 259-268.
- Pommier, Y., Leo, E., Zhang, H., and Marchand, C. (2010). DNA topoisomerases and their poisoning by anticancer and antibacterial drugs. Chemistry & Biology *17*, 421-433.
- Prekeris, R., Mayhew, M.W., Cooper, J.B., and Terrian, D.M. (1996). Identification and localization of an actin-binding motif that is unique to the epsilon isoform of protein kinase C and participates in the regulation of synaptic function. The Journal of Cell Biology *132*, 77-90.
- Qi, X., and Mochly-Rosen, D. (2008). The PKCdelta -Abl complex communicates ER stress to the mitochondria - an essential step in subsequent apoptosis. Journal of Cell Science *121*, 804-813.
- Rao, K.E., and Lown, J.W. (1990). Mode of action of saframycin antitumor antibiotics: sequence selectivities in the covalent binding of saframycins A and S to deoxyribonucleic acid. Chemical Research in Toxicology *3*, 262-267.
- Rappeneau, S., Baeza-Squiban, A., Jeulin, C., and Marano, F. (2000). Protection from Cytotoxic Effects Induced by the Nitrogen Mustard Mechlorethamine on Human Bronchial Epithelial Cells in Vitro. Toxicological Sciences *54*, 212-221.
- Reddig, P.J., Dreckschmidt, N.E., Zou, J., Bourguignon, S.E., Oberley, T.D., and Verma, A.K. (2000). Transgenic Mice Overexpressing Protein Kinase Cε in Their Epidermis Exhibit Reduced Papilloma Burden but Enhanced Carcinoma Formation after Tumor Promotion. Cancer Research *60*, 595-602.
- Regala, R.P., Weems, C., Jamieson, L., Copland, J.A., Thompson, E.A., and Fields, A.P. (2005). Atypical protein kinase Ciota plays a critical role in human lung cancer cell growth and tumorigenicity. The Journal of Biological Chemistry *280*, 31109-31115.
- Ringden, O. (2007). Immunotherapy by allogeneic stem cell transplantation. Advances in Cancer Research *97*, 25-60.
- Rotenberg, S.A., Huang, M.H., Zhu, J., Su, L., and Riedel, H. (1995). Deletion analysis of protein kinase C inactivation by calphostin C. Molecular Carcinogenesis *12*, 42-49.
- Sadeghi, M., Enferadi, M., and Shirazi, A. (2010). External and internal radiation therapy: past and future directions. J Cancer Res Ther *6*, 239-248.
- Sahasranaman, S., Howard, D., and Roy, S. (2008). Clinical pharmacology and pharmacogenetics of thiopurines. European Journal of Clinical Pharmacology *64*, 753-767.
- Sant, M., Capocaccia, R., Coleman, M.P., Berrino, F., Gatta, G., Micheli, A., Verdecchia, A., Faivre, J., Hakulinen, T., Coebergh, J.W., *et al.* (2001). Cancer survival increases in Europe, but international differences remain wide. European journal of cancer *37*, 1659-1667.
- Sant, M., Francisci, S., Capocaccia, R., Verdecchia, A., Allemani, C., and Berrino, F. (2006). Time trends of breast cancer survival in Europe in relation to incidence and mortality. International Journal of Cancer *119*, 2417-2422.

- Santiago-Walker, A.E., Fikaris, A.J., Kao, G.D., Brown, E.J., Kazanietz, M.G., and Meinkoth, J.L. (2005). Protein kinase C delta stimulates apoptosis by initiating G1 phase cell cycle progression and S phase arrest. The Journal of Biological Chemistry *280*, 32107-32114.
- Sarasin, A. (2003). An overview of the mechanisms of mutagenesis and carcinogenesis. Mutat Res *544*, 99-106.
- Schaufelberger, D.E., Koleck, M.P., Beutler, J.A., Vatakis, A.M., Alvarado, A.B., Andrews, P., Marzo, L.V., Muschik, G.M., Roach, J., Ross, J.T., *et al.* (1991). The large-scale isolation of bryostatin 1 from Bugula neritina following current good manufacturing practices. Journal of Natural Products *54*, 1265-1270.
- Schönwasser, D.C., Marais, R.M., Marshall, C.J., and Parker, P.J. (1998). Activation of the Mitogen-Activated Protein Kinase/Extracellular Signal-Regulated Kinase Pathway by Conventional, Novel, and Atypical Protein Kinase C Isotypes. Molecular and Cellular Biology *18*, 790-798.
- Schultz, A., Jonsson, J.I., and Larsson, C. (2003). The regulatory domain of protein kinase Ctheta localises to the Golgi complex and induces apoptosis in neuroblastoma and Jurkat cells. Cell Death and Differentiation *10*, 662-675.
- Seeff, L.B., and Hoofnagle, J.H. (2006). Epidemiology of hepatocellular carcinoma in areas of low hepatitis B and hepatitis C endemicity. Oncogene *25*, 3771-3777.
- Sellers, A.H. (1971). The clinical classification of malignant tumours: the TNM system. Canadian Medical Association Journal *105*, 836-passim.
- Shen, X., Xiong, G.L., Jing, Y., Xiao, H., Cui, Y., Zhang, Y.F., Shan, Y.J., Xing, S., Yang, M., Liu, X.L., *et al.* (2015). The protein kinase C agonist prostratin induces differentiation of human myeloid leukemia cells and enhances cellular differentiation by chemotherapeutic agents. Cancer Letters *356*, 686-696.
- Shih, T., and Lindley, C. (2006). Bevacizumab: an angiogenesis inhibitor for the treatment of solid malignancies. Clinical Therapeutics *28*, 1779-1802.
- Siomboing, X., Gressier, B., Dine, T., Brunet, C., Luyckx, M., Cazin, M., and Cazin, J.C. (2001). Investigation of the inhibitory effects of chelerythrine chloride on the translocation of the protein kinase C betaI, betaII, zeta in human neutrophils. Farmaco *56*, 859-865.
- Song, Y., Li, X., Zeng, Z., Li, Q., Gong, Z., Liao, Q., Li, X., Chen, P., Xiang, B., Zhang, W., *et al.* (2016). Epstein-Barr virus encoded miR-BART11 promotes inflammation-induced carcinogenesis by targeting FOXP1. Oncotarget *7(24)*, 36783-36799
- Soto-Guzman, A., Navarro-Tito, N., Castro-Sanchez, L., Martinez-Orozco, R., and Salazar, E.P. (2010). Oleic acid promotes MMP-9 secretion and invasion in breast cancer cells. Clinical & Experimental Metastasis *27*, 505-515.
- Spano, D., Heck, C., De Antonellis, P., Christofori, G., and Zollo, M. (2012). Molecular networks that regulate cancer metastasis. Seminars in Cancer Biology *22*, 234-249.
- Spiegel, R.J. (1986). Intron A (interferon alfa-2b): clinical overview and future directions. Seminars in Oncology *13*, 89-101.
- Stallings-Mann, M., Jamieson, L., Regala, R.P., Weems, C., Murray, N.R., and Fields, A.P. (2006). A novel small-molecule inhibitor of protein kinase Ciota blocks transformed growth of non-small-cell lung cancer cells. Cancer Research *66*, 1767-1774.
- Stein, U., Walther, W., Arlt, F., Schwabe, H., Smith, J., Fichtner, I., Birchmeier, W., and Schlag, P.M. (2009). MACC1, a newly identified key regulator of HGF-MET signaling, predicts colon cancer metastasis. Nature Medicine *15*, 59-67.
- Struewing , J.P., Hartge , P., Wacholder , S., Baker , S.M., Berlin , M., McAdams , M., Timmerman , M.M., Brody , L.C., and Tucker , M.A. (1997). The Risk of Cancer Associated with Specific Mutations of BRCA1 and BRCA2 among Ashkenazi Jews. New England Journal of Medicine *336*, 1401-1408.

- Sun, R., Gao, P., Chen, L., Ma, D., Wang, J., Oppenheim, J.J., and Zhang, N. (2005). Protein kinase C zeta is required for epidermal growth factor-induced chemotaxis of human breast cancer cells. Cancer Research *65*, 1433-1441.
- Sun, X.G., and Rotenberg, S.A. (1999). Overexpression of protein kinase Calpha in MCF-10A human breast cells engenders dramatic alterations in morphology, proliferation, and motility. Cell Growth & Differentiation *10*, 343-352.
- Szallasi, Z., and Blumberg, P.M. (1991). Prostratin, a nonpromoting phorbol ester, inhibits induction by phorbol 12-myristate 13-acetate of ornithine decarboxylase, edema, and hyperplasia in CD-1 mouse skin. Cancer Research *51*, 5355-5360.
- Takahashi, I., Kobayashi, E., Asano, K., Yoshida, M., and Nakano, H. (1987). UCN-01, a selective inhibitor of protein kinase C from Streptomyces. The Journal of Antibiotics *40*, 1782-1784.
- Takai, Y., Kishimoto, A., Inoue, M., and Nishizuka, Y. (1977). Studies on a cyclic nucleotide-independent protein kinase and its proenzyme in mammalian tissues. I. Purification and characterization of an active enzyme from bovine cerebellum. The Journal of Biological Chemistry *252*, 7603-7609.
- Takai, Y., Kishimoto, A., Iwasa, Y., Kawahara, Y., Mori, T., and Nishizuka, Y. (1979). Calcium-dependent activation of a multifunctional protein kinase by membrane phospholipids. The Journal of Biological Chemistry *254*, 3692-3695.
- Tan, S.-L., and Parker, P.J. (2003). Emerging and diverse roles of protein kinase C in immune cell signalling. Biochemical Journal *376*, 545-552.
- Tenzer, A., Zingg, D., Rocha, S., Hemmings, B., Fabbro, D., Glanzmann, C., Schubiger, P.A., Bodis, S., and Pruschy, M. (2001). The phosphatidylinositide 3'-kinase/Akt survival pathway is a target for the anticancer and radiosensitizing agent PKC412, an inhibitor of protein kinase C. Cancer Research *61*, 8203-8210.
- Tsai, J.H., Hsieh, Y.S., Kuo, S.J., Chen, S.T., Yu, S.Y., Huang, C.Y., Chang, A.C., Wang, Y.W., Tsai, M.T., and Liu, J.Y. (2000). Alteration in the expression of protein kinase C isoforms in human hepatocellular carcinoma. Cancer Letters *161*, 171-175.
- Urtreger, A.J., Kazanietz, M.G., and Bal de Kier Joffe, E.D. (2012). Contribution of individual PKC isoforms to breast cancer progression. IUBMB Life *64*, 18-26.
- Valastyan, S., and Weinberg, R.A. (2011). Tumor Metastasis: Molecular Insights and Evolving Paradigms. Cell *147*, 275-292.
- Vallentin, A., Lo, T.C., and Joubert, D. (2001). A single point mutation in the V3 region affects protein kinase Calpha targeting and accumulation at cell-cell contacts. Mol Cell Biol *21*, 3351-3363.
- Vandeven, N., and Nghiem, P. (2014). Pathogen-Driven Cancers and Emerging Immune Therapeutic Strategies. Cancer Immunology Research *2*, 9-14.
- Vong, S., and Kalluri, R. (2011). The Role of Stromal Myofibroblast and Extracellular Matrix in Tumor Angiogenesis. Genes & Cancer *2*, 1139-1145.
- Wagner, J.C., Sleggs, C.A., and Marchand, P. (1960). Diffuse pleural mesothelioma and asbestos exposure in the North Western Cape Province. British Journal of Industrial Medicine *17*, 260-271.
- Wainwright, M. (2008). Photodynamic therapy: the development of new photosensitisers. Anti-cancer Agents in Medicinal Chemistry *8*, 280-291.
- Walboomers, J.M., Jacobs, M.V., Manos, M.M., Bosch, F.X., Kummer, J.A., Shah, K.V., Snijders, P.J., Peto, J., Meijer, C.J., and Munoz, N. (1999). Human papillomavirus is a necessary cause of invasive cervical cancer worldwide. The Journal of Pathology *189*, 12-19.
- Waldron, R.T., Whitelegge, J.P., Faull, K.F., and Rozengurt, E. (2007). Identification of a novel phosphorylation site in c-jun directly targeted in vitro by protein kinase D. Biochemical and Biophysical Research Communications *356*, 361-367.

- Wang, J., Wan, W., Sun, R., Liu, Y., Sun, X., Ma, D., and Zhang, N. (2008). Reduction of Akt2 expression inhibits chemotaxis signal transduction in human breast cancer cells. Cellular Signalling *20*, 1025-1034.
- Wang, M.T., Holderfield, M., Galeas, J., Delrosario, R., To, M.D., Balmain, A., and McCormick, F. (2015). K-Ras Promotes Tumorigenicity through Suppression of Non-canonical Wnt Signaling. Cell *163*, 1237-1251.
- Weinblatt, M.E. (2013). Methotrexate in Rheumatoid Arthritis: A Quarter Century of Development. Transactions of the American Clinical and Climatological Association *124*, 16-25.
- Wheeler, D.L., Martin, K.E., Ness, K.J., Li, Y., Dreckschmidt, N.E., Wartman, M., Ananthaswamy, H.N., Mitchell, D.L., and Verma, A.K. (2004). Protein Kinase C ε Is an Endogenous Photosensitizer That Enhances Ultraviolet Radiation-Induced Cutaneous Damage and Development of Squamous Cell Carcinomas1. Cancer Research *64*, 7756-7765.
- Woodage, T., King, S.M., Wacholder, S., Hartge, P., Struewing, J.P., McAdams, M., Laken, S.J., Tucker, M.A., and Brody, L.C. (1998). The APCI1307K allele and cancer risk in a community-based study of Ashkenazi Jews. Nature Genetics *20*, 62-65.
- Wu, T.T., Hsieh, Y.H., Hsieh, Y.S., and Liu, J.Y. (2008). Reduction of PKC alpha decreases cell proliferation, migration, and invasion of human malignant hepatocellular carcinoma. Journal of Cellular Biochemistry *103*, 9-20.
- Wynder, E.L., and Graham, E.A. (1950). Tobacco smoking as a possible etiologic factor in bronchiogenic carcinoma; a study of 684 proved cases. Journal of the American Medical Association *143*, 329-336.
- Xiao, L., Gonzalez-Guerrico, A., and Kazanietz, M.G. (2009). PKC-mediated secretion of death factors in LNCaP prostate cancer cells is regulated by androgens. Molecular Carcinogenesis *48*, 187-195.
- Xu, G., McMahan, C.A., Hildreth, K., Garcia, R.A., Herbert, D.C., and Walter, C.A. (2012). Ionizing Radiation-Induced Mutant Frequencies Increase Transiently in Male Germ Cells of Older Mice. Mutation Research *744*, 135-139.
- Yang, B.H., Bray, F.I., Parkin, D.M., Sellors, J.W., and Zhang, Z.F. (2004). Cervical cancer as a priority for prevention in different world regions: an evaluation using years of life lost. International Journal of Cancer *109*, 418-424.
- Yao, G.Y., Zeng, M.S., Lin, P., Song, L.B., Zhang, X., He, J.H., Yang, M.T., and Rong, T.H. (2006). Effects of MT1-MMP on the in vitro invasiveness of breast cancer cells. Zhonghua zhong liu za zhi *28*, 650-653.
- Yarden, Y. (2001). Biology of HER2 and Its Importance in Breast Cancer. Oncology *61(suppl 2)*, 1-13.
- Yoshida, K. (2007). PKCdelta signaling: mechanisms of DNA damage response and apoptosis. Cellular Signalling *19*, 892-901.
- Yoshida, M., Yokokura, H., Hidaka, H., Ikekawa, T., and Saijo, N. (1998). Mechanism of antitumor action of PKC activator, gnidimacrin. International Journal of cancer *77*, 243-250.
- Yoshiji, H., Kuriyama, S., Ways, D.K., Yoshii, J., Miyamoto, Y., Kawata, M., Ikenaka, Y., Tsujinoue, H., Nakatani, T., Shibuya, M., *et al.* (1999). Protein Kinase C Lies on the Signaling Pathway for Vascular Endothelial Growth Factor-mediated Tumor Development and Angiogenesis. Cancer Research *59*, 4413-4418.
- Young, L.H., Balin, B.J., and Weis, M.T. (2005). Go 6983: a fast acting protein kinase C inhibitor that attenuates myocardial ischemia/reperfusion injury. Cardiovascular Drug Reviews *23*, 255-272.
- Zafar, A., Hardy, K., Wu, F., Li, J., and Rao, S. (2015). The role of protein kinase-C theta in control of epithelial to mesenchymal transition and cancer stem cell formation. Genomics Data *3*, 28-32.

- Zhang, G., Kazanietz, M.G., Blumberg, P.M., and Hurley, J.H. (1995). Crystal structure of the cys2 activator-binding domain of protein kinase C delta in complex with phorbol ester. Cell *81*, 917-924.

Chapter 2

Experimental Procedures

2.1 Introduction

Experimental procedures of all the experiments carried out during this thesis work has been described in details in this chapter so that research work described can be easily reproduced elsewhere. Procedures of specific experiments of a particular chapter is described in the corresponding chapters.

2.2 Cell culture and treatments

MDAMB-231 cells and MCF-7 breast cancer cells were cultured in DMEM:F12, supplemented with 10 % foetal bovine serum (FBS) and 1% penicillin-streptomycin antibiotic solution (100 units/ml penicillin and 100 µg/ml streptomycin sulfate). Cells were grown at 37°C in a humidified environment with 5% CO_2 incubator. Cells were seeded on poly L-Lysine coated 96 well cell culture plate/35 mm/60 mm/100 mm cell culture dishes and allowed to adhere to the cell culture plate. Prior to different compound treatments, cells were washed twice with cell culture grade phosphate buffer saline (PBS) and then they were subjected to various treatments in serum free media. In order to test the effects of antioxidants, cells were pre-incubated with antioxidants for 2 h before treatment.

2.3 Cell viability assay

The dye MTT (3-(4,5-Dimethylthiazol-2-yl)-2,5-Diphenyltetrazolium Bromide) was used to measure cellular viability by MTT viability assay (Arkusz et al., 2006; van Meerloo et al., 2011). MTT solution was prepared in sterile phosphate buffered saline (PBS) to a concentration of 0.5 mg/ml. Ten thousand (10,000) cells were seeded in each well of a 96 well plate in a total volume of 0.2 ml DMEM:F12 complete medium. After overnight incubation, cells were washed twice with cell culture grade phosphate buffer saline (PBS) and were subsequently incubated with different concentrations (0-100 µg/ml) of various compounds (agonists) in 0.2 ml of serum free medium (incomplete medium) for the fixed time period of 48 h. Cells treated with incomplete medium alone were considered as 100% viable. Mitomycin-C was considered as positive anti-cancer drug control. After the treatment period, the cells were washed twice with PBS and incubated with 100 µl of MTT (0.5 mg/ml) solution for 4 h at 37°C with 5% CO_2. Then, MTT solution was removed and the formazan crystals were dissolved in 100 µl cell culture grade DMSO. The optical density was determined using a spectrophotometer (SpectraMax M2) at 570 nm and 660 nm (to subtract scattering effects of crystals). Results were expressed as the percent survival in comparison to the control.

2.4 Cell cycle analysis

Propidium Iodide was used to quantitate the DNA content of cells by flow cytometry. Hundred thousand (10^5) cells were seeded in each well of a 6 well plate in DMEM:F12 complete medium for overnight. On the next morning, according to different experiments, cells were treated with different PKC ligands (either drugs, phytochemicals or alkyl cinnamates) in DMEM:F12 serum free medium for 24 h at different concentrations. Post treatment, cells were washed twice with cell-culture grade PBS and then detached from wells using 0.6% EDTA solution prepared in sterile PBS. Cells were centrifuged and re-suspended in 500 µl of PBS. Next, staining was done according to methods described by Keeton et. al. (Keeton and Brown, 2005) with a final concentration of propidium iodide of 10 µg/ml. Stained cells were analyzed immediately at room temperature with BD FACS Caliber flow cytometer. Fifty thousand ($5x10^4$) cells per sample was analysed by flow cytometry. Sample was excited at 488 nm and emission was collected at 585/42 nm filter (FL-2). Distribution of different cell cycle phase cells were analysed by Modfit software (BD Biosciences, USA). Cells treated with only medium was considered as control.

2.5 Acridine Orange & Propidium Iodide (PI) staining of apoptotic and dead cells

Identification of apoptotic or dead cells was done by staining the cells with acridine orange and ethidium bromide staining method as described by leigler at al. (Liegler et al., 1995) and V.Trivedi et. al. (Deshmukh and Trivedi, 2014). Fifty thousand (50,000) cells were seeded into each well of a 24-well plate for overnight in DMEM:F12 complete medium. In each of the experiments, the next morning, cells were treated with different compounds at various concentrations prepared in serum free medium for 24 h time periods. Next, cells were detached from 24-well culture plates with PBS containing 0.6% EDTA. Cells were centrifuged and re-suspended in 500 µl of PBS. Acridine Orange (1 µg/ml) and Propidium Iodide (10 µg/ml) were used to stain cells by incubating for 30 min at room temperature. Stained cells were analyzed immediately with BD FACS Caliber and analysed by Cell Quest pro software (BD Biosciences, USA). Both fluorophores were excited at 488 nm but the emission signals of acridine orange was collected at 530/30 nm filter (FL-1) whereas propidium iodide emission signals was collected at 650 nm filter (FL-3). Quadrant analysis was choosen to differentiate the healthy (lower left), early apoptotic (lower right), late apoptotic (upper right) and necrotic (upper left) cells from the total population of cells. Cells treated with serum free medium alone was considered as control and used to draw initial quadrant.

2.6 DNA-fragmentation assay

DNA fragmentation assay is used to distinguish between healthy, apoptotic and necrotic cells. Lysis of cells and subsequent agarose gel run of genomic DNA produces laddering pattern of apoptotic

cells while shearing pattern in necrotic cells (Nanji and Hiller-Sturmhofel, 1997). Two hundred thousand (2×10^5) cells were seeded in a 6-well plate for overnight in DMEM:F12 complete medium. The following morning the cells were treated with the appropriate concentrations of the various compounds (drugs, phytochemicals or alkyl cinnamates) for 24 h at 37°C in serum free medium. Cells treated with serum free medium were considered as control. Post treatment, cells were washed twice with sterile ice cold PBS and then lysed with lysis buffer (100 mM Tris-HCl pH 8.0 containing 2 mM EDTA and 0.8% w/v SDS). To remove RNA present in the sample the lysate was treated with 2 µl of DNase free RNase A (50 mg/ml) at 37°C for 30 min. After that, Proteinase K (10 µl of 20 mg/ml) was added to samples and incubated for 2 h at 55°C. Samples were then mixed with 6x DNA loading buffer (NEB, USA) and resolved on 1.8% agarose gel containing ethidium bromide (0.3 µg/ml) at 50 mA for 6 h at 4°C. Fragments of DNA were visualized under UV-light and images were captured with a Bio-Rad gel imaging system.

2.7 Intracellular ROS measurement

The intracellular ROS generated was measured with the help of 2′, 7′- dichlorofluorescein diacetate (DCFH-DA), a ROS sensitive fluorescent probe (Cambos and Scorza, 2011; Eruslanov and Kusmartsev, 2010). The DCFH-DA inside the cell is rapidly hydrolyzed by esterases to non-fluorescent DCFH. In presence of ROS molecule, this non-fluorescent DCFH gets converted to highly fluorescent 2′,7′-dichlorofluorescein (DCF). Thirty thousand cells (3×10^4) were seeded in each well of a 24-well plate for overnight in DMEM:F12 complete medium. The following day, one set of cells were treated with compounds alone while the other set was pre-treated for 2 h with 5 mM NAC prior to compound treatment for different time periods. The compounds were used in various concentrations and time periods according to the specific experiment used. Control and compound treated cells were washed with PBS and incubated for 30 min with 10 µM DCFH-DA dye. Next, cells were detached from 24-well culture plates with PBS containing 0.6% EDTA and then cells were centrifuged and re-suspended in 500 µl of PBS. Then, cells were sorted by BD FACS Calibur and analysed by Cell Quest pro software (BD Biosciences, USA). Sample was excited at 488nm and emission was collected at 525/20-nm filter (FL-1).

2.8 Immuno-localization of PKC-α in MDAMB-231 cells

Immuno-fluorescence technique was used to detect immunolocalization of PKC-α after treatment with PKC agonists. Twenty thousand (20,000) cells were seeded in square glass coverslips in DMEM:F12 complete medium and allowed to adhere overnight at 37°C. The following day, coverslips were washed twice with sterile cell culture grade PBS. Next, the cells were treated with respective compounds (drugs, phytochemicals or alkyl cinnamates) prepared in serum-free medium at appropriate concentrations for defined time periods. Cells treated only with serum-free medium served as control. Post-treatment, cells

were washed with PBS and permeabilized & fixed with ice-cold methanol treatment. Next, samples were washed with PBS and blocked with 3% BSA (low fat) prepared in sterile PBS and incubated at room temperature for one hour. Samples were next incubated with anti-PKC-α antibody (BD biosciences) for 16 h at 4°C with intermittent shaking. 1:1000 dilution ratio was maintained for all antibody preparations. Next, cells were again washed with sterile PBS and incubated with anti-mouse antibody conjugated with either alexa-flour-555 dye or FITC dye for 4 h at 37°C with intermittent shaking. However, final steps were performed in two slightly different ways in separate sets of experiments. i) In some experiments, after secondary antibody treatment step, cells were washed twice with PBS and again incubated with filipin dye at 50 µg/ml concentration for 1 h to stain the plasma membrane. Finally, the cells grown over coverslips were washed with PBS, then mounted in clean slides, allowed to dry for 15 min after which they were immediately observed in a Nikon Eclipse 80i fluorescence microscope. ii) In other sets of experiments, instead of filipin, DAPI was used to localize the nucleus. After secondary antibody treatment, the coverslips were washed twice with PBS and mounted in clean slides in DAPI containing mounting medium. Then they were allowed to dry for 15 min after which they were immediately observed in a Nikon Eclipse 80i fluorescence microscope.

2.9 Preparation of membrane and cytosolic fractions

After the treatment phases of experiments, the cells were washed with sterile cell culture grade PBS and then detached with PBS containing 0.6% EDTA and centrifuged at 1000 rpm (~250 xg). The cell pellet was dissolved again in sterile PBS and centrifuged at 1000 rpm as a period of washing. The pellet was hypotonically lysed in 10 mM HEPES buffer (pH 7.4) by passing through a sterile syringe 10 times. The lysate was centrifuged at 1000 xg at 4°C for 5 min. The supernatant obtain was collected and re-centrifuged at 15,000 rpm at 4°C for 30 min. The supernatant and pellet were separated. This supernatant served as cytosolic fraction while the pellet was considered to be as a crude membrane fraction. This pellet was further dissolved in 10 mM HEPES buffer and further centrifuged at 15000 rpm at 4°C for 30 min. The supernatant was discarded while the pellet was again reconstituted in 10 mM HEPES buffer which served as pure membrane fraction. The membrane preparation protocol was validated by doing the marker analysis by the 5'-nucleotidase assay (Section 2.19) and LDH assay (Section 2.11). The membrane and cytosolic fractions were found to be ok as there was no cross-contamination of membrane or cytosolic species to each other.

2.10 Immuno-blotting to detect PKC-α translocation

Level of the presence of PKC-α on membrane and cytosolic fractions was estimated by immunoblotting experiment. MDAMB-231 cells were grown on 6 cm cell culture plates (5×10^5 cells on

each plate) for overnight in DMEM:F12 complete medium. The following day, cells were washed with sterile cell culture grade PBS and treated with the specific compounds (drugs, phytochemicals or alkyl cinnamates) at appropriate concentrations in serum free medium for different time periods. Post treatment, cells were detached and the membrane and cytosolic fractions were accordingly prepared (section 2.9). The amount of total protein was quantified by lowry's method and equal quantity of protein (~40-50 µg) was loaded on a 10% SDS PAGE to separate the proteins. After completion of electrophoresis, the proteins were transferred from the gel to the PVDF membrane (Hybond, GE Healthcare) by western blotting at 110 V for 2 h. Blocking was performed overnight with 5% skim milk prepared in sterile PBS and 0.1% Tween 20. Incubation with anti-PKC-α primary antibody was done at 4°C for 16 h followed by anti-mouse HRP tagged secondary antibody for 8 h at 4°C. Presence of PKC-α on the membrane and cytosolic fractions was detected by chemi-luminescence substrate from chemi-luminescence peroxidase Kit from Sigma Aldrich. Intensity of bands was calculated using ImageJ software. Percentage translocation was calculated as the ratio between membrane and total fractions.

2.11 Lactate Dehydrogenase Assay

Lactate dehydrogenase assay was performed along with immunoblotting experiments for detection of PKC-α. MDAMB-231 cells were grown on 6 cm cell culture plates (5×10^5 cells per plate) for overnight in DMEM:F12 complete medium. Then, cells were treated with the alkyl cinnamates for a period of 30 min at their respective concentrations. Cells treated with serum free medium alone were considered as control. The cells were harvested and cytosolic and membrane fractions were separated as described in section 2.9. Proteins were quantified by Lowry's method and equal quantity of protein was loaded in a 1 ml standard quartz cuvette which contained 0.13 mM NADH and 1 mM sodium pyruvate dissolved in 1 ml of 0.2 M Tris-HCl (pH 7.3). Appropriate blanks were established earlier. The reaction velocity was determined by a decrease in absorbance at 340 nm resulting from the oxidation of NADH (Bergmeyer, 1974). Appropriate blank to nullify the reading of buffer alone was established and subtracted from all the readings. The enzyme (LDH) activity was calculated by the following equation, and expressed as moles of NADH/min/mg .

$$\text{Units (moles) of NADH per min per mg} = \left(\left(\frac{\Delta A340}{\text{min}}\right)\text{sample} - \left(\frac{\Delta A340}{\text{min}}\right)\text{blank}\right) \text{x reaction volume} \; / (6.22 \text{ x } 0.033 \text{ x concentration of original fraction(mg/ml)})$$

Where,

$(\Delta A340/\text{min})_{\text{sample}}$ = The difference between final and initial absorbance of sample at 340 nm ;

$(\Delta A340/min)_{blank}$ = The difference between final and initial absorbance of Blank at 340 nm

Reaction volume = 1 ml

6.22 = The millimolar extinction coefficient of NADH at 340 nm whose unit is in $(mM)^{-1}\ cm^{-1}$

0.033 = Sample volume (ml)

2.12 Immunoblotting to detect phospho-threonine proteins

MDAMB-231cells were grown on 10 cm dishes ($2x10^6$ cells per plate) overnight in DMEM:F12 complete medium. The following day, cells were washed with sterile cell culture grade PBS and treated with 'Danazol (70 µg/ml)' or 'PMA (100 ng/ml)' or PMA+Danazol' in serum free medium for 30 min. The lysate, cytosol and membrane fractions were prepared in the same way as described in section 2.10. The amount of total protein was quantified by lowry's method and equal quantity of protein was loaded on a 10% SDS PAGE to separate the proteins. After completion of electrophoresis, the proteins were transferred from the gel to the PVDF membrane by western blotting at 110 V for 2 h. Blocking was performed overnight with 5% BSA prepared in TBST. Incubation with anti-phospho-threonine primary antibody was done at 4°C for 16 h followed by anti-mouse HRP tagged secondary antibody for 8 h at 4°C. Presence of threonine-phosphorylated proteins on the membrane, lysate and cytosolic fractions was detected by chemi-luminescence substrate from Sigma Aldrich. All bands in the blot were detected by PyElph software.

2.13 Measurement of change in mitochondrial membrane potential

MDAMB-231 cells were seeded (10,000 cells per well) in 96 well plates for overnight in DMEM:F12 complete medium. Next morning, cells were treated with different compounds (drugs, phytochemicals or alkyl cinnamates) with their respective concentrations for 24 h at 37°C in serum free medium. Cells treated with serum free medium were considered as control. Post treatment, cells were washed twice with sterile ice cold PBS and incubated with JC-1 dye (1X in 1X assay buffer) according to kit manufacturer's protocol (BD-Biosciences) for 20 min at 37°C, 5% CO_2 incubator. Finally, cells were gently washed once in PBS and then the bright field and fluorescence images were acquired by using Cytell system (GE Healthcare).

2.14 Immuno-localization to study cytochrome-c (cyt-c) release

MDAMB-231 cells were seeded (10,000 cells per well) in 96 well plates for overnight in DMEM:F12 complete medium. In other experiments, 10,000 cells were seeded in coverslips for overnight.

The next morning, cells were treated with different compounds (drugs, phytochemicals or alkyl cinnamates) at their respective concentrations for 24 h in serum free medium. Post-treatment, cells were washed with PBS and were incubated with mitotracker-Red at 200 nM concentration (as per manufacturer's instructions) prepared in serum free medium for 45 min to stain mitochondria. After that the cells were washed once in PBS and incubated with primary anti-cyt-c antibody (BD biosciences, mouse origin) for 16 h at 4°C to stain cyt-c. Cells were again washed with sterile PBS and incubated with anti-mouse antibody conjugated with FITC for 4 h at 37°C with intermittent shaking. Finally, the cells were washed twice with PBS and then the bright field and fluorescence images were acquired by using Cytell system (GE Healthcare). In case of coverslips, finally, the coverslips were washed twice with PBS and mounted on clean slides, allowed to dry for 15 min, and observed with a Nikon Eclipse 80i fluorescence microscope.

2.15 Caspase-3 assay

Caspase-3 assay was carried out by BD-Pharmingen caspase-3 assay kit, Cat no: 556485. The kit contains Ac-DEVD-AMC, a synthetic tetrapeptide fluorogenic substrate that is cleaved between D and AMC, releasing the fluorescent AMC which can be quantified in cell lysates by ultraviolet (UV) spectrofluorometry using an excitation wavelength of 380 nm and an emission wavelength range of 420-460 nm. MDAMB-231 cells ($2x10^6$) cells were grown on 10 cm well plates for overnight in DMEM:F12 complete medium. The next morning cells were treated with various compounds at IC_{50} concentrations for 24 h in serum free medium. Cells treated with serum-free medium alone served as controls. Post treatment, the cells were washed twice with sterile PBS and resuspended in cold-cell lysis buffer (Component No: 51-6636KC) for 30 min. The amount of total protein for each sample was quantified by lowry's method. For each reaction or time point, 5 µl reconstituted caspase-3 fluorogenic substrate Ac-DEVD-AMC (Component No. 51-66081U) was added to a well containing 200 µl of 1X HEPES buffer (Component No: 51-6637KC). To it, equal quantity of cell-lystae proteins (~100 µg) was added. Reaction mixtures were incubated for 1 h at 37°C. Reaction mixture with Ac-DEVD-AMC only and without cell-lysate served as blank. The amount of AMC liberated from Ac-DEVD-AMC was measured using a plate reader (Spectramax, M2) with an excitation wavelength of 380 nm and an emission wavelength range of 420-460 nm.

2.16 Caspase-9 assay

Caspase-9 assay was carried out by Invitrogen caspase-9 colorimetric kit,Cat no:KHZ0101. The kit contains the colorometric substrate LEHD-pNA, a synthetic peptide (sequence: LEHD) conjugated to the chromophore, p-nitroanilide (pNA). Upon cleavage of the substrate by caspase-9, absorption of light

by free pNA can be quantified using a spectrophotometer or a microtiter plate reader at 400 or 405 nm. MDAMB-231 cells ($2x10^6$) cells were grown on 10 cm well plates for overnight in DMEM:F12 complete medium. The next morning cells were treated with various compounds at IC_{50} concentrations for 24 h in serum free medium. Cells treated with serum-free medium alone served as controls. Cells were then detached with PBS containing 0.6 % EDTA and centrifuged at 1000 rpm. The cell pellet was dissolved again in 50 µl of chilled Cell Lysis Buffer (provided along with kit) and incubated on ice for 10 min. Next, cell-lystae was re-centrifuged for 1 min (10,000 x g) and the supernatant obtained was transferred to a fresh tube and put on ice. The total protein concentration in each ample was assayed by lowry's method and was accordingly adjusted to ~100 µg/50 µl. Then, 50 µl of sample was put into each well of a 96-well microtitre plate. Next, to each well 50 µl of 2x Reaction Buffer (provided in kit) containing 10 mM dithiothreitol, DTT was added. Then, to each well 5 µl of the 4 mM LEHD-pNA substrate (200 µM final concentration) was added. The reaction plate was incubated at 37°C for 2 h in dark condition. Finally, samples were read at 405 nm in a microplate reader (Spectramax, M2). Fold-increase in Caspase-9 activity was determined by direct comparison to the level of the uninduced control.

2.17 Estimation of lipid peroxidation level

MDAMB-231 cells were seeded as thirty thousand (30,000) cells per well in a 24 well plate for overnight in DMEM:F12 complete medium. The following day, cells were treated with different compounds for the appropriate time periods (30 min to 4 h). Next, cells were immediately lysed with 1% Triton X-100 in cold environment (4°C). Small amount of cell lysate (20 µl) was used to measure the protein level by Lowrys' method. 200 µl of lysate were mixed with equal volume of ice cold (4°C) trichloro acetic acid (TCA - 10%) and left it for 15 min in ice flakes for protein precipitation. TCA-cell lysate mixture was centrifuged at 3000 rpm (~1000 xg) for 15 min at 4°C and 300 µl of supernatant was heated with equal volume of thiobarbituric acid (0.67%) in a boiling water bath for 10 min. Developed pink coloured solution was measured at 532 nm colorimetrically (Spectramax, M2). Obtained values are matched with the standard curve and the final lipid peroxidation values were normalized with the total protein present in the lysate. Compound untreated samples were used as control and used to calculate the fold changes (Trivedi et al., 2005).

2.18 Estimation of protein carbonyl level

To measure the protein carbonyl level, till the compound treated cell lysate step, preparation process was followed as described in section 2.17. Then cell lysate was aliquoted equally and labelled as blank as well as sample. Further both aliquotes were treated with equal volume of ice cold TCA (10 %). After 15 min incubation, samples were centrifuged at 3000 rpm for 15 min at 4°C and obtained sample-

pellet was incubated with 500 µl of dinitrophenylhydrazine (DNPH - 0.2 %) in 2 N HCl for 2 h at 37°C. Simultaneously, blank-pellet was incubated with 2N HCl. All the samples were again treated with 55 µl of TCA (100%) and centrifuged at 8000 rpm for 10 min at room temperature (RT). Samples were washed thrice with ethanol:ethylacetate (1:1) mixture. Pelletes are dissolved in 600 µl of guanidine HCl (6M) in 20 mM sodium phosphate buffer (pH 6.5) and measured at 370 nm calorimetrically (Spectramax, M2). Molar extinction coefficient value for the protein carbonyl is 21 mM at 370 nm which was used to calculate the protein carbonyl level. Blank values were used to substract the corresponding samples protein carbonyl level. Values were recalculated according to the proteins level present in the samples and converted into folds as mentioned earlier in section 2.2.4 (Trivedi et al., 2005).

2.19 Detection of 5'-nucleotidase in membrane fraction

5'-nucleotidase is an enzyme which is exclusively present in the cell-membrane of mammalian cells. Presence or absence of this enzyme in different centrifuged fractions can serve to prove the purity of membrane fractions after centrifugation. MDAMB-231 cells were seeded in 60 mm cell-culture plates as $5x10^5$ cells per plate and treated with the concerned compounds for defined time periods at their respective concentrations. Next, the cells were washed once with sterile PBS and then detached with PBS containing 0.6% EDTA and separated into membrane and cytosolic fractions as described earlier section 2.9. The final membrane and cytosolic fractions obtained were separated in two 10% SDS PAGE gels and both the gels were electro-blotted into two PVDF membranes. The membranes were blocked in skim milk at 4°C overnight and then washed with sterile TBST buffer. One membrane was probed with anti-PKC-α antibody (1:1000 dilution & mouse origin) while the other membrane was probed with anti-5'-nucleotidase antibody (1:1000 dilution & rabbit origin) at 4°C overnight. Next, membranes were washed gently with TBST buffer and re-probed with anti-mouse HRP tagged antibody and anti-rabbit HRP tagged antibody for 8 h at 4°C respectively. Presence of PKC-α and 5'-nucleotidase were detected by chemi-luminescence peroxidase kit.

2.20 References

- Arkusz, J., Stepnik, M., Trzaska, D., Dastych, J., and Rydzynski, K. (2006). Assessment of usefulness of J774A.1 macrophages for the assay of IL-1beta promoter activity. Toxicology in Vitro *20*, 109-116.
- Bergmeyer, H.U., and Bernt, E. (1974). Methods of Enzymatic Analysis; Bergmeyer, H.U., 2nd ed. Academic Press: New York, NY *Volume II*, 574-579.
- Cambos, M., and Scorza, T. (2011). Robust erythrophagocytosis leads to macrophage apoptosis via a hemin-mediated redox imbalance: role in hemolytic disorders. Journal of Leukocyte Biology *89*, 159-171.
- Deshmukh, R., and Trivedi, V. (2014). Phagocytic uptake of oxidized heme polymer is highly cytotoxic to macrophages. PloS One *9*, e103706.

- Eruslanov, E., and Kusmartsev, S. (2010). Identification of ROS using oxidized DCFDA and flow-cytometry. Methods in Molecular Biology *594*, 57-72.
- Keeton, E.K., and Brown, M. (2005). Cell cycle progression stimulated by tamoxifen-bound estrogen receptor-alpha and promoter-specific effects in breast cancer cells deficient in N-CoR and SMRT. Molecular Endocrinology *19*, 1543-1554.
- Liegler, T.J., Hyun, W., Yen, T.S., and Stites, D.P. (1995). Detection and quantification of live, apoptotic, and necrotic human peripheral lymphocytes by single-laser flow cytometry. Clinical and Diagnostic Laboratory Immunology *2*, 369-376.
- Nanji, A.A., and Hiller-Sturmhofel, S. (1997). Apoptosis and necrosis: two types of cell death in alcoholic liver disease. Alcohol Health and Research World *21*, 325-330.
- Trivedi, V., Chand, P., Srivastava, K., Puri, S.K., Maulik, P.R., and Bandyopadhyay, U. (2005). Clotrimazole inhibits hemoperoxidase of Plasmodium falciparum and induces oxidative stress. Proposed antimalarial mechanism of clotrimazole. The Journal of Biological Chemistry *280*, 41129-41136.
- van Meerloo, J., Kaspers, G.J., and Cloos, J. (2011). Cell sensitivity assays: the MTT assay. Methods in Molecular Biology *731*, 237-245.

2.21 Appendix I

Materials: Acridine Orange (AO), Agarose, Propidium Iodide (PI), 2′, 7′- dichlorofluorescein diacetate, Dulbecco's modified eagle's medium, Ethidium Bromide (Et-Br), Glutaraldehyde, Guanidine hydrochloride, Methemoglobin, N-acetylcysteine (NAC), Paraformaldehyde, Tetramethylethylenediamine (TEMED), Thiobarbituric acid, Thiourea, 2',7'-3-(4,5-dimethylthiazol-2-yl)-2,5-diphenyltetrazoliumbromide (MTT), 1,1',3,3' tetraethoxy propane (malonaldehyde) were purchased from Sigma (St. Louis, USA). DMSO, Foetal Bovine Serum (FBS), Guaiacol, Penicillin-Streptomycin (100X) antibiotic solution, Phosphate Buffer Saline (PBS), Proteinase K, RNase A, Sodium Azide, Trypan blue and Trypsin-EDTA were purchased from Himedia (Mumbai, India). Ethylenediaminetetraacetic acid (EDTA), Ethanol 100%, Ethylacetate, Hydrogen peroxide (H_2O_2), Sodium chloride, Trichloroacetic acid (TCA) and TritonX-100 was purchased from Merck (Massachusetts, USA). Anti-PKC-α and anti-cyt-c antibodies, Mitotracker Red and JC-1 dye were from BD-biosciences (New Jersey, USA). Anti-5'-nucleotidase antibody was purchased from Cell Signalling Technology (Massachusetts, USA). PVDF membrane was from brand Hybond which was purchased from GE Healthcare (Chicago, USA). Caspase-3 assay kit was from BD-Pharmingen (New Jersey, USA). Caspase-9 colorometric kit was from Invitrogen Corporation (Waltham, USA). DMEM:F12 was purchased from Hyclone (Logan, USA). All the cell culture plates and dishes were purchased from Corning (New York, USA). MDAMB-231 and MCF-7 cell lines were procured from Tissue & Cell

Culture Unit, Central Drug Research Institute (Lucknow, India). All other reagents and chemicals were of analytical grade purity.

2.22 Appendix II

Buffer, reagents and culture growth media

A. Dulbecco's modified eagle's medium:F12 (DMEM:F12): This medium was used for breast cancer cell culture. The composition and method of preparation is as follows:

Table 2.1: Composition of DMEM:F12 medium

Components	Composition
DMEM F12	15.6 gm/l
Sodium bicarbonate	1.2 gm/l
HEPES	15 mM
Fetal bovine serum (FBS)	10% (v/v)
100X Antibiotic (Penicillin –Streptomycin)	1% (v/v)

Preparation: For making one litre media around 880 ml of cell culture grade (milliQ) water is collected. After that 15.6 gm of DMEM F12 powder is slowly dissolved in the water with the aid of a magnetic stirrer. After the powder is completely dissolved, 1.2 gm of sodium bicarbonate is added and allowed to dissolve completely. Next, the pH is adjusted to 7.1 using 1N NaOH or 1N HCl (as during filtration the pH of bicarbonate buffered solutions usually rises by 0.1 - 0.2 units). Finally, the total volume is adjusted to 890ml with the same cell culture grade water. This is considered as the unfiltered incomplete medium. This incomplete medium is then passed through a sterile filtration unit fitted with 0.22 μm membrane filter to prepare sterile incomplete medium. This incomplete medium is now added with supplements 10% (100 ml) fetal bovine serum and 1% (10 ml) penicillin–streptomycin antibiotic solution (100 units/ml penicillin and 100 μg/ml streptomycin sulfate) and again passed through a sterile filtration unit fitted with 0.22 μm membrane filter to prepare 1 litre of complete media.

B. Lysis buffer (RIPA): 100 mM Tris-Cl pH 8 containing 2 mM EDTA and 0.8% w/v SDS and 0.5% Triton

C. Hypotonic buffer (HEPES): 10 mM HEPES buffer pH 7.4

D. SDS-PAGE: Sodium dodecyl sulphate polyacrylamide gel electrophoresis was used for the electrophoretic separation of proteins. Stock solution for SDS-PAGE were prepared as described in Table 2.2. The components for preparing running buffer of electrophoresis and sample loading buffer is given

in Table 2.5. The resolving gel (Table 2.3) and stacking gel (Table 2.4) were prepared using the components described in Table 2.2. All the solutions were prepared in de-ionized water.

Table 2.2: Recipe for the preparation of stock reagents for SDS-PAGE.

Stock reagent	Preparation
Acrylamide solution (30%)	1 gm of N'N'-methylene-bis acrylamide was dissolved in 50 ml ultra pure deionized water collected at 18 MΩcm (Millipore, Milli-Q water purification system) in amber colored bottle. On complete dissolving,29 gm acrylamide was added to it and stirred on a magnetic stirrer till the clear solution was formed. The final volume was adjusted to 100 ml. The solution was filtered (Whatman No. 1) and stored at 4°C in dark.
Tris HCl (1.5 M, pH 8.8)	54.45 gm Tris base was dissolved in 150 ml deionized water. The pH of solution was adjusted to 8.8 using HCl and volume made to 300 ml. It was stored at 4°C.
Tris HCl (1M, pH 6.8)	Tris base 6 gm was dissolved in 60 ml deionized water. The pH of solution was adjusted to 6.8 using HCl and volume made to 100 ml. Itwas stored at 4°C.
SDS (10%, w/v)	10 gm sodium dodecyl sulfate (SDS) was dissolved in 60 ml deionized water. The volume made to 100 ml.
APS (10%, w/v)	100 mg ammonium per sulfate (APS) was dissolved in 1 ml water.

Table 2.3: Recipe for the preparation of resolving gel of SDS-PAGE (10 ml)

Components (ml)	8%	10%	12%	15 %
Deionized water	2.3	1.9	1.6	1.1
30% acrylamide solution	1.3	1.7	2.0	2.5
1.5 M Tris (pH 8.8)	1.3	1.3	1.3	1.3
10% (w/v) SDS solution	0.05	0.05	0.05	0.05
10% (w/v) APS solution	0.05	0.05	0.05	0.05
TEMED	0.003	0.002	0.002	0.002

Table 2.4: Recipe for the preparation of 5% stacking gel

Components (ml)	5 ml	10 ml
Deionized water	3.4	6.8
30% acrylamide solution	0.83	2.0
1 M Tris (pH 6.8)	0.63	2.5
10% (w/v) SDS solution	0.05	0.1
10% (w/v) APS solution	0.05	0.1
TEMED	0.005	0.010

Table 2.5: Recipe for the preparation of 5X running buffer and loading buffer	
Solution	**Preparation**
5x Running buffer	15 gm Tris base, 5 gm SDS and 72 gm glycine were dissolved in 800 ml ofde-ionized water. The pH was adjusted to 8.3 and volume was adjusted to1000 ml. The solution was filtered (Whatman, Filter No. 1) and stored at 4°C. The buffer (5X) was diluted to 1X and pre-warmed at 37°C before use.
5x Loading buffer	10 ml 0.5 M Tris (pH 6.8), 1.6 ml SDS 10%, 10 ml glycerol, 0.4 ml β-mercaptoethanol and 0.4 ml 0.5% (w/v) bromophenol blue were dissolved in 3 ml deionized water and pH was adjusted to 6.8. The final concentration of buffer was 1X by mixing 1 volume of 5X sample loading buffer to 4 volumes of sample (protein) before loading in gel.

Table 2.6: Recipe for the preparation of 1X tank buffer for SDS-PAGE (1 litre)	
Components(ml)	**Quantity gm)**
Tris	3 gm
Glycine	14.4 gm
SDS	1 gm

Finally, adjust the volume to one litre with MQ water

Table 2.7: Recipe for the preparation of Transfer Buffer for Western Blot (2 litre)	
Components(ml)	**Quantity**
Glycine	22.52 gm
Tris Base	4.84 gm
Methanol	400 ml

Finally, adjust the volume to two litre with MQ water

Table 2.8: Recipe for the preparation of Wash Buffer for Western Blot (2 litre),with final pH 7.5 (adjusted)	
Components (ml)	**Quantity**
Tris Base	4.856 gm
NaCl	17.532 gm
Tween	1 ml

Finally, adjust the volume to two litre with MQ water

E. Sample preparation and running of SDS-PAGE: The 36 µl of sample was mixed with 4 µl of 10x loading buffer and was loaded on the 10% SDS-PAGE. Electrophoresis was carried out in 1X running buffer with a constant current of 50 V for first1 hr (to stack the protein) and then 75 V after samples moves out of the stacking gel. Electrophoresis continued until dye front reaches to the other end of the gel.

F. Protein estimation by Lowry's method

Procedure: To 20 µl of sample containing protein, 1ml of reagent C was added. After 15 mins, 100 µl of phenol reagent was added and the solution was mixed. The absorbance at 660 nm (A660) was measured after 30 mins against a blank and the protein concentration was calculated from BSA standard curve of (0.1-10 mg/ml).

Table 2.9: Recipe for preparation of reagents used in Lowry's method

Reagents	Components	Amount	Procedure
Reagent A	Sodium carbonate	2.0 gm	Both the components were dissolved in de-ionized water and volume was made to 100 ml.
	Sodium hydroxide	0.4 gm	
Reagent B1	Sodium potassium tartarate	2% (w/v)	1 gm was dissolved in 50 ml de-ionized water.
Reagent B2	Cupric sulphate	1% (w/v)	0.5 gm was dissolved in 50 ml in de-ionizedwater.
Reagent C	Freshly prepared by mixing Reagent B1, Reagent A and Reagent B2 in the ratio 1:100:1.		
Folin-Ciocalteu reagent(2N)	2N Folin-Ciocalteu reagent (1ml) was dissolved in 1 ml de-ionized water		

Table 2.10: Recipe for preparation of MTT solution

MTT powder	10 mg
Sterile PBS	20 ml

Dissolve the MTT powder in PBS and finally filter with a 0.22 µm syringe filter.

Chapter 3

Identification of PKC-directed ligands from different sources.

3.1 Introduction

Protein Kinase C is the most prominent signalling protein that responds to stress/growth-linked signalling pathways. A structurally diverse range of compounds (Fujiki and Sugimura, 1987; Hecker, 1968; Hecker et al., 1983; Lewin et al., 1991; Shao et al., 2001) have been recognized in addition to diacylglycerols (DAGs) that can bind to the C1 domain of PKC. Diverse PKC ligands differentially translocate PKC to different micro-domains of a variety of biological membranes in the cell. This translocation properties directly result in different biological responses of PKC signalling. PKC signalling is modulated in cancer to modulate the growth or apoptotic signals (Castagna et al., 1982; Santiago-Walker et al., 2005). PKC acts as the downstream signalling molecule of many anti-cancer agents (Mackay and Twelves, 2003; Marengo et al., 2011). Thus, PKC is being probed to design new therapeutic agents which are in clinical trials (Chu and O'Brian, 2005; Deissler and Lang, 2016; Kim et al., 2011; Mackay and Twelves, 2003; Mizuno et al., 1993; Verdelli et al., 2009; Young et al., 2005). Hence, PKC has emerged as an important molecule for chemotherapy as PKC can mediate cell-cycle arrest or induce apoptosis in many types of cancer cells (Nakagawa et al., 2005; Sun and Rotenberg, 1999; Yoshida, 2007).

This chapter discusses the strategies (workflow in Figure 3.1) undertaken to identify novel ligands for PKC with a prospect to develop an anti-cancer therapy based on modulation of PKC signalling. For that purpose, diverse molecules were collected from different sources (chemical libraries and phytochemical databases). These molecules were tested under the in-silico virtual screening platforms to identify the molecules that bind to the C1b domain of PKC. Then, these were verified by an agonist competition assay to understand whether the interaction is specific or non-specific towards the C1b domain. Docking results from chemical libraries produced hits which were utilized to identify already approved drug molecules from DrugBank that were structurally at least 70% or more similar to the top-hit heterocyclic molecules. For phytochemicals, top hits (from the docking results) were selected which were known to possess medicinal property and were readily available for further studies. In-depth interaction analysis of the chosen ligands and the receptor were undertaken in order to understand the basis of higher affinity between the candidate ligands and PKC. This chapter is devoted to describing the complete details of identification of the PKC-directed molecules that can potentially be used in anti-cancer therapy for breast cancer.

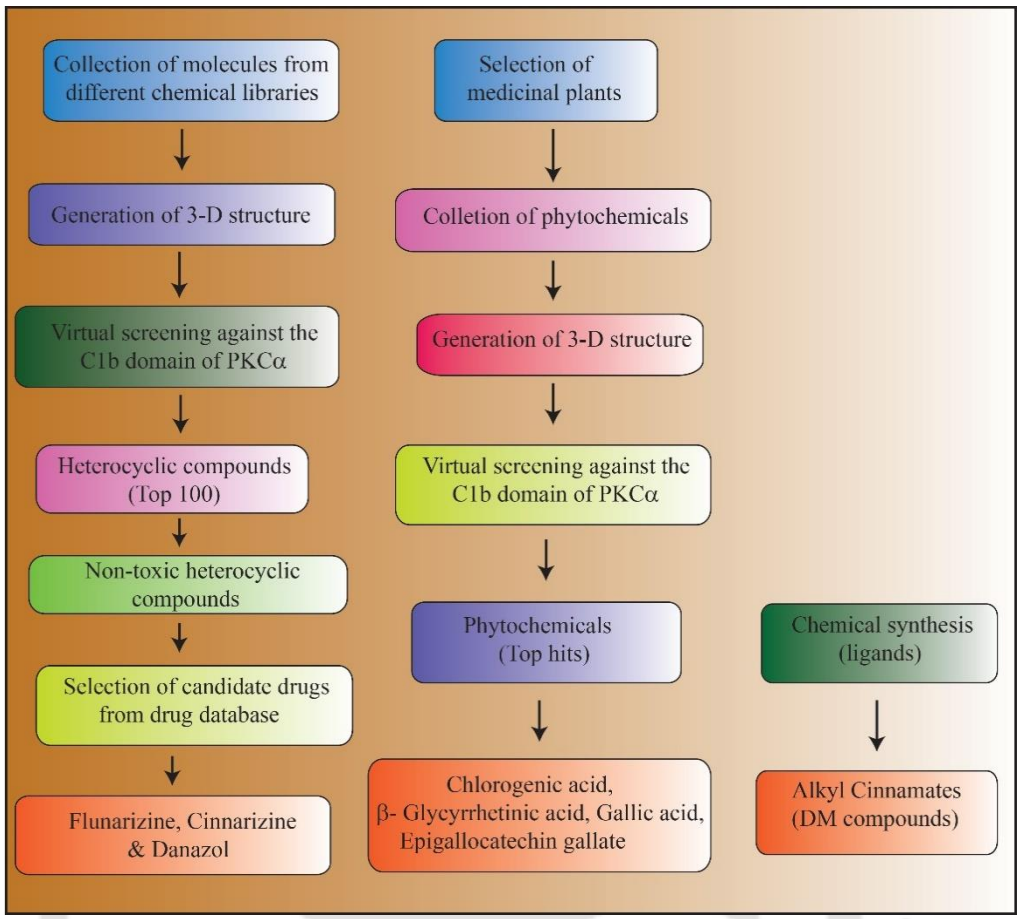

Figure 3.1: Illustration of experimental approach pursued in Chapter 3

3.2 Experimental procedures

3.2.1 Collection of heterocyclic molecules from chemical libraries: Zinc database (http://zinc.docking.org/) is a good source of drugs and heterocyclic compounds with their detailed 3-Dimensional (3-D) structures. This database was chosen to select the subset of all drug-like compounds. The 3-D structures of these molecules (approximately 8,000 molecules) were downloaded in mol2 format. The mol2 structures were then converted to PDB format and used for docking to the C1b domain of PKC-α as the drug target.

3.2.2 Collection of phytochemicals from medicinal plants found in north-eastern (NE) India: The list of plants present in north-eastern India with known medicinal properties was collected through literature search. A comprehensive list of these plants is given in Appendix I and names of selected plants is given in Table 3.1. The phytochemicals present in each plant were collected from Dr.Duke's phytochemical and ethnobotanical databases (https://phytochem.nal.usda.gov/phytochem/search). A unique set of phytochemicals representing all plants was prepared. Then, amongst all the phytochemicals, we selected only the phytochemicals with a previously known medicinal property. Finally, ~100

phytochemicals were selected for our study. The 3-D structures of all these phytochemicals were downloaded from various libraries (PubChem, zinc database, ChemSpider, etc.). Finally, all the structures were converted to PDB format with the help of Open Babel software (openbabel.org/).

Table 3.1: List of selected medicinal plants present in north-eastern India

S no.	Botanical Name	Common Name	Ethnobotanical uses
1.	*Camelia sinensis*	Tea	Used as a beverage. Also used as a carminative, CNS stimulant and also possess anti-cancer property.
2.	*Coffea arabica L*	Coffee	Used as a beverage. Also used as a cardiotonic, CNS stimulant, treatment of asthma and headache.
3.	*Curcuma longa*	Indian Saffron; Turmeric	Key spice of many South Asian and Middle Eastern cooking. Extracts from turmeric have antifungal and antibacterial properties.
4.	*Curcuma xanthorrhiza*	Temu Lawak; Javan Turmeric	It is used as a spice. Useful for treating digestive disorders and anti-inflammation.
5.	*Zingiber officinale*	Ginger	Used as a spice. It is used to treat digestive disorders, treatment of fever, nausea and vomiting and possess anti-microbial property.
6.	*Capsicum annuum*	Paprika; Green Pepper; Cherry Pepper; Bell Pepper; Cone Pepper; Sweet Pepper	Used as a spice. It is used in combination homeopathic and natural preparations. It is used as a relief of oral discomfort or toothache, external analgesia, as a digestive aid, in menstrual conditions, and in cosmetics as cleansers and bath products.
7.	*Arnica montana*	Arnica; Dagtutunu	Used in the treatment of fever, as a cardiotonic and in the treatment of cancer.
8.	*Acacia nilotica*	Babli; Gumarabic	Used as a decongestant, treatment of gall-bladder, spleen and as an anti-cancer agent.
9.	*Hibiscus sabdariffa*	Roselle; Oseille De Guinee; Vinagrillo; Maravilla; Kerkedeh; Chai Kujarat; Afrika Bamyasi	Used as a flavouring agent. Also used to lower pressure in hypertension.
10.	*Nicotiana tabacum*	Tabigh; Tobacco; Tabaco	Used for curing toothache, antidote to bee-sting, centipede bites,scorpion-bites. Used in asthma. Used as Parasiticide, anti-cancer agent and CNS stimulant.

Selected list of plants with medicinal value selected from Dr. Duke's database. See Appendix 1 for full list.

3.2.3 Molecular Modeling and Docking Studies: The NMR 3-D structure of the C1b domain of PKC-α (PDB ID: 2ELI) was downloaded from Protein Data Bank in PDB format. The average structure was drawn taking the rmsd values of all the conformations. The 3-D structures of the ligands were downloaded from Zinc database. The virtual docking experiment was performed by AutoDock 4.1 program suite of MGL Tools 1.5.4 software (Morris et al., 2009). For PKC-α, polar hydrogen, Kollman charges, and atomic solvation charges were defined, and a grid of 0.375Å was centred around the potential ligand binding

pocket of the C1b domain using the autogrid module of autodock 4.1. Next, the Grid Parameter File (GPF) was defined. For the ligand molecules polar hydrogens, atomic charges, and flexible torsions were accordingly defined. A number of docking parameters such as the number of generations, energy evaluation, and the GA run were set as 27000, 2500000 and 100 respectively. Genetic algorithm was used to perform docking simulations. Binding energy obtained from docking experiments are reported in kcal/mol.

3.2.4 In-silico agonist competition assay: The top-hit molecules from initial docking experiments were used for the agonist competition assay. Agonist competition gives us a real idea to what extent the candidate ligands can mimic the binding pattern of a well-known agonist such as PMA. Hence, ligand molecules were docked again but this time the molecules were docked against the structure of PMA bound C1b domain complex (C1b-PMA) instead of the native C1b domain. The receptor and ligand preparations, grid and docking parameters remained the same as for initial docking using the native C1b domain of PKC. The results of competition docking experiments were taken into consideration for selection of the ligands. Final lists of selected molecules were prepared by subtracting binding energy of competition assay from the binding energy of docking results with the native C1b domain of PKC-α.

3.2.5 In-silico toxicity determination of heterocyclic compounds: Heterocyclic compounds are known in their potential carcinogenic hazard towards mammalian life, whereas phytochemicals are of no concern in this aspect as they are readily available in edible beverages, fruits, vegetables and plants. The toxicity and carcinogenic potential of the top hit heterocyclic compounds was determined to select the non-carcinogenic and non-toxic molecules for further studies. The toxicity and mutagenic potentials of the top-hit heterocyclic molecules were predicted by ToxPredict (toxpredict.org/)(Willighagen et al., 2011). Toxpredict (www.toxpredict.net) is a server that is used to estimate the chemical hazard of any chemical structure. ToxPredict was utilized to calculate the carcinogenic and mutagenic potential of the heterocyclic compounds. Tox Predict utilizes open Tox API-v1.1 web services to estimate the chemical hazard any chemical structure. ToxPredict can also predict if any compound is non-carcinogenic in single-cell, rat and hamster based carcinogenicity models.

3.2.6 Analysis of PKC-ligand docked complexes and interaction analysis: After the docking simulation was over, each of the PKC-ligand molecular models was taken for analysis. The PKC-ligand molecular models were analyzed in PyMOL v0.99 (Schrodinger, 2010) and interaction analysis was performed by LigPlot^{+} software (Wallace et al., 1995). The PKC residues were numbered as per the convention followed in the PDB of PKC 3-D structure.

3.3 Results

3.3.1 PKC directed molecules can be found amongst heterocyclic molecules: The virtual screening technique has identified around 300 molecules that may be potential ligands of PKC-α. The binding energy of PMA to PKC-α was found to be -3.24 kcal/mol. It is observed that most of the compounds showed a better binding energy to the C1b domain compared to PMA. Docked molecular complexes of ligands with C1b domain indicated that different ligands bind to slightly different positions of the polar groove of the C1b domain.

The top 300 molecules in the earlier docking experiment were arranged according to the binding energies. These 300 molecules were used for the agonist competition assay as described in Chapter 3 (Section 3.2.4). The agonist competition assay showed that many molecules indeed bind in a similar manner to PMA to the C1b domain. But some molecules do bind differently and hence are excluded from further analysis. Based on the results of the agonist competition assay, only 60 molecules were chosen out of the initially identified 300 molecules. The docking results of the chosen top 60 molecules are presented in Table 3.2. Thus, the top 60 molecules (Table 3.2) that have shown almost negligible non-specific binding are finally selected

Table 3.2:Top-hit heterocyclic compounds from molecular docking experiments

Serial No.	Zinc ID	Binding Energy (PKC-α alone) (kcal/mol) (A)	Binding Energy (PKC-α+PMA) (kcal/mol) (B))	Difference (A-B) (kcal/mol)
1.	ZINC04097427	-7.63	42.7	-50.33
2.	ZINC53683151	-7.25	41.06	-48.31
3.	ZINC03780340	-7.14	30.86	-38
4.	ZINC03995608	-7.94	19.32	-27.26
5.	ZINC52955754	-7.36	17.66	-25.02
6.	ZINC14255250	-7.41	16.12	-23.53
7.	ZINC11592877	-7.38	9.16	-16.54
8.	ZINC03830288	-7.47	3.06	-10.53
9.	ZINC13760709	-7.11	1.83	-8.94
10.	ZINC05561290	-7.25	1.68	-8.93
11.	ZINC03830840	-7.34	1.24	-8.58
12.	ZINC11592705	-7.36	1.12	-8.48
13.	ZINC03873789	-7.08	1.36	-8.44
14.	ZINC01494900	-8.17	-0.2	-7.97
15.	ZINC11592633	-7.26	0.28	-7.54
16.	ZINC14880002	-7.51	-0.09	-7.42
17.	ZINC27439698	-7.14	0	-7.14
18.	ZINC11592704	-7.33	-0.33	-7
19.	ZINC11592703	-7.45	-0.46	-6.99

20.	ZINC27305632	-7.45	-0.47	-6.98
21.	ZINC04215623	-7.29	-0.39	-6.9
22.	ZINC34853956	-7.64	-0.84	-6.8
23.	ZINC11592631	-7.86	-1.55	-6.31
24.	ZINC04217387	-7.25	-0.95	-6.3
25.	ZINC00608041	-7.26	-1.08	-6.18
26.	ZINC11592737	-7.47	-1.36	-6.11
27.	ZINC01493454	-7.12	-1.16	-5.96
28.	ZINC03830599	-7.32	-1.38	-5.94
29.	ZINC03985982	-7.23	-1.53	-5.7
30.	ZINC05458886	-7.25	-1.68	-5.57
31.	ZINC00538564	-7.18	-1.76	-5.42
32.	ZINC04212747	-7.44	-2.1	-5.34
33.	ZINC00597691	-7.39	-2.06	-5.33
34.	ZINC04084618	-7.15	-2.01	-5.14
35.	ZINC13298436	-7.33	-2.24	-5.09
36.	ZINC00538119	-7.22	-2.19	-5.03
37.	ZINC03872177	-7.19	-2.23	-4.96
38.	ZINC00900663	-7.17	-2.32	-4.85
39.	ZINC01490477	-7.37	-2.53	-4.84
40.	ZINC01482030	-7.08	-2.38	-4.7
41.	ZINC04217507	-7.44	-2.76	-4.68
42.	ZINC22026394	-7.21	-2.54	-4.67
43.	ZINC03830838	-7.33	-2.69	-4.64
44.	ZINC03830796	-7.19	-2.63	-4.56
45.	ZINC00388658	-7.47	-2.91	-4.56
46.	ZINC22010289	-7.19	-2.7	-4.49
47.	ZINC04102205	-7.22	-2.75	-4.47
48.	ZINC04215736	-7.29	-2.83	-4.46
49.	ZINC22001688	-7.32	-2.94	-4.38
50.	ZINC03830794	-7.31	-2.98	-4.33
51.	ZINC01481814	-8.11	-3.82	-4.29
52.	ZINC11592646	-7.47	-3.23	-4.24
53.	ZINC43707316	-7.1	-2.88	-4.22
54.	ZINC03875518	-7.08	-2.89	-4.19
55.	ZINC03830738	-7.15	-3.02	-4.13
56.	ZINC03830883	-7.15	-3.02	-4.13
57.	ZINC00538633	-7.37	-3.25	-4.12
58.	ZINC21985528	-8.02	-3.9	-4.12
59.	ZINC00000828	-7.17	-3.12	-4.05
60.	ZINC13298661	-7.09	-3.04	-4.05
61.	PMA	-3.24	not applicable	not applicable

Binding energies of top 60 heterocyclic compounds after docking simulations using Autodock 4.1

3.3.2 Most of the top-hit heterocyclic compounds are non-toxic and non-carcinogenic: Toxicity & carcinogenicity predictions were performed with Toxpredict (Section 3.2.5). Toxpredict indicates that a sizeable number of the top compounds are non-mutagenic in bacterial system (Salmonella) and mammalian cell system (Table 3.3). ToxPredict also notified which of the compounds were non-carcinogenic in single-cell, rat and hamster based carcinogenicity models (Table 3.3). These results were taken into consideration. The finally selected molecules were the ones with no toxicity aspects.

Table 3.3: Mutagenic and Carcinogenic Descriptors of Top Hit Heterocyclic Compounds

Molecule	Mutagenicity	Kazius-Bursi Salmonella mutagenicity	Carcinogenic Potency in Single Cell	Carcinogenic Potency in Rat:	Carcinogenic Potency in Hamster
ZINC00388658	non-mutagenic	non-mutagenic	non-carcinogen	non-carcinogen	non-carcinogen
ZINC11592646	non-mutagenic	non-mutagenic	non-carcinogen	non-carcinogen	non-carcinogen
ZINC01482030	non-mutagenic	non-mutagenic	non-carcinogen	non-carcinogen	non-carcinogen
ZINC03872177	non-mutagenic	non-mutagenic	non-carcinogen	non-carcinogen	non-carcinogen
ZINC04102205	non-mutagenic	non-mutagenic	non-carcinogen	non-carcinogen	non-carcinogen
ZINC04215736	non-mutagenic	non-mutagenic	non-carcinogen	non-carcinogen	non-carcinogen
ZINC05458886	non-mutagenic	non-mutagenic	non-carcinogen	non-carcinogen	non-carcinogen
ZINC13298436	non-mutagenic	non-mutagenic	non-carcinogen	non-carcinogen	non-carcinogen
ZINC14880002	non-mutagenic	non-mutagenic	non-carcinogen	non-carcinogen	non-carcinogen
ZINC22026394	non-mutagenic	non-mutagenic	non-carcinogen	non-carcinogen	non-carcinogen

The toxicity and mutagenic potentials of the drug molecules were predicted by ToxPredict server (.http://opentox.net/tutorials-category/toxpredict).

3.3.3 Top-hit heterocyclic compounds have many structurally similar drug counterparts available in the market: The top non-carcinogenic heterocyclic compounds identified were not available for further experiments. So, we have approached through an alternate strategy**.** We decided to find their structural analogues in the form of already prevailing clinical drugs that are easily available in the market. The website DrugBank (http://www.drugbank.ca/chemquery) was explored which would enable us to identify structurally similar approved drugs that are in vogue. Smiles (alphanumeric codes) of the top hit compounds were put into the chemquery structure search toolbox, and the similarity threshold was set at 70%. The query identified many regularly approved clinical drugs (Table 3.4) that were used for many different types of diseases such as anti-histamine for asthma type disorders, neurological disorders, antibiotic, parasitic worm infection and birth-control (Barbieri and Ryan, 1981; Desmedt et al., 1975;

Parving et al., 2001). The drugs Flunarizine, Cinnarizine and Danazol (Figure 3.3) were chosen for our study as they were available at an affordable price.

Table 3.4: Similarity of Heterocyclic Compounds with clinical drugs.

Compound Code	Name of Drug and % Similarity				
ZINC14880002	Dihydroergotamine 100	Ergoloidmesylate 93.8	Ergotamine 84.9	Bromocriptine 77.6	
ZINC05458886	3-Methylfentanyl 100	Fentanyl 94.6	Alpha-methylfentanyl 90.6	Beta-hydroxy-3-methylfentanyl 89.6	Acetyl-alpha-methylfentanyl 88.9
ZINC13298436	Irbesartan 100				
ZINC03872177	Permethrin 83.3				
ZINC01482030	Deptropine 100	Benzatropine 79.3			
ZINC22026394	Cinnarizine 85.3	Flunarizine 82.6	Chlorcyclizine 77.5	Meclizine 73.8	Buclizine 73.8
ZINC00388658	Matairesinol 88.5				
ZINC04102205	Dihydromorphine 100	Dihydrocodeine 99.1	Dihydroetorphine 97.7	Buprenorphine 97.3	Diprenorphine 97.3
ZINC11592646	Danazol 100				
ZINC04215736	Dihydrocodeine 100	Dihydromorphine 99.1	Dihydroetorphine 96.9	Buprenorphine 96.4	Diprenorphine 96.4

Many of the commonly available drugs in the market are found to be similar to the top-hit hetrocyclic compounds. SMILES of the top non-toxic heterocyclic compounds were used as inputs to the drug database (www.drugbank.ca/chemquery) to identify similar clinical drugs.

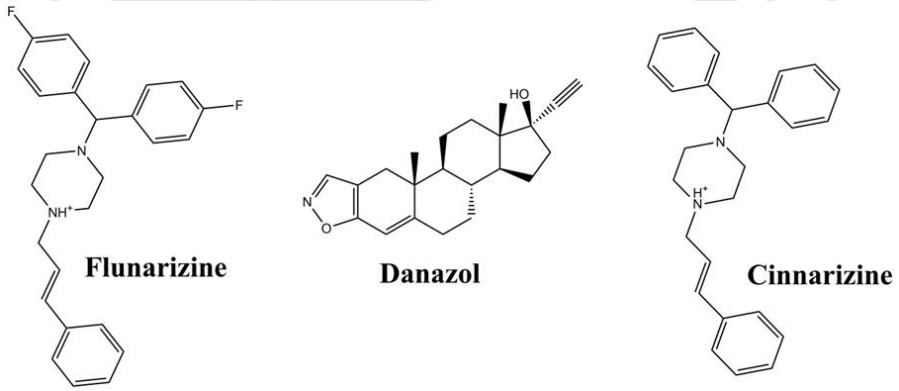

Figure 3.2: Chemical structure of selected drugs.

Having identified the drugs Danazol, Flunarizine and Cinnarizine as the molecules for further studies, we checked their binding affinity to PKC by docking (Section 3.2.3) in order to confirm that we have indeed selected the right molecules. The binding energy of Danazol to the C1 domain was calculated to be -6.77 kcal/mol, while Flunarizine and Cinnarizine binds to PKC-α with a binding energy of -6.68 kcal/mol and -6.08 kcal/mol respectively.

3.3.4 PKC directed molecules are found in phytochemicals from plants of north-eastern India: Newer molecular biology research has identified the active participation of phytochemicals in numerous important signal transduction pathways that serve to halt the progress of malignant cancer cells.

Table 3.5: Top-hit phytochemicals after molecular docking against C1b domain

S. No	Name of Compound	Binding Energy (PKC-α alone) (kcal/mol) (A)	Binding Energy (PKC-α+PMA) (kcal/mol) (B)	Difference (A-B) (kcal/mol)
1.	Theaflavin	-5.32	+767.66	-772.98
2.	Glycyrrhetinic acid	-6.42	+22.1	-28.52
3.	Isopteropodine	-6.86	+17.23	-24.09
4.	Gossypol	-4.15	+15.84	-19.99
5.	Euperfolitin	-5.17	+2.71	-7.88
6.	Emetine	-6.07	-0.09	-5.98
7	Isomitraphylline	-7.19	-1.37	-5.82
8.	Curcumin	-6.00	-0.72	-5.28
9.	Tocopherol	-4.73	+0.15	-4.88
10.	Gallic acid	-5.42	-0.28	-5.14
11.	L-Chichoric Acid	-4.35	+0.42	-4.77
12.	Mitraphylline	-7.05	-2.78	-4.27
13.	Isorhynchophylline	-6.21	-2.11	-4.10
14.	Chlorogenic Acid	-5.19	-1.39	-3.8
15.	Arctigenin	-5.45	-1.72	-3.73
16.	Epigallocatechin Gallate	-4.72	-1.72	-3.00
17.	PMA	-3.24	not applicable	not applicable

Binding energies of top hit phytochemicals after docking simulations using Autodock 4.1. Both receptor and ligands were prepared as given in Section 3.2.3 and docked using Autodock 4.1

We have also extensively searched for the phytochemicals that could serve as PKC ligands. Medicinal plants from north-eastern India (Table 3.1 & Appendix I) and their corresponding phytochemicals were selected. Molecular docking was performed with the 3-D structure of PKC-α as the drug target (Section 3.2.3).

Completion of molecular docking experiments indicated that many phytochemicals fit into the polar groove of the C1b domain and had better binding energy than PMA. Further, an agonist competition assay (Chapter 3, Section 3.2.4) identified the top 16 molecules that are depicted in Table 3.5, and chemical structure of selected molecules are shown in Figure 3.3.

Having identified the top molecules on the basis of docking scores, our next task was to choose a few molecules amongst them to pursue further experiments. In order to have the phytochemicals at our hand, our choice must be those molecules which are easily accessible and affordable to us. Thus, to know the readily available molecules out of those 16 top hit molecules, we re-looked into the original plant source of these 16 molecules. So, it was finally decided to obtain all molecules available with commercial vendors for further studies. Thus, we have finally selected the molecules Chlorogenic acid, Gallic acid, β-Glycyrrhetinic acid and Epigallocatechin gallate for further studies.

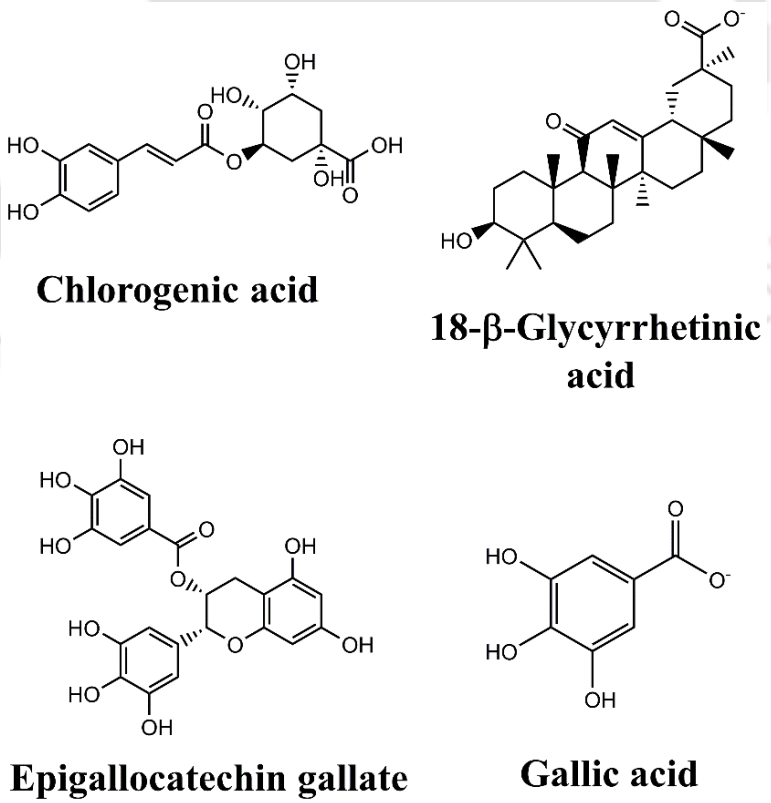

Figure 3.3: Structures of a few selected top-hit phytochemicals. Smiles of individual phytochemicals were downloaded from various chemical libraries and structures were sketched in 'ChemBioDraw Ultra-version-14' software.

3.3.4 Selected molecules bind strongly to PKC under in-silico conditions and form many interactions with the C1b domain of PKC: After the docking simulation was over, the PKC-ligand molecular models were taken for analysis. This final PKC-ligand structure was analyzed in molecular visualization software PyMOL v0.99 (Schrodinger, 2010). Molecular docking study indicates that Danazol, Flunarizine and Cinnarizine fits well into the polar binding groove of the C1b domain of PKC-α (Figure 3.4).

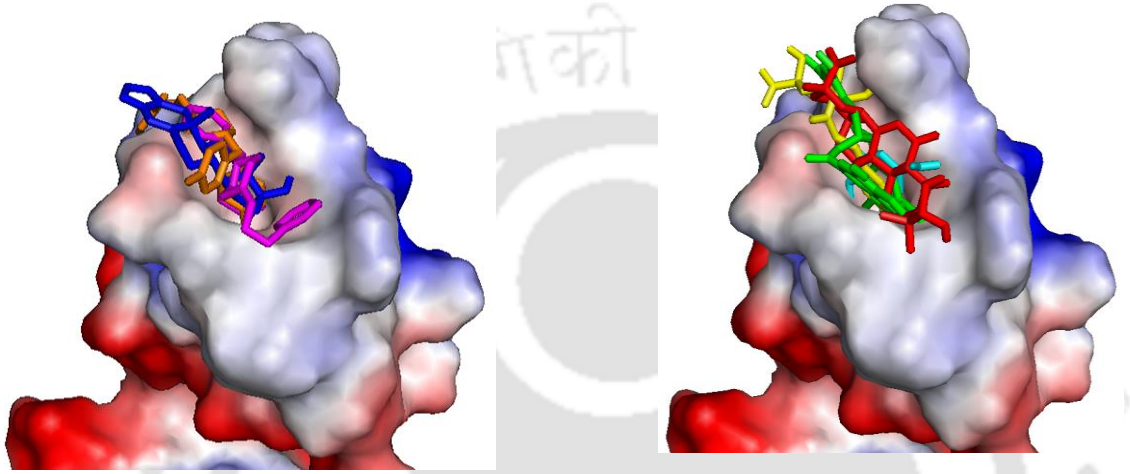

Figure 3.4: Selected molecules fit well into the C1b domain. Danazol (blue), Flunarizine (orange), Cinnarizine (magenta), Chlorogenic acid (yellow), Epigallocatechin gallate (green), Gallic acid (cyan) and β-Glycyrrhetinic acid (red) fit well into C1b domain. All the molecules bind to the polar ligand binding pocket of the C1b domain of PKC-α. Docked complexes of the ligands with the C1b domain were visualized in pyMOL using the "vaccum electrostatics" option.

Similarly, docking studies have also revealed that many phytochemicals bind to the C1b domain at the same binding site as PMA albeit with minor variations in the ligand orientations about the lipophilic binding pocket (Figure 3.4).The molecular interactions between ligand and receptor help us to understand better the affinity of a particular ligand for a receptor. These molecular interactions between bound ligand molecules and PKC C1b domain residues were sketched using LigPlot^{+} software (Wallace et al., 1995). All the three selected drugs Danazol, Flunarizine and Cinnarizine, were analysed for interactions with PKC C1b domain. It is seen that all the three drugs fit well & deep, as well as span the entire binding pocket of the C1b domain. They form many hydrophobic interactions as well as strong hydrogen bonding interactions which indicate strong binding characteristics. Robust hydrophobic and hydrogen bonding interactions (Figure 3.5) is expected to confer a high level of stability to ligand-PKC complexes.

The Danazol-PKC molecular model analysis indicates extensive interaction of bound Danazol with the protein residues lining the C1b domain. It forms many hydrophobic interactions as well as strong

hydrogen bonding interactions. Danazol makes hydrophobic interaction with Pro 28, Tyr 25, Leu 41, Gly26, Tyr 39, Gln44, Ser 27 and Thr 29 (Figure 3.5). Also, it makes two hydrogen bonds with Leu 38 and Gly 40. Flunarizine forms hydrophobic interactions with the amino acid residues His 23, Thr 24, Leu 41, Gly 26, Pro 28, Gly 40, Gln 44, Ser 27 and Leu 38 of the C1b polar binding pocket (Figure 3.5). It also forms hydrogen bonding interactions with Tyr 25 and Thr 29. Similarly, Cinnarizine formed hydrophobic interactions with the amino acid residues Leu 37, Tyr 39, Leu 38, Gln 44, Gly 40, Thr 29, Tyr 25, Ser 27, Gly 26, Leu 41 and Pro 28 of the polar binding pocket (Figure 3.5). But cinnarizine doesn't form any hydrogen bonding interaction.

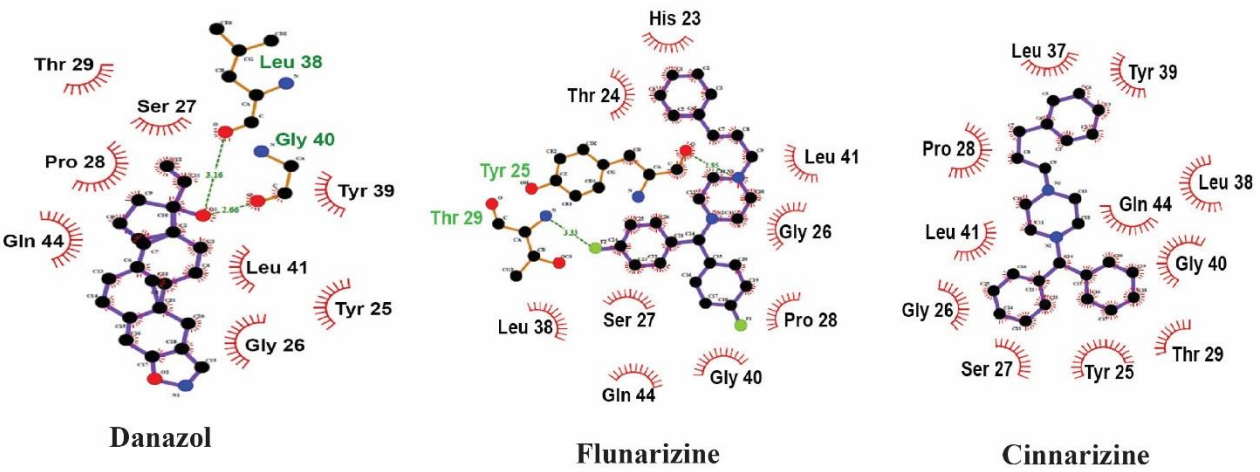

Figure 3.5: Molecular interaction of PKC-α with Danazol, Flunarizine and Cinnarizine. Danazol, Flunarizine andCinnarizine form stronger hydrogen bonding interactions with PKC. The PKC-ligand molecular models were used to draw molecular interaction using LigPlot^{+} software.

Similarly, it was revealed that many other molecules utilize a combination of hydrogen bonding and hydrophobic interactions to position themselves most efficiently for binding to the lipophilic pocket. This strategy ultimately results in an optimal reduction of free energy of the system which is relatively indicated by the docking scores predicted by Autodock software. Similarly, the selected phytochemicals β-Glycyrrhetinic acid, Gallic acid, Epigallocatechin gallate & Chlorogenic acid were also analysed for interactions with PKC C1b domain. All the selected phtochemicals also fit well & deep, as well as span the entire binding pocket of the C1b domain. In addition, they form many hydrophobic interactions as well as strong hydrogen bonding interactions. The interaction analysis of the molecules Chlorogenic acid, Gallic acid, Epigallocatechin gallate and β-Glycyrrhetinic acid are summarized in Figure 3.6.

Except for β-Glycyrrhetinic acid, all other phytochemicals are observed to utilize hydrogen bonding interactions in addition to hydrophobic interactions for binding to the ligand binding domain of C1b domain. Chlorogenic acid makes hydrophobic interaction with Pro 28, Gln 44, Leu 37, Ser 27, Tyr

25, Gly 26 and Thr 24 (Figure 3.6). In addition, it makes three hydrogen bonds with Thr 29, Leu 41 and Leu 38. On the other hand, Gallic acid makes hydrophobic interaction with Pro 28, Gln 44, Gly 26 and Tyr 39, whereas it makes hydrogen bonding interactions with Thr 29, Gly 40, Leu 38, Tyr 25 and Ser 27 (Figure 3.6). Epigallocatechin gallate makes hydrophobic interactions with Tyr 25, Leu 41, Gly 26, Pro 28, Ser 27, Leu 37 and Gly 40, while it makes hydrogen bonding interactions.

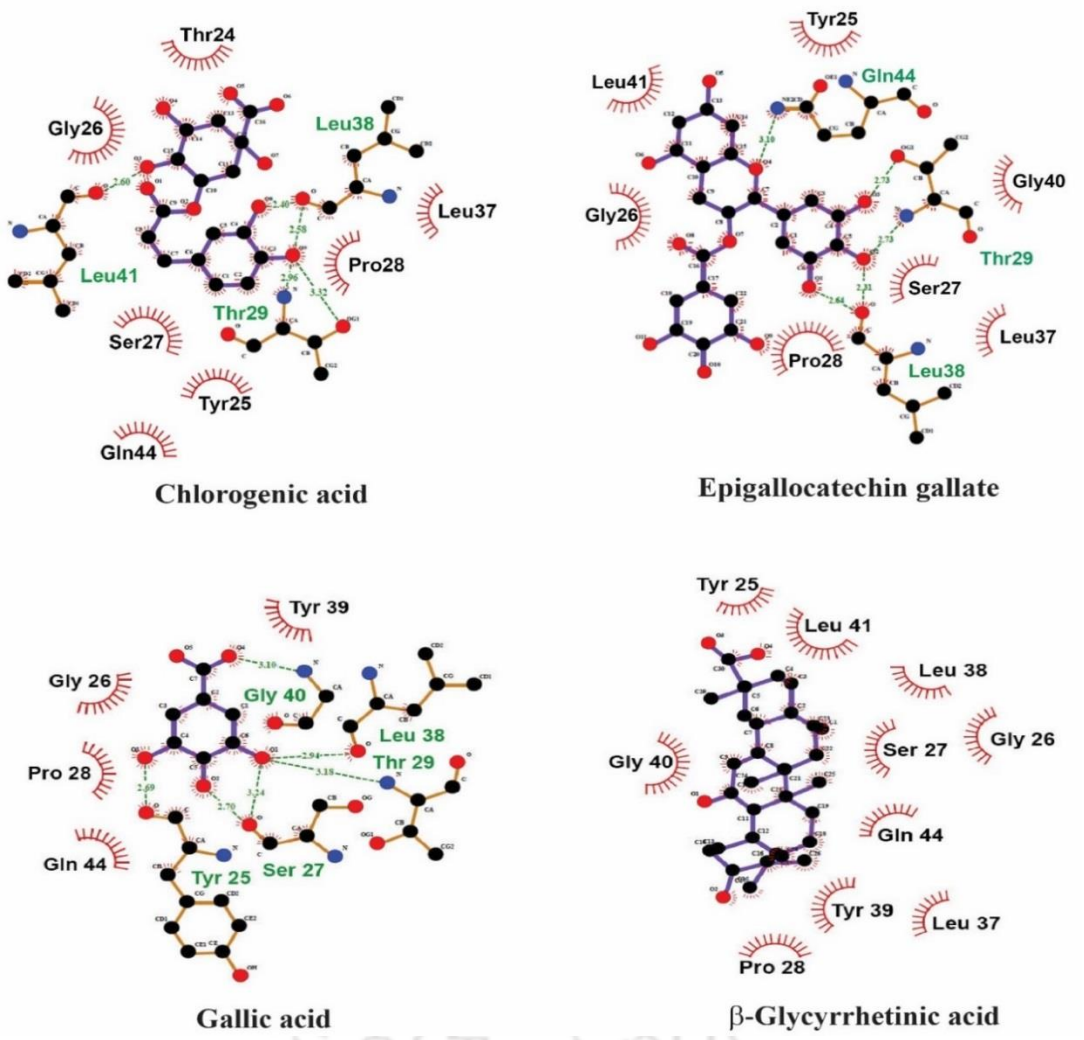

Figure 3.6: Molecular interaction of PKC-α with phytochemicals. Except β-Glycyrrhetinic acid, all other phytochemicals form stronger hydrogen bonding interactions with PKC. The PKC-ligand molecular models were used to draw molecular interaction using LigPlot^{+} software.

with Gln 44, Thr 29 and Leu 38. However, β-Glycyrrhetinic acid only makes hydrophobic interactions with Tyr 25, Leu 41, Leu 38, Gly 26, Ser 27, Gln 44, Leu 37, Tyr 39, Pro 28 and Gly 40 (Figure 3.6).

To further understand the strong binding affinity of these ligands to the C1b domain of PKC, all the selected PKC-directed molecules were sent to Dr. Debasis Manna's laboratory, Department of Chemistry, IIT Guwahati for in-vitro ligand binding assay. The dissociation constant (K_D) of each ligand

was determined and given to us by them. The dissociation constant (K_D) of Flunarizine, Cinnarizine, Danazol, Chlorogenic acid, β-Glycyrrhetinic acid, Gallic acid and Epigallocatechin gallate towards PKC is given in Table 3.6.

Table 3.6: Dissociation constants (K_D) of PKC-directed molecules

S No.	Molecule	Dissociation constant, K_D (μM)
1.	Danazol	5.64±1.27
2.	Flunarizine	4.51±0.51
3.	Cinnarizine	10.75±1.87
4.	Chlorogenic acid	28.84±3.95
5.	β-Glycyrrhetinic acid	10.14 ± 1.13
6.	Gallic acid	0.91 ± 0.11
7.	Epigallocatechin gallate	0.88 ± 0.14

The dissociation constant (K_D) of in-vitro binding of PKC directed molecules towards the C1b domain of PKC. Each of the K_D values was calculated by a fellow student in Dr. Debasis Manna's laboratory, Department of Chemistry, IIT Guwahati.

Thus, all the top hit molecules make extensive interactions with most of the amino acid residues lying around the periphery of the ligand binding pocket of the C1 domain. The binding of all the ligands to the C1b domain under in-silico and in-vitro conditions confirms that Danazol, Flunarizine, Cinnarizine, Chlorogenic acid, β-Glycyrrhetinic acid, Gallic acid and Epigallocatechin gallate are strong ligands of PKC.

3.4 Discussion

It is now well-known that structurally diverse molecules can serve as ligands for PKC. Detailed structural analysis of diverse PKC ligands, as well as their mode of binding to PKC, has been revealed. It is now understood that the C1 domain functions as a hydrophobic switch (Steinberg, 2008). The ligand binding site of the C1 domain is a hydrophilic cleft formed by strands of β-sheets (Steinberg, 2008). The upper surface area around this cleft is comprised of hydrophobic amino acids (Steinberg, 2008). Thus, ligands insert their hydrophilic domains in this ligand binding cleft and project their hydrophobic domains outwards. Hence, ligand binding to the C1 domain forms a uniform hydrophobic upper surface on the C1 domain which serves to penetrate the ligand-C1 domain complex to appropriate lipid membranes (Blumberg et al., 2010; Steinberg, 2008). The coverage of the hydrophilic cleft of the C1 domain is very similar amongst different molecules, but the hydrophobic side chains protruding outwards vary among structurally diverse ligands (Blumberg et al., 2010). This different hydrophobic side chains bring about

substantial diversity in the preference of the ligand-C1b domain complex for various biological membranes and even for different lipid micro-domains in the same membrane. This differential translocation potential of diverse ligands to different micro-domains of a variety of biological membranes in the cell directly results in different biological responses of PKC signalling.

Phytochemicals have been designed by evolution to target important cellular signalling networks that result in modulation of key physiological processes (Cojocneanu Petric et al., 2015; Surh, 2003). Phytochemicals also serve as lead molecules for the design and synthesis of advanced derivatives targeted against important human ailments (Cojocneanu Petric et al., 2015). However, isolation of a new phytochemical from natural sources is time-consuming. Moreover, it is tough to isolate every phytochemical in the purest form from the crude plant extract preparations. Chemical synthesis of phytochemicals as well as their analogues in the laboratory is costly and also a time-consuming affair. It is indeed in such situations where virtual docking techniques come handy (Geromichalos, 2007). Virtual docking approaches significantly enhance the number of molecules screened as well as eliminate the need for in-vitro analysis of each and every pre-considered natural or synthetic molecule (Meng et al., 2011).In the current study, molecular docking was performed by Autodock 4.1 software in order to screen two broad categories of ligands, heterocyclic compounds and phytochemicals. Top-hit ligands against the C1b domain of PKC were identified amongst both heterocyclic compounds and phytochemicals. An agonist competition assay enabled the selection of only those ligands that bind in a similar manner to a previously well-known agonist. We have also obtained a series of novel chemically synthesized molecules known as alkyl cinnamates from our collaborator lab. Design, synthesis, molecular docking analyses and in-vitro ligand binding analyses of these alkyl cinnamates by Mamidi et. al. showed that some of these compounds strongly interact with the C1b subdomain (Mamidi et al., 2012). K_D values of in-vitro PKC binding ranged from 3 μM to 21 μM (Mamidi et al., 2012). As it has already been confirmed by in-silico and in-vitro studies that alkyl cinnamates interact with PKC by our colleagues, we haven't repeated any such experiments again. Hence, in the current chapter experiments related to alkyl cinnamates are not presented. Any subsequent experiments with alkyl cinnamates are described in detail in later chapters. The following figure (Figure 3.7) illustrates the structure of all of the alkyl cinnamates. Curcumin is the parent molecule of alkyl cinnamates which is designated as 'DM 2-CRMN'.

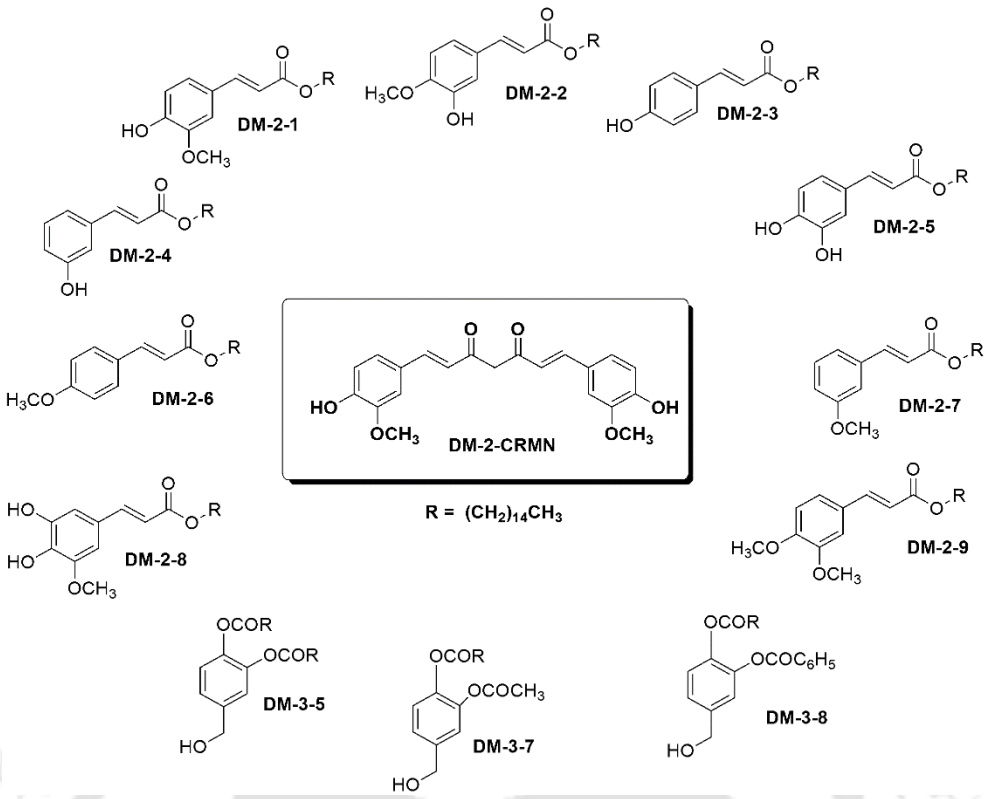

Figure 3.7: Chemical structure of different alkyl cinnamates with their respective compound codes. DM 2-CRMN is curcumin.

Agonist binding to a receptor is dictated by the strength of the interactions (inter-molecular forces) between the ligand and receptor. Hydrogen bonding and hydrophobic interactions are considered to be more significant interactive forces operating between ligands and receptors apart from other interactions such as ionic, salt bridges and van der Waals forces (Patil et al., 2010). This is due to the fact that generally the hydrogen bonding and hydrophobic interactions are numerous between ligand and receptor; as such, they outweigh the contribution of sparingly present other kinds of interactive inter-molecular forces. Virtual docking softwares rely mainly on calculations from the hydrogen bonding and hydrophobic interactions between ligand and receptor (Meng et al., 2011; Patil et al., 2010). In the current study, in-silico screening experiments complemented with in-vitro ligand binding studies actively suggest that certain compounds exist in all the three categories of molecules screened that can serve as excellent ligands for PKC. Thus, PKC ligands prevail in all possible classes of molecules existing throughout the world. Finding them is only a matter of effort and time.

A few conclusions can be inevitably drawn from the experiments described in this chapter.

1. Detailed interaction analysis revealed that the top hit ligands are bound to the receptor by both hydrophobic and hydrogen bonding interactions.

2. Visualization of ligand-receptor complexes also highlighted that ligands can be structurally different but bind to the same binding site with very similar binding energy. These structurally different ligands utilize different portions of themselves to bind to the same site of the C1 domain. Having identified the strongest ligands on the basis of their binding affinity to PKC, it was inevitably intriguing to explore the effects on cancer-cell cellular physiology on the treatment of these molecules.

3.5 References

- Barbieri, R.L., and Ryan, K.J. (1981). Danazol: endocrine pharmacology and therapeutic applications. American Journal of Obstetrics and Gynecology *141*, 453-463.
- Blumberg, P.M., Kedei, N., Lewin, N.E., Yang, D., Tao, J., Telek, A., and Geczy, T. (2010). Phorbol Esters and Diacylglycerol: The PKC Activators. In Protein Kinase C in Cancer Signaling and Therapy, M.G. Kazanietz, ed. Humana Press, pp. 25-53.
- Castagna, M., Takai, Y., Kaibuchi, K., Sano, K., Kikkawa, U., and Nishizuka, Y. (1982). Direct activation of calcium-activated, phospholipid-dependent protein kinase by tumor-promoting phorbol esters. The Journal of Biological Chemistry *257*, 7847-7851.
- Chu, F., and O'Brian, C.A. (2005). PKC sulfhydryl targeting by disulfiram produces divergent isozymic regulatory responses that accord with the cancer preventive activity of the thiuram disulfide. Antioxidants & Redox signaling *7*, 855-862.
- Cojocneanu Petric, R., Braicu, C., Raduly, L., Zanoaga, O., Dragos, N., Monroig, P., Dumitrascu, D., and Berindan-Neagoe, I. (2015). Phytochemicals modulate carcinogenic signaling pathways in breast and hormone-related cancers. OncoTargets and Therapy *8*, 2053-2066.
- Deissler, H.L., and Lang, G.E. (2016). The Protein Kinase C Inhibitor: Ruboxistaurin. Developments in Ophthalmology *55*, 295-301.
- Desmedt, L.K., Niemegeers, C.J., and Janssen, P.A. (1975). Anticonvulsive properties of cinnarizine and flunarizine in rats and mice. Arzneimittel-Forschung *25*, 1408-1413.
- Fujiki, H., and Sugimura, T. (1987). New classes of tumor promoters: teleocidin, aplysiatoxin, and palytoxin. Advances in Cancer Research *49*, 223-264.
- Geromichalos, G.D. (2007). Importance of molecular computer modeling in anticancer drug development. Journal of BUON *12 Suppl 1*, S101-118.
- Hecker, E. (1968). Cocarcinogenic principles from the seed oil of Croton tiglium and from other Euphorbiaceae. Cancer Research *28*, 2338-2349.
- Hecker, E., Adolf, W., Hergenhahn, M., Schmidt, R., and Sorg, B. (1983). Irritant diterpene ester promoters of mouse skin: contributions to etiologies of environmental cancer and to biochemical mechanisms of carcinogenesis. Princess Takamatsu Symposia *14*, 3-36.
- Kim, J., Thorne, S.H., Sun, L., Huang, B., and Mochly-Rosen, D. (2011). Sustained inhibition of PKCalpha reduces intravasation and lung seeding during mammary tumor metastasis in an in vivo mouse model. Oncogene *30*, 323-333.

- Lewin, N.E., Pettit, G.R., Kamano, Y., and Blumberg, P.M. (1991). Binding of [26-3H]-epi-bryostatin 4 to protein kinase C. Cancer Communications *3*, 67-70.
- Mackay, H.J., and Twelves, C.J. (2003). Protein kinase C: a target for anticancer drugs? Endocrine-related Cancer *10*, 389-396.
- Mamidi, N., Gorai, S., Sahoo, J., and Manna, D. (2012). Alkyl cinnamates as regulator for the C1 domain of protein kinase C isoforms. Chemistry and Physics of Lipids *165*, 320-330.
- Marengo, B., De Ciucis, C., Ricciarelli, R., Pronzato, M.A., Marinari, U.M., and Domenicotti, C. (2011). Protein Kinase C: An Attractive Target for Cancer Therapy. Cancers *3*, 531-567.
- Meng, X.-Y., Zhang, H.-X., Mezei, M., and Cui, M. (2011). Molecular Docking: A powerful approach for structure-based drug discovery. Current Computer-aided Drug Design *7*, 146-157.
- Mizuno, K., Saido, T.C., Ohno, S., Tamaoki, T., and Suzuki, K. (1993). Staurosporine-related compounds, K252a and UCN-01, inhibit both cPKC and nPKC. FEBS Letters *330*, 114-116.
- Morris, G.M., Huey, R., Lindstrom, W., Sanner, M.F., Belew, R.K., Goodsell, D.S., and Olson, A.J. (2009). AutoDock4 and AutoDockTools4: Automated docking with selective receptor flexibility. Journal of Computational Chemistry *30*, 2785-2791.
- Nakagawa, M., Oliva, J.L., Kothapalli, D., Fournier, A., Assoian, R.K., and Kazanietz, M.G. (2005). Phorbol ester-induced G1 phase arrest selectively mediated by protein kinase Cdelta-dependent induction of p21. The Journal of Biological Chemistry *280*, 33926-33934.
- Parving , H.-H., Lehnert , H., Bröchner-Mortensen , J., Gomis , R., Andersen , S., and Arner , P. (2001). The Effect of Irbesartan on the Development of Diabetic Nephropathy in Patients with Type 2 Diabetes. New England Journal of Medicine *345*, 870-878.
- Patil, R., Das, S., Stanley, A., Yadav, L., Sudhakar, A., and Varma, A.K. (2010). Optimized Hydrophobic Interactions and Hydrogen Bonding at the Target-Ligand Interface Leads the Pathways of Drug-Designing. PLoS ONE *5*, e12029.
- Santiago-Walker, A.E., Fikaris, A.J., Kao, G.D., Brown, E.J., Kazanietz, M.G., and Meinkoth, J.L. (2005). Protein kinase C delta stimulates apoptosis by initiating G1 phase cell cycle progression and S phase arrest. The Journal of Biological Chemistry *280*, 32107-32114.
- Schrodinger, LLC (2010). The PyMOL Molecular Graphics System, Version 1.3r1.
- Shao, L., Lewin, N.E., Lorenzo, P.S., Hu, Z., Enyedy, I.J., Garfield, S.H., Stone, J.C., Marner, F.J., Blumberg, P.M., and Wang, S. (2001). Iridals are a novel class of ligands for phorbol ester receptors with modest selectivity for the RasGRP receptor subfamily. Journal of Medicinal Chemistry *44*, 3872-3880.
- Steinberg, S.F. (2008). Structural Basis of Protein Kinase C Isoform Function. Physiological Reviews *88*, 1341-1378.
- Sun, X.G., and Rotenberg, S.A. (1999). Overexpression of protein kinase Calpha in MCF-10A human breast cells engenders dramatic alterations in morphology, proliferation, and motility. Cell Growth & Differentiation *10*, 343-352.
- Surh, Y.-J. (2003). Cancer chemoprevention with dietary phytochemicals. Nat Rev Cancer *3*, 768-780.

- Verdelli, D., Nobili, L., Todoerti, K., Intini, D., Cosenza, M., Civallero, M., Bertacchini, J., Deliliers, G.L., Sacchi, S., Lombardi, L., *et al.* (2009). Molecular targeting of the PKC-beta inhibitor enzastaurin (LY317615) in multiple myeloma involves a coordinated downregulation of MYC and IRF4 expression. Hematological oncology *27*, 23-30.
- Wallace, A.C., Laskowski, R.A., and Thornton, J.M. (1995). LIGPLOT: a program to generate schematic diagrams of protein-ligand interactions. Protein Engineering *8*, 127-134.
- Willighagen, E.L., Jeliazkova, N., Hardy, B., Grafström, R.C., and Spjuth, O. (2011). Computational toxicology using the OpenTox application programming interface and Bioclipse. BMC Research Notes *4*, 487-487.
- Yoshida, K. (2007). PKCdelta signaling: mechanisms of DNA damage response and apoptosis. Cellular signalling *19*, 892-901.
- Young, L.H., Balin, B.J., and Weis, M.T. (2005). Go 6983: a fast acting protein kinase C inhibitor that attenuates myocardial ischemia/reperfusion injury. Cardiovascular drug reviews *23*, 255-272.

3.6 Appendix I

Full list of selected plants for study

Table 3.7: List of 50 medicinal plants explored for therapeutic phytochemicals

S No.	Botanical Name	Common Name	Ethnobotanical uses
1.	*Camellia sinensis*	Tea	Used as a beverage. Also used as a carminative, CNS stimulant and also possess anti-cancer property.
2.	*Coffea arabica L*	Coffee	Used as a beverage. Also used as a cardiotonic, CNS stimulant, treatment of asthma and headache.
3.	*Curcuma longa*	Indian Saffron; Turmeric	Key spice of many South Asian and Middle Eastern cooking. Extracts from turmeric have antifungal and antibacterial properties.
4.	*Curcuma xanthorrhiza*	Temu Lawak; Javan Turmeric	It is used as a spice. Useful for treating digestive disorders and anti-inflammation.
5.	*Zingiber officinale*	Ginger	Used as a spice. It is used to treat digestive disorders, treatment of fever, nausea and vomiting and possess anti-microbial property.
6.	*Capsicum annuum*	Paprika; Green Pepper; Cherry Pepper; Bell Pepper; Cone Pepper; Sweet Pepper	Used as a spice. It is used in combination of homeopathic and natural preparations. It is used as a relief of oral discomfort or toothache, external analgesia, as a digestive aid, in menstrual conditions, and in cosmetics as cleansers and bath products.
7.	*Capsicum frutescens*	Cayenne; Chilli; Tabasco; Hot Pepper; Spur Pepper; Red Chili	Similar use as Capsicum annuum.

8.	*Pisum sativum*	Pea	Used as food.It is recommended for heart diseases, diabetes and nervous system disorders.
9.	*Hibiscus sabdariffa*	Roselle; Oseille De Guinee; Vinagrillo; Maravilla; Kerkedeh; Chai Kujarat; Afrika Bamyasi	Used as a flavouring agent. Also used to lower pressure in hypertension.
10.	*Nicotiana tabacum*	Tabigh; Tobacco; Tabaco	Used for curing toothache, antidote to bee-sting, centipede bites,scorpion-bites. Used in asthma. Used as Parasiticide, anti-cancer agent and CNS stimulant.
11.	*Uncaria tomentosa*	Cats Claw	Reduce pain and inflammation of rheumatism, arthritis and other types of inflammatory problems. Has anti-tumor and anti-cancer properties and is useful for treatment of gastric ulcers and intestinal complaint.
12.	*Uncaria catechu*	khoyer	Catechu is used for diarrhea, swelling of the nose and throat, dysentery, swelling of the colon (colitis), bleeding, indigestion, osteoarthritis, and cancer. Also used for treatment of skin-diseases.
13.	*Sophora pachycarpa*	Kowhai	Possess anti-bacterial and anti-allergic properties. Considered as a potential chemotherapeutic agent in cancer treatment.
14.	*Syringa vulgaris*	Lilac	Used in homeopathy. Also used to treat fever and malaria.
15.	*Citrus limon*	Lemun Tresh; Limonero; Lemun Hamedh; Lemon; Miski; Limon	Used to treat cold, fever, inflammation, diarrhoea, dysentery and digestive disorders.
16.	*Allium sativum*	Garlic	Used to cure any kind of ache in the body. Used as antiseptic, antidote, arthritis, asthma, bronchitis, malaria, as a vasodilator and most importantly in the treatment of cancer.
17.	*Brassica napus var. napobrassica*	Turnip; Naveterinary; Nabo	Used bin the treatment of cold, gout and as anti-cancer agent.
18.	*Triticum aestivum*	Common wheat	Known to be used to treat fever and diarrhoea.
19.	*Aloe vera*	Djadam arab; Jadam; Nu Hui	Treatment of fever, cough, asthma and cancer.
20.	*Eupatorium perfoliatum*	Eupatorio; Indian Sage; Hempweed	Used in the treatment of cough, cold, dengue, as a laxative and in malaria.
21.	*Arnica montana*	Arnica; Dagtutunu	Used in the treatment of fever, as a cardiotonic and in the treatment of cancer.

22.	*Acacia nilotica*	Babli; Gumarabic	Used as a Decongestant, treatment of gall-bladder, spleen and as an anti-cancer agent.
23.	*Artemisia annua*	Kuso-Ninzin; Huang Hua Hao	Used as bacteriocide, treatment of abscess, eye, fever, jaundice, skin-disease, stomach ache and dysentery.
24.	*Dionaea muscipula*	Venus' Fly Trap	Used in the treatment of HIV, Crohn's disease and skin cancer.
25.	*Myroxylon balsamum*	Balsam Of Tolu	Used as an antibacterial and antiseptic.
26.	*Illicium verum*	Pa Chio Yu	Used as diuretic, antiseptic, in the treatment of dyspepsia, constipation and dysentery.
27.	*Ocimum basilicum*	Great basil; Saint-Joseph's-wort	Used to cure ache (ear, head, tooth, stomach), antidote, as a carminative, treatment of kidney diseases, nausea, gout, sinus, spasm and possess anti-cancer properties.
28.	*Coccinia grandis*	Ivy gourd	Used to treat leprosy, fever, asthma, bronchitis, and jaundice. Possesses mast cell-stabilizing, antianaphylactic, and antihistaminic potential. Used in the treatment of scabies.
29.	*Lawsonia inermis*	Henna, Jetuka	Used tro treat stomach ache, headache, as an astringent, bacteriocide, fungicide, as hair-dye and treatment of inflammation and jaundice.
30.	*Berberis vulgaris*	Agracejo; Epine Vinette; Amberparis	Used as antiseptic, diuretic, laxative and ion the treatment of jaundice, fever, dyspepsia and dysentery.
31.	*Eschscholzia californica*	Khishkhash Kalifornia; Kaliforniya Hashasi	Used as analgesic and soporific.
32.	*Mahonia aquifolium*	Oregongrape; Oregon Grape	Known to possess bactericidal preoperties.
33.	*Thymus vulgaris*	Common Thyme	Used as antiseptic, carminative, in the treatment of bronchitis, cancer and digestive disorders.
34.	*Rheum officinale*	Huang Liang; Kelembak; Chiang Chun	Used in the treatment of boil, burns, dysentery, diarrhoea and cancers of cervix and stomach.
35.	*Zanthoxylum americanum*	Prickly Ash; Ache(Tooth) Tree	Used in the treatment of rheumatism, cough, cold, colitis and gonorrhoea.
36.	*Podophyllum pleianthum*	Mayapple	Used as Cathartic, treatment of warts, rheumatoid arthritis, and possess anti-cancer properties.
37.	*Arctium lappa L*	Kewe; Bardana; Waisar; Burdock; Lampazo Mayor	Used as antidote, bactericide, carminative, treatment of cough and cold, fever, flu, gonorrhoea, gout, infection, measles, piles, pneumonia, tonsillitis, syphilis and cancer.

38.	*Sorbus aucubaria L*	Rowan Tree; Serbal Silvestre; Uvez Agaci; European Mountainash	Used as an astringent, diuretic and in the treatment of gall-bladder, dyspepsia and rectal cancer.
39.	*Solanum tuberosum*	Potato	Used mainly as a food. But also known to be used in the treatment of peptic ulcers rheumatic joints, swellings, skin rashes and haemorrhoids.
40.	*Lycopersicon esculentum*	Tomato	Primarily used as food. Also used as antiseptic, treatment of cough, cold, fever and for digestive disorders.
41.	*Vitis vinifera*	European Grape	Used as astringent, expectorant, diuretic, laxative and in the treatment of cancer.
42.	*Glycyrrhiza glabra L.*	Madhuka; Licorice	Used in the treatment of cough, cold, as antidote, diuretic, expectorant and treatment of cancer.
43.	*Thespesia populnea*	Grand Mahaut	Treatment of headache, insect bites, cholera, cold, fever, scabies, stomachache, warts and dysentery.
44.	*Glycine max*	Soybean	Used as food. Also used as antidote, laxative, treatment of burns, malaria and cancer.
45.	*Cephaelis ipecacuanha*	Altim Koku; Tokon	Treatment of amebiasis, dysentery and cancer.
46.	*Artemisia vulgaris*	Sundamala	Used as an aphrodisiac, antidote of snake bite, treatment of dysmenorrhea, digestive disorders and dysentery.
47.	*Mitragyna speciosa*	Bia; Ketum; Biak; Kutum	Used in the treatment of fever
48.	*Echinacea angustifolia*	Coneflower	Used as antiseptic, aphrodisiac, treatment of cough, cold and digestive disorders.
49.	*Chimaphila umbellata L*	Pipsissewa; Chimaphile; Spotted Wintergreen	Used in the treatment of diabetes, kidney disorders, fever and digestive problems.
50.	*Oryza sativa*	Asian rice	Used mainly as a food. However it is also used as an antidote, diarrhoea and various bowel disorders.

Chapter 4

PKC-directed molecules affects breast cancer cells in multiple ways.

4.1 Introduction

Recent research has put great emphasis on the identification of novel therapeutics for the treatment of cancer. PKC-directed cancer therapy is emerging as a newer approach to treat cancer. Different molecules have been identified that act through PKC to exert their anti-cancer property. Many inhibitors of PKC generate stress in cancer cells (Kaul and Maltese, 2009; Kuo et al., 2011). This PKC mediated generated stress leads to cell-cycle arrest in cancer cells (Frey et al., 1997; Leszczynski, 1995; Minana et al., 1992; Rodriguez-Lirio et al., 2015). Stress-mediated cell-cycle arrest might lead to loss of viability in cancer cells. Thus, identification of newer and robust PKC regulators holds a great promise in cancer therapeutics.

In Chapter 3, we have discussed about the exploration and identification of PKC-directed molecules from various sources. We have identified PKC-directed molecules from reservoir phytochemicals, clinical drugs as well as chemically synthesized novel alkyl cinnamates. The selected compounds were found to bind firmly to the C1b regulatory domain of PKC. They also formed numerous hydrogen bonding & hydrophobic interactions with the ligand binding pocket of the C1b domain.

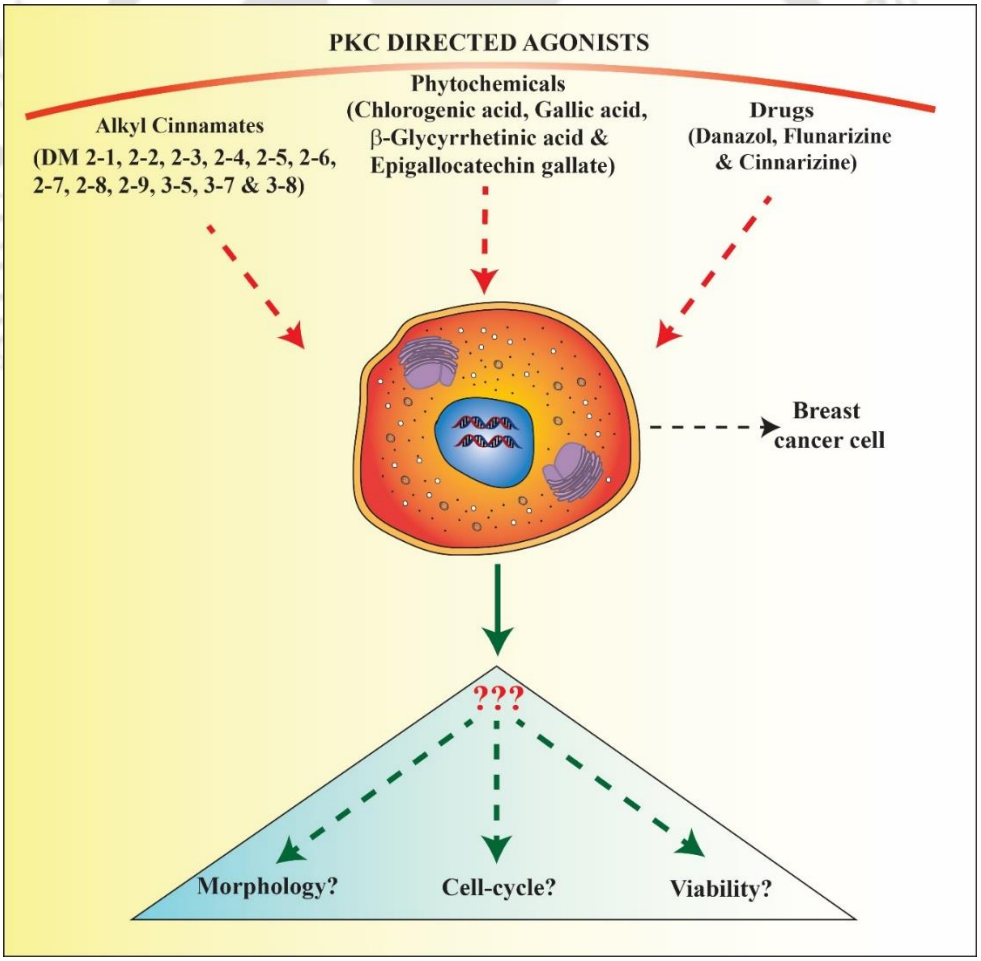

Figure 4.1: Schematic representation of hypothesis that leads to the experimental strategy in Chapter4.

Thus, having confirmed that the selected molecules bind strongly to PKC, it is very intriguing to ask the questions as to how these molecules might affect the physiology of cancer cells? Few of the changes in which we are interested are morphological changes, cell cycle changes and ultimately whether these molecules cause any change in viability (Figure 4.1). Thus, the current chapter describes the experiments undertaken to understand the effects on breast cancer cells on treatment with the selected PKC-directed molecules.

4.2 Experimental procedures

4.2.1 Cell-culture: MDAMB-231 cells and MCF-7 breast cancer cells were cultured in DMEM:F12, supplemented with 10% foetal bovine serum (FBS) and 1% penicillin-streptomycin antibiotic solution (100 units/ml penicillin and 100µg/ml streptomycin sulfate). Cells were grown at 37°C in a humidified environment in a 5% CO_2 incubator. On the day of the experiments, cells were washed twice with cell-culture-grade phosphate buffer saline (PBS) and subjected to various treatments in serum-free medium as described in Results section (Section 4.3).

4.2.2 Investigation of cellular morphology: MDAMB-231 and MCF-7 breast cancer cells (10,000 cells) were seeded into each well of 96-well plates and allowed to adhere for overnight. Next, cells were treated individually with different concentrations (0-100 µg/ml) of all the selected PKC-directed molecules in serum-free media. The plates were left undisturbed for 48 hrs at 37°C in a humidified environment in a 5% CO_2 incubator. The morphological changes in breast cancer cells were observed with Nikon Eclipse TS-100F inverted microscope using 20x and 40x objectives and images of cells were taken with a high resolution Nikon L22 camera.

4.2.3 Cell cycle analysis: MDAMB-231 breast cancer cells (10^5 cells) were seeded into each well of a 6-well plate in DMEM:F12 complete media and were allowed to adhere for overnight. Next, cells were individually treated with IC_{50} concentration of molecules (different drugs, phytochemicals and alkyl cinnamates) prepared in serum-free media for a period of 24 hrs. Post treatment, cells were washed with PBS, detached from the wells with 0.6% EDTA prepared in PBS and then stained with propidium iodide. Fifty thousand ($5x10^4$) cells per sample were analysed by flow cytometry as described in Chapter 2 (Section 2.4).

4.2.4 Measurement of cellular viability: MDAMB-231 and MCF-7 breast cancer cells (10,000 cells) were seeded into each well of 96-well plates and allowed to adhere for overnight. Next, cells were treated individually with different concentrations (0-100 µg/ml) of all the selected PKC-directed molecules in serum-free media except Cinnarizine which was used in the concentrations of 0-200 µg/ml. The plates were left undisturbed in 37°C in a 5% CO_2 incubator for a period of 48 hrs. After treatment, cells were

analysed for viability with MTT assay that is described in detail in Chapter 2 (Section 2.3). Obtained data was analysed, and viability curves were accordingly plotted.

4.3 Results

4.3.1 PKC directed molecules induce morphological abnormalities in breast cancer cells: MDAMB-231 and MCF-7 breast cancer cells were treated individually with different concentrations (0-100 µg/ml) of Danazol, Flunarizine and Cinnarizine prepared in serum-free media for 48 hrs at 37°C in a humidified environment in a 5% CO_2 incubator. After treatment, the cells were observed under an inverted microscope to detect morphological changes (Section 4.2.2). Danazol, Flunarizine & Cinnarizine (Figure 4.2) treated cells showed aberrant membrane blebbing patterns and cytoplasmic shrinkage which are indicative of cells under intense stress. In contrast, untreated cells appeared to be spindle-shaped and evenly spread-out, indicative of healthy morphology and no stress condition (Figure 4.2). All the Danazol treated cells at higher concentration (100 µg/ml) appeared to have highly shrunk morphology (Figure 4.2-A). However, a lesser number of such shrunk cells were observed at lower concentrations of Danazol (50 µg/ml). Similarly, Flunarizine or Cinnarizine treatment also appeared to affect the cellular morphology of both MDAMB-231 and MCF-7 breast cancer cells in a dose-dependent manner. It can be easily inferred by visual observation that Flunarizine or Cinnarizine at the concentration of 25 µg/ml affected the morphology of almost every cell in that panel (Figure 4.2-B, C). Whereas, the effect of Flunarizine or Cinnarizine at 6 µg/ml on morphology of breast cancer cells was far less. It was also observed that Flunarizine is more potent to affect the morphology of breast cancer cells than Cinnarzine or Danazol. It suggests that Flunarizine might have better anti-cancer activity than Cinnarzine or Danazol. It is also noteworthy that MCF-7 cells appeared to be more susceptible to every individual drug treatment than MDAMB-231 cells. This might be due to the fact that MDAMB-231 are triple negative breast cancer cells and are generally more robust and stubborn to drug treatment than MCF-7 cells.

In addition, MDAMB-231 and MCF-7 cells were also individually treated with different phytochemicals as described in Section 4.2.2. Amongst the phytochemicals, β-Glycyrrhetinic acid is seen to cause abnormal morphological effects on MDAMB-231 breast cancer cells at 25 µg/ml (Figure 4.3-A). Gallic acid and Epigallocatechin gallate were seen to have the most profound effects on the morphology of breast cancer cells, especially at higher concentrations (Figure 4.3-B, C). Gallic acid or Epigallocatechin gallate were observed to induce aberrant morphology in both MDAMB-231 and MCF-7 breast cancer cells at 13 µg/ml (Figure 4.3-B, C). However, this aberrant morphology inducing effect was a little reduced at lower concentration (3 µg/ml). Thus, β-Glycyrrhetinic acid seems to be a bit inferior in its potency in this aspect when compared to Gallic acid and Epigallocatechin gallate (Figure 4.3-A, B, C). We found that Chlorogenic acid is not as potent as the other three phytochemicals in affecting breast cancer cell morphology (Figure 4.3-D). Chlorogenic acid could induce visible morphological blebbing

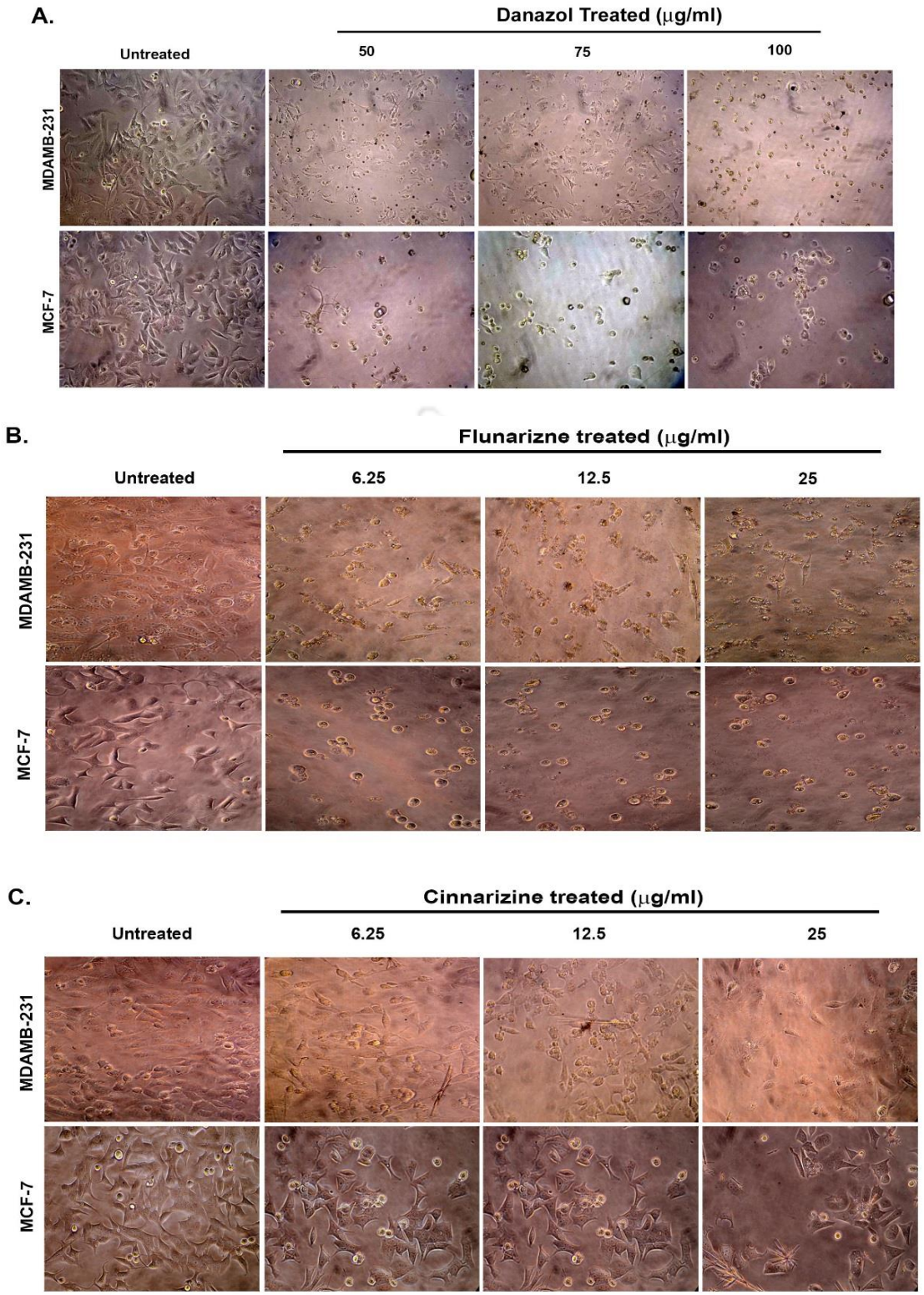

Figure 4.2: Morphological deformities in MDAMB-231 or MCF-7 breast cancer cells treated individually with different drugs (0-100 µg/ml) in serum-free media for 48 hrs. Cells were treated with (A) Danazol (0, 50, 75 and 100 µg/ml), (B) Flunarizine (0, 6.25, 12.5 and 25 µg/ml) and (C) Cinnarizine (0, 6.25, 12.5 and 25 µg/ml) induce cell death and morphological deformities in triple negative and ER+ve breast cancer cells. Post incubation, cells were observed under inverted microscope TS-100F (Nikon), and images of 10 different random fields were captured with a high resolution digital camera Nikon Coolpix L22. Drug treated cells appear with morphological deformities when compared with untreated cells which appear to be healthy.

patterns in cells only at much higher concentrations (50 µg/ml to 100 µg/ml). Overall, all the three phytochemicals β-Glycyrrhetinic acid, Gallic acid and Epigallocatechin gallate affected the morphology of both MDAMB-231 and MCF-7 breast cancer cells in a dose-dependent manner. However, as usual, MCF-7 were susceptible to all the phytochemicals at comparatively lower concentrations compared to MDAMB-231 cells. In Figure 4.3, it is clearly observed that cells treated with serum-free media alone didn't show any sign of membrane blebbing or other morphological deformities which prove that they were very healthy and fine.

In chapter 3, we have mentioned about the synthesis of a novel series of compounds alkyl cinnamates (Mamidi et al., 2012). At first, we looked into the morphological features of breast cancer cells to individual alkyl cinnamate treatment. Curcumin is considered as the parent compound of alkyl cinnamates (Chapter 3, Figure 3.8) and hence it was included in the study as a reference molecule. Alkyl cinnamates treated cells also exhibited cytoplasmic shrinkage and membrane blebbing patterns indicating a high proportion of cells progressing towards death (Figure 4.4). However, different alkyl cinnamates varied in their potency to induce abnormalities in breast cancer cells. Some of the alkyl cinnamates such as DM 2-1, DM 2-2, DM 2-3, DM 2-4 and DM 2-5 were very potent in affecting the morphology of breast cancer cells at much lower concentrations (≤ 3 µg/ml, Figure 4.4). Whereas, DM 2-8, DM 3-7 and DM 3-8 can be considered as moderate molecules in their potency to induce morphological abnormality. All the alkyl cinnamates dose-dependently affected the morphology of both MDAMB-231 and MCF-7 breast cancer cells. However, different alkyl cinnamates started affecting cellular morphology from a particular concentration specific to each alkyl cinnamate which undoubtedly indicated their individual potency. We also observed in the study that MCF-7 cells were more susceptible to alkyl cinnamates than MDAMB-231 cells. In contrast, cells treated with serum-free media alone didn't show any morphological abnormality and appear to be healthy and fine.

The experiments concluded that the PKC-directed molecules were affecting the cellular morphology of cancer cells which indicated that they were causing stress in breast cancer cells. That probably is affecting their cellular morphology. The stress developed could have an impact on physiological processes such as cell cycle. A prolonged halting of cell cycle can compromise the viability of cancer cells. So, the immediate next set of experiments was designed to investigate possible changes in the breast cancer cell cycle on treatment with individual PKC-directed molecules. Thus, morphological differences between agonist-treated and untreated samples in these experiments indicate that different PKC-directed molecules induce potent stress on breast cancer cells which might pave the way for cell-death.

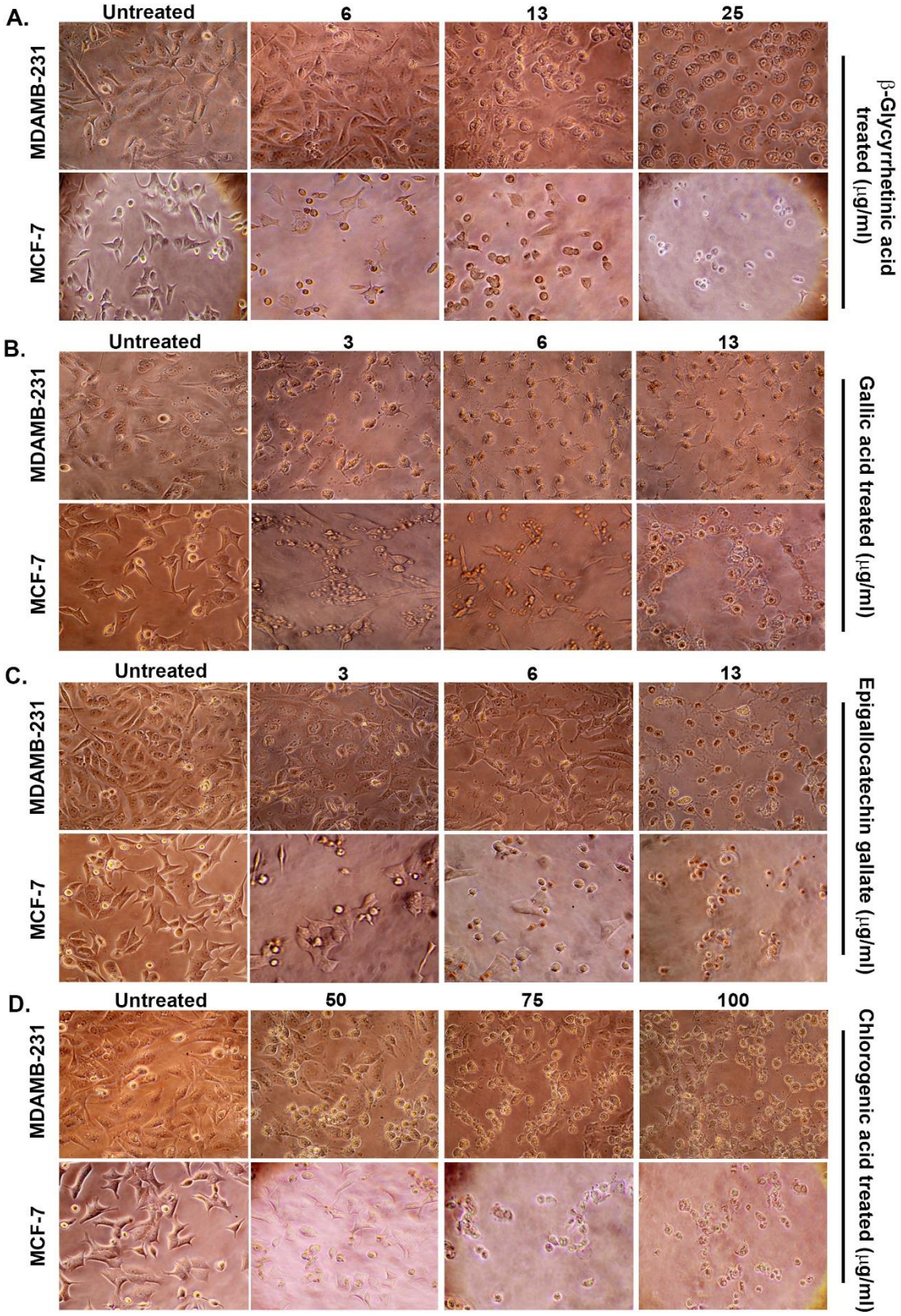

Figure 4.3: Morphological deformities in MDAMB-231 or MCF-7 breast cancer cells treated individually with different phytochemicals (0-100 µg/ml) in serum-free media for 48 hrs. (A) β-Glycyrrhetinic acid (0, 6, 13 and 25 µg/ml), (B) Gallic acid (0, 3, 6 and 13 µg/ml), (C) Epigallocatechin gallate (0, 3 ,6 and 13 µg/ml) and (D) Chlorogenic acid (0, 50, 75 and 100 µg/ml). Post incubation, the cells were observed under inverted microscope TS-100F (Nikon), and images of 10 different random fields were captured with a high resolution digital camera Nikon Coolpix L22.

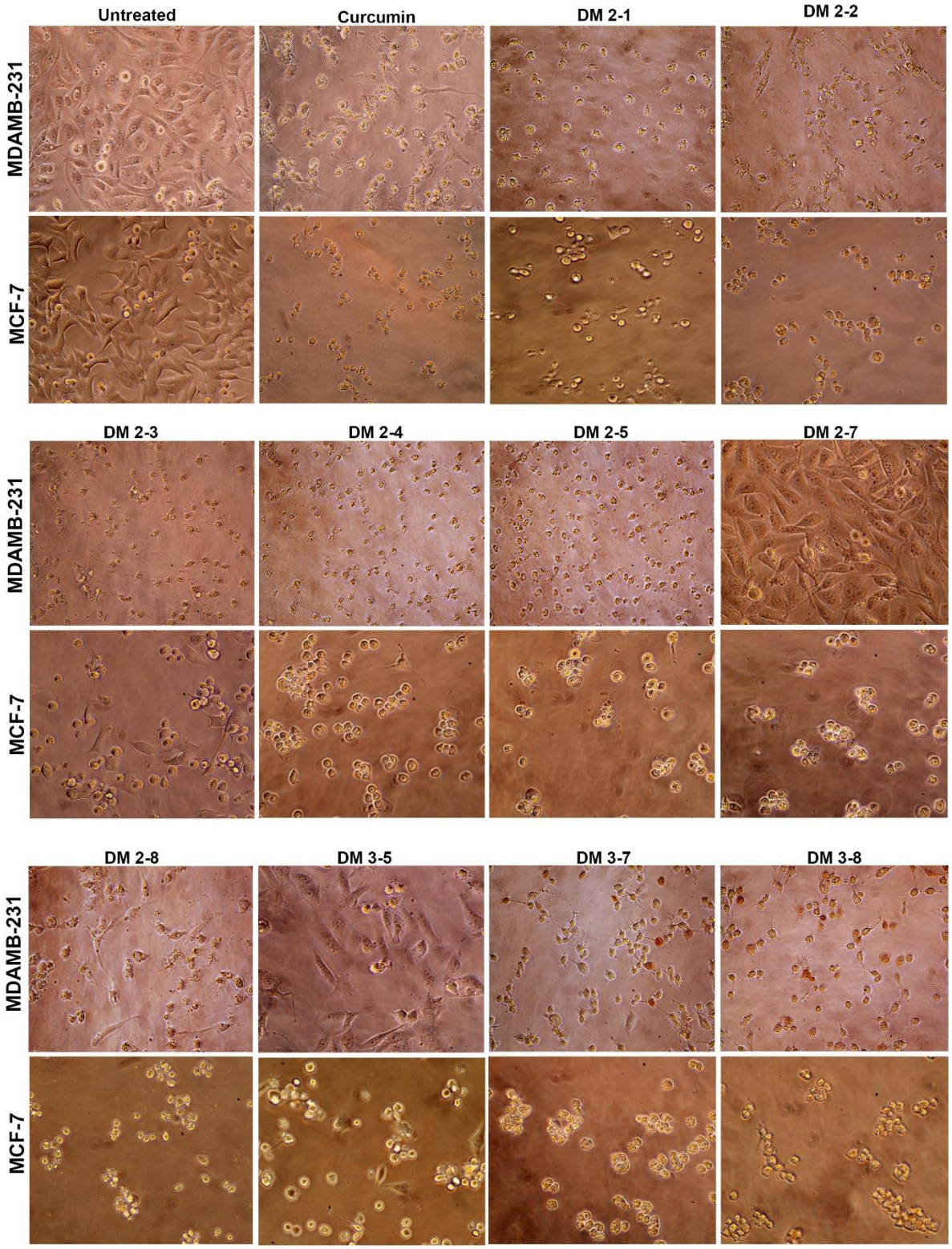

Figure 4.4: Morphological deformities in MDAMB-231 or MCF-7 breast cancer cells treated individually with Curcumin (13 µg/ml), DM 2-1 (3 µg/ml), DM 2-2 (3 µg/ml), DM 2-3 (1.5 µg/ml), DM 2-4 (3 µg/ml), DM 2-5 (6 µg/ml), DM 2-7 (75 µg/ml), DM 2-8 (6 µg/ml), DM 3-5 (75 µg/ml), DM 3-7 (6 µg/ml) and DM 3-8 (13 µg/ml). Cells treated with different alkyl cinnamates at different concentrations (0-100 µg/ml) for 48hrs in serum-free media**.** Post incubation, the cells were observed under inverted microscope TS-100F (Nikon) and images were taken with high resolution Nikon L22 camera.

.4.3.2 PKC agonists disrupt the cell cycle of breast cancer cells:

It has been revealed by many studies that PKC-mediated signalling pathways has profound influences on the cell cycle (Black and Black, 2012; Poli et al., 2014). MDAMB-231 cells are very actively growing cancer cells and have a very efficient cell cycle (Pervin et al., 2001). The effect of PKC agonists on the morphology of MDAMB-231 cells insisted us to understand the effects on MDAMB-231 cell cycle on the application of the selected PKC-directed molecules. MDAMB-231 cells were individually treated with Danazol (70 µg/ml), Flunarizine (5.9 µg/ml) or Cinnarizine (54 µg/ml) for 24 hrs, and distribution of cells in different phases of cell cycle was studied by flow cytometry as described in Chapter 2 (Section 2.4). In untreated cells, 45.22 ± 2.63% of cells were present in the G1 phase, 39.44 ± 1.85% of cells were present in the S phase while 15.34 ± 0.76% of cells in the G2/M phase (Figure 4.5). Whereas, cells treated with Danazol, Flunarizine or Cinnarizine showed a change in cell cycle distribution pattern within the cellular population. Cells treated with Danazol exhibited 55 ± 1.75% cells in G1 phase, 30 ± 1.08% cells in S phase and 15 ± 1.18% in G2/M phase. Similarly, during individual Flunarizine or Cinnarizine treatments, the percentage of the cell-population in the S phase was 26.86 ± 1.37% and 26.94 ± 2.08% respectively. Whereas, the percentage of the cell-population in the G1 phase were 51.51 ± 2.31% and 53 ± 2.75% respectively. The percentage of the cell-population in the G2/M phase during individual Flunarizine or Cinnarizine treatment were 21.63 ± 2.14% and 20.06 ± 1.31% respectively. Thus, the cell cycle analysis indicates that Danazol, Flunarizine and Cinnarizine were reducing proportion of cells in S-phase (the stage with active DNA synthesis and required for proliferation) with a concomitant increase in G1 and G2 phases (the phase with low metabolic activity). Reduction of S phase and halting of cells at G1 or G2 phase indicate that the cells had stop proliferating.

Similarly, we have also tested the effect of individual phytochemicals on the distribution of MDAMB-231 cells in different phases of cell cycle. MDAMB-231 cells were treated individually with Chlorogenic acid (75 µg/ml), β-Glycyrrhetinic acid (10 µg/ml), Gallic acid (2.5 µg/ml) and Epigallocatechin gallate (6.5 µg/ml) for 24 hrs. The population of cells in different phases of cell cycle was monitored by staining the cells with propidium iodide dye and analysed by flow cytometry as described in Chapter 2 (Section 2.4). Cells treated with phytochemicals showed a shift in the population of cells in S phase to the quiescent G1 phase or the G2 phase. In Chlorogenic acid treated MDAMB-231 cells, 55.77 ± 2.32% cells were in the G1 phase, 29.69 ± 0.78% cells were in the S phase while 14.54 ± 0.37% cells were in the G2/M phase. This shows that Chlorogenic acid treatment halted MDAMB-231 breast cancer cells at G0/G1 phase. β-Glycyrrhetinic acid was the most uncommon amongst all the PKC-directed molecule tested. Treatment of MDAMB-231 cells with β-Glycyrrhetinic acid produced a cell-

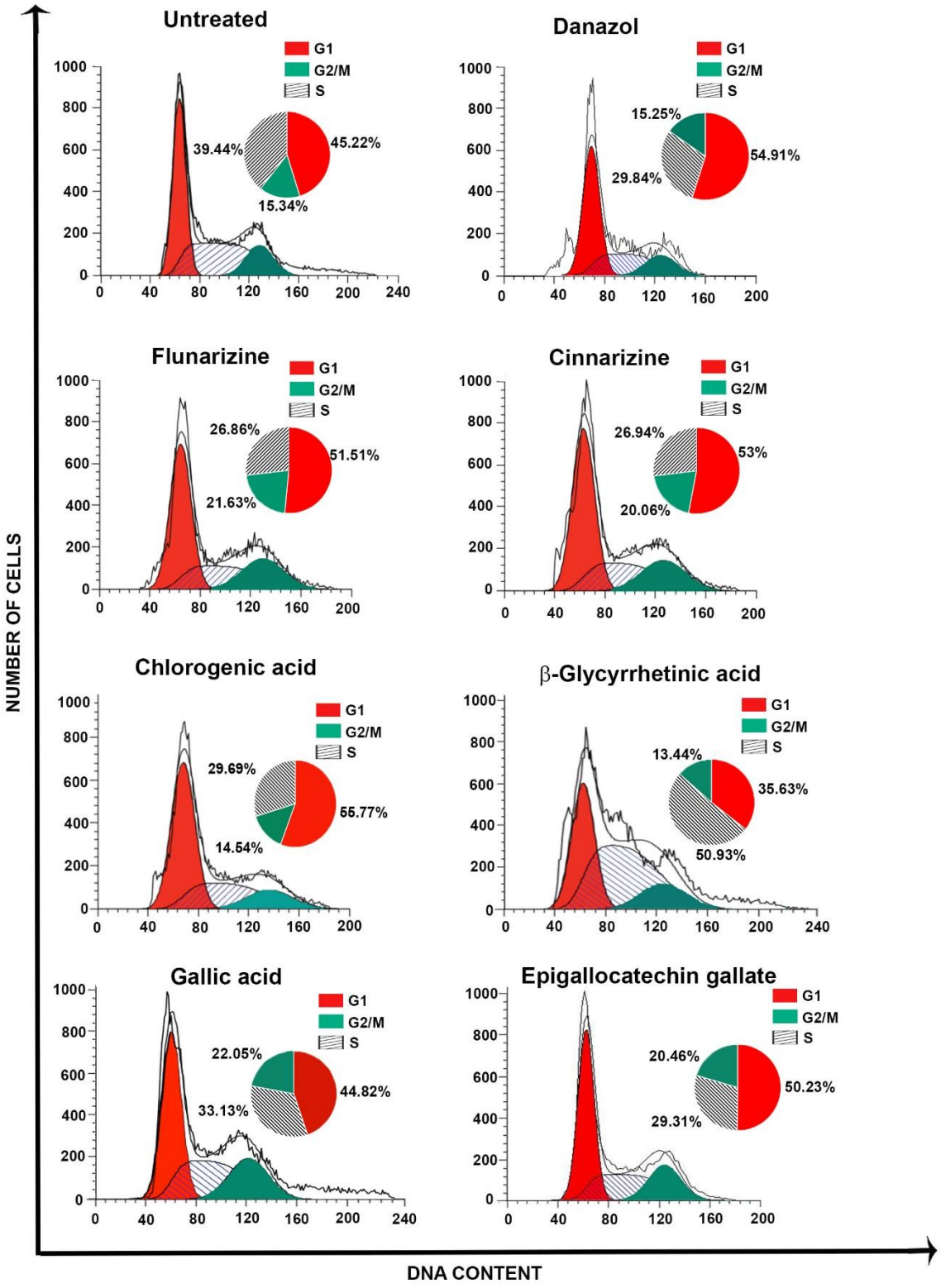

Figure 4.5: Drug and phytochemical PKC-directed molecules disturb the cell cycle of breast cancer cells. MDAMB-231 cells were treated individually with Danazol (70 µg/ml), Flunarizine (5.9 µg/ml), Cinnarizine (54 µg/ml), Chlorogenic acid (75 µg/ml), β-Glycyrrhetinic acid (10 µg/ml), Gallic acid (2.5 µg/ml) and Epigallocatechin gallate (6.5 µg/ml) for 24 hrs. Cell-cycle phases were analyzed by flow cytometry as described in Chapter 2 (Section 2.4).

cycle phase distribution of MDAMB-231 cells as follows: 35.63 ± 1.37% cells in G1 phase, 50.93 ± 1.67% cells in S phase and 13.44 ± 0.56% cells in G2/M phase. Thus, there is an extensive arrest of MDAMB-231 cells in S phase on the treatment of β-Glycyrrhetinic acid. The other candidate phytochemical, Gallic acid has also been implicated earlier in the arrest of cell cycle of bladder carcinoma cells at the G2/M phase (Ou et al., 2010) and as such was expected to show similar effects against MDAMB-231 cells. We also found out that Gallic acid mediated mainly G2/M phase arrest of MDAMB-231 cells predominantly. The phase distribution of Gallic acid treated MDAMB-231 cells were as follows: 44.82 ± 2.73% cells in G1 phase, 33.13 ± 0.63% cells in S phase and 22.05 ± 1.11% cells in G2/M phase. Epigallocatechin gallate has also been earlier pursued for anti-cancer therapy and has been reported to arrest NBT-II bladder tumour cells and biliary tract cancer cells at G0/G1 phases (Chen et al., 2004; Mayr et al., 2015). We have obtained a phase distribution of Epigallocatechin gallate treated MDAMB-231 cells as follows: 50.23 ± 0.45% cells in G1 phase, 29.31 ± 0.48% cells in S phase and 20.46 ± 1.55% cells in G2/M phase. This data shows a clear shifting of cells to G1 as well as G2/M phase confirming arrest of cell cycle of breast cancer cells.

Similarly, alkyl cinnamates were also found to affect cell cycle phase distribution in MDAMB-231 cells (Figure 4.6). MDAMB-231 cells were also individually treated with different alkyl cinnamates for 24 hrs, and the population of cells in different phases of cell cycle was monitored by staining the cells with propidium iodide dye and analysed by flow cytometry as described in Chapter 2 (Section 2.4). Untreated cells were exhibiting 41 ± 1.16% cells in G1 phase, 39 ± 1.27% cells in S phase and 18 ± 1.12 % cells in the G2/M phase (Figure 4.6-A). Whereas, cells stimulated with different alkyl cinnamates exhibited the disturbance of cell cycle stages. The population of cells in the G1 and G2/M phases increased with a concomitant decrease of cells in the S phase (Figure 4.6-A). DM 2-8 had the most profound effect on the S phase of treated cells and causes ~50% decrease in the S phase population (Figure 4.6-B).Thus, all PKC-directed molecules have the ability to shift population of MDAMB-231 cells from the S phase to G1 or G2 phases. The decrease in population of MDAMB-231 breast cancer cells in the DNA synthesis or S phase after treatment with individual PKC-directed molecules might signify a decrease in DNA synthesis. This change in the distribution of MDAMB-231 cells in different phases of the cell cycle after PKC-directed molecule treatment may significantly affect the cellular ability to survive or proliferate.

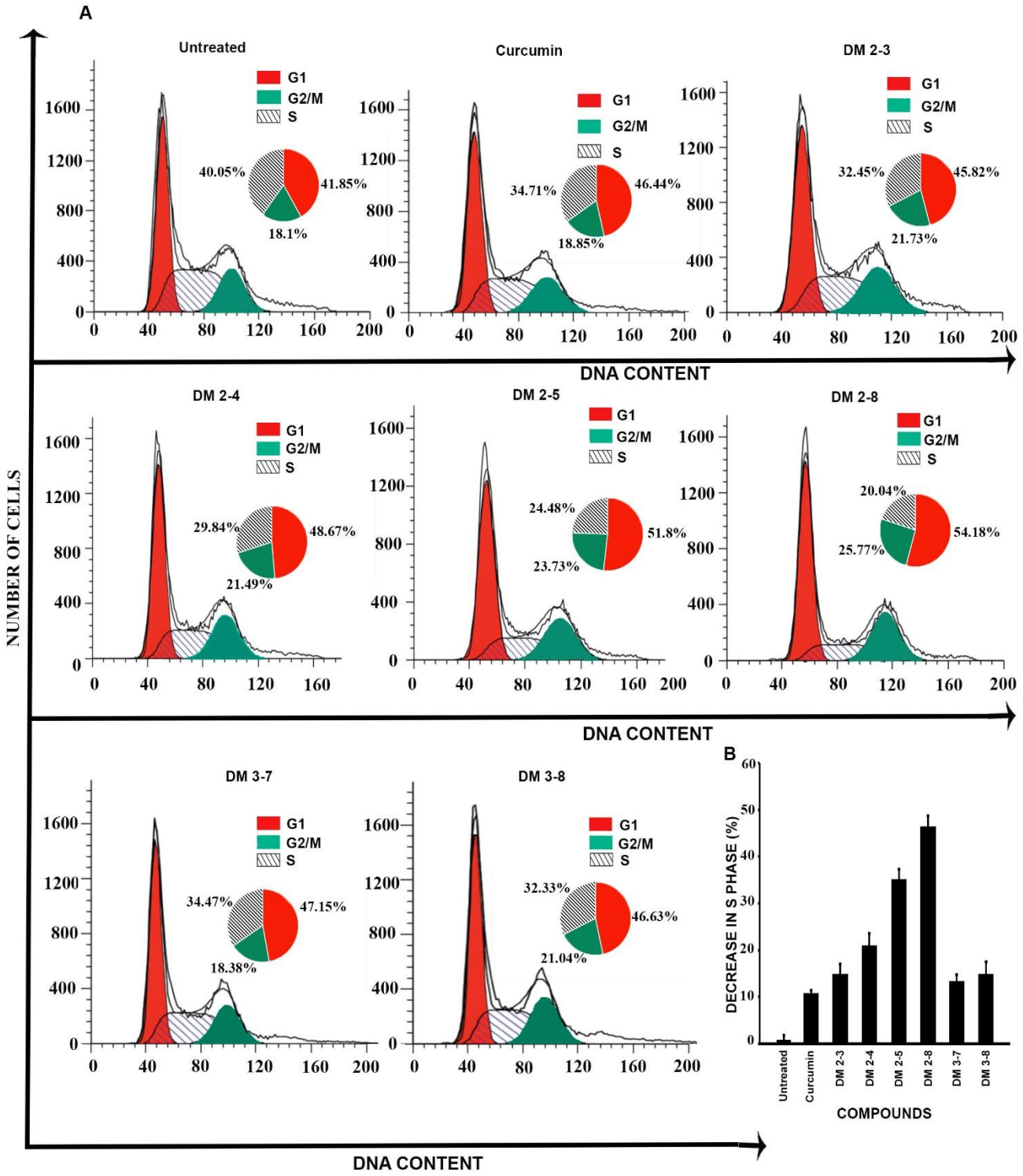

Figure 4.6: Alkyl-cinnamates disturb cell cycle in MDAMB-231 cells. (A) Cells were treated with different alkyl cinnamates; curcumin (13µg/ml), DM 2-3 (1.5µg/ml), DM 2-4 (3µg/ml), DM 2-5 (6µg/ml), DM 2-8 (6µg/ml), DM 3-7 (6µg/ml) and DM 3-8 (13µg/ml) for 24 hrs in incomplete media, stained with PI as given in Section 4.2.3. Next, cells were immediately analyzed by flow cytometry. Concentration against individual alkyl cinnamate is indicated to the right in parentheseis. Alkyl cinnamate treated cells show a reduction of S phase and increase in G1 and G2 phases. (**B**) Plot of reduction in S-Phase against each alkyl cinnamates. DM 2-8 show the highest change in S phase (50%).

4.3.3 Viability of breast cancer cells is compromised on treatment with PKC-directed molecules:

Morphological observations and cell cycle assays have shown that candidate drugs are profoundly capable of disturbing the normal functioning of breast cancer cells. The cells were observed to be under intense stress (Section 4.3.1) on treatment with PKC-directed molecules. Also, halting of the cell-cycle (Section 4.3.2), indicated that the cells might have stopped proliferating. The disturbance in morphology indicated that under this combined effect (stress & halting of cell cycle at G1/G2), viability may be compromised. To answer these questions, MDAMB-231 and MCF-7 cells were treated individually with different concentrations (0-100 µg/ml) of the molecules (Danazol and Flunarizine), and cellular viability was measured by MTT reduction assay as described in Chapter 2 (Section 2.3). Cells were also treated with Cinnarizine at different concentrations (0-200 µg/ml) to measure cellular viability. Danazol, Flunarizine and Cinnarizine were seen to reduce the viability of MDAMB-231 and MCF-7 cells in a dose-dependent manner. Danazol, Flunarizine and Cinnarizine were killing MDAMB-231 cells with IC_{50} concentrations of 65 ± 4.27 µg/ml, 5.88 ± 0.37 µg/ml and 53.7 ± 5.22 µg/ml respectively (Figure 4.7). Besides, Danazol, Flunarizine and Cinnarizine were killing MCF-7 cells with IC_{50} concentrations of 31 ± 2.63 µg/ml, 1.24 ± 0.06 µg/ml and 33 ± 2.93 µg/ml respectively (Figure 4.7).

We have also measured the individual effect of phytochemicals and alkyl cinnamates on the cellular viability of breast cancer cells. All the selected phytochemicals are observed to reduce the cellular viability of MDAMB-231 and MCF-7 cells dose-dependently. Chlorogenic acid, β-Glycyrrhetinic acid, Gallic acid and Epigallocatechin gallate were killing MDAMB-231 cells with IC_{50} concentrations of 75.88 ± 4.54 µg/ml, 9.7 ± 1.45 µg/ml, 2.6 ± 0.42 µg/ml and 6.6 ± 0.47 µg/ml respectively (Figure 4.7). Similarly, Chlorogenic acid, β-Glycyrrhetinic acid, Gallic acid and Epigallocatechin gallate were killing MCF-7 cells with IC_{50} concentrations of 29 ± 3.61 µg/ml, 3.1 ± 0.65 µg/ml, 1.1 ± 0.11 µg/ml and 5.88 ± 0.86 µg/ml respectively (Figure 4.7). Thus, Chlorogenic acid appeared to be the weakest phytochemical as far as potency is concerned. Other three phytochemicals were similar in their anti-cancer potency. It is also noteworthy that the MCF-7 cells have comparatively lower IC_{50} concentrations than MDAMB-231 cells for each phytochemical. Thus, MDAMB-231 cell line can be considered as a little bit more resistant to the selected phytochemicals.

Viability measurements showed that alkyl cinnamates dose-dependently induce cell-death in breast cancer cells. Overall, most of the compounds were highly active against breast cancer cells (MCF-7 and MDAMB-231) with IC_{50} concentrations ranging from 1.1 to 58 µg/ml (Table 4.1). Compounds DM 2-1, DM 2-2, DM 2-3 and DM 2-4 were the most active compounds. Whereas, compound DM 3-5 and DM 2-7 were the least active against MCF-7 cells and were ineffective against MDAMB-231 cells. DM

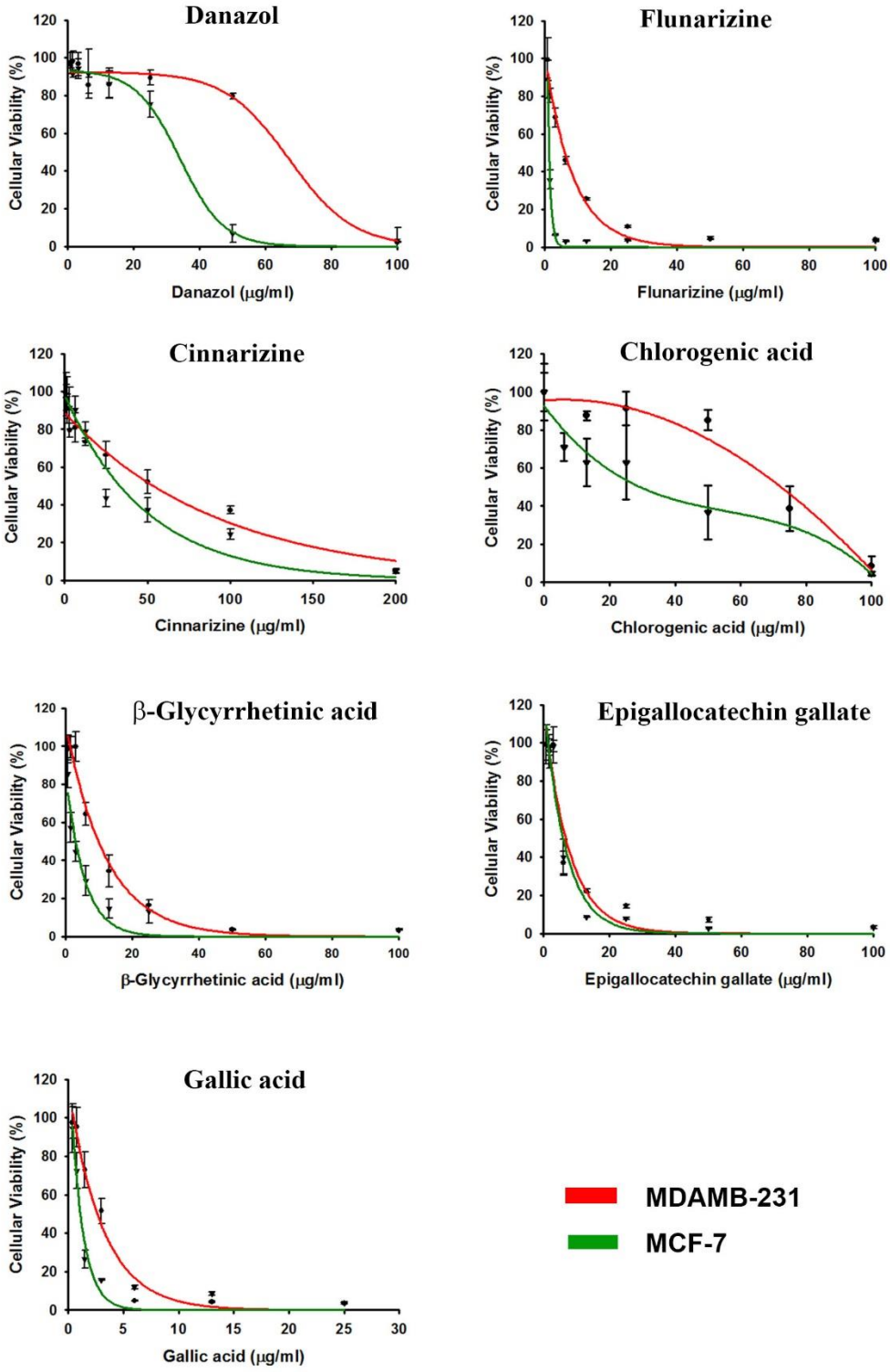

Figure 4.7:PKC-directed molecules reduce the viability of triple negative and ER+ve breast cancer cells in a dose dependent manner. MDAMB-231 or MCF-7 cells breast cancer cells were treated with different concentrations (0-100µg/ml) of Danazol, Flunarizine, Cinnarizine, Chlorogenic acid, β-Glycyrrhetinic acid, Epigallocatechin gallate and Gallic acid in serum-free media for 48 hrs and cellular viability was measured by MTT reduction assay as described in Section 4.2.4.

2-3 and DM 2-4 showed anti-cancer activity against MDAMB-231 with IC_{50} concentrations of 1.5 ± 0.14 µg/ml and 1.9 ± 0.1 µg/ml respectively. The viability assay confirmed that alkyl cinnamates were inducing cell-death both in MDAMB-231 and MCF-7 breast cancer cell lines. (Table 4.1 and Figure 4.8).

Table 4.1: Activity of Novel alkyl cinnmates against breast cancer cells.

		Anticancer Activity (IC_{50} ±SD)	
S No	**Compound Code**	**MCF-7**	**MDAMB-231**
1	Curcumin	5.0 ±0.81	11±3
2	DM-2-1	1.9 ± 0.22	2.7 ± 0.4
3	DM-2-2	2.8 ± 0.21	3.4± 0.82
4	DM-2-3	0.97 ± 0.12	1.5± 0.14
5	DM-2-4	1.1 ± 0.20	1.9 ± 0.1
6	DM-2-5	1.3 ± 0.11	3.90 ± 0.25
7	DM-2-6	2.86 ± 0.47	58.2± 4.67
8	DM-2-7	6.9 ± 1.0	Not Active
9	DM-2-8	1.2 ± 0.17	4.13 ± 0.27
10	DM-2-9	3.2 ± 0.35	39.4 ± 4.1
11	DM-3-5	6.3 ± 0.38	Not Active
12	DM-3-7	4.1 ± 0.54	6.4 ± 2
13	DM-3-8	4.7 ± 0.31	8.6 ± 0.89

MDAMB-231 or MCF-7 cells breast cancer cells were treated with different concentrations (0-100µg/ml) of alkyl cinnamates in serum-free media for 48 hrs. Post incubation, cellular viability was measured by MTT reduction assay as described in Chapter 2 (Section 2.3). Viability curves were plotted in SigmaPlot software and the half maximal inhibitory concentration (IC_{50}) values of all the alkyl cinnamates were accordingly calculated.

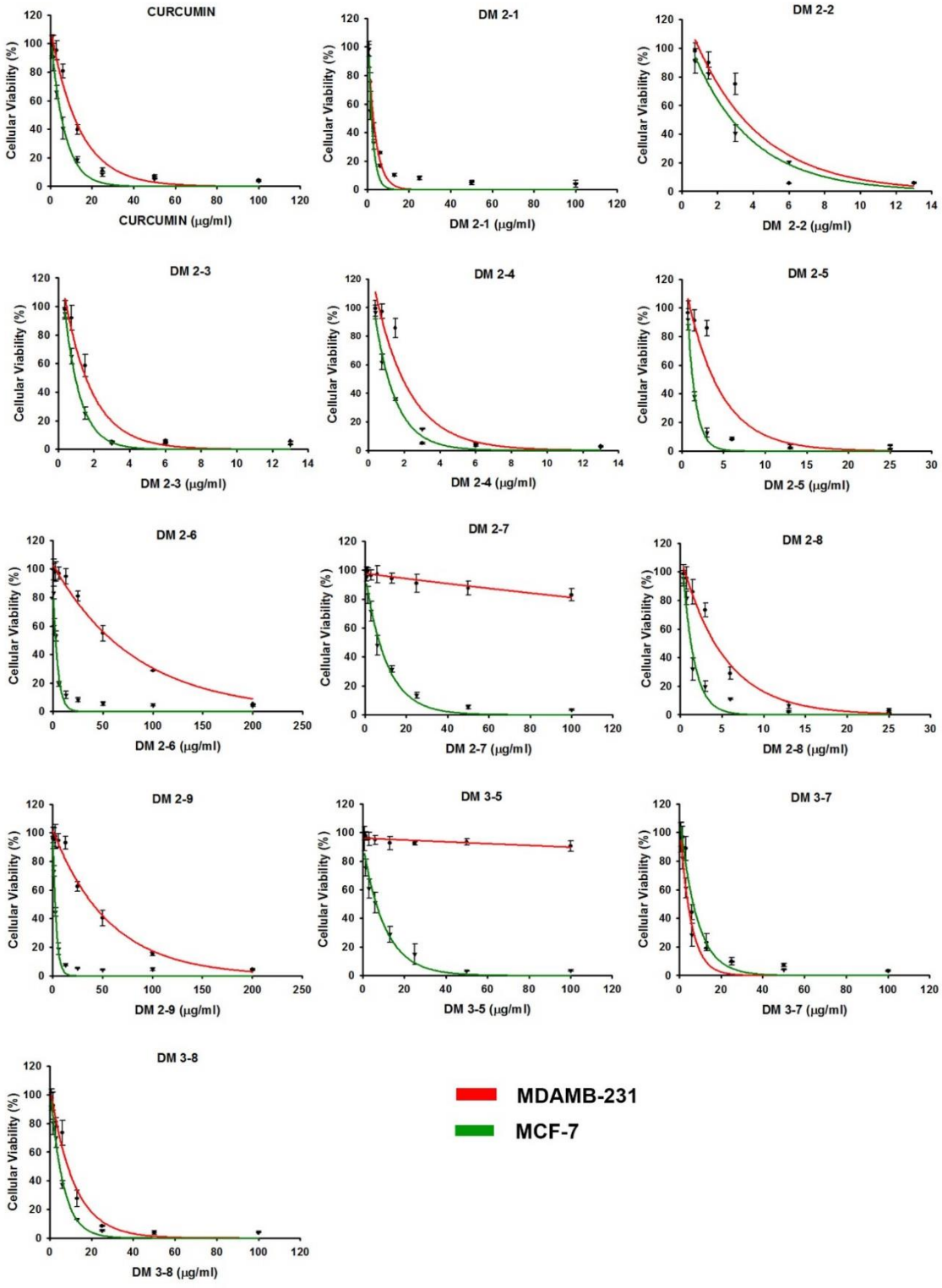

Figure 4.8: Alkyl cinnamates reduce the viability of triple negative and ER+ve breast cancer cells in a dose dependent manner. MDAMB-231 or MCF-7 breast cancer cells were treated with different concentrations of alkyl cinnamates (0-100 µg/ml) in serum-free media for 48 hrs. Post incubation, cellular viability was measured by MTT reduction assay as described in Chapter 2 (Section 2.3). Values were plotted and graph was drawn in sigma plot software and IC_{50} values were accordingly calculated.

4.4 Discussion

Activated PKC has been implicated in the activation of stress-linked kinases, the p38 and c-Jun N-terminal kinase (JNK) (Nakajima et al., 2004). Activation of the p38 kinase by PKC induces apoptosis in prostate cancer cells (Tanaka et al., 2003). PKC also actively regulates the JNK pathway (Brandlin et al., 2002). PKC isozymes are known to mediate apoptosis via activation of JNK (Matassa et al., 0000). Activation of JNK by PKC mediates endoplasmic reticulum stress dependent apoptosis of human vascular smooth muscle cells (Larroque-Cardoso et al., 2013). Activated JNK can also translocate to mitochondria to generate mitochondrial ROS production (Aoki et al., 2002). Production of ROS in mitochondria is usually accompanied by lower NADH and ATP levels. Thus, stress-linked signalling results in lower NADH and ATP availability for cell cycle progression (da Veiga Moreira et al., 2015; Murphy, 2009; Tiwari et al., 2002). Depletion of ATP levels by drugs arrest cell cycle in prostate cancer cells which lead to apoptosis (Obajimi and Melera, 2008). Thus, activation of PKC by PKC directed molecules serve as a platform to induce p38 kinase or JNK mediated stress-linked signalling in breast cancer cells.

The experiments depicted in the present chapter were designed to assess the effect on breast cancer cell physiology on treatment with the various PKC-directed molecules that had been identified in the previous Chapter 3. Treatment of both MDAMB-231 and MCF-7 cells have shown that the identified PKC-directed molecules dose-dependently affected the morphology of both MDAMB-231 and MCF-7 breast cancer cells. This aberrant morphology is indicative of stress generation inside breast cancer cell which indicated their anti-cancer potential. Amongst the clinical drugs, Flunarizine was more potent at affecting the cellular morphology of breast cancer cells. Earlier studies have indicated promising anti-cancer activity of Flunarizine both as an anticancer drug alone (Abdul and Hoosein, 2002) or in conjunction with already established anti-cancer drugs (Orlandl et al.). Similarly, Cinnarizine has also been reported to reduce the viability of myeloma and lymphoma cell lines in a dose-dependent manner (Schmeel et al., 2015). The current study indicates that these drugs have anti-cancer activity against breast cancer cells. Amongst the phytochemicals, Gallic acid and Epigallocatechin gallate are more potent at affecting cellular morphology. The anti-cancer potential of Epigallocatehin gallate had been earlier reported against HCT-116 and SW-480 human colorectal cancer cells (Du et al., 2012). Its activity against MDAMB-231 and MCF-7 breast cancer cells further substantiate its anti-cancer potential. Different alkyl cinnamates also varied immensely in their potency at affecting cellular morphology. It was also observed that MCF-7 cells are more susceptible to all the PKC-directed molecule induced morphological changes than MDAMB-231 cells.

This change in cellular morphology brought about by PKC-directed molecules indicated a probable effect on the breast cancer cell cycle on treatment with these molecules. It is well documented in scientific literature that halting of the cell cycle at the G1 or G2 phases for prolonged periods induces activation of cell-death pathways (Atashpour et al., 2015). Investigations into the highly active cell cycle of MDAMB-231 breast cancer cells by flow cytometry techniques found that PKC-directed molecule treatment can halt the cell cycle at the G1, G2 or even at the S phase. Flunarizine, Cinnarizine, Danazol as well as alkyl cinnamate treatments significantly shifted the population of cells from S to G1 phase. On the other hand, phytochemicals were preferentially selective on the shifting of cells to the G1, G2 or S phases, depending upon the individual phytochemical. While there are earlier reports which suggested that Chlorogenic acid treatment arrested the cell cycle at the G0/G1 phase in leukaemia cells (Liu et al.), there is no any earlier report about the cell cycle arrest at S phase by β-Glycyrrhetinic acid. It had only been reported that β-Glycyrrhetinic acid induces G1-phase cell cycle arrest in human non-small cell lung cancer cells (Zhu et al., 2015). Similarly, Epigallocatechin gallate had also been reported to induce cell cycle arrest in bladder tumor cell-line (Chen et al., 2004). Hence, although there are no previous reports about the arrest of cell-cycle by Flunarizine, Cinnarizine and Danazol, the halting of cell cycle by most of the phytochemicals is in accordance with many earlier studies.

Morphological observations (Section 4.3.1) and cell-cycle assays (Section 4.3.2) under individual PKC-directed molecule treatment have enabled us to conclude that different molecules varied in their potency to induce morphological abnormalities in breast cancer cells. The cellular viability of breast cancer cells on the treatment of PKC-directed molecules was subsequently measured. Viability assays on both MDAMB-231 and MCF-7 cell lines have shown that all PKC-directed molecules reduce the viability of both types of breast cancer cells in a dose-dependent manner. All the molecules have lower IC_{50} concentrations for the MCF-7 cell line than the MDAMB-231 cell line. Strikingly, viability measurements were in full agreement with morphological assay results described earlier (Section 4.3.1). Amongst drugs, Flunarizine had the lowest IC_{50} against breast cancer cells, which was in accordance with morphological observations (Section 4.3.1). Amongst alkyl cinnamates, compounds DM 2-1, DM 2-2, DM 2-3 and DM 2-4 were the most active compounds in accordance with earlier morphological observations (Section 4.3.1). Likewise, compound DM 3-5 and DM 2-7 were the least active against MCF-7 and were ineffective against MDAMB-231, again in accordance with earlier morphological observations (Section 4.3.1). In a nutshell, the experiments presented in this chapter have discovered the anti-cancer role of PKC-directed molecules against triple negative and ER+ve breast cancer cells. These findings have undoubtedly

complemented the earlier reported anti-cancer activity of some of these PKC-directed molecules against different cancer cell lines (prostrate, lung, bladder and colorectal).

Thus, in the current study, all the selected PKC-directed molecules have induced cell-death after induction of morphological abnormalities and halting of the cell cycle in breast cancer cells. In short, till now, we have confirmed the development of aberrant morphology, cell cycle dysregulation and loss of breast cancer cellular-viability (Figure 4.9). However, the mechanistic details from the point of halting of cell cycle till the induction of cell-death need to be answered. Thus, many questions remain unexplored (Figure 4.9). A schematic illustration of the hypothesis depicting the mechanism of action of PKC-directed molecules is shown in Figure 4.9. These are exactly the questions what we have tried to explore in subsequent experiments that are described in detail in the next chapter.

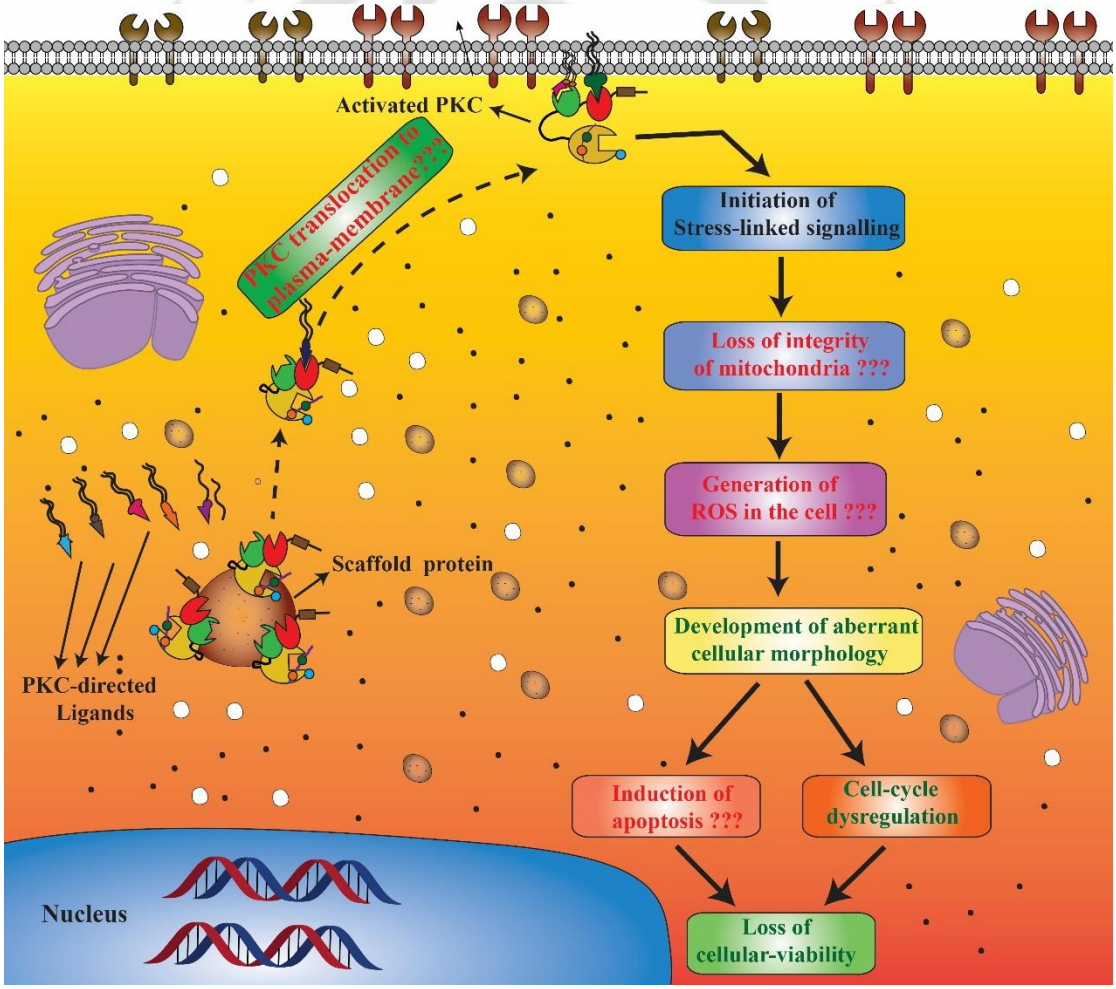

Figure 4.9: Probable pathway of PKC-directed molecules mediated loss of cellular-viability in breast cancer cells. Green letter-headings indicates phenomena that have been verified. Whereas, red letter-headings indicates phenomena not verified yet.

4.5 References

- Abdul, M., and Hoosein, N. (2002). Voltage-gated sodium ion channels in prostate cancer: expression and activity. Anticancer Research *22*, 1727-1730.
- Aoki, H., Kang, P.M., Hampe, J., Yoshimura, K., Noma, T., Matsuzaki, M., and Izumo, S. (2002). Direct Activation of Mitochondrial Apoptosis Machinery by c-Jun N-terminal Kinase in Adult Cardiac Myocytes. Journal of Biological Chemistry *277*, 10244-10250.
- Atashpour, S., Fouladdel, S., Movahhed, T.K., Barzegar, E., Ghahremani, M.H., Ostad, S.N., and Azizi, E. (2015). Quercetin induces cell cycle arrest and apoptosis in CD133(+) cancer stem cells of human colorectal HT29 cancer cell line and enhances anticancer effects of doxorubicin. Iranian Journal of Basic Medical Sciences *18*, 635-643.
- Black, A.R., and Black, J.D. (2012). Protein kinase C signaling and cell cycle regulation. Frontiers in Immunology *3*, 423.
- Brandlin, I., Eiseler, T., Salowsky, R., and Johannes, F.J. (2002). Protein kinase C(mu) regulation of the JNK pathway is triggered via phosphoinositide-dependent kinase 1 and protein kinase C(epsilon). The Journal of Biological Chemistry *277*, 45451-45457.
- Chen, J.J., Ye, Z.Q., and Koo, M.W. (2004). Growth inhibition and cell cycle arrest effects of epigallocatechin gallate in the NBT-II bladder tumour cell line. BJU International *93*, 1082-1086.
- da Veiga Moreira, J., Peres, S., Steyaert, J.-M., Bigan, E., Paulevé, L., Nogueira, M.L., and Schwartz, L. (2015). Cell cycle progression is regulated by intertwined redox oscillators. Theoretical Biology & Medical Modelling *12*, 10.
- Du, G.-J., Zhang, Z., Wen, X.-D., Yu, C., Calway, T., Yuan, C.-S., and Wang, C.-Z. (2012). Epigallocatechin Gallate (EGCG) Is the Most Effective Cancer Chemopreventive Polyphenol in Green Tea. Nutrients *4*, 1679-1691.
- Frey, M.R., Saxon, M.L., Zhao, X., Rollins, A., Evans, S.S., and Black, J.D. (1997). Protein Kinase C Isozyme-mediated Cell Cycle Arrest Involves Induction of p21waf1/cip1 and p27kip1 and Hypophosphorylation of the Retinoblastoma Protein in Intestinal Epithelial Cells. Journal of Biological Chemistry *272*, 9424-9435.
- Kaul, A., and Maltese, W.A. (2009). Killing of Cancer Cells by the Photoactivatable Protein Kinase C Inhibitor, Calphostin C, Involves Induction of Endoplasmic Reticulum Stress. Neoplasia *11*, 823-834.
- Kuo, T.-c., Huang, W.-j., and Guh, J.-h. (2011). WJ9708012 exerts anticancer activity through PKC-α related crosstalk of mitochondrial and endoplasmic reticulum stresses in human hormone-refractory prostate cancer cells. Acta Pharmacologica Sinica *32*, 89-98.
- Larroque-Cardoso, P., Swiader, A., Ingueneau, C., Nègre-Salvayre, A., Elbaz, M., Reyland, M.E., Salvayre, R., and Vindis, C. (2013). Role of protein kinase C δ in ER stress and apoptosis induced by oxidized LDL in human vascular smooth muscle cells. Cell Death & Disease *4*, e520.
- Leszczynski, D. (1995). Regulation of cell cycle and apoptosis by protein kinase C in rat myeloid leukemia cell line. Oncology Research *7*, 471-480.
- Liu, Zhou, Qiu, Lu, and Wang (2013). Chlorogenic acid induced apoptosis and inhibition of proliferation in human acute promyelocytic leukemia HL60 cells. Mol. Med. Rep *8(4)*, 1106-10
- Mamidi, N., Gorai, S., Sahoo, J., and Manna, D. (2012). Alkyl cinnamates as regulator for the C1 domain of protein kinase C isoforms. Chemistry and Physics of Lipids *165*, 320-330.

- Matassa, A.A., Kalkofen, R.L., Carpenter, L., Biden, T.J., and Reyland, M.E. (0000). Inhibition of PKC[alpha] induces a PKC[delta]-dependent apoptotic program in salivary epithelial cells. Cell Death Differ *10*, 269-277.
- Mayr, C., Wagner, A., Neureiter, D., Pichler, M., Jakab, M., Illig, R., Berr, F., and Kiesslich, T. (2015). The green tea catechin epigallocatechin gallate induces cell cycle arrest and shows potential synergism with cisplatin in biliary tract cancer cells. BMC Complementary and Alternative Medicine *15*, 194.
- Minana, M.D., Felipo, V., and Grisolia, S. (1992). Differential effects of the protein kinase C inhibitors H7 and calphostin C on the cell cycle of neuroblastoma cells. Brain Research *596*, 157-162.
- Murphy, Michael P. (2009). How mitochondria produce reactive oxygen species. Biochemical Journal *417*, 1-13.
- Nakajima, K., Tohyama, Y., Kohsaka, S., and Kurihara, T. (2004). Protein kinase C alpha requirement in the activation of p38 mitogen-activated protein kinase, which is linked to the induction of tumor necrosis factor alpha in lipopolysaccharide-stimulated microglia. Neurochemistry International *44*, 205-214.
- Obajimi, O., and Melera, P.W. (2008). The depletion of cellular ATP by AG2034 mediates cell death or cytostasis in a hypoxanthine-dependent manner in human prostate cancer cells. Cancer Chemotherapy and Pharmacology *62*, 215-226.
- Orlandl, L., Zaffaroni, N., Costa, A., Villa, R., and Silvestrini, R. Flunarizine and lonidamine as modulators of anticancer drug activity in human colon adenocarcinoma cells. European Journal of Cancer *29*, S114.
- Ou, T.T., Wang, C.J., Lee, Y.S., Wu, C.H., and Lee, H.J. (2010). Gallic acid induces G2/M phase cell cycle arrest via regulating 14-3-3beta release from Cdc25C and Chk2 activation in human bladder transitional carcinoma cells. Molecular Nutrition & Food Research *54*, 1781-1790.
- Pervin, S., Singh, R., and Chaudhuri, G. (2001). Nitric oxide-induced cytostasis and cell cycle arrest of a human breast cancer cell line (MDA-MB-231): potential role of cyclin D1. Proceedings of the National Academy of Sciences of the United States of America *98*, 3583-3588.
- Poli, A., Mongiorgi, S., Cocco, L., and Follo, M.Y. (2014). Protein kinase C involvement in cell cycle modulation. Biochemical Society Transactions *42*, 1471-1476.
- Rodriguez-Lirio, A., Perez-Yarza, G., Fernandez-Suarez, M.R., Alonso-Tejerina, E., Boyano, M.D., and Asumendi, A. (2015). Metformin Induces Cell Cycle Arrest and Apoptosis in Drug-Resistant Leukemia Cells. Leukemia Research and Treatment *2015*, 516460.
- Schmeel, L.C., Schmeel, F.C., Kim, Y., Blaum-Feder, S., Endo, T., and Schmidt-Wolf, I.G. (2015). In vitro efficacy of cinnarizine against lymphoma and multiple myeloma. Anticancer Research *35*, 835-841.
- Tanaka, Y., Gavrielides, M.V., Mitsuuchi, Y., Fujii, T., and Kazanietz, M.G. (2003). Protein kinase C promotes apoptosis in LNCaP prostate cancer cells through activation of p38 MAPK and inhibition of the Akt survival pathway. The Journal of Biological Chemistry *278*, 33753-33762.
- Tiwari, B.S., Belenghi, B., and Levine, A. (2002). Oxidative Stress Increased Respiration and Generation of Reactive Oxygen Species, Resulting in ATP Depletion, Opening of Mitochondrial Permeability Transition, and Programmed Cell Death. Plant Physiology *128*, 1271-1281.
- Zhu, J., Chen, M., Chen, N., Ma, A., Zhu, C., Zhao, R., Jiang, M., Zhou, J., Ye, L., Fu, H., *et al.* (2015). Glycyrrhetinic acid induces G1phase cell cycle arrest in human nonsmall cell lung cancer cells through endoplasmic reticulum stress pathway. International Journal of Oncology *46*, 981-988.

Chapter 5

PKC-directed molecules translocate PKC and induce apoptosis in breast cancer cells following mitochondrial pathway.

5.1 Introduction

Newer research suggests that PKC-α plays an active role in inhibiting proliferation and inducing apoptosis in many types of cancer cells. These include colon cancer cells, non-small cell lung cancer cells (NSCLC) (Oliva et al., 2008; Oster and Leitges, 2006), breast cancer (Kerfoot et al., 2004) and pancreatic cancer cells. This understanding can be a novel paradigm shift in the design of effective anti-cancer drugs that utilize PKC-α as a therapeutic target.

In Chapter 3, we have discussed about the identification of molecules that fit with high affinity to PKC C1b domain, through molecular docking experiments and interaction analysis. In chapter 4, we have evaluated that these molecules cause morphological abnormalities, dysregulate the cell cycle and cause cell-death in breast cancer cells. Now we have a set of excellent PKC-directed molecules which are showing a potent anti-cancer activity. These experiments allow us to develop an experimental model as illustrated in Figure 5.1. Thus, we would like to test the utilities of these molecules in cancer drug development. The questions which are pertinent for this purpose are:

(1) Whether these molecules bind to PKC and induce its translocation to the cell membrane? The earlier experiments described in Chapter 3 or Chapter 4 still didn't address the point whether the observed effects in breast cancer cells (impairment of cell cycle and reduction of viability) is due to the activation of PKC in cancer cells after treatment with PKC-directed molecules. It is interesting to explore whether these molecules after binding to PKC can induce its translocation to cell membrane (as an indicator of agonist activity).

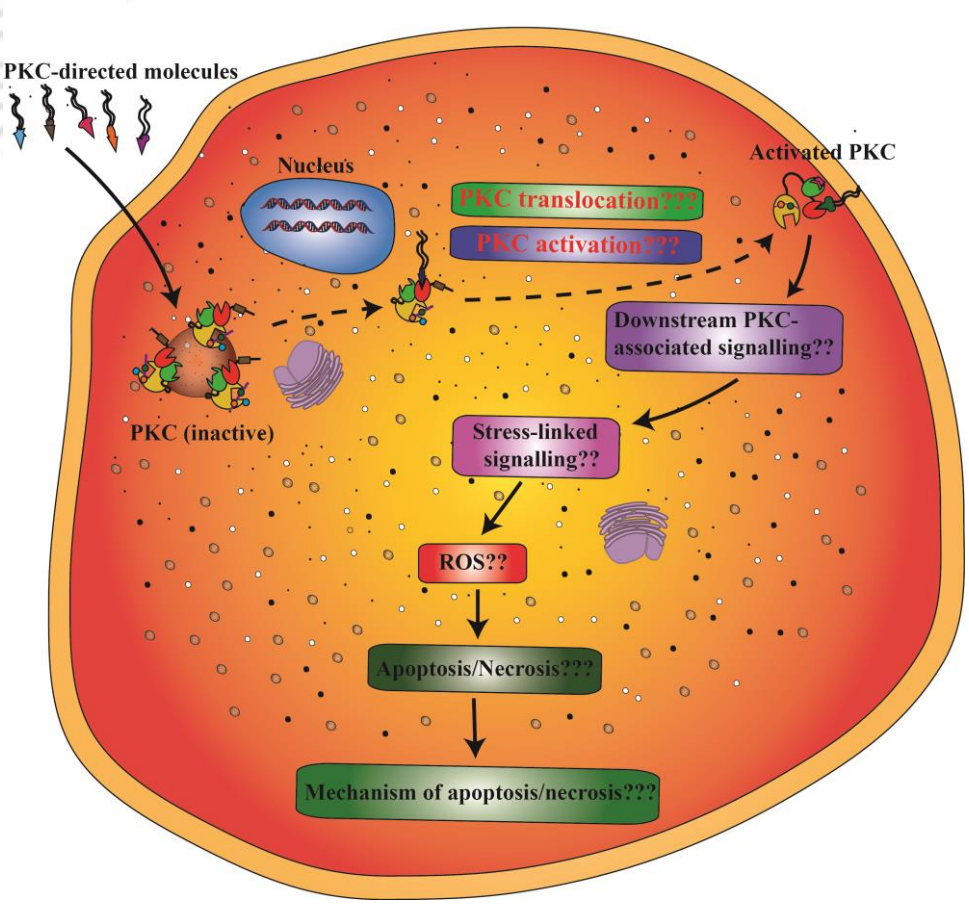

Figure 5.1: Schematic diagram about different questions explored in Chapter 5.

(2) What is the mode (apoptosis/necrosis) of death in cancer cells? We also don't know about the mechanism of cell-death caused by PKC directed molecules in breast cancer cells. We would like to investigate whether the death follows apoptotic, necrotic or any other pathway.

(3) What is the molecular mechanism of cell-death and what are the crucial cellular factors involved? We also follow-up with the investigation into the molecular mechanism of the mode of cell-death. Thus, we intend to explore the mechanistic details of observed cell-death in breast cancer cells that have been brought about by the selected PKC-directed molecules.

To understand these questions, biochemical/molecular-biology/cell-biology approaches have been undertaken. These approaches are being ellaborated in experimental procedures (Section 5.2).

5.2 Experimental Procedures

5.2.1 Cell-culture: MDAMB-231 and MCF-7 breast cancer cells were cultured in DMEM:F12 media, supplemented with 10% foetal bovine serum (FBS) and 1% penicillin-streptomycin antibiotic solution (100 units/ml penicillin and 100 µg/ml streptomycin sulfate). Cells were grown at 37°C in a humidified 5% CO_2 incubator. On the day of the experiments, cells were washed twice with cell-culture-grade phosphate buffer saline (PBS) and subjected to various treatments in serum free medium as described in details in Chapter 2 (Section 2.2).

5.2.2 Immunoblotting to detect PKC-α translocation: MDAMB-231 breast cancer cells (5×10^5) were seeded in 60 mm dishes overnight. Next, according to different experiments, cells were treated with different PKC-directed molecules (either drugs, phytochemicals or alkyl cinnamates) for different time periods in serum-free media. Cells treated with serum-free media alone served as control. Post treatment, cells were gently washed twice with sterile PBS and then detached from wells using 0.6% EDTA solution prepared in sterile PBS. After that, the cytosolic and membrane fractions were prepared as described in Chapter 2 (section 2.9). The fractions were next resolved in 10% SDS PAGE and transferred to PVDF membrane for immuno-blotting with anti-PKC-α antibody as described in detail in Chapter 2 (Section 2.10).

5.2.3 Immuno-localization experiments: Immuno-localization experiments were performed to detect PKC-α in MDAMB-231 cells. Twenty thousand (2×10^4) cells were seeded in square glass coverslips for overnight attachment in DMEM:F12 media. Next, according to different experiments, cells were treated different PKC-directed molecules (either drugs, phytochemicals or alkyl cinnamates) for different time periods in serum-free media. After treatments, cells were washed with sterile PBS and prepared for antibody ('anti-PKC-α alone' or 'anti-PKC-α + anti-5′-nucleotidase') staining to be finally observed by fluorescence microscopy that is described in details in Chapter 2 (Section 2.8).

5.2.4 Acridine Orange (AO) and Propidium Iodide (PI) staining: Propidium iodide (10 µg/ml) and acridine orange (1 µg/ml) at final concentrations were used to stain and distinguish live, apoptotic, necrotic and dead cells on treatment with different compounds. Fifty thousand (5×10^4) cells were

seeded into each well of a 24-well plate overnight. In each of the experiments, the next morning, cells were treated with compounds prepared in serum-free media for 24 hrs. Post treatment, cells were detached from wells using 0.6% EDTA solution prepared in sterile PBS. Next, cells were prepared for AO/PI staining to be finally analysed by flow cytometry as described in details in Chapter 2 (Section 2.5).

5.2.5 DNA fragmentation assay: MDAMB-231 cells were seeded as two lakh (2×10^5) cells per well of a 6-well plate in DMEM F:12 media for overnight. Next, the cells were treated with the appropriate concentrations of the various compounds for 24 hrs at 37°C. Cells treated with serum-free medium alone were considered as control. Post-treatment cells were washed with ice-cold sterile PBS and prepared for DNA laddering assay as described in Chapter 2 (Section 2.6).

5.2.6 Immuno-blotting to detect phosphor-threonine proteins: MDAMB-231 cells were seeded in 60 mm cell-culture dishes (5×10^5 cells per dish) overnight in DMEM:F12 complete media. Next, cells were washed with sterile cell-culture-grade PBS and treated with 'Danazol (70 µg/ml)' or 'PMA (100 ng/ml)' or 'PMA + Danazol' in serum-free media for 30 minutes. The lysate, cytosol and membrane fractions were accordingly prepared as described in Chapter 2 (Section 2.9) and immune-blotting was performed as described in Chapter 2 (Section 2.12). All bands in the blot were detected and analysed by PyElph software.

5.2.7 Lactate Dehydrogenase Assay: MDAMB-231 cells were treated with the different compounds for a period of 30 mins at their respective concentrations in serum-free media. The cells were harvested, and the cytosolic & membrane fractions were prepared as described in Section 2.9. Proteins were quantified by lowry's method, and then the activity of lactate dehydrogenase was estimated as described in Chapter 2 (Section 2.11).

5.2.8 Detection of 5′-nucleotidase in membrane fraction: Post treatment of cells with different compounds, cells were detached and the membrane and cytosolic fractions were prepared as described in Section 2.9. Proteins were quantified by lowry's method and the proteins were separated in SDS gels. Next, proteins were transferred to PVDF membrane, and presence of 5′-nucleotidase was detected as described in Chapter 2 (Section 2.19).

5.2.9 Intracellular ROS measurement: MDAMB-231 cells were seeded as thirty thousand (3×10^4) cells per well of a 24-well plate in DMEM:F12 complete media for overnight. Next, one set of cells were treated with compounds alone while the other set was pre-treated for 2 hrs with 5 mM NAC prior to compound treatment for different time periods. The compounds were used in various concentrations according to the specific experiment used. Post treatment, cells were washed with sterile PBS, detached and prepared for analysis by flow cytometry as described in Chapter 2 (Section 2.7).

5.2.10 Lipid peroxidation assay: MDAMB-231 cells were seeded as thirty thousand (3×10^4) cells per well of a 24-well plate in DMEM:F12 complete media for overnight. Next, cells were treated with compounds for a time period of 4 hrs. Post treatment, cells were prepared for lipid peroxidation level estimation as described in Chapter 2 (Section 2.17).

5.2.11 Protein carbonyl assay: MDAMB-231 cells were seeded as thirty thousand (3×10^4) cells per well of a 24-well plate in DMEM:F12 complete media for overnight. Next, cells were treated with compounds for a time period of 4 hrs. Post treatment, cells were prepared for protein carbonyl estimation as described in Chapter 2 (Section 2.18).

5.2.12 Measurement of change in mitochondrial membrane potential: MDAMB-231 cells were seeded as ten thousand (10,000) cells per well of a 96 well plate in DMEM:F12 complete media for overnight. Next, cells were treated with different compounds (at their respective concentrations) for 24 hrs at 37°C in serum-free media. Cells treated with serum-free medium alone were considered as control. Post treatment, mitochondrial membrane potential was determined as described in Chapter 2 (Section 2.13).

5.2.13 Immuno-localization to study cyt-c release: MDAMB-231 cells were seeded as ten thousand (10,000) cells per well of a 96 well plate in DMEM:F12 complete media for overnight. Next, cells were treated with different compounds at their respective concentrations for 24 hrs in serum-free media. Post-treatment, cells were washed with PBS and prepared for immuno-blotting to detect cyt-c release as described in Chapter 2 (Section 2.14).

5.2.14 Caspase-3 and caspase-9 assay: MDAMB-231 cells were seeded in 100 mm cell-culture dishes (2×10^6 cells per dish) for overnight in DMEM:F12 complete media. Subsequently, cells were treated with compounds at IC_{50} concentrations for 24 hrs in serum-free media. Post treatment, the cells were washed twice with sterile PBS. Then the caspase-3 and caspase-9 assays were carried out as described in Chapter 2 (Section 2.15 & Section 2.16).

5.3 Results:

5.3.1 PKC-directed molecules translocate PKC-α from the cytosol to the plasma membrane in breast cancer cells: We decided to investigate if the selected PKC-directed molecules have the potential to translocate PKC to the plasma membrane in breast cancer cells. MDAMB-231 cells were stimulated individually with Danazol (70 µg/ml), Flunarizine (5.9 µg/ml) or Cinnarizine (54 µg/ml) for 30 mins in serum-free media, and PKC-α translocation was investigated as described in Chapter 2 (Section 2.10). In the cells stimulated with Danazol, 12.5 ± 1.28% PKC-α translocation was found compared to unstimulated cells with only 2 ± 0.43% translocation (Figure 5.2-A). On the other hand, cells stimulated with Flunarizine or Cinnarizine gave 18.5 ± 1.35% and 27.8 ± 2.17% PKC-α translocation respectively compared to unstimulated cells with only 4.7 ± 0.22% translocation

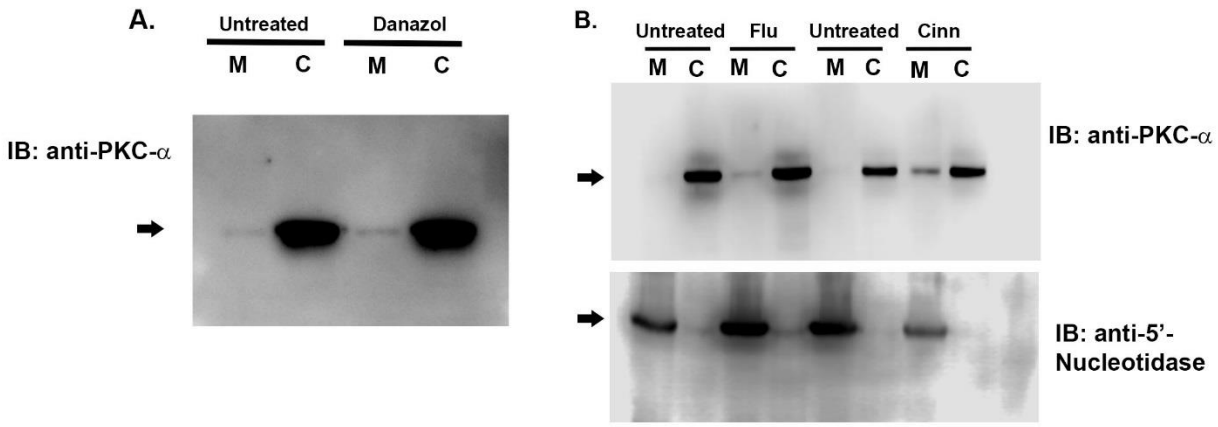

Figure 5.2: Danazol, Flunarizine and Cinnarizine induce translocation of PKC-α to the plasma membrane. (A) Cells stimulated with Danazol (70 µg/ml) for 30 mins show intense PKC band in membrane fractions compared to untreated sample. **(B) Flunarizine (5.9 µg/ml) or Cinnarizine (54 µg/ml) treated breast cancer cells show PKC-α in membrane fractions.** Treated and untreated samples were loaded in parallel as in the original order of the Flunarizine or Cinnarizine stimulation experiment. The immune-blotted proteins were probed separately with anti-PKC-α (Upper Blot) or anti-5′-nucleotidase antibody (Lower Blot) as described in Chapter 2 (Section 2.19).

(Figure 5.2-B). Purity of the membrane and the cytosolic fractions was assessed by 5′-nucleotidase assay as described in Chapter 2 (Section 2.19). The results clearly show that 5′-nucleotidase was present in the membrane fractions only to prove the purity of the membrane fractions.

The immuno-blotting results were further confirmed by immuno-localization study in the PKC-directed molecule stimulated cells. MDAMB-231 cells were stimulated with Danazol (70 µg/ml) for 30 mins at 37ºC in serum-free media. The PKC was localized using anti-PKC-α antibodies as described in Chapter 2 (Section 2.8). The plasma membrane was identified by cholesterol staining fluorescent dye, filipin. Danazol stimulated cells show a high signal of PKC-α with a large proportion of cells showing PKC signal on the plasma membrane (Figure 5.3). In these cells, PKC signal matched well with the filipin stain and indicated significant PKC translocation (Figure 5.3, superimposed).

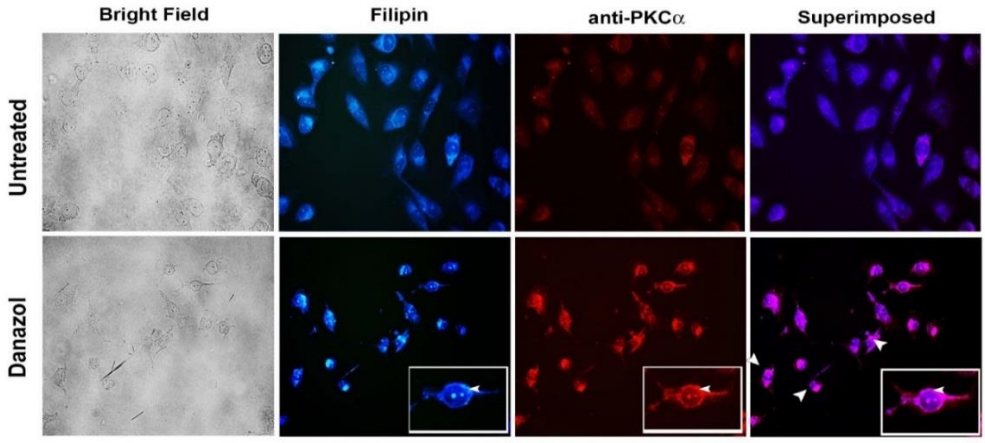

Figure 5.3: Immuno-fluorescence experiments also prove that Danazol induce translocation of PKC-α to the plasma membrane. Cells were stimulated with Danazol (70 µg/ml) for 30 mins and presence of PKC signal was detected by **immuno-fluorescence** as described in "Chapter 2 (Section 2.8)". Membrane lipids are stained with filipin (blue) while PKC-α is detected with anti-PKC- α antibody (red).

Similarly, an immuno-localization experiment was also designed to observe the effect of Flunarizine and Cinnarizine treatment on PKC-α. MDAMB-231 cells were stimulated individually with Flunarizine (5.9 µg/ml) and Cinnarizine (54 µg/ml) for 30 mins at 37ºC in serum-free media. The nuclei were identified with dapi dye (blue color in Figure 5.4) which specifically binds to DNA while membrane was identified by 5′-nucleotidase antibody (green color in Figure 5.4). PKC-α was identified by anti-PKC-α antibody (red color in Figure 5.4).In untreated sample, all the cells showed a uniform distribution of PKC throughout the cytosol with a very little PKC-α signal on the plasma membrane indicating basal translocation of PKC. But in Flunarizine and Cinnarizine treated samples, most of the cells showed an increased signal of PKC-α on the plasma membrane that was co-localizing very well with the 5′-Nucleotidase signal (Figure 5.4).

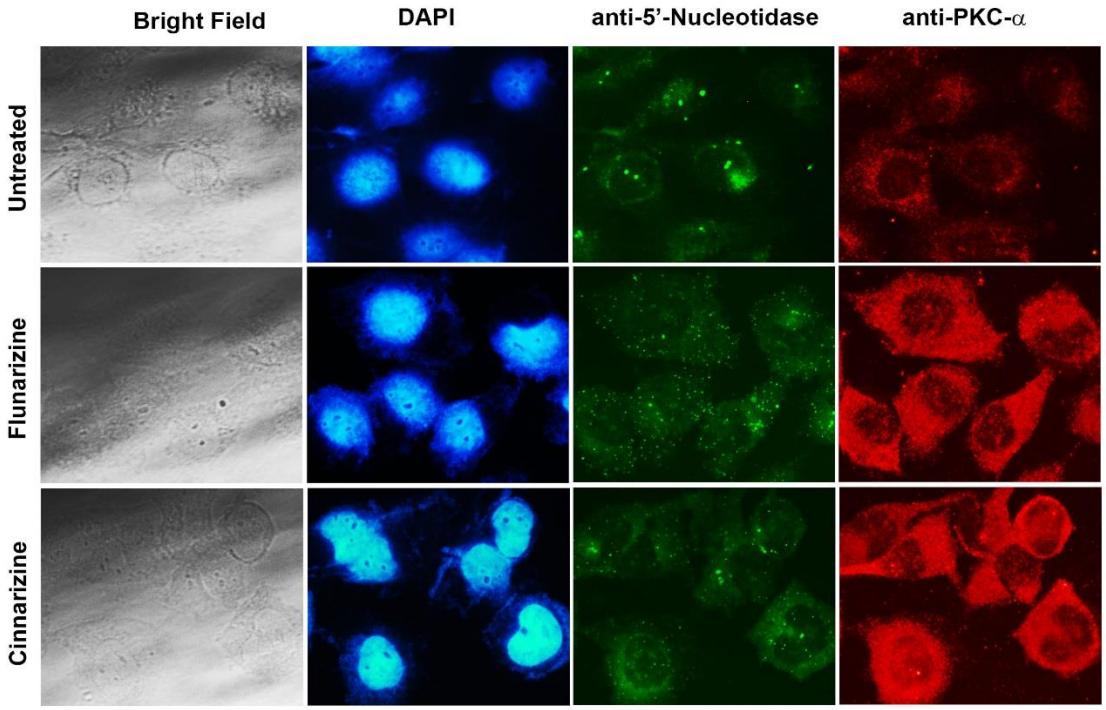

Figure 5.4: Immunofluorescence experiments further demonstrate that Flunarizine and Cinnarizine induce translocation of PKC-α to the plasma membrane. Cells were stimulated with Flunarizine (5.9 µg/ml) or Cinnarizine (54 µg/ml) for 30 mins and presence of PKC signal was detected by immunofluorescence as described in Chapter 2 (Section 2.8). Nucleus is stained with dapi (blue), 5′-nucleotidase antibody is detected by secondary antibody conjugated with FITC (green) while PKC-α is detected with anti-mouse secondary antibody conjuated with Alexa fluor-555 (red).

MDAMB-231 cells were also stimulated individually with Chlorogenic acid (75 µg/ml), β-Glycyrrhetinic acid (10 µg/ml), Gallic acid (2.5µg/ml) and Epigallocatechin gallate (6.5 µg/ml) for 30 mins in serum-free media. PKC-α translocation was investigated as described in Chapter 2 (Section 2.10). In the cells stimulated with Chlorogenic acid, 10.5 ± 1.36% PKC-α translocation was found compared to unstimulated cells with only 4.1 ± 0.36% translocation (Figure 5.5-A). In the cells stimulated with β-Glycyrrhetinic acid, 26.36 ± 4.21% PKC-α translocation was found compared to unstimulated cells with only 4.97 ± 1.16% translocation (Figure 5.5-B). Similarly, in the cells

stimulated with Gallic acid or Epigallocatechin gallate, 15.1 ± 2.18% and 16.03 ± 3.88% of PKC-α translocation were found respectively compared to unstimulated cells with only 5.5 ± 1.53% of PKC translocation (Figure 5.5-C).

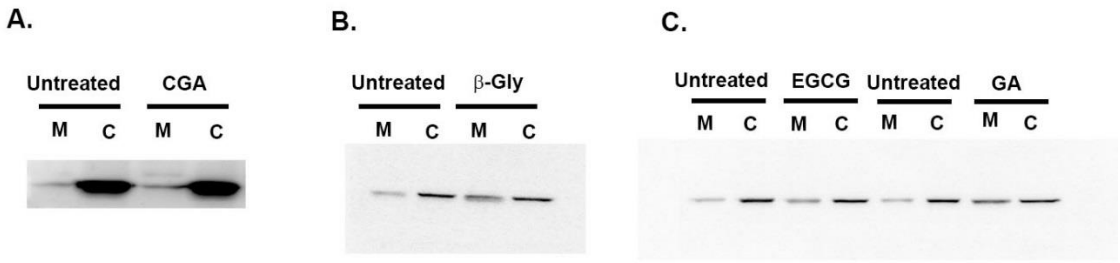

Figure 5.5: CGA (Chlorogenic acid), β-Gly (β-Glycyrrhetinic acid), GA (Gallic acid) and EGCG (Epigallocatechin gallate) induce translocation of PKC-α from the cytosol to the plasma membrane as revealed by immuno-blotting. Cells stimulated with **(A)** CGA **(**75 µg/ml) **(B)** β-gly (10 µg/ml) and **(C)** EGCG (6.5 µg/ml) and GA (2.5 µg/ml) for 30 mins show intense PKC band in membrane fractions compared to untreated cells.

An immuno-localization experiment was also designed to reconfirm the results of immuno-blotting experiments.MDAMB-231 cells were stimulated with Chlorogenic acid (75 µg/ml) for 30 mins in serum-free media. PKC-α was identified by anti-PKC-α antibody as described in Chapter 2 (Section 2.8). Plasma membrane was identified with cholesterol staining filipin dye. In Chlorogenic acid treated samples, most of the cells displayed a high signal of PKC in the plasma membrane, overlapping with the signal of filipin (Figure 5.6). In contrast, untreated cells showed a basal level of PKC signal in the plasma membrane and displayed a uniform distribution of PKC in the cytosol.

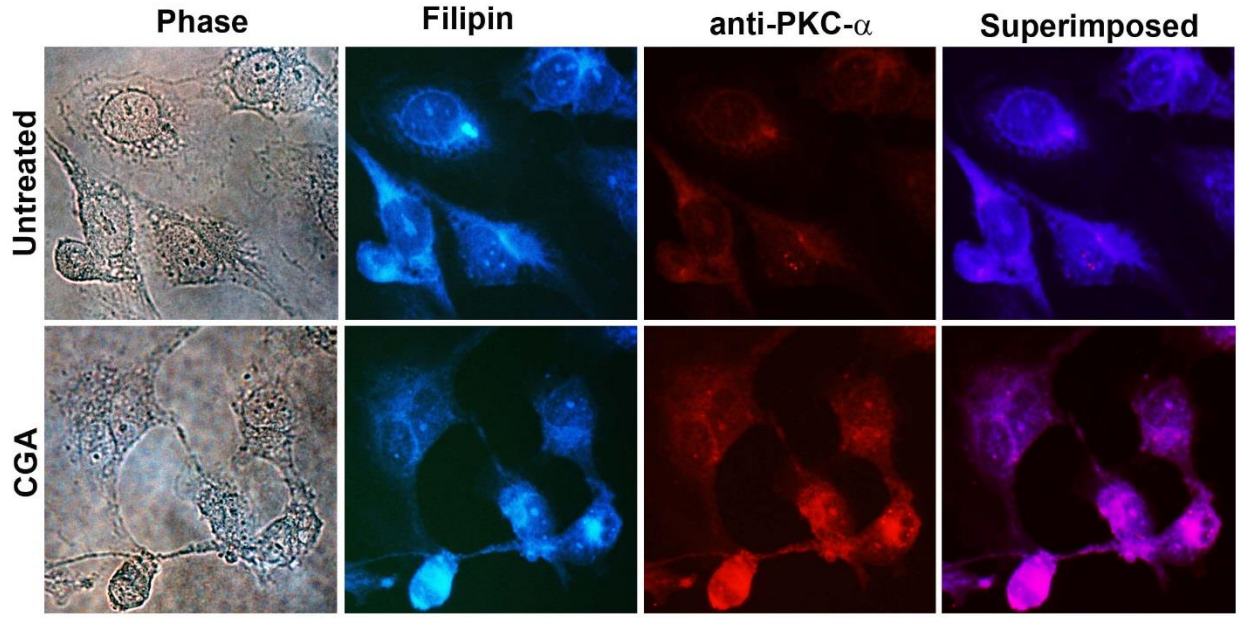

Figure 5.6: Immuno-fluorescence experiments to demonstrate that CGA (Chlorogenic acid) induce translocation of PKC-α to the plasma membrane. Cells were stimulated with CGA (75 µg/ml) for 30 mins and presence of PKC signal was detected by immuno-fluorescence as described in Chapter 2 (Section 2.8). PKC-α is detected with anti-mouse secondary antibody conjuated with Alexa fluor-555 (red) whereas membrane lipids are stained with filipin (blue).

Similarly, MDAMB-231 cells were stimulated individually with β-Glycyrrhetinic acid (10 µg/ml), Gallic acid (2.5 µg/ml) and Epigallocatechin gallate (6.5 µg/ml) for 30 mins in serum-free media for the immuno-localization experiment. PKC-α was identified by anti-PKC-α antibody while the nucleus was distinguished by DAPI dye. In phytochemical treated samples, most of the cells displayed a high signal of PKC in the plasma membrane (Figure 5.7, green in color). In contrast, untreated cells showed a basal level of PKC signal in the plasma membrane and displayed a uniform distribution of PKC in the cytosol.

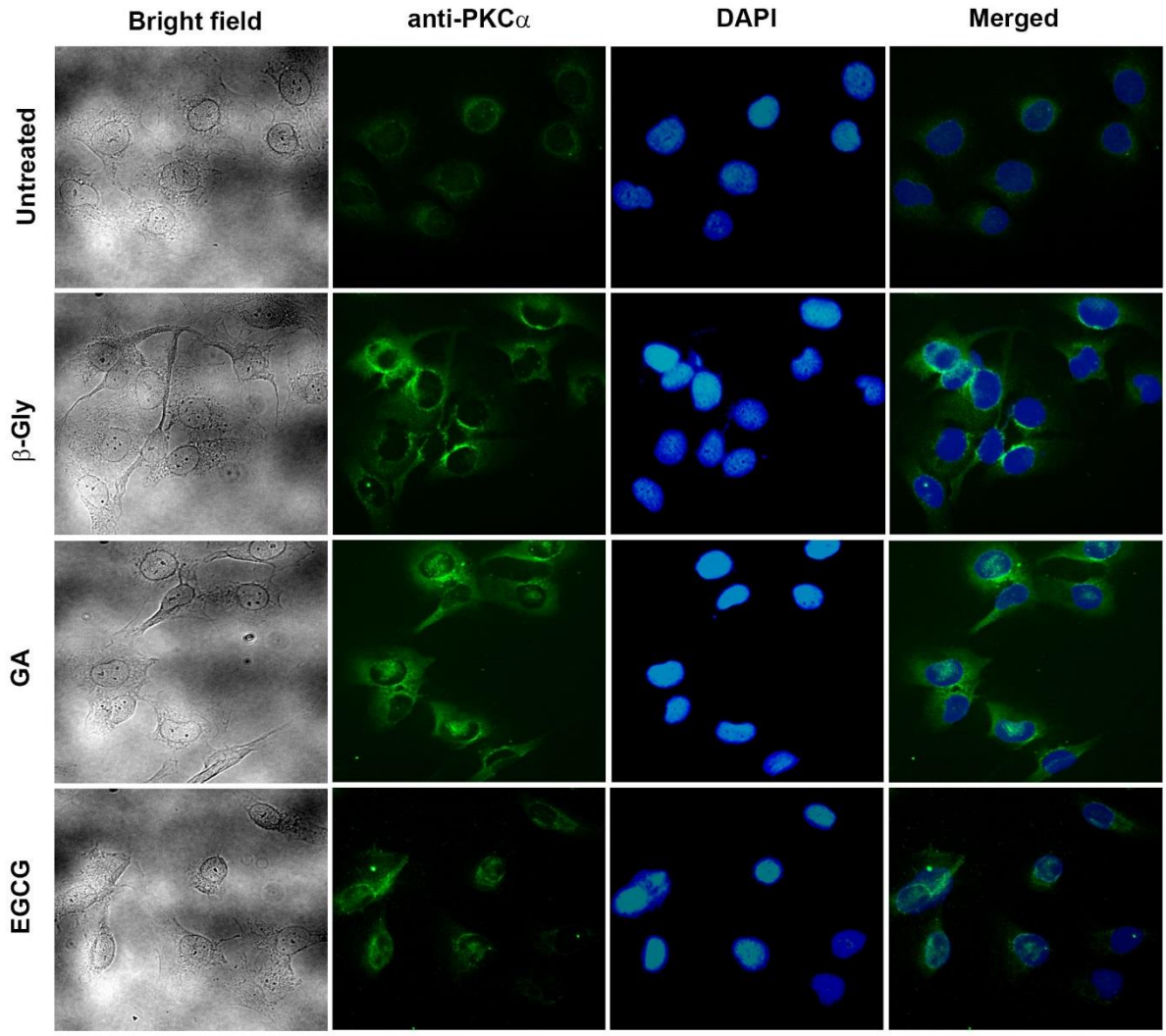

Figure 5.7: Immunofluorescence experiments further demonstrate that β-Gly (β-Glycyrrhetinic acid), GA (Gallic acid) and EGCG (Epigallocatechin gallate) induce translocation of PKC-α to the plasma membrane. (A) Cells were stimulated with β-Gly (10 µg/ml), EGCG (6.5 µg/ml) and GA (2.5 µg/ml) for 30 mins and presence of PKC signal was detected by **immunofluorescence** as described in Chapter 2 (Section 2.8). PKC-α is detected with anti-mouse secondary antibody conjuated with fitc (green) while nuclei are stained by dapi (blue).

We have also tested the ability of alkyl cinnamates to induce PKC translocation from cytosol to the plasma membrane after binding to the C1b domain. MDAMB-231 breast cancer cells were stimulated with different alkyl cinnamates for 30 mins. The membrane and cytosolic fractions were

prepared, resolved on SDS-PAGE and PKC-α translocation was probed using anti-PKC-α antibody as described in Chapter 2 (Section 2.10). In addition, purity of cytosolic or membrane fractions were characterized by re-probing blot with anti-5′-nucleotidase (plasma membrane marker) antibody as described in Chapter 2 (Section 2.19). The level of PKC-α in the cytosolic fraction was used to calculate the percentage translocation in different conditions. MDAMB-231 cells stimulated with DM 2-8 exhibited 16.6 ± 1.7% translocation of PKC from cytosol to the plasma membrane fractions (Figure 5.8). The level of PKC translocation in cells stimulated with DM 2-5 & curcumin, were found to be 8.2 ± 0.93% and 17 ± 1.88% respectively. Under the similar condition, cells stimulated with serum-free medium alone exhibited low level (~0.7 ± 0.23%) of PKC translocation. Interestingly, cells stimulated with low-affinity compound DM 3-5 didn't show any significant PKC signal in plasma membrane fraction. These results are in accordance to the binding affinities of alkyl cinnamates towards PKC (Mamidi et al., 2012), their effect towards disturbing cell-cycle, morphological changes and viability (Chapter 4). Thus, there is a sharp contrast in the distribution of PKC-α between alkyl cinnamate treated and untreated samples. Hence, data in Figure 5.8 bolstered the notion that the PKC interaction with alkyl cinnamates mediates robust translocation of PKC-α from the cytosol to the plasma membrane. This indicates that alkyl cinnamates, either by directly binding to PKC or indirectly caused PKC-α to translocate from the cytosol to the plasma membrane in breast cancer cells.

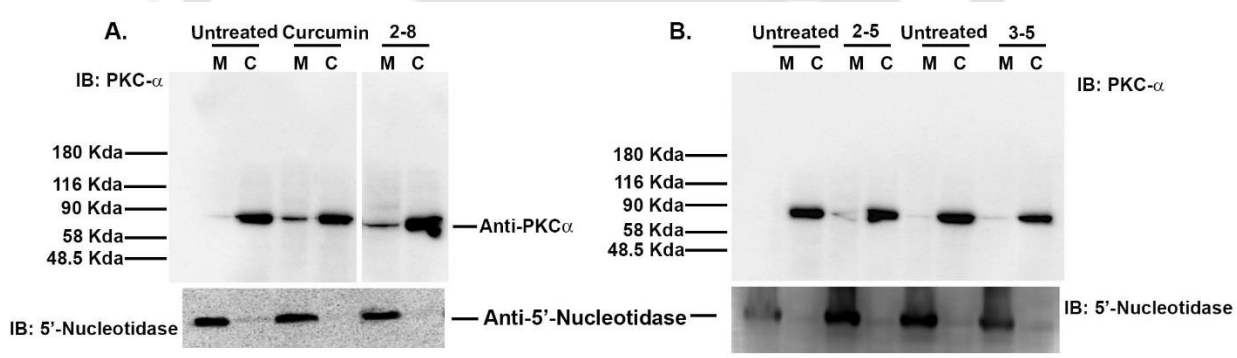

Figure 5.8: Alkyl Cinnamates have the potential to exhibit PKC-α translocation from cytosol to the plasma membrane in MDAMB-231 cells. Immuno-blotting of PKC-α in MDAMB-231 treated with different alkyl cinnamates to monitor PKC translocation from cytosol to plasma membrane. MDAMB-231 cells were treated and PKC-α Immuno-localization was done as described in Chapter 2 (Section 2.10).Untreated cells show a basal level of PKC-α at plasma membrane whereas a high level of PKC-α was found in alkyl cinnamate treated cells. The purity of cytosolic or membrane fraction was assessed by testing the presence 5′-nucleotidase in these fractions. Assay for the presence of 5′-nucleotidase was done by immuno-blotting with anti-5′-nucleotidase antibodies as described in Chapter 2 (Section 2.19).

Quantitative immuno-blotting observations (Figure 5.8) were further validated in the qualitative immuno-localization technique. MDAMB-231 breast cancer cells were stimulated with different alkyl cinnamates for 30 mins at 37ºC. Post treatment, the PKC was localized using anti-PKC-α antibodies (red color in Figure 5.10) while plasma membrane lipids were identified with chlolesterol staining filipin dye as described in Chapter 2 (Section 2.8). A substantial increase in PKC signal in

alkyl cinnamate treated cells was seen in comparison to untreated cells (Figure 5.9). Also, the ineffective compound DM 3-5 didn't produce a strong PKC signal in agreement with immuno-blotting results observed earlier.

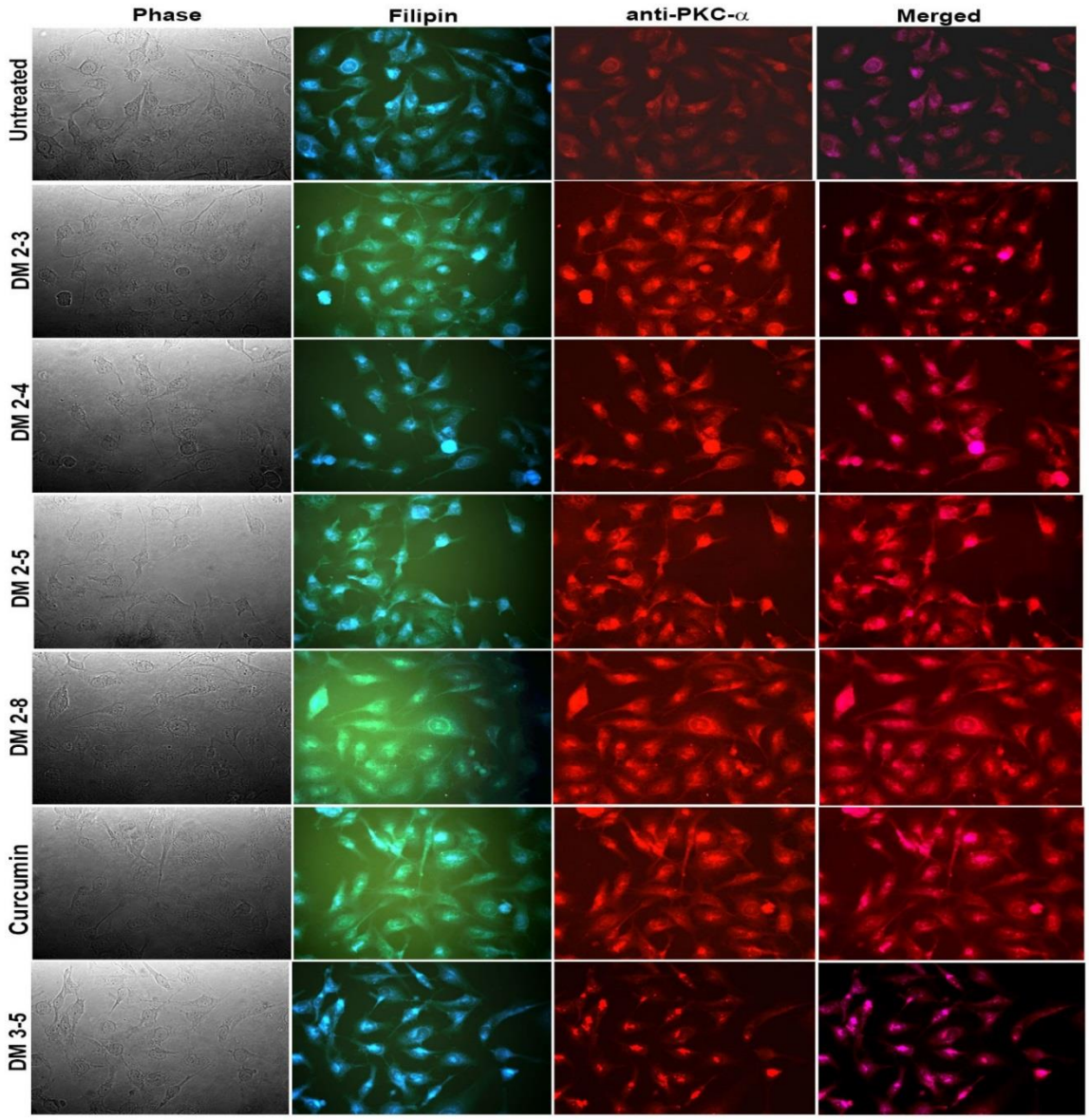

Figure 5.9: Immunofluorescence experiments further prove that alkyl cinnamates have the potential to exhibit PKC-α translocation from cytosol to the plasma membrane in MDAMB-231 cells. Immuno-localization experiment of PKC-α in MDAMB-231 treated with different alkyl cinnamates was accordingly performed to monitor PKC translocation from cytosol to plasma membrane. MDAMB-231 cells were treated with alkyl cinnamates and PKC-α immuno-localization was done as described in Chapter 2 (Section 2.8). In each panel, bright field, PKC-α (red), membrane lipids (Blue) and superimposed images are shown. Untreated cells show a low level of PKC- α at plasma membrane compared to significant signal in alkyl cinnamate treated cells.

5.3.2: The PKC-directed molecules cause prolonged PKC translocation in treated cells: Immuno-blotting experiments were also designed to study the time-dependent translocation of PKC-α to the plasma membrane on stimulation of MDAMB-231 cells with PKC-directed molecules. MDAMB-231 cells were stimulated individually with Flunarizine and Cinnarizine for a period of 30

mins, 60 mins and 120 mins (Figure 5.10). The intensity of the immune-reactive bands were quantified. It was observed that in case of Flunarizine, there was time-dependent increase of PKC-α levels in the membrane fractions. Whereas, Cinnarizine induced maximal PKC-α translocation in the membrane fraction at 30 mins with a progressive decline in PKC-α levels at 1 hr and 2 hrs time points. Flunarizine treated cells showed a PKC-α translocation level of 15.02 ± 1.18% (30 mins), 19.2 ± 1.82% (60 mins) and 26.13 ± 2.08% (120 mins) compared to unstimulated cells with very little PKC translocation in each of these time-points (Figure 5.10-A). On the other hand, Cinnarizine treated cells showed a PKC-α translocation level of 25.2 ± 3.27% (30 mins), 16.2 ± 2.55% (60 mins) and 11.7 ± 0.63% (120 mins) compared to unstimulated cells with minimal PKC translocation in each of these time-points (Figure 5.10-B).

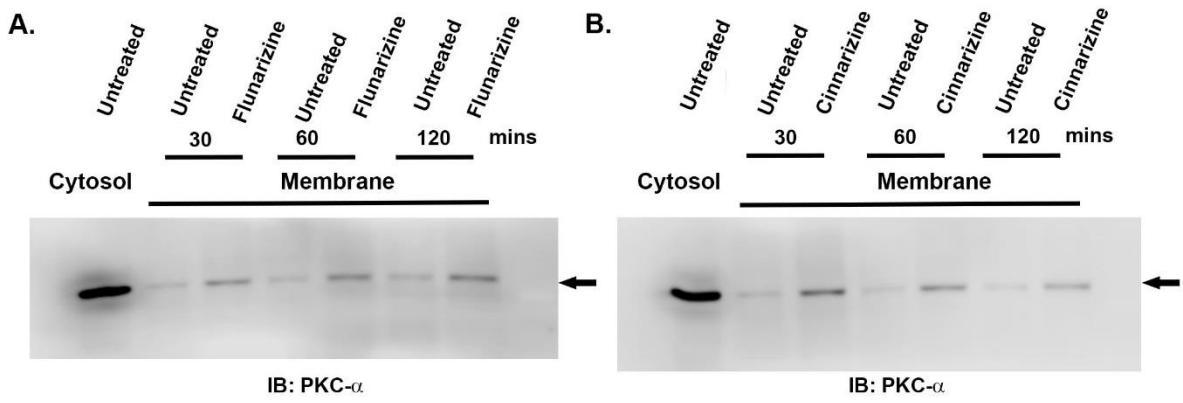

Figure 5.10: Flunarizine and Cinnarizine cause prolonged translocation of PKC-α from the cytosol to the plasma membrane as revealed by immuno-blotting. Cells were stimulated with **(A)** Flunarizine (5.9 µg/ml) and **(B)** Cinnarizine (54 µg/ml) for 30 mins, 60 mins and 120 mins respectively to study time-dependent translocation of PKC-α to the plasma membrane in MDAMB-231 breast cancer cells.

Similarly, in another experiment, cells were stimulated individually with Chlorogenic acid (75 µg/ml) for 30 mins, 60 mins and 120 mins in serum-free media (Figure 5.11-A). Chlorogenic acid treated cells showed a PKC-α translocation level of 9.5 ± 0.75% (30 mins), 12.1 ± 0.56% (60 mins) and 12.3 ± 0.81% (120 mins). An experiment to study the time-dependent kinetics of PKC translocation on individual β-Glycyrrhetinic acid (10 µg/ml) and Gallic acid (2.5 µg/ml) stimulation of MDAMB-231 cells was also performed (Figure 5.11-B & C). β-Glycyrrhetinic acid treated cells showed a PKC-α translocation level of 2.85 ± 0.51% (0 min), 03.824 ± 0.32% (60 mins), 10.45 ± 1.26 % (120 mins) and 4.57 ± 1.12% (240 mins). On the other hand, Gallic acid treated cells showed a PKC-α translocation level of 8.98 ± 0.37% (30 mins), 9.25 ± 1.94% (60 mins), 10.81 ± 2.11% (120 mins), 14.89 ± 2.27% (180 mins), 15.93 ± 1.96%(240 mins) and 8.45 ± 1.67% (480 mins).Thus, each of the molecules has a distinct time-dependent kinetics of PKC-α translocation.

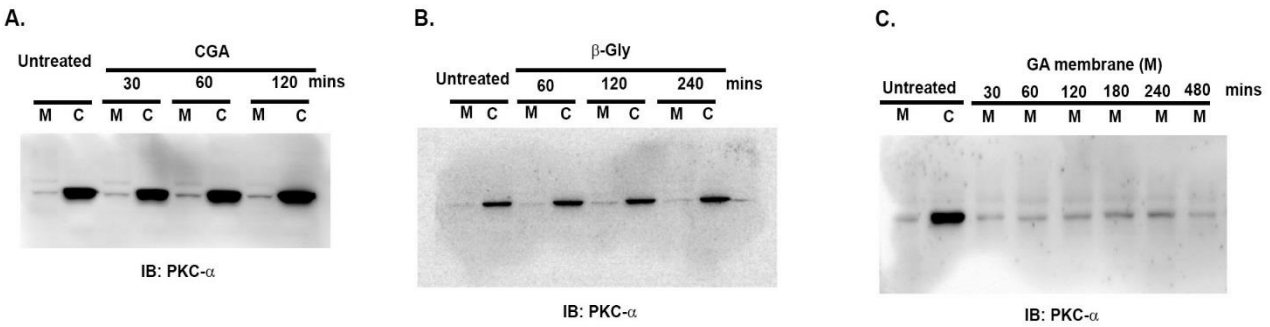

Figure 5.11: CGA (Chlorogenic acid), β-Gly (β-Glycyrrhetinic acid) and GA (Gallic acid) cause prolonged translocation of PKC-α from the cytosol to the plasma membrane as revealed by immune-blotting. (A) Cells were stimulated with CGA (75 µg/ml) for 30 mins, 60 mins and 120 mins to study time-dependent translocation of PKC-α to the plasma membrane. **(B)** Cells were stimulated with β-Gly (10 µg/ml) for 60 mins, 120 mins and 240 mins to study time-dependent translocation of PKC-α to the plasma membrane in MDAMB-231 cells. **(C)** Cells were stimulated with GA (2.5 µg/ml) for 30 mins, 60 mins, 120 mins, 180 mins, 240 mins and 480 mins respectively to study time-dependent translocation of PKC-α to the plasma membrane in MDAMB-231 cells on stimulation with GA.

5.3.3 Danazol treatment causes downstream phosphorylation signal in MDAMB-231 cells: MDAMB-231 cells were stimulated with Danazol (70µg/ml) for 30mins in serum-free media. Phosphorylated proteins in cell lysate, cytosol and membrane fractions were identified by immuno-blotting using anti-phosphothreonine antibodies as described in detail in Chapter 2 (Section 2.12). MDAMB-231 cells stimulated with Danazol (70µg/ml) gave phosphorylated proteins in lysate, cytosol and membrane fractions in comparison to the cells stimulated with incomplete media ("untreated"). Cells stimulated with Danazol gave 21 and 22 phosphorylated proteins in lysate and membrane fractions respectively (Figure 5.12). Cell lysate of Danazol stimulated cells gave phosphorylated proteins in the native molecular weight range of 13-156 kDa (Figure 5.12). The phosphorylated proteins appearing in cell lysate could be due to either direct effect of Danazol on cellular receptor and resulting down-stream signalling or indirect through the development of stress such as oxidative stress. The molecular weight of phosphorylated band was used to identify the probable protein using phosphoSiteplus server (http://www.phosphosite.org). As molecular weight is not very specific to a particular protein, there are multiple proteins possible for a particular band. A thorough and in-depth phospho-proteomics study is further on the way in the laboratory to explore this part of the study.

5.3.4 Danazol abolishes tumorogenic (PMA) specific phosphorylation signal in MDAMB-231 Cells: We further asked whether Danazol has the potential to disrupt carcinogenic PMA specific phosphorylation signal in MDAMB-231 cells. MDAMB-231 cells were stimulated with PMA (100 ng/ml) in absence or presence of Danazol (70 µg/ml) for 30mins in serum free media. Phosphorylated proteins in cell lysate, cytosol and membrane fractions were identified by immuno-blotting using anti-phosphothreonine antibodies as described in Chapter 2 (Section 2.12). MDAMB-231 cells stimulated with PMA (100 ng/ml) gave phosphorylated proteins in lysate, cytosol and membrane fractions in comparison to the cells stimulated with serum-free media ("untreated"). Cells stimulated with PMA

gave 23 and 20 phosphorylated proteins in lysate and membrane fractions respectively (Figure 5.12). Cell lysate of PMA stimulated cells gave phosphorylated proteins in the molecular weight range of 13-156 kDa (Figure 5.12). In the presence of Danazol, PMA stimulated cells gave 17 and 19 phosphorylated proteins in lysate and membrane fractions respectively (Figure 5.12). Danazol was specifically targeting phosphorylated proteins with a native molecular weight of 156.3, 137.9, 120.7, 82 and 11.7 kDa (Figure 5.12, denoted by "*"). These phosphorylated bands were common in cells stimulated with PMA or Danazol, and PMA didn't show these bands in presence of Danazol. This is probably due to competitive inhibition or feedback inhibition via over-activation. There were additional bands appearing in all the three treatments (PMA, Danazol or PMA in the presence of

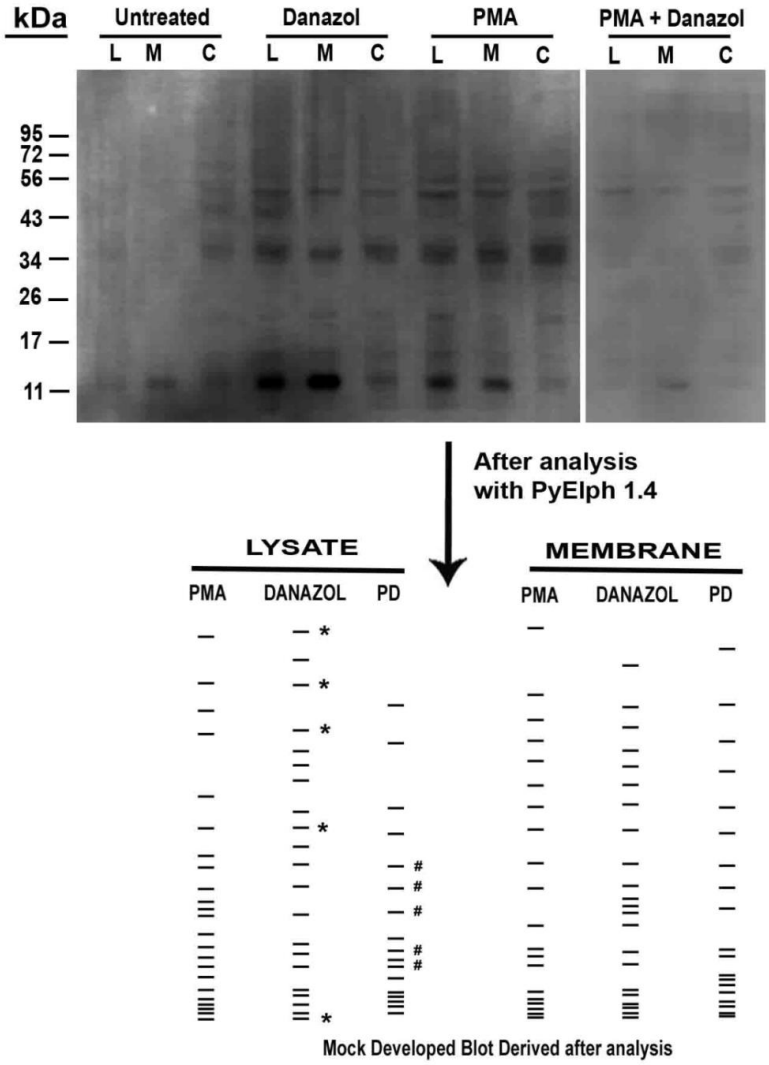

Figure 5.12: MDAMB-231 cells respond to Danazol and Danazol treatment affects PMA induced cell signaling in cancer cells. MDAMB-231 cells were stimulated with PMA (100ng/ml), Danazol (70µg/ml) or PMA (100ng/ml) in presence of Danazol (100µg/ml) for 30mins and phosphorylated proteins were identified by immunoblotting as described in Chapter 2 (section 2.12). The developed blot was analyzed by PyElph 1.4 and a mock blot representing pattern of phosphorylated protein in each treatment is given. The details of molecular weight of each phosphorylated protein in each treatment is yet to be identified. The bands in Danazol lane are marked with "*" to denote phosphorylated protein disappeared in PMA stimulated cells due to Danazol whereas bands are marked with "#" to denote phosphorylated protein appearing probably due to stress in cells.

danazol) to cancer cells, and probably represent stress linked signalling molecules (Figure 5.12, denoted by "#"). These results are initial observations that Danazol was affecting PMA induced phosphorylation signal in MDAMB-231 cells but an in-depth phospho-proteomics study is required to confirm the findings.

5.3.5 PKC-directed molecules induce apoptosis to kill breast cancer cells: MDAMB-231 breast cancer cells were treated with Danazol (70 µg/ml) in serum-free media for 24 hrs. Apoptosis was assessed by Acridine Orange & Propidium Iodide (AO/PI) staining as described in detail in Chapter 2 (Section 2.5). Quadrant analysis of the cell populations for appearance of healthy (lower left), early apoptotic (lower right), late apoptotic (upper right) and necrotic (upper left) phases was performed. Untreated cells showed mostly healthy cells (~83 ± 2.48%) which was evident from a lower intake of propidium iodide into their genomic DNA. Danazol treated cells showed a lesser number of healthy cells with a concomitant increase of cells in the apoptotic (early and late) or death phases (Figure 5.13-A). At 70 µg/ml, it exhibited the proportion of cells in the early apoptotic (9.8 ± 0.82%) & late apoptotic (57.5 ± 3.13%) phases and only 30 ± 1.62% healthy cells (Figure 5.13-A). The flow cytometric analysis indicates that the cell-death caused by Danazol might be following apoptotic rather than necrotic pathways. Likewise, MDAMB-231 cells were also treated either with Flunarizine (5.9 µg/ml) or Cinnarizine (54 µg/ml) for a period of 24 hrs. Apoptosis was assessed by flow cytometry by AO/PI method as described in Chapter 2 (Section 2.5). AO/PI staining indicated that a significant

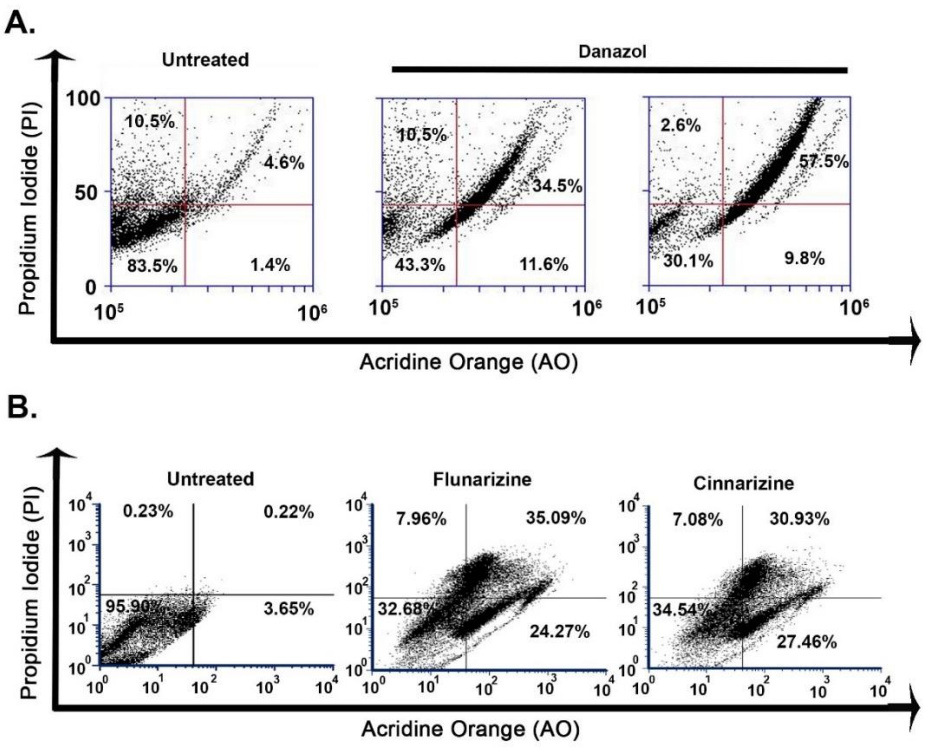

Figure 5.13: Danazol, Flunarizine and Cinnarizine causes cell death in cancer cell due to induction of apoptosis: MDAMB-231 cells were treatment with **(A)** Danazol (70 µg/ml) **(B)** Flunarizine (5.9 µg/ml) & Cinnarizine (54 µg/ml) in serum-free media for 24 hrs and stained with Acridine orange (AO)/Propidium iodide (PI) as given in Chapter 2 (Section 2.5). Cells treated with serum-free media served as control.

proportion of treated cells are shifted to the right corner with a significant proportion of late apoptotic cells in Flunarizine (35.09 ± 4.51%) as well as Cinnarizine treated (30.93 ± 3.57%) cells (Figure 5.13-B). There was also a significant proportion of early apoptotic cells in Flunarizine treated (24.27 ± 1.81 %) and Cinnarizine treated (27.46 ± 2.34%) cells.

Likewise, phytochemicals were also evaluated for their ability to induce apoptosis in cancer cells. MDAMB-231 cells were treated individually with Chlorogenic acid (75 µg/ml), β-Glycyrrhetinic acid (10 µg/ml) and Gallic acid (2.5 µg/ml) for a period of 24 hrs. In Chlorogenic acid treated cells, the proportion of cells in early apoptotic was 0.3±0.12%, late apoptotic was 44.2±3.56 % and necrotic was 25.9± 1.66% (Figure 5.14-A). Whereas in untreated cells, the proportion of cells in early apoptotic was 8.3±1.52%, late apoptotic was 17.1±2.85% and necrotic was 13.8±0.48%. Chlorogenic acid treated cells showed quite lesser number of healthy cells (29.6±2.33%), with a significant increase of cells in the apoptotic (early and late) or death phases (Figure 5.14-A). Similarly, in β-Glycyrrhetinic acid, Epigallocatechin gallate and Gallic acid treatments, there was a significant shift of healthy cells to the early apoptotic and late apoptotic phases in comparison to untreated cells.

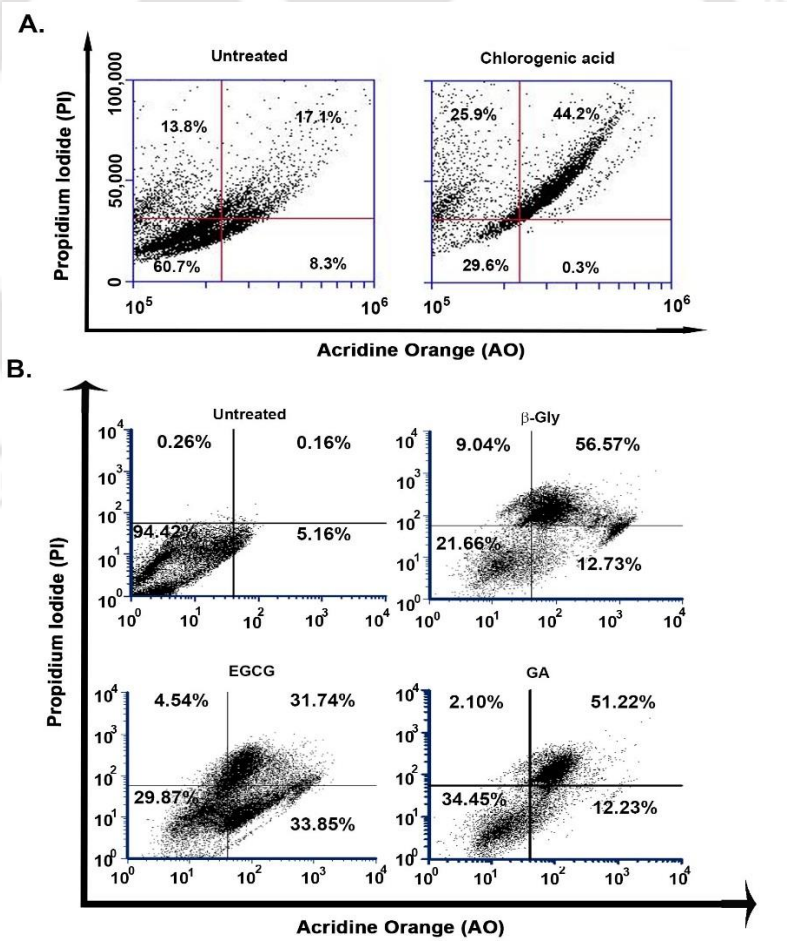

Figure 5.14: Evidence of apoptotis as a mode of death in CGA (Chlorogenic acid), β-Gly (β-Glycyrrhetinic acid) and GA (Gallic acid) treated breast cancer cells. MDAMB-231 cells were treated with CGA (75 µg/ml), β-Gly (10 µg/ml) and GA (2.5 µg/ml) in serum-free media for 24 hrs and stained with acridine orange (AO)/Propidium iodide (PI) as described in Chapter 2 (Section 2.5). Cells treated with serum-free media served as control.

In β-Glycyrrhetinic acid treated cells, 12.73 ± 1.63% and 56.57 ± 5.21% cells were in the early and late apoptotic phases respectively while those statistics in case of Epigallocatechin gallate treated cells were 33.85 ± 4.26% and 31.74 ± 2.95% respectively. Similarly, in Gallic acid treated cells 12.23 ± 1.45%, and 51.22 ± 6.21% cells were in the early and late apoptotic phases respectively (Figure 5.14-B).

We also explored the alkyl cinnamates mediated cell death of breast cancer cells and the underlying molecular mechanism (necrotic or apoptotic). MDAMB-231 breast cancer cells were treated with the different alkyl cinnamates in serum-free medium for a period of 24 hours at 37ºC at their respective IC_{50} concentration. The differential population of healthy, apoptotic (early or late), necrotic and dead cells were identified by Acridine orange & Propidium iodide (AO/PI) double staining method described in Chapter 2 (Section 2.5). Untreated cells showed mostly healthy cells (70 ± 2.69%), and this was evident from a lower intake of propidium iodide into their genomic DNA. Alkyl cinnamate treated cells showed a lesser number of healthy cells with a concomitant increase of cells in the apoptotic (early and late) or death phases (Figure 5.15). DM 2-8 was the most potent molecule and exhibited the highest proportion of cells in the necrotic phase (39.66 ± 3.72%) and 24.68 ± 2.54% in the late apoptotic phase. It was followed by DM 2-4 and DM 2-3 which showed late apoptotic cells at 38.04 ± 3.63% and 35.69 ± 2.92 % respectively. Thus, all the candidate molecule treatment pushed a significant fraction of cells towards apoptosis. The flow cytometric analysis indicates that the cell-death caused by alkyl cinnamates might be following apoptotic rather than necrotic pathways.

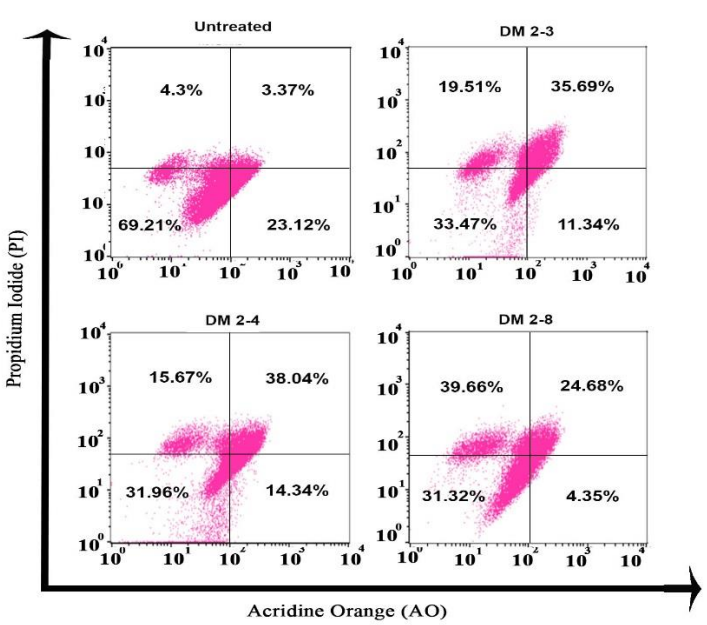

Figure 5.15: Alkyl cinnamates cause death of MDAMB-231 cells following apoptosis. MDAMB-231 treated with different alkyl cinnamates and distribution of healthy, dead, apoptotic and necrotic cells. Cells were treated alkyl cinnamates (IC_{50} for 24 h), stained with acridine orange and propidium iodide and analyzed by flow cytometry.

5.3.6 PKC directed molecules induce degradation of genomic DNA during apoptosis of MDAMB-231 breast cancer cells: MDAMB-231 cells were treated individually with Danazol (70 µg/ml), Flunarizine (5.9 µg/ml) or Cinnarizine (54 µg/ml) for 24 hrs in serum-free media. Subsequently, genomic DNA was isolated and examined for DNA cleavage pattern by resolving of that genomic DNA in agarose gel-electrophoresis as described in Chapter 2 (Section 2.6). Untreated cells gave intact genomic DNA with no evidence of smear or laddering pattern (Figure 5.16-A, Lane 1). In contrast, cells treated with Danazol showed appearance of DNA fragments with different sizes mimicking characteristic laddering pattern (Figure 5.16-A, Lane 2). Similarly, cells treated with Flunarizine and Cinnarizine for 24 hrs produced a clear laddering pattern of DNA fragments in the 1.8 % agarose gel (Figure 5.16-B, C, Lanes 2).

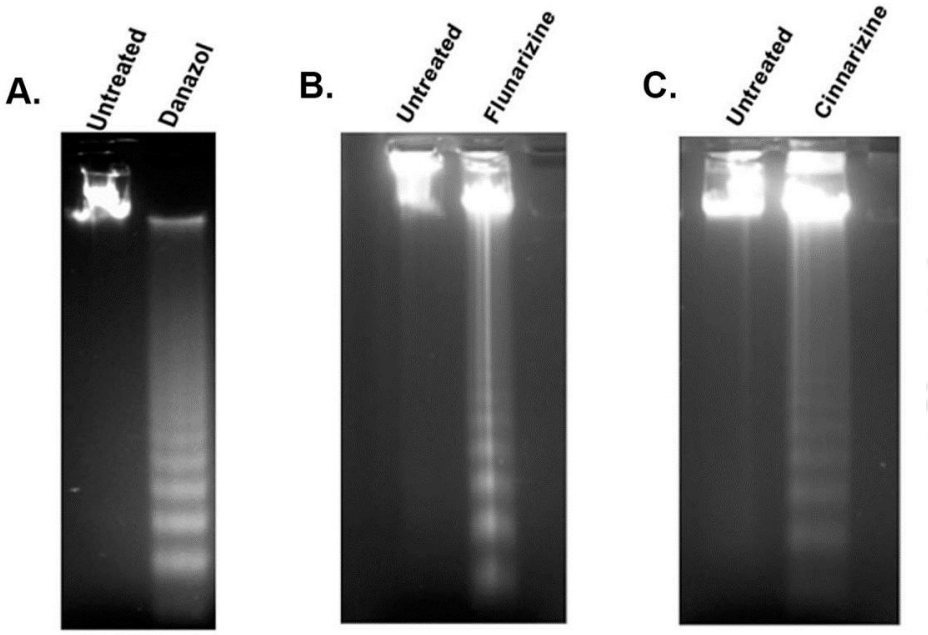

Figure 5.16: DNA fragmentation as an evidence of apoptosis by drugs. MDAMB-231 cells were individually treated with **(A)** Danazol (70µg/ml), **(B)** Flunarizine (5.88µg/ml) and **(C)** Cinnarizine (25µg/ml) in serum-free media for 24 hrs and samples were processed for DNA laddering analysis as described in Chapter 2 (Section 2.6). Intact genomic DNA was observed in untreated cells whereas the laddering pattern of DNA is observed in Danazol, Flunarizine and Cinnarizine treated cells.

Similarly, cells treated with Chlorogenic acid showed a clear laddering pattern of different sized DNA fragments which is indicative of apoptosis (Figure 5.17-A, Lane 2). Such laddering pattern was absent in untreated cells sample (Figure 5.17-A, Lane 1). Likewise, MDAMB-231 breast cancer cells treated with β-Glycyrrhetinic acid, Gallic acid and Epigallocatechin produced distinct laddering pattern when run in agarose gel (Figure 5.17-B, C). In contrast, untreated cells didn't produce any such pattern.

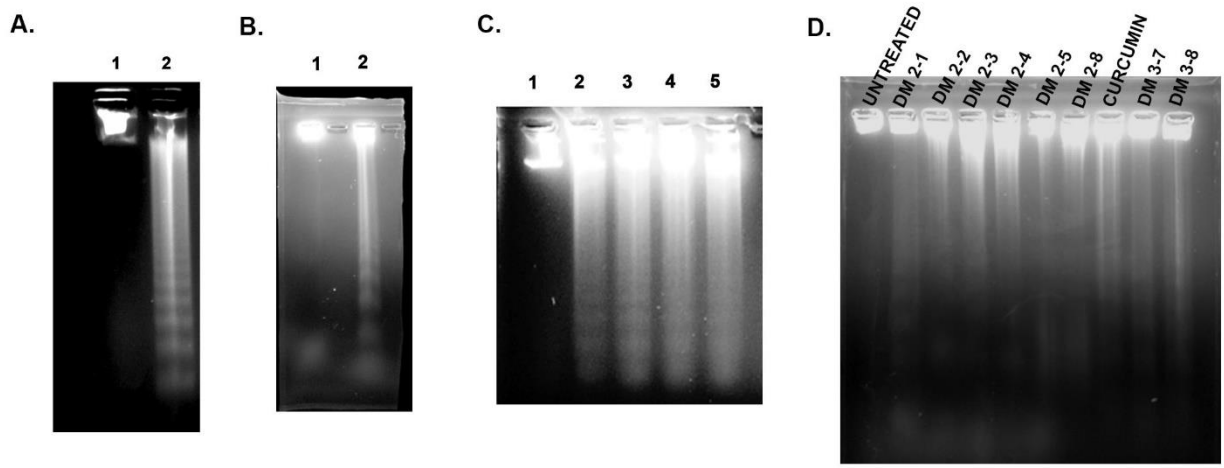

Figure 5.17: DNA fragmentation in MDAMB-231 cells treated with different phytochemicals and alkyl cinnamates. (A) Chlorogenic acid; lane 1= untreated, lane 2= treated (75 µg/ml)**., (B)** β-Glycyrrhetinic acid; lane 1= untreated, lane 2= treated (10 µg/ml), **(C)** Epigallocatechin gallate (lane 2= 6.5 µg/ml, & lane 3= 13 µg/ml,) and Gallic acid (lane 4= 2.5 µg/ml, & lane 5= 5 µg/ml,); lane 1= untreated **(D)** Different alkyl cinnamates (at their IC_{50} concentrations) for 24 hrs in serum-free media and samples were processed for DNA laddering analysis as described in Chapter 2 (Section 2.6). A laddering pattern of DNA is observed in PKC-directed molecule treated cells compared to the intact genomic DNA in untreated cells.

MDAMB-231 cells were also treated individually with different alkyl cinnamates (at their respective IC_{50} concentrations) for 12 hrs in serum-free media to subsequently analyze for probable DNA laddering pattern. Untreated cells showed an intact genomic DNA with no sign of DNA fragments/smear (Figure 5.17-D, Lane 1). In contrast, cells treated with alkyl cinnamates (IC_{50} concentration) gave laddering pattern with the appearance of DNA fragments of different sizes (Figure 5.17-D, Lanes 2-10). DM 2-1, DM 2-3, DM 2-4, DM 2-8 and curcumin produced distinct bands which were absent in untreated cells. Hence, DNA fragmentation assays confirm that the chosen candidate molecules cause breast cancer cell death following apoptotic pathways rather than necrosis.

5.3.7 The apoptosis in breast cancer cells follow mitochondrial pathway:

A) PKC directed molecules disrupt the mitochondrial membrane potential: MDAMB-231 cells were treated individually with Danazol (70 µg/ml), Flunarizine (5.9 µg/ml) and Cinnarizine (54 µg/ml) in serum-free media for 24 hrs. Cells were stained with JC-1 as described in Chapter 2 (Section 2.13) and observed by Cytell imaging system (GE Healthcare).JC-1 is a dye that accumulates in the cytosol or mitochondria depending upon the membrane potential of mitochondria. The dye generally tends to accumulate inside mitochondria in healthy cells. This accumulation within mitochondria brings the JC-1 monomers into close proximity and the JC-1 aggregates fluoresce orange under stimulation with light of the wavelength in UV range. However, in apoptotic cells, there is rapid depolarization of mitochondria which leads to leakage of JC-1 to the cytosol where they are evenly spread. Under the same UV stimulation, these JC-1 monomers in the cytosol fluoresce green. Thus, this feature of JC-1 dye helps to distinguish apoptotic cells from healthy cells. Untreated cells were found to be healthy

with an orange fluorescence that indicated the accumulation of the dye aggregates inside the mitochondrion (Figure 5.18). Whereas, Danazol, Flunarizine and Cinnarizine treated cells were

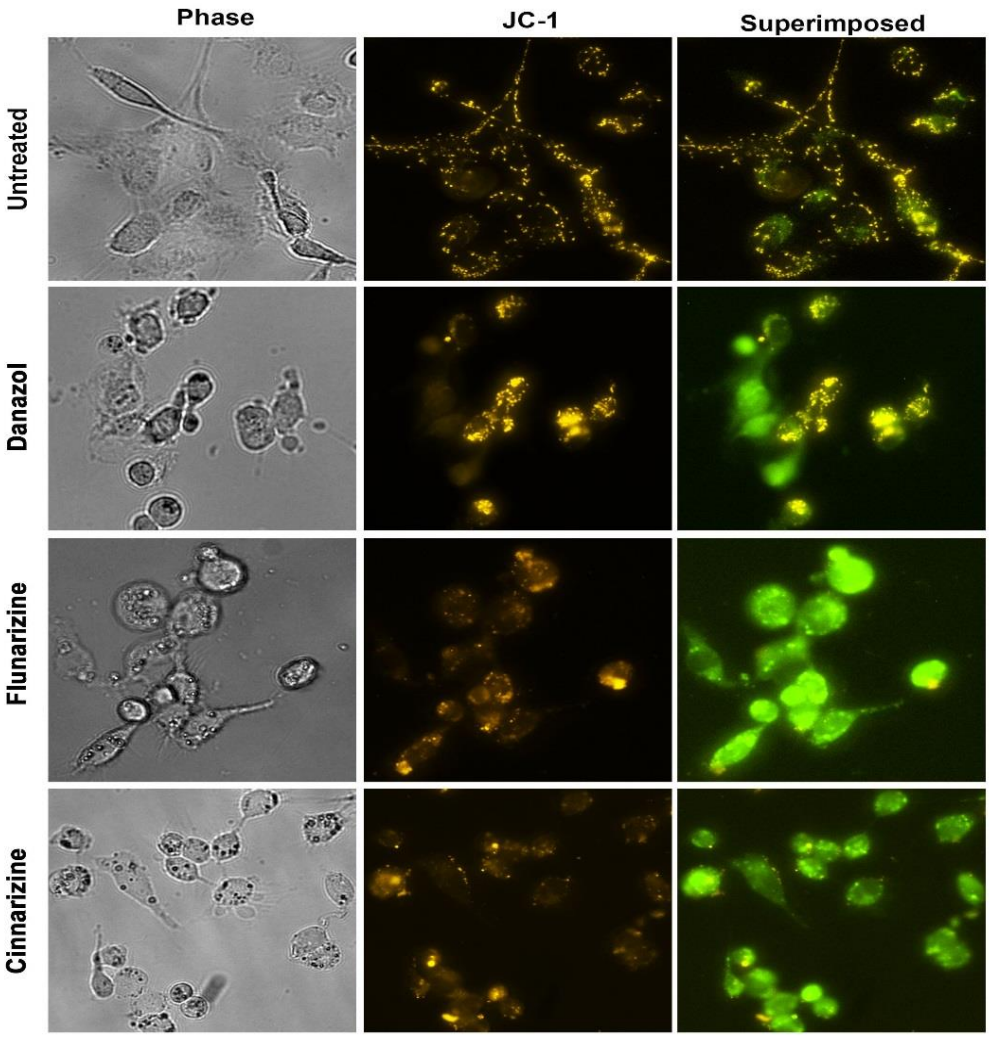

Figure 5.18: Loss of mitochondrial membrane potential in Danazol, Flunarizine and Cinnarizine treated breast cancer cells. MDAMB-231 breast cancer cells were treated with Danazol (70µg/ml), Flunarizine (at 5.9 µg/ml) and Cinnarizine (at 54 µg/ml) in serum-free media for 24 hrs. Post-treatment cells were stained with JC-1 dye for 20 minutes and were observed in Cytell imaging system (GE Healthcare). Danazol, Flunarizine and Cinnarizine treated cells show a decrease in mitochondrial membrane potential as indicated by loss of orange and appearance of green fluorescence.

showing green fluorescence spread evenly throughout the cytosol with little orange fluorescence (Figure 5.18). This indicates the leaky behavior of mitochondria and disruption of mitochondrial membrane potential; as evident by no accumulation of JC-1 dye aggregates inside the mitochondria.

In phytochemical treated cells, JC-1 monomers were observed to be evenly spread throughout the cytosol of MDAMB-231 cells (Figure 5.19). In those cells, there was emission of green fluorescence throughout the cytosol in almost all the cells. This indicates that mitochondrial membrane potential is compromised on phytochemical treatment of breast cancer cells. In untreated cells, there was emission of bright orange fluorescence that is indicative of healthy intact mitochondrial potential (Figure 5.19).

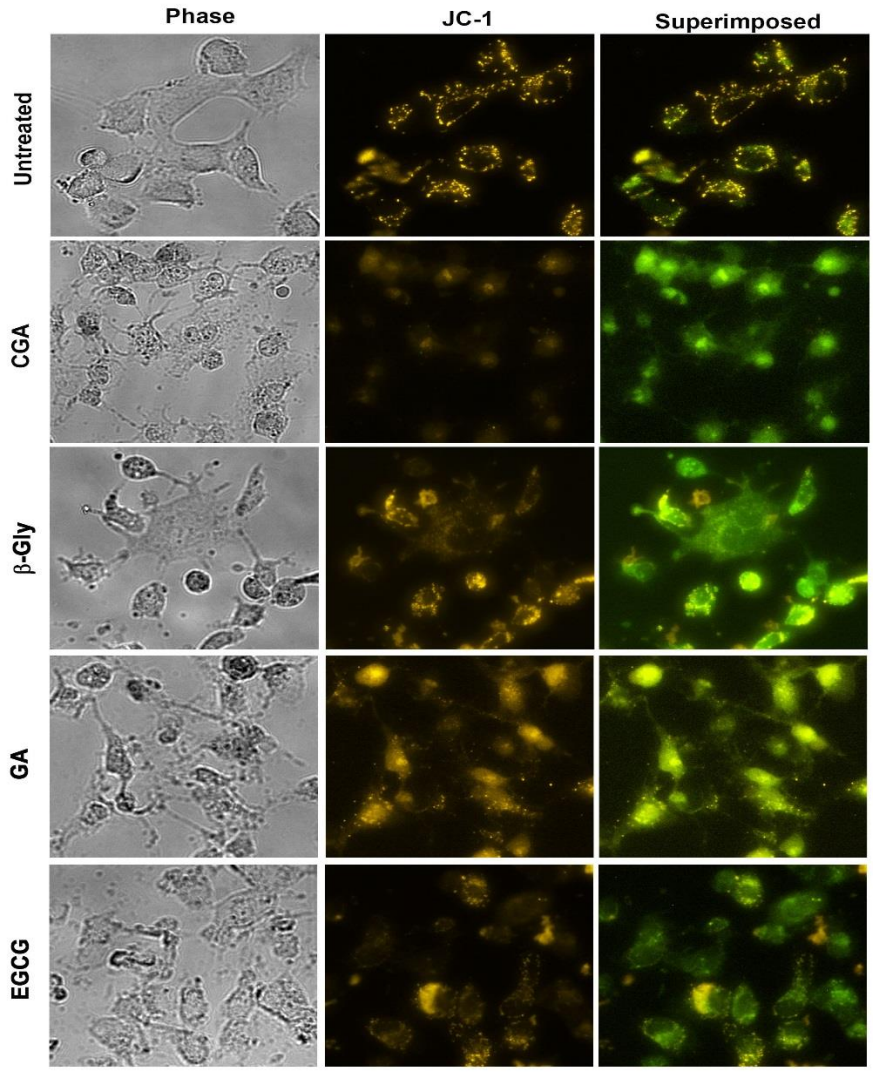

Figure 5.19: CGA (Chlorogenic acid), β-Gly (β-Glycyrrhetinic acid), GA (Gallic acid) and EGCG (Epigallocatechin gallate) treated breast cancer cells exhibit loss of mitochondrial membrane potential. MDAMB-231 breast cancer cells were treated with CGA (75 µg/ml), β-Gly (10 µg/ml), EGCG (6.5 µg/ml) and GA (2.5 µg/ml) in serum-free media for 24 hrs. Post-treatment, cells were stained with JC-1 dye for 20 minutes and were observed in Cytell imaging system (GE Healthcare).

Similarly, alkyl cinnamate (at their respective IC_{50} concentrations) treated MDAMB-231 cells were showing green fluorescence spread evenly throughout the cytosol with little orange fluorescence. This condition is indicative of apoptosis (Figure 5.20).

B) Release of cytochrome-c from breast-cancer cells undergoing apoptosis: We further explored the release of cytochrome-c (cyt-c) from mitochondria in PKC-directed molecule treated MDAMB-231 cells. MDAMB-231 cells were treated individually with Danazol (70 µg/ml), Flunarizine (5.9 µg/ml) and Cinnarizine (54 µg/ml) for a period of 24 hrs in serum free media and release of cyt-c was assessed as described in Chapter 2 (Section 2.14). Location of mitochondria was identified by MitoTracker Red dye which localizes inside the mitochondrion irrespective of any mitochondrial membrane potential (Poot et al., 1996). Immuno-staining in untreated cells showed that signal of cyt-c was highly specific to distinct locations inside the cell. It was observed that the cyt-c signal was co-

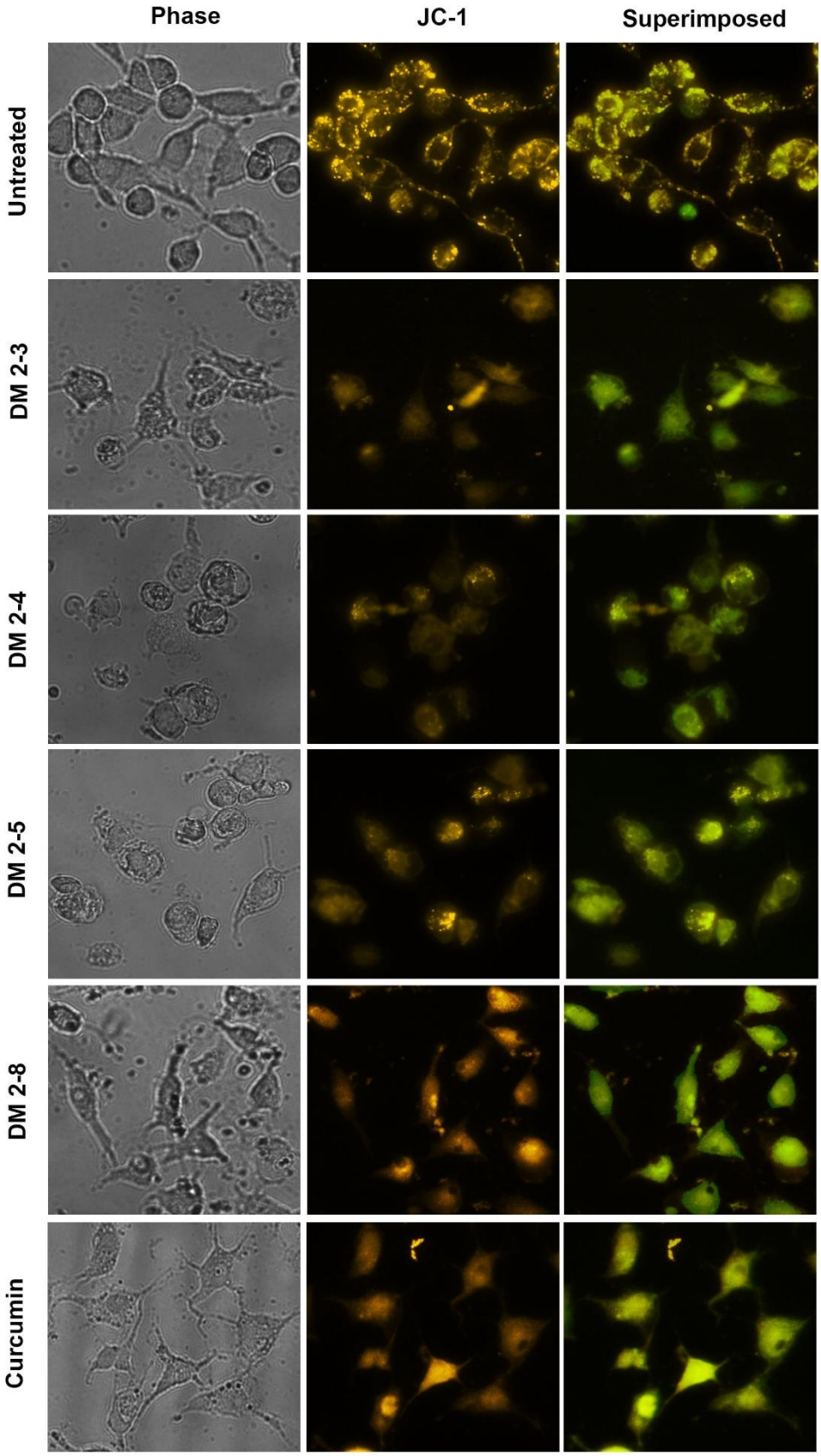

Figure 5.20: Loss of mitochondrial membrane potential in alkyl cinnamate treated MDAMB-231 breast cancer cells. MDAMB-231 breast cancer cells were treated with alkyl cinnamates (IC_{50} concentration) in serum-free media for 24 hrs. Post treatment cells were stained with JC-1 dye for 20 minutes and were observed in Cytell imaging system (GE Healthcare). Alkyl cinnamate treated cells show a decrease in mitochondrial membrane potential as indicated by loss of orange and appearance of green fluorescence**.**

localizing with MitoTracker Red signal. It indicates the presence of cyt-c inside the intact mitochondria in untreated cells (Figure 5.21). In Danazol, Flunarizine and Cinnarizine treated cells; cyt-c was almost evenly distributed throughout the cytosol; was not co-localizing with the MitoTracker Red signals (Figure 5.21). This proves that candidate drug treatment results in compromised mitochondrial membrane integrity with the release of cyt-c.

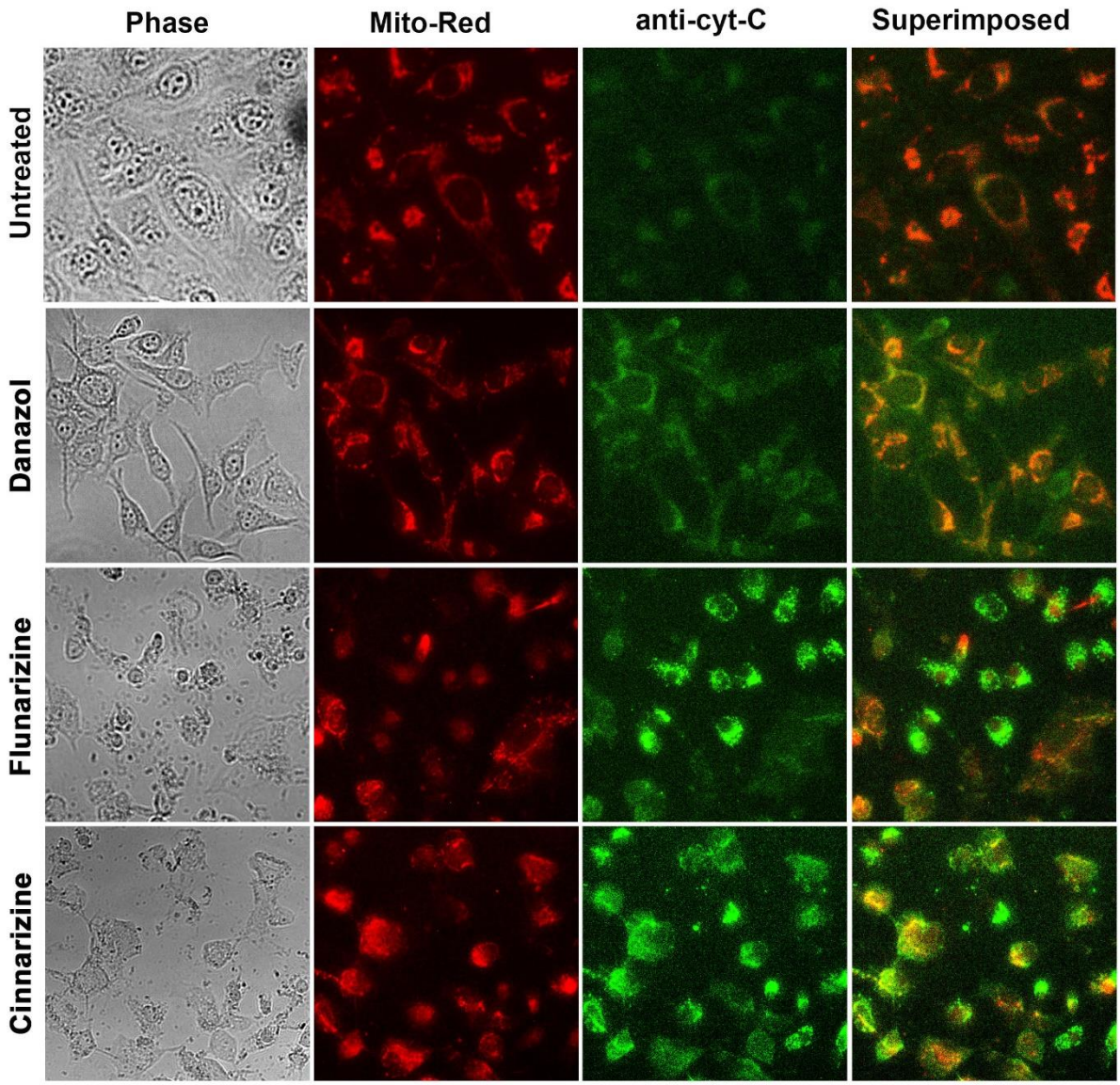

Figure 5.21: The release of cytochrome-c from Danazol, Flunarizine and Cinnarizine treated breast cancer cells. MDAMB-231 breast cancer cells were treated with Danazol (70µg/ml), Flunarizine (5.9 µg/ml) and Cinnarizine (54 µg/ml) in serum-free media for 24 hrs. Post treatment, cells were stained for cyt-c and location of mitochondria in MDAMB-231 cells was determined by loading the cells with MitoTracker Red (200 nM for 45 mins) as described in Chapter 2 (Section 2.14). Labelled cells were observed in Cytell imaging system (GE Healthcare). Untreated cells seem healthy with the cyt-c signal overlapping with MitoTracker signal. High resolution imaging detected the release of cyt-c from drug treated cells.

The similar effect of even distribution of cyt-c throughout the cytosol was observed in Chlorogenic acid, β-Glycyrrhetinic acid, Gallic acid and Epigallocatechin gallate (Figure 5.22) treated

cells. This indicates release of cyt-c into the cytosol from mitochondria. Untreated cells displayed a co-localization of cyt-c and MitoTracker signals indicating no significant release of cyt-c from mitochondria.

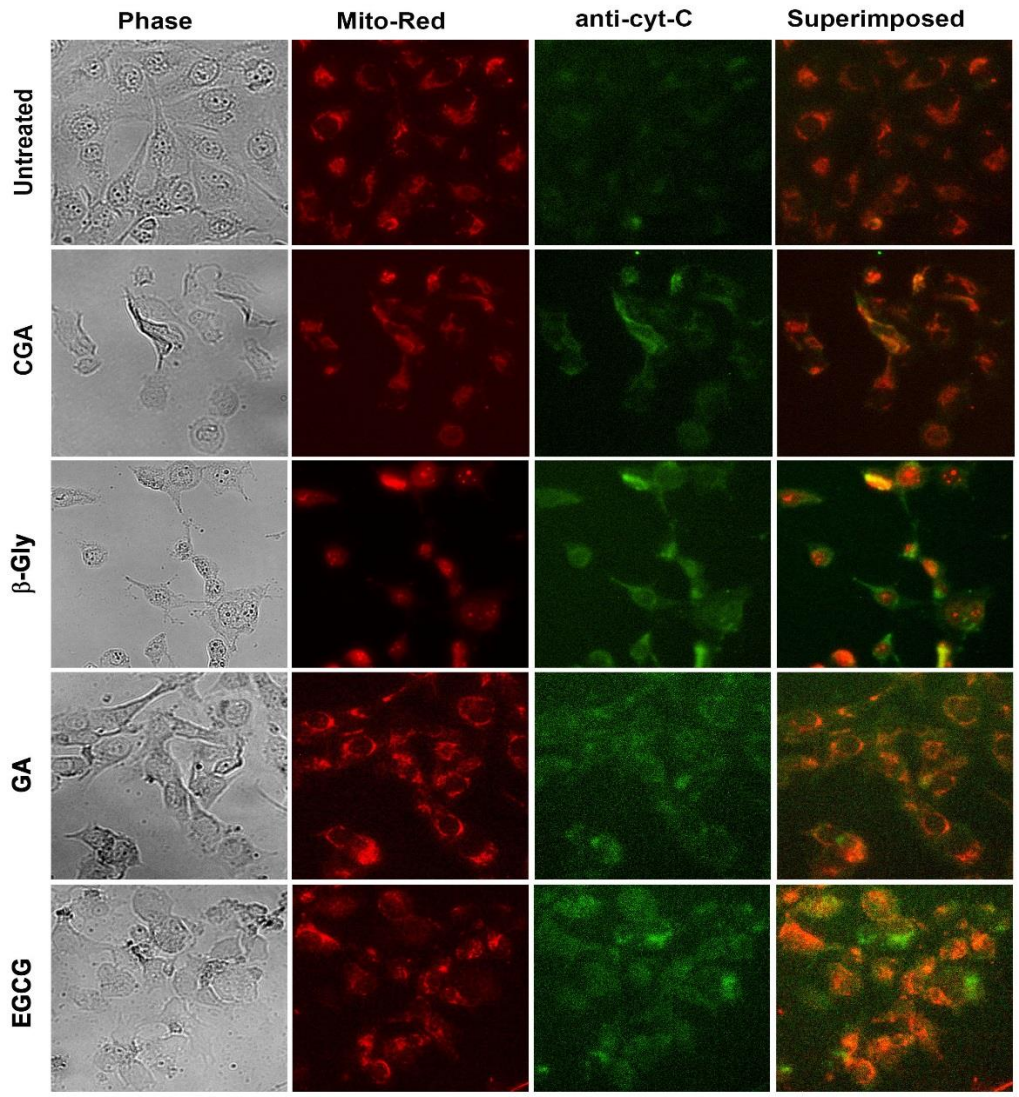

Figure 5.22: CGA (Chlorogenic acid), β-Gly (β-Glycyrrhetinic acid), GA (Gallic acid) and EGCG (Epigallocatechin gallate) treated breast cancer cells release cyt-c from the mitochondria. MDAMB-231 breast cancer cells were treated with CGA (75 µg/ml), β-Gly (10 µg/ml), EGCG (6.5 µg/ml) and GA (2.5 µg/ml) in serum-free media for 24 hrs. Post treatment, anti-cyt-c antibodies were used to stain cytochrome-C in cells. The location of mitochondria in MDAMB-231 cells was determined by loading the cells with MitoTracker Red (200 nM for 45mins) as described in Chapter 2 (Section 2.14). Labelled cells were observed in Cytell imaging system (GE Healthcare).

We further explored the release of cyt-c from mitochondria in alkyl cinnamates treated breast cancer cells. Alkyl cinnamate treated cells showed a cyt-c signal which is almost evenly distributed throughout the cytosol. Untreated cells showed a clear co-localization of cyt-c and MitoTracker signal. It can be easily comprehended from the immunostaining data that there is release of cyt-c from mitochondria to the cytosol in cancer cells undergoing apoptosis after treatment (Figure 5.23). Thus, PKC-directed molecules are capable of inducing apoptosis via the mitochondrial pathway which involves mitochondrial depolarization followed by release of cyt-c.

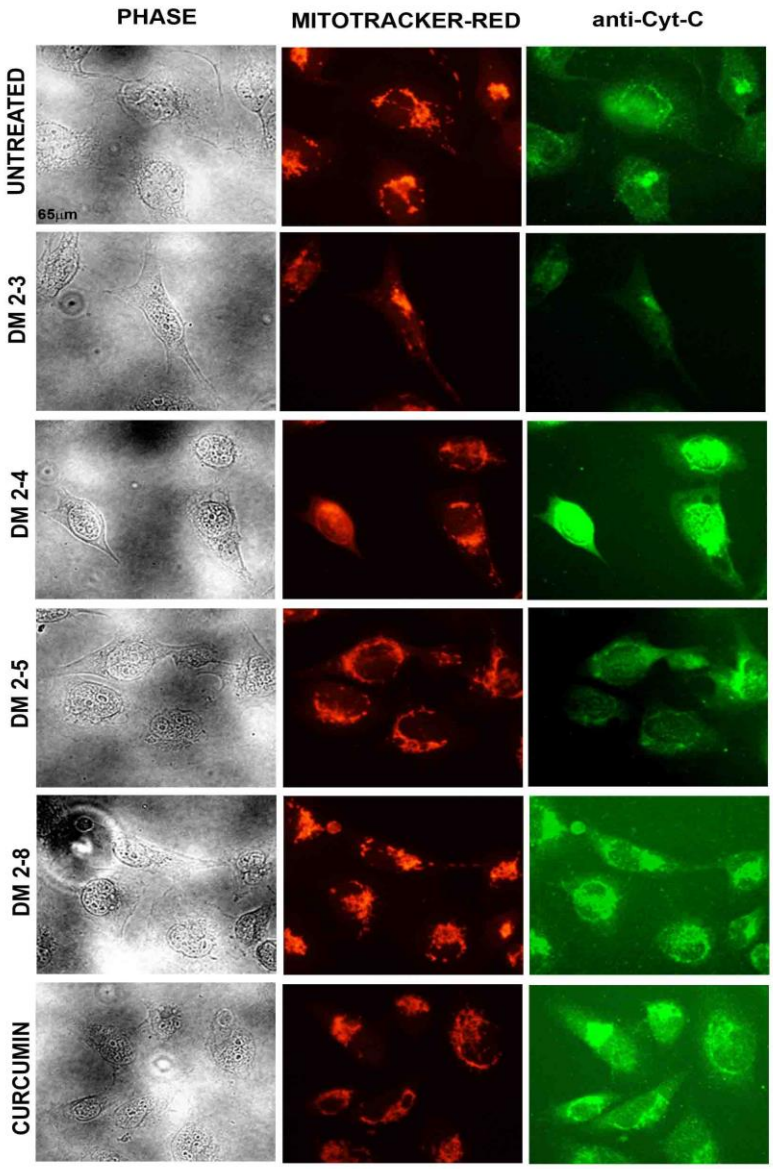

Figure 5.23: Release of cytochrome-c from alkyl cinnamate treated MDAMB-231 breast cancer cells. MDAMB-231 breast cancer cells were treated with alkyl cinnamates (IC_{50} concentration) in serum free media for 24 hrs. Post treatment, cells were stained for cytochrome-c and location of mitochondria in MDAMB-231 cells is determined by loading the cells with MitoTracker (200 nM for 45mins) as given in material and methods. Labelled cells were observed in Nikon Eclipse 80i fluorescence microscope. In each panel, bright field, cyt-c (green), mitotracker Red (red) is given. Release of cyt-c is detected from DM 2-3, DM 2-4, DM 2-5 and curcumin treated cells.

(C) Caspases are activated downstream of release of cytochrome-c from the mitochondria in breast cancer cells: Cytochrome-c released from mitochondrion combines with Apaf-1 and activates downstream caspases involved in modulating the apoptotic pathway. Caspase-9 and caspase-3 are principal caspases involved in the intrinsic mitochondrial pathway of apoptosis (Fulda and Debatin, 2006; Xue et al., 2014). Hence, the activity of caspase -3 was assayed as a consequence of mitochondrial depolarization and cyt-c release on treatment of MDAMB-231 cells for 24 hrs as described in Chapter 2 (Section 2.15). As expected Flunarizine (at 5.9 µg/ml) and Cinnarizine (at 54 µg/ml) treated MDAMB-231 cells displayed a 124 ± 3.5% and 70 ± 2.5% increment in caspase-3

activity (Figure 5.24) compared to untreated cells. This finding confirms that Flunarizine and Cinnarizine treated breast-cancer cells follow the mitochondrial pathway of apoptosis.

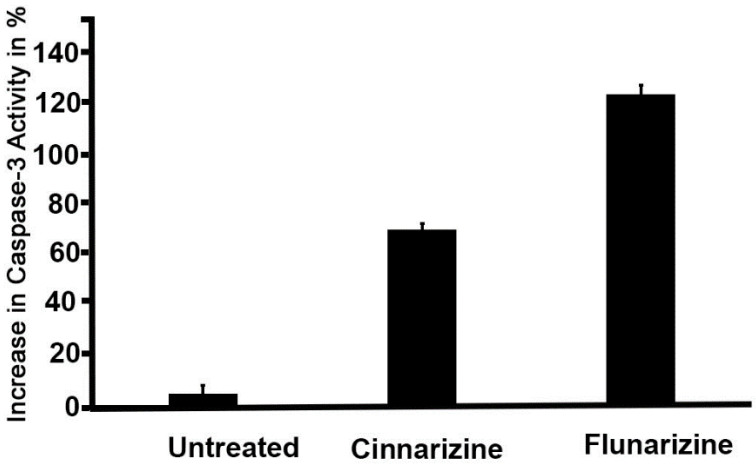

Figure 5.24: Increase in caspase-3 activity in Flunarizine (5.9 µg/ml) and Cinnarizine (54 µg/ml) treated MDAMB-231 cells.

Similarly, MDAMB-231 cells treated with curcumin or DM 2-8 for 24 hrs showed an increase in caspase-9 activity compared to untreated sample (Figure 5.26-A) as described in Chapter 2 (Section 2.16). Cells treated with curcumin or DM 2-8 gave 35% and 48% increase in caspase-9 activity respectively (Figure 5.25-A). Similarly, DM 2-8 or curcumin treated cell showed 90% and 65% increase in caspase-3 activity respectively (Figure 5.25-B). These experiments indicate that the PKC-agonists utilize intrinsic pathway to induce apoptosis in MDAMB-231 breast cancer cells.

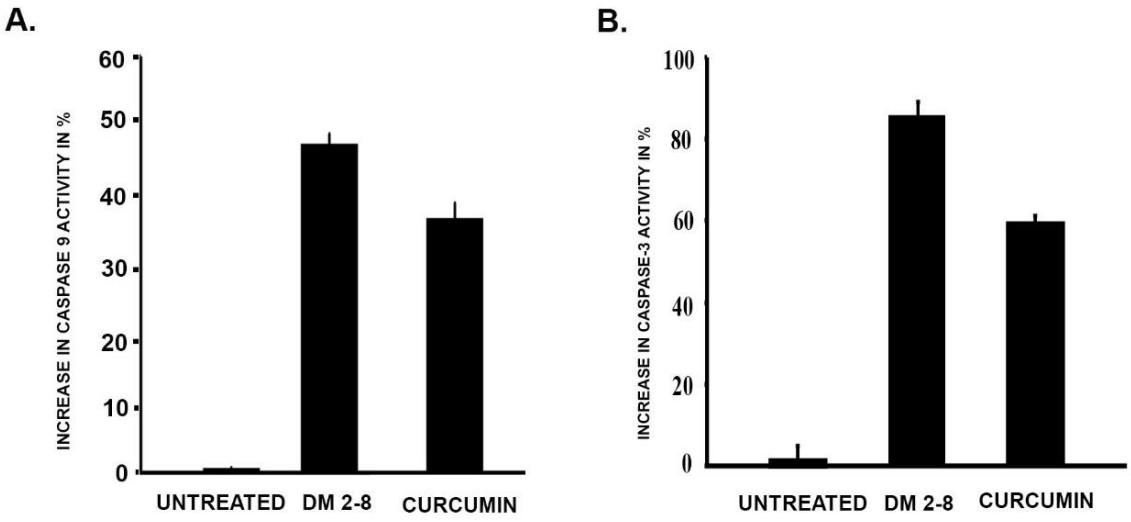

Figure 5.25: Cytochrome-c release activates down-stream cytosolic caspases. (A) Caspase-9 and **(B)** Caspase-3 activity in MDAMB-231 cells treated with alkyl cinnamates. Caspase-3 activity levels increased by 90 percent and 65 percent in DM 2-8 and curcumin treated cells respectively.

5.3.8: PKC-directed molecule treatment causes ROS accumulation in cancer cells: MDAMB-231 cells were treated individually with Flunarizine (5.9 µg/ml), β-Glycyrrhetinic acid (10 µg/ml) for 24 hrs for the assessment of ROS levels with DCF dye as described in Chapter 2 (Section 2.7). Cells incubated only in serum-free media alone served as control. Flow cytometric analysis suggested a significant generation of ROS in Flunarizine and β-Glycyrrhetinic acid treated cells as compared to untreated cells (Figure 5.26). We also investigated the role of oxidative stress in alkyl cinnamates (IC_{50} concentration) mediated cell death in MDAMB-231 breast cancer cells. Cells incubated only in incomplete (serum-free) media served as control. Alkyl cinnamate treated MDAMB-231 cells showed an increased level of ROS compared to untreated cells (Figure 5.28-A).

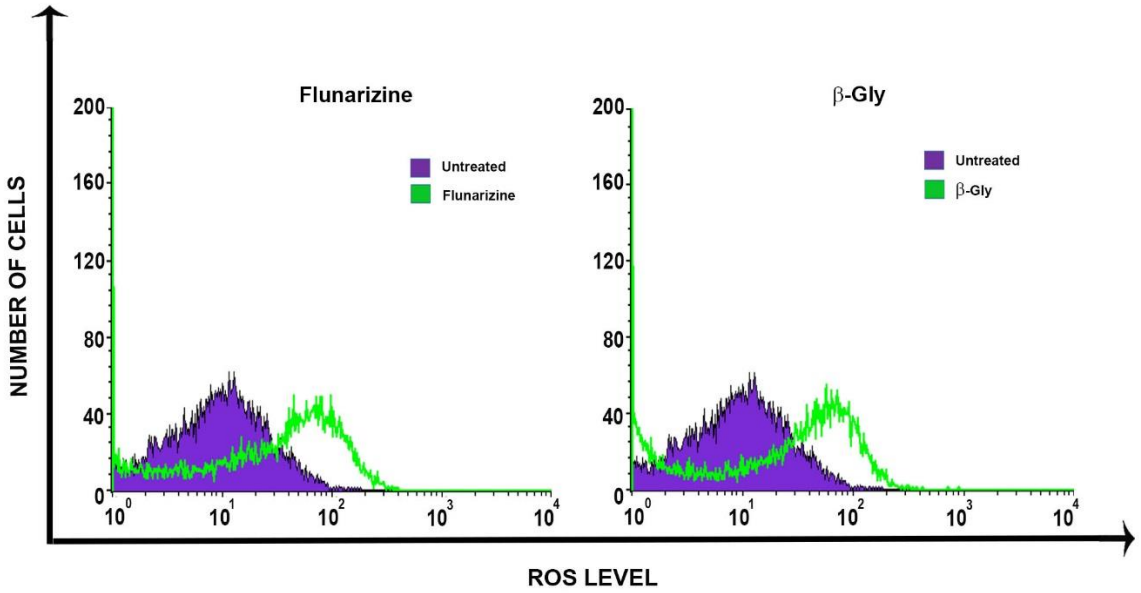

Figure 5.26: Flow cytometry analysis reveal accumulation of ROS in Flunarizine and β-Gly (β-Glycyrrhetinic acid) treated cells. Cells were treated with Flunarizine (5.9 µg/ml) and β-Gly (10 µg/ml) for 24 hrs timepoint. DCF-DHA was used as a ROS probe. Flunarizine and β-Glycyrrhetinic acid treated cells show an increased level of ROS compared to untreated cells.

5.3.9 PKC directed molecules cause protein carbonyl and lipid peroxidation in cancer cells: Usually, oxidative stress is associated with increase in lipid peroxidation levels and formation of protein carbonyls inside cell cytosol. In order to explore any possible generation of lipid peroxidation products and protein carbonyls, MDAMB-231 cells were treated with β-Glycyrrhetinic acid (10 µg/ml) or different alkyl cinnamates (at their IC_{50}) concentrations for 4 hrs. Then, estimation of lipid peroxidation and protein carbonyl levels were done as described in Chapter 2 (Section 2.17 and Section 2.18 respectively). (Figure 5.27-A & B and Table 5.1). Estimation of lipid peroxidation and protein carbonyl levels confirm a much higher level of oxidative stress in β-Glycyrrhetinic acid treated cells. The level of malonaldehyde (MDA) in β-Glycyrrhetinic acid treated cells reached 200 nmoles/mg and the protein carbonyl levels reached 10,000 nmoles/mg which is much higher than untreated cells. Similarly, lipid peroxidation and protein carbonyl levels were also found to be considerably higher in

alkyl cinnamate treated cells (Table 5.2) compared to untreated cells. In this aspect, DM 2-5 was the compound which showed the highest levels of malonaldehyde (80 nmoles/mg) and protein carbonyl (9000 nmoles/mg) levels followed by DM 2-4 and DM 2-8. Thus, PKC-directed molecules cause oxidative stress in MDAMB-231 breast cancer cells.

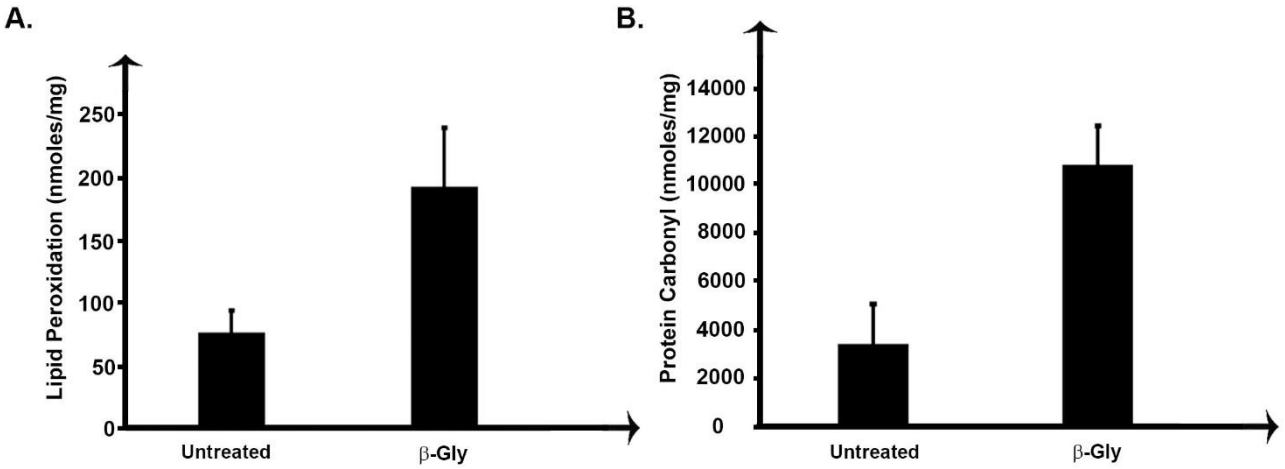

Figure 5.27: Lipid peroxidation and protein carbonyl levels in β-Gly (β-Glycyrrhetinic acid) treated MDAMB-231cells. β-gly treated cells (10 µg/ml) for 4 hrs show an increased level of lipid peroxidation and protein carbonyl levels compared to untreated cells**.**

Table 5.1: Measurement of oxidative stress indices in alkyl cinnamate treated MDAMB-231 cells.

S.No	Compound	Lipid Peroxidation(nmoles/mg)	Protein Carbonyl Level(nmoles/mg)
1.	Untreated	31.4 ± 3.1	3848.5 ± 669.6
2.	DM 2-CRMN	47.6 ± 9.9	6636.4 ± 737.5
3.	DM 2-3	42.9 ± 6.7	5931.8 ± 1174.6
4.	DM 2-4	54.4 ± 8.4	5242.4 ± 1033.9
5.	DM 2-5	80.5 ± 15.0	9068.2 ± 880.5
6.	DM 2-8	47.8 ± 4.1	5401.5 ± 854.7

Lipid Peroxidation and Protein carbonyl levels were determined as described in Chapter 2 (Section 2.17 & Section 2.18). Cells are treated with different alkyl cinnamates at their respective IC_{50} concentrations. Considerable increase in lipid peroxidation and protein carbonyl levels are seen in alkyl cinnamate treated cells.

5.3.10 Oxidative stress within breast cancer cells is responsible for apoptosis: We further explored the possible role of oxidative stress in the induction of apoptosis, cellular damage and death in cancer cells treated with alkyl cinnamates. Alkyl cinnamate treated MDAMB-231 cells showed an increased level of ROS compared with that of untreated cancer cells (Figure 5.28-A). In the presence of NAC (5 mM), ROS level was reduced in alkyl cinnamate treated cancer cells (Figure 5.28-A). Subsequently, MDAMB-231 cells were treated with DM 2-8 or curcumin in the absence or presence of NAC (5 mM), genomic DNA was extracted from treated cells and analysed on 1.8% agarose gel. Untreated cells

showed an intact genomic DNA with no sign of DNA fragments/smear (Figure 5.28-B, Lane 1). Whereas, cells treated with DM 2-8 or curcumin gave DNA fragments of different sizes (Figure 5.28-B, Lanes 3 and 5). In contrast, cells pre-incubated with NAC (5 mM) and then treated with DM-2-8 or curcumin, gave intact genomic DNA with no visible appearance of DNA fragments (Figure 5.28-B, Lanes 4 and 6). Subsequently, we found that removal of oxidative stress in MDAMB-231 cells restores cell morphology compared to cells treated with alkyl cinnamates (Figure 5.29).

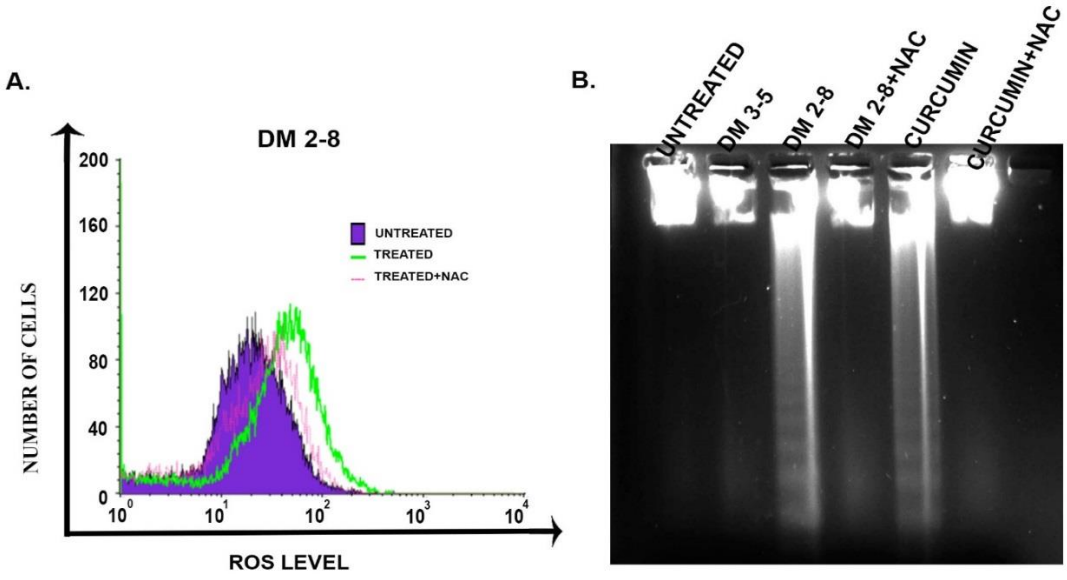

Figure 5.28: Flow cytometric measurements reveals elevated ROS levels in alkyl cinnamate treated breast cancer cells. (A) Cells were treated with alkyl cinnamates (IC_{50} concentration) for 4 hrs and DCF-DHA was used as a ROS probe. In this figure, DM 2-8 is used as an example. DM-2-8 treated cells show an increased level of ROS compared to untreated cells. The pre-incubation of cells in NAC reduces ROS level in treated cell.**(B)** Cells were treated with DM 2-8 or curcumin in the absence or presence of NAC (5mM) and presence of NAC gives intact genomic DNA with no visible appearance of DNA fragments.

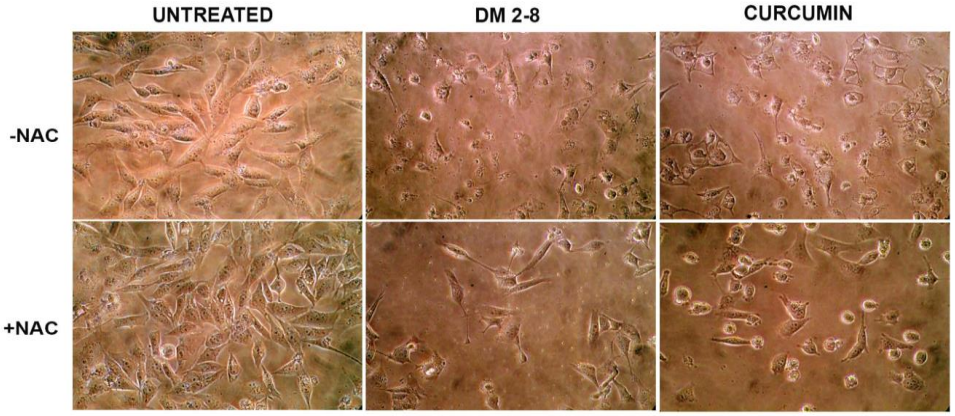

Figure 5.29: Microscopic Observation of MDAMB-231 cells treated with DM 2-8 or curcumin for 48 hrs in absence or presence of NAC. Images were taken with high resolution Nikon L22 camera. Cells pre-incubated with NAC gives an improved cellular morphology compared to DM 2-8 or curcumin treated cells.

5.4 Discussion

The results of immuno-blotting and immuno-fluorescence experiments confirm that the chosen PKC-directed molecules can mediate effective translocation of PKC from the cytosol to the plasma membrane. All the molecules also caused prolonged translocation of PKC to the plasma membrane. However, different molecules varied in their efficacy at mediating translocation of PKC. Flunarizine and Cinnarizine behaved differently in translocating PKC. Flunarizine mediated translocation was minimal at 30 mins and started increasing to maximal at 120 mins timepoint. On the other hand, Cinnarizine showed maximal translocation of PKC at 30 mins followed by a decrease in translocation untill minimal at 120 mins. Chlorogenic acid induced similar translocation levels of PKC at 60 mins and 120 mins timepoints. β-Glycyrrhetinic acid had maximal translocation of PKC at 120 mins timepoint followed by a decline in translocation of PKC at 240 mins timepoint. On the other hand, Gallic acid induced a steady increase in PKC translocation till the 240 mins timepoint which was followed by a decrease in translocation levels of PKC at 480 mins timepoint. Generally, the consequence of PKC translocation leads to an active form of the enzyme that culminate in either proliferation of the cancer cells or cell-death (Huang, 1989). However, in our case, the PKC-directed molecules are effective in the induction of dose-dependent cell-death in MDAMB-231 breast cancer cells. As such, results of PKC translocation experiments enabled us to design newer experiments. These experiments helped us to understand the mechanistic details of MDAMB-231 breast cancer cells cell-death induced by PKC-directed molecule treatment.

Apoptosis is a programmed process of cell-death which is initiated by the packaging of cellular contents into different granules (apoptosome) rather than leakage to the extracellular environment (Cain et al., 2002). These granules serve as efficient opsonins that are easily phagocytosed by circulating macrophages and neutrophils, preventing any inflammatory response (Elmore, 2007; Hochreiter-Hufford and Ravichandran, 2013). Whenever a cell is mauled by toxic external agents, the cell undergoes necrosis which is characterized by haphazard release of cellular contents into the surrounding extracellular space (Golstein and Kroemer, 2007). Such release of cellular contents readily invites an inflammatory response which causes localized edema. Thus, necrosis is an unselective phenomenon. On the other hand, apoptosis is mediated by very specific modulatory proteins such as receptors, enzymes and transcription factors and is a carefully controlled process (Elmore, 2007; Hassan et al., 2014). A desirable quality of any future anti-cancer drug is to kill cancer cells following apoptosis rather than necrosis. Apoptosis would ensure safe and efficient killing of targeted cancer cells without invoking inflammatory reactions in the patient (Elmore, 2007). In the current study, we have found that the cell-death mediated by identified molecules through active PKC signalling is apoptotic in nature. PKC-directed molecule treated cells show a higher uptake of AO and PI dyes which indicates a compromised cell membrane and confirms induction of apoptosis. DNA

degradation in the form of laddering was observed in all the molecule treated breast cancer cells. Involvement of the mitochondrial pathway of apoptosis was confirmed by the clear evidence of depolarization of mitochondrial membrane. Hence, our study proves that different PKC-directed molecules from diverse sources have the potential to modulate PKC dynamics in breast cancer cells to induce apoptosis.

There are generally two types of apoptotic programs: the intrinsic/ mitochondrial pathway and the extrinsic/death-receptor pathway (Figure 5.30). The death receptor pathway is initiated by external ligands (ligands from outside the cell) that bind to their associated receptors on the cell surface (Fulda and Debatin, 2006). These receptors are known as death receptors and consists of FAS, DR4, DR5, DR3 and TNFR1 receptor families (Guicciardi and Gores, 2009). Activation of these receptors by their corresponding ligands leads to the association of their cytoplasmic tails to another protein which is termed FADD (Fas-associated death domain protein). This complex recruits pro-caspase-8 and pro-caspase-10 which undergo self-cleavage to activated forms. These caspases cleave the executioner caspases, caspase-3, caspase-6 and caspase-7. The mitochondrial pathway is characterized by the activation of Bax, BAD, Bak, and Bid proteins and cleavage of Bcl-2 protein (Estaquier et al., 2012). Bax, BAD, Bak, and Bid proteins after activation by cleavage, form pores in the mitochondrial membrane leading to release of cyt-c molecules to the cytosol. Cyt-c released from mitochondria combines with Apaf-1 and activates downstream caspases involved in modulating the apoptotic pathway (Fulda and Debatin, 2006). The extrinsic and the intrinsic pathways converge at the point of activation of caspase-3. Initial signalling through extrinsic pathway activates caspase-3 which in turn can cleave Bid protein to reveal its active form called truncated Bid (tBid). These tBid molecules can form pores in the mitochondrial membrane leading to the release of cyt-c molecules to the cytosol. Cyt-c in turn combines with Apaf-1 to activate caspase-9. The current study has proven the involvement of the mitochondrial pathway in apoptosis mediated by PKC directed-molecules in breast cancer cells. We have found the involvement of caspase-3. However, there is always a possibility of the involvement of the extrinsic pathway in the activation of caspase -3 (Figure 5.30) which remains to be explored. Generated ROS has been earlier reported to activate the death-receptor pathway via generation of self-death ligands.

Development of oxidative stress is one of the mechanisms by which many phytochemicals and anti-cancer drugs predispose cancer cells towards apoptosis (Gorrini et al., 2013; Liu and Wang, 2015). A limited concentration of reactive oxidative species always exists in every cell and these ROS serves as signalling molecules to provide growth stimulus in the cell. A high level of ROS within cell will have disastrous effects on cell-viability and will predispose any cell towards programmed cell-death. Studies have revealed that the phytochemical curcumin exhibits differential roles for healthy cells and cancer cells as the generation of oxidative stress is concerned. Curcumin has been known as an

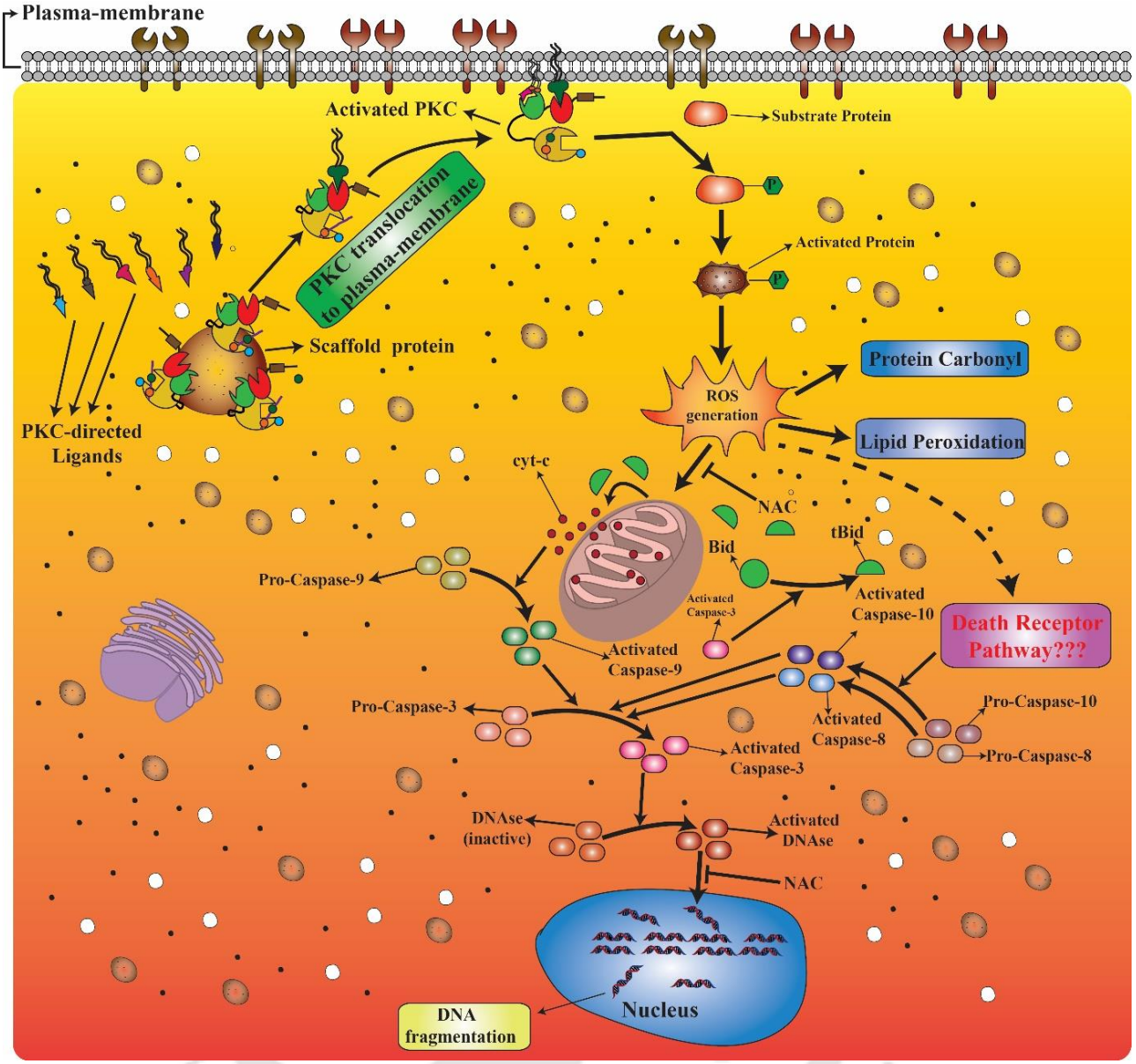

Figure 5.30: Conclusion of the mechanism of action of PKC directed molecules on breast cancer cells.

oxidative stress inducer in many cancer cell lines whereas being a protector of oxidative stress in many healthy cell lines (Khar et al., 1999; Oyama et al., 1998; Sun et al., 2009). In the current study, PKC-directed molecule treated MDAMB-231 cells showed an increased level of ROS compared to untreated cells (Figure 5.27 and 5.28). In the presence of N-acetyl cysteine (NAC), oxidative stress level in PKC-directed molecule treated cells was reduced (Figure 5.29-A). Interestingly, NAC treatment even caused reversal of apoptosis and viability (Figure 5.29-B) which prove that oxidative stress is an important factor in the induction of apoptosis by PKC-directed molecules. Generation of oxidative stress was undoubtedly responsible for the mitochondrial pathway of apoptosis induced by PKC-directed molecules in MDAMB-231 cells. However, any possible connection of this generated ROS with the death-receptor pathway has not been explored by us due to financial and time constraints at our lab. However, the involvement of death-receptor pathway is considered to be explored by future students at our lab.

In the results outlined in the present thesis, few of the experiments are performed only with a few representative molecules. For example, we have seen that Danazol abolishes carcinogenic signalling induced by PMA, but we have not explored this feature with other molecules. Time and resource constraints prevented us from performing these seemingly redundant experiments. Since, these are going to be superfluous data, that's why for these few experiments we just went with one representative molecule to show that this was actually happening. Although we are not sure if the similar mechanism is also followed by other molecules, it is very likely that they also follow that mechanism But the follow up experiments with the other molecules is required to finally validate that these mechanisms are also followed with other molecules as well.

Overall, the work incorporated in this thesis has the following message to be taken.

1) Re-purposing of clinically approved drugs is an alternative to design anti-cancer drug: Drugs such as Danazol, Flunarizine and Cinnarizine that have been long used for the treatment of diseases other than cancer, can now also be viewed as having potent anti-cancer properties. Thus, we have identified an additional important property of these drugs that they also interact with PKC to induce apoptosis in cancer cells as revealed by the current study. This process is also known as clinical repurposing of existing drugs which assigns an additional new therapeutic identity to the molecule. Clinical repurposing relies on pre-existing clinical safety and drug development data of the concerned molecule. Pre-existing clinical drugs have a distinct advantage over the designing of a de-novo drug. For instance, pre-clinical drugs are exempted from the rigors of clinical trials that rejects more than 90% of de-novo drug candidates. Thus, repurposed drugs have no toxicity concerns and can be promptly approved for therapeutic use.

2) **Importance of inclusion of herbal beverages such as tea to delay cancer progression:** Our study reveals that phytochemicals such as Epigallocatechin gallate, Gallic acid and Chlorogenic acid that are found in natural herbs & beverages can potentially act as ligands for PKC-α and can stimulate apoptosis in highly aggressive breast cancer cells. Green tea is a good source of Chlorogenic acid, β-Glycyrrhetinic acid and Epigallocatechin gallate. Grapes and red wine are good sources of Gallic acid. Many such phytochemicals identified as good PKC-directed molecules in Chapter 3 have yet to be explored for potential anti-cancer property. Thus, regular intake of herbs and beverages enriched in these anti-cancer phytochemicals is highly recommended to boost the immune system against malignant cancer cells. They can also be taken as a part of cancer therapy, especially as additional immune therapy during radiotherapy or chemotherapy practices.

3) Chemical synthesis of novel molecules targeting PKC can open up new avenues for anti-cancer drug development: Our study has also shown that the novel chemicals (alkyl cinnamates) synthesized

in the collaborator lab as PKC-directed molecules, were capable of inducing the mitochondrial pathway of apoptosis in breast cancer cells. However, synthesis of these alkyl cinnamates have been inspired from the natural phytochemical curcumin as a template.

Thus, the current study emphasizes that natural molecules can serve as templates for the synthesis of novel derivatives that can potentially be very effective PKC ligands. There is no dearth of natural molecules that can serve as ligands of PKC. One can readily choose a natural molecule and chemically synthesize many derivatives that can be more potent than the parent compound. This approach enables us to design effective PKC-directed anti-cancer molecules at economic research budgets that can potentially qualify as suitable candidates for anti-cancer drug discovery programme.

5.5 References

- Cain, K., Bratton, S.B., and Cohen, G.M. (2002). The Apaf-1 apoptosome: a large caspase-activating complex. Biochimie *84*, 203-214.
- Elmore, S. (2007). Apoptosis: A Review of Programmed Cell Death. Toxicologic Pathology *35*, 495-516.
- Estaquier, J., Vallette, F., Vayssiere, J.L., and Mignotte, B. (2012). The mitochondrial pathways of apoptosis. Advances in Experimental Medicine and Biology *942*, 157-183.
- Fulda, S., and Debatin, K.M. (2006). Extrinsic versus intrinsic apoptosis pathways in anticancer chemotherapy. Oncogene *25*, 4798-4811.
- Golstein, P., and Kroemer, G. (2007). Cell death by necrosis: towards a molecular definition. Trends in Biochemical Sciences *32*, 37-43.
- Gorrini, C., Harris, I.S., and Mak, T.W. (2013). Modulation of oxidative stress as an anticancer strategy. Nat Rev Drug Discov *12*, 931-947.
- Guicciardi, M.E., and Gores, G.J. (2009). Life and death by death receptors. The FASEB Journal *23*, 1625-1637.
- Hassan, M., Watari, H., AbuAlmaaty, A., Ohba, Y., and Sakuragi, N. (2014). Apoptosis and Molecular Targeting Therapy in Cancer. BioMed Research International *2014*, 150845.
- Hochreiter-Hufford, A., and Ravichandran, K.S. (2013). Clearing the Dead: Apoptotic Cell Sensing, Recognition, Engulfment, and Digestion. Cold Spring Harbor Perspectives in Biology *5*.
- Huang, K.P. (1989). The mechanism of protein kinase C activation. Trends in Neurosciences *12*, 425-432.
- Kerfoot, C., Huang, W., and Rotenberg, S.A. (2004). Immunohistochemical analysis of advanced human breast carcinomas reveals downregulation of protein kinase C alpha. The Journal of Histochemistry and Cytochemistry *52*, 419-422.
- Khar, A., Ali, A.M., Pardhasaradhi, B.V., Begum, Z., and Anjum, R. (1999). Antitumor activity of curcumin is mediated through the induction of apoptosis in AK-5 tumor cells. FEBS Letters *445*, 165-168.
- Liu, J., and Wang, Z. (2015). Increased Oxidative Stress as a Selective Anticancer Therapy. Oxidative Medicine and Cellular Longevity *2015*, 12.
- Mamidi, N., Gorai, S., Sahoo, J., and Manna, D. (2012). Alkyl cinnamates as regulator for the C1 domain of protein kinase C isoforms. Chemistry and Physics of Lipids *165*, 320-330.

- Oliva, J.L., Caino, M.C., Senderowicz, A.M., and Kazanietz, M.G. (2008). S-Phase-specific activation of PKC alpha induces senescence in non-small cell lung cancer cells. The Journal of Biological Chemistry *283*, 5466-5476.
- Oster, H., and Leitges, M. (2006). Protein kinase C alpha but not PKCzeta suppresses intestinal tumor formation in ApcMin/+ mice. Cancer Research *66*, 6955-6963.
- Oyama, Y., Masuda, T., Nakata, M., Chikahisa, L., Yamazaki, Y., Miura, K., and Okagawa, M. (1998). Protective actions of 5'-n-alkylated curcumins on living cells suffering from oxidative stress. European Journal of Pharmacology *360*, 65-71.
- Poot, M., Zhang, Y.Z., Kramer, J.A., Wells, K.S., Jones, L.J., Hanzel, D.K., Lugade, A.G., Singer, V.L., and Haugland, R.P. (1996). Analysis of mitochondrial morphology and function with novel fixable fluorescent stains. The journal of Histochemistry and Cytochemistry *44*, 1363-1372.
- Sun, A., Lu, Y.J., Hu, H., Shoji, M., Liotta, D.C., and Snyder, J.P. (2009). Curcumin analog cytotoxicity against breast cancer cells: exploitation of a redox-dependent mechanism. Bioorganic & Medicinal Chemistry Letters *19*, 6627-6631.
- Xue, X., Yu, J.L., Sun, D.Q., Kong, F., Qu, X.J., Zou, W., Wu, J., and Wang, R.M. (2014). Curcumin induces apoptosis in SGC-7901 gastric adenocarcinoma cells via regulation of mitochondrial signaling pathways. Asian Pacific Journal of Cancer Prevention *15*, 3987-3992.

List of Publications

- "Alkyl cinnamates bind and translocate PKC to plasma membrane; induce apoptosis in breast cancer cells via mitochondrial pathway". **Suman Jyoti Deka**, Narsimha Mamidi, Debasis Manna and Vishal Trivedi. "**Journal of Breast Cancer**". Vol. 19; No. 4, 2016.

- "Danazol has potential to cause PKC translocation, cell-cycle dysregulation and apoptosis in breast cancer cells". **Suman Jyoti Deka**, Ashalata Roy, Vibin Ramakrishnan, Debasis Manna and Vishal Trivedi. "**Chemical Biology and Drug Design**".DOI: 10.1111/cbdd.12921.

- "Evidence of PKC Binding and Translocation to explain the anticancer mechanism of chlorogenic acid in breast cancer cells". **Suman Jyoti Deka**, SukhamoyGorai, Debasis Manna and Vishal Trivedi. Manuscript accepted for publication in the journal "**Current Molecular Medicine**".

- "Nitrobenzofurazan derivatives of *N′*-hydroxyamidines as potent inhibitors of indoleamine-2,3-dioxygenase 1." Saurav Paul, Ashalata Roy, **Suman Jyoti Deka**, Subhankar Panda, Vishal Trivedi and Debasis Manna. **European Journal of Medicinal Chemistry**.Volume 121, 4 October 2016, Pages 364–375.

- Fused Heterocyclic Compounds as Potent Indoleamine-2,3-dioxygenase 1 Inhibitors. Subhankar Panda, Ashalata Roy, **Suman Jyoti Deka**, Vishal Trivedi and Debasis Manna. ***ACS Med. Chem. Lett.*, Article ASAP,** DOI: 10.1021/acsmedchemlett.6b00359,Publication Date (Web): October 15, 2016.

- "Virtual Screening of drug database to identify potential anti-cancer drugs". **Suman Jyoti Deka**, Ashalata Roy, Debasis Manna and Vishal Trivedi. Manuscript submitted for publication in the journal **"Molecular Biosystems" (Manuscript in Communication).**

- "3-Substituted 2-Indolinonesas Mechanism-based Inhibitors of Indoleamine 2,3-Dioxygenase-1". Saurav Paul, Ashalata Roy, **Suman Jyoti Deka**, Subhankar Panda, Gopal N Srivastava, Vishal Trivedi and Debasis Manna. Manuscript submitted for publication in the journal "**European Journal of Medicinal Chemistry**" **(Manuscript in Communication)**.

Conference Presentations

- Presented a poster entitled "**Mechanistic Details of Alkyl Cinnamates in Driving Pro-Apoptotic Pathways in Breast Cancer Cells through PKC Activity Modulation**" by **Suman Jyoti Deka**, Narsimha Mamidi, Debasis Manna and Vishal Trivedi at 83rd Annual Meeting of The Society of Biological Chemists (India) held at KIIT University, Bhubaneswar, India from 18th Dec to 21st Dec 2014.

- Delivered an oral talk entitled **"Docking and Virtual Screening to Identify PKC agonists: Potentials in Anticancer Therapeutics"** at National Conference on Cancer Research held at IIT, Guwahati on 4th to 5th Dec 2014.

- Presented a poster entitled **"Biochemical and structural characterization of PF14_0660 from Plasmodium Falciparum: potentials in anti-malarial drug development"**, at 9th TCS Annual Event and Flow Cytometry Workshop on "Flow Applications in Basic, Applied and Clinical Biology" (FABACTCS) held at IIT Guwahati, Guwahati, India from 3rd Nov to 5th Nov 2016.

Journal of Breast Cancer

J Breast Cancer 2016 December; 19(4): 358-371 https://doi.org/10.4048/jbc.2016.19.4.358

ORIGINAL ARTICLE

Alkyl Cinnamates Induce Protein Kinase C Translocation and Anticancer Activity against Breast Cancer Cells through Induction of the Mitochondrial Pathway of Apoptosis

Suman Jyoti Deka, Narsimha Mamdi[1], Debasis Manna[1], Vishal Trivedi

Malaria Research Group, Department of Biosciences and Bioengineering, and [1]Laboratory of Biological Chemistry, Department of Chemistry, Indian Institute of Technology Guwahati, Guwahati, India

Purpose: The protein kinase C (PKC) family of serine-threonine kinases plays an important role in cancer cell progression. Thus, molecules that target PKC have potential as anticancer agents. The current study aims to understand the treatment of breast cancer cells with alkyl cinnamates. We have also explored the mechanistic details of their anticancer action and the underlying molecular signaling. **Methods:** 3-(4,5-Dimethylthiazol-2-yl)-2,5-diphenyltetrazolium bromide (MTT) assay was performed to measure the viability of MDAMB-231 breast cancer cells to assess the anticancer activity of these compounds. In addition, flow cytometry was performed to study the effect of alkyl cinnamates on the cell cycle and apoptosis. Immunoblotting and immunofluorescence techniques were performed to study PKC translocation, cytochrome c release, and modulation of the mitochondrial membrane potential in breast cancer cells targeted with alkyl cinnamates. **Results:** The PKC agonist DM-2-8 translocated 16.6%±1.7% PKCα from cytosol to the plasma membrane and showed excellent anticancer activity with an half maximal inhibitory concentration (IC_{50}) of 4.13±0.27 μg/mL against cancer cells. The treated cells had an abnormal morphology and exhibited cell cycle defects with G2/M arrest and reduced S phase. Cancer cells treated with DM-2-3, DM-2-4, or DM-2-8 underwent apoptosis as the major pathway of cell death, further confirmed by genomic DNA fragmentation. Furthermore, the mitochondrial membrane potential was perturbed, indicating involvement of the mitochondrial pathway of apoptosis. Immunolocalization studies revealed cytochrome c release from mitochondria to cytosol. Cancer cells treated with DM-2-8 and curcumin showed activation of caspase-9 and caspase-3 as downstream molecular components of the apoptotic pathway. Alkyl cinnamates also caused oxidative stress, which regulates the apoptotic machinery (DNA fragmentation), cell death, and morphological abnormalities in cancer cells. **Conclusion:** Alkyl cinnamates specifically target cancer cells through induction of PKC translocation and the mitochondrial pathway of apoptosis, and could be promising anticancer drugs.

Key Words: *Apoptosis, Caspases, Neoplasms, Oxidative stress, Protein kinase C*

INTRODUCTION

Cancer is a life-threatening disease and is responsible for about 7.6 million deaths every year worldwide. Cancer cells exhibits features of unlimited cell proliferation due to key changes in several crucial signal transduction pathways [1]. Canonical mitogen-activated protein kinase (MAPK) signaling, nuclear factor κB (NF-κB) signaling, and cell cycle regulatory networks are disrupted through the modulation of one or more key regulatory proteins [1]. Protein kinase C (PKC)-mediated signaling is an essential pathway that is modulated by cancer cells to acquire a tumorigenic phenotype [2]. The PKC family of serine/threonine kinases plays a central role in cellular signal transduction. A multifamily of proteins that are activated upon association with cellular membranes [3], they are implicated in numerous intracellular signaling events such as cell growth, determination of cell polarity, cell migration, cell proliferation, differentiation, tumor promotion, and apoptosis. PKCs are implicated downstream of a wide range of G protein-coupled receptors, tyrosine kinase receptors, and other growth factor-dependent receptors. Studies have revealed that PKC-mediated signaling is generally growth-supportive and stimulate cell division when activated in both normal and

Correspondence to: Vishal Trivedi
Malaria Research Group, Department of Biosciences and Bioengineering, Indian Institute of Technology Guwahati, Guwahati, India
Tel: +91-361-258-2217, Fax: +91-361-258-2249
E-mail: vtrivedi@iitg.ernet.in/vishalash_1999@yahoo.com

This work was partially supported by the National Tea Research Foundation (NTRF), Tea Board of India to V.T. S.J.D. acknowledges the financial support in the form of a fellowship from Indian Institute of Technology Guwahati, Assam, India.

Received: July 18, 2016 **Accepted:** November 12, 2016

Received Date : 13-Aug-2016

Revised Date : 23-Oct-2016

Accepted Date : 21-Nov-2016

Article type : Research Article

DANAZOL HAS POTENTIAL TO CAUSE PKC TRANSLOCATION, CELL-CYCLE DYSREGULATION AND APOPTOSIS IN BREAST CANCER CELLS.

Suman Jyoti Deka[1], Ashalata Roy[2], Vibin Ramakrishnan[3], Debasis Manna[2] and Vishal Trivedi[1#]

[1]Malaria Research Group, Department of Biosciences and Bioengineering, Indian Institute of Technology-Guwahati, Guwahati-781039, Assam, India.

[2]Department of Chemistry, Indian Institute of Technology-Guwahati, Guwahati-781039, Assam, India.

[3]Molecular Informatics & Design Laboratory, Department of Biotechnology, Indian Institute of Technology-Guwahati, Guwahati 781039, Assam, India.

[#]Address correspondence to:
Dr. Vishal Trivedi, Malaria Research Group, **Department of Biosciences and Bioengineering, Indian Institute of Technology-Guwahati, Guwahati-781039, Assam, India.** Email: vtrivedi@iitg.ernet.in, Vishalash_1999@yahoo.com, Phone : +91-361-2582217, Fax : +91-361-258-2249

Abstract: Danazol, the established clinical drug has given promising therapeutic results in a series of clinical trials with breast cancer patients. Danazol shares structural similarities with several known PKC agonists and fits well into the C1 domain. Danazol binds to the C1b domain of PKC with K_d of 5.64±1.27 μM. MD simulation studies further support that the PKC-Danazol molecular model is stable and showing minimum distortion to the structure during the simulation period. Immunofluorescence and western-blotting studies indicate that MDAMB-231 cells stimulated with danazol exhibit translocation of PKCα to the plasma membrane. Cells stimulated with Danazol causes appearance of several phosphorylated proteins in lysate and plasma membrane. In addition, Danazol affects carcinogenic molecule (PMA) induced intracellular signaling in cancer cells. It halted the cancer cells in the G1-phase of the cell-cycle and reduced the viability of ER^{+ve} and triple-negative breast cancer cells with an IC_{50} of 31±2.63 and 65±4.27μg/ml respectively. DNA fragmentation and flow cytometry experiments revealed that the cell death follow the apoptotic pathway. It affects mitochondrial membrane potentials and releases cytochrome-c from mitochondria to induce down-stream apoptosis in breast cancer cells. Hence, the current study may help clinicians to re-design their treatment strategy to optimize therapeutic potentials of the molecule.

This article has been accepted for publication and undergone full peer review but has not been through the copyediting, typesetting, pagination and proofreading process, which may lead to differences between this version and the Version of Record. Please cite this article as doi: 10.1111/cbdd.12921

European Journal of Medicinal Chemistry 121 (2016) 364–375

Contents lists available at ScienceDirect

European Journal of Medicinal Chemistry

journal homepage: http://www.elsevier.com/locate/ejmech

Research paper

Nitrobenzofurazan derivatives of *N*′-hydroxyamidines as potent inhibitors of indoleamine-2,3-dioxygenase 1

Saurav Paul [a, 1], Ashalata Roy [a, 1], Suman Jyoti Deka [b], Subhankar Panda [a], Vishal Trivedi [b, **], Debasis Manna [a, *]

[a] Department of Chemistry, Indian Institute of Technology Guwahati, Assam 781039, India
[b] Department of Bioscience and Bioengineering, Indian Institute of Technology Guwahati, Assam 781039, India

ARTICLE INFO

Article history:
Received 1 March 2016
Received in revised form
25 May 2016
Accepted 26 May 2016
Available online 28 May 2016

Keywords:
N′-hydroxyamidines
Mechanism-based drug design
IDO1 inhibition
High selectivity
Low cytotoxicity

ABSTRACT

Tryptophan metabolism through the kynurenine pathway is considered as a crucial mechanism in immune tolerance. Indoleamine 2,3-dioxygenase 1 (IDO1) plays a key role in tryptophan catabolism in the immune system and it is also considered as an important therapeutic target for the treatment of cancer and other diseases that are linked with kynurenine pathway. In this study, a series of nitrobenzofurazan derivatives of *N*′-hydroxybenzimidamides (**1**) and *N*′-hydroxy-2-phenylacetimidamides (**2**) were synthesized and their inhibitory activities against human IDO1 enzyme were tested using in-vitro and cellular enzyme activity assay. The optimization leads to the identification of potent compounds, **1d**, **2i** and **2k** (IC_{50} = 39–80 nM), which are either competitive or uncompetitive inhibitors of IDO1 enzyme. These compounds also showed IDO1 inhibition potencies in the nanomolar range (IC_{50} = 50–71 nM) in MDA-MB-231 cells with no/negligible amount of cytotoxicity. The stronger selectivity of the potent compounds for IDO1 enzyme over tryptophan 2,3-dioxygenase (TDO) enzyme (312–1593-fold) also makes them very attractive for further immunotherapeutic applications.

1. Introduction

Cancer immunotherapy by targeting indoleamine 2,3-dioxygenase 1 (IDO1) and tryptophan 2,3-dioxygenase (TDO) enzymes is considered as an exciting approach for drug development [1,2]. Both IDO1 and TDO enzymes catalyze the initial and rate limiting step in the catabolism of L-tryptophan (*L*-Trp) to *N*-formylkynurenine by oxidative cleavage of the pyrrole ring through kynurenine pathway [3,4]. Uncontrolled metabolism of *L*-Trp abets tumor cells to escape from the immune responses [1,4]. Reduction in local concentrations of *L*-Trp and uninhibited formation of kynurenine and other metabolites, including neurotransmitters serotonin and melatonin, excitotoxin quinolinic acid, *N*-methyl-D-aspartate receptor antagonist kynurenic acid, and the production of nicotinamide adenine dinucleotide (NAD) assists IDO1 enzyme to suppress the local immune response by hindering the proliferation of T-lymphocyte in the G1-phase of the cell cycle [1,2,5,6]. Cytokines like interferon-γ are primarily responsible for the over-expression of IDO1 enzyme in the macrophages, epithelial and dendritic cells [7]. TDO enzyme is mainly expressed in the liver and catabolizes more than 90% of the *L*-Trp. This catabolism of *L*-Trp in the liver by the TDO enzyme systematically regulates *L*-Trp balance in response to dietary intake. The over-expression of IDO1 enzyme is interconnected with poor prognosis in different cancers, including, ovarian and pancreatic [1,3,8]. However, recently it is reported that endothelial IDO1 expression in kidney tumors is associated with a better prognosis [9,10]. Cellular IDO1 activities are also related with neurodegenerative disorder HIV-1 encephalitis and age related cataract [1,11–14].

Recent studies demonstrated that inhibition of IDO1 activity with small molecules successfully restrain the abnormal growth of tumors and also showed complemented effect with chemotherapeutic and radiotherapeutic treatment of malignant tumors [6,15]. TDO enzyme is highly selective and preferably binds to *L*-Trp. Whereas, the active site of IDO1 enzyme is amenable to small molecules. Hence, IDO1 has emerged as an attractive target in

Abbreviations used: IDO1, indoleamine 2,3-dioxygenase 1; TDO, tryptophan 2,3-dioxygenase; *L*-Trp, *L*-tryptophan; HTS, High throughput screening; UV–Vis, ultraviolet–visible; HPLC, high-performance liquid chromatography.

* Corresponding author.
** Corresponding author.
E-mail address: dmanna@iitg.ernet.in (D. Manna).

[1] S.P. and A.R. contributed equally to this work.

http://dx.doi.org/10.1016/j.ejmech.2016.05.061
0223-5234/

ACS Medicinal Chemistry Letters

Letter

pubs.acs.org/acsmedchemlett

Fused Heterocyclic Compounds as Potent Indoleamine-2,3-dioxygenase 1 Inhibitors

Subhankar Panda,[†,§] Ashalata Roy,[†,§] Suman Jyoti Deka,[‡] Vishal Trivedi,[‡] and Debasis Manna*[,†]

[†]Department of Chemistry and [‡]Department of Bioscience and Bioengineering, Indian Institute of Technology, Guwahati, Assam 781039, India

Supporting Information

ABSTRACT: Uncontrolled metabolism of L-tryptophan (L-Trp) in the immune system has been recognized as a critical cellular process in immune tolerance. Indoleamine 2,3-dioxygenase 1 (IDO1) enzyme plays an important role in the metabolism of a local L-Trp through the kynurenine pathway in the immune systems. In this regard, IDO1 has emerged as a therapeutic target for the treatment of diseases that are associated with immune suppression like chronic infections, cancer, and others. In this study, we synthesized a series of pyridopyrimidine, pyrazolopyranopyrimidine, and dipyrazolopyran derivatives. Further lead optimizations directed to the identification of potent compounds, **4j** and **4l** (IC_{50} = 260 and 151 nM, respectively). These compounds also exhibited IDO1 inhibitory activities in the low nanomolar range in MDA-MB-231 cells with very low cytotoxicity. Stronger selectivity for the IDO1 enzyme (>300-fold) over tryptophan 2,3-dioxygenase (TDO) enzyme was also observed for these compounds. Hence, these fused heterocyclic compounds are attractive candidates for the advanced study of IDO1-dependent cellular function and immunotherapeutic applications.

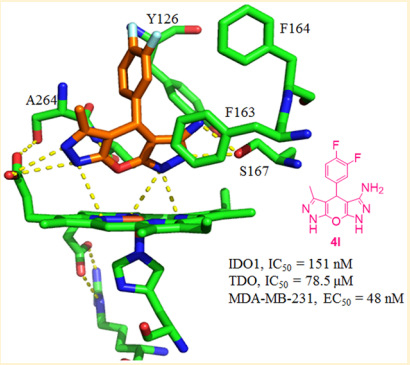

KEYWORDS: *Indoleamine 2,3-dioxygenase 1 inhibition, fused heterocyclic compounds, halogen substituents, low IC_{50} and EC_{50} values, low cytotoxicity*

Immunotherapy is currently considered as one of the most promising approaches in the battle against cancer.[1−3] Recent accomplishment with the immune checkpoint inhibitors against a wide range of cancers has made cancer immunotherapy one of the most exciting developments. It has been also shown that cancer immunotherapy and traditional chemotherapy or radiotherapy could also be benefited from combinatorial strategies against tumor-induced immunosuppression.[1,2,4] Induced metabolism of L-tryptophan (L-Trp) through kynurenine pathway and consequential production of kynurenine, 3-hydroxy kynurenine, kynurenic acid, excitotoxin quinolinic acid, and other metabolites are primarily responsible for local immunosuppression.[4−6]

In nonhepatic cells, indoleamine 2,3-dioxygenase 1 (IDO1) catalyze the rate limiting step of the L-Trp catabolism through kynurenine pathway. IDO1 activity is generally low in healthy humans and has insignificant physiological effects. However, within the immune system IDO1 gets highly up-regulated in response to inflammatory signals under pathophysiological conditions (e.g., in tumor cells). Up-regulation of IDO1 is interrelated with poor prognosis in different types of cancers, including pancreatic, ovarian, colorectal, and others.[5,6] Recent reports also suggest that neurodegenerative disorder, HIV-1 encephalitis, and other diseases are also associated with the up-regulated IDO1 activity.[7,8] IDO1 promotes a tolerogenic state in the tumor cells and its lymph nodes by suppressing the T cells and enhancing the local regulatory T cells. IDO1 expression is strongly up-regulated by cytokines like interferon-γ. Cytotoxic T lymphocytes produce this interferon-γ, which perhaps indulges the efficacy of other immune therapy against cancer.[3] A variety of preclinical studies with cancer models suggests that IDO1 assists cancer progression and metastasis.[9,10] All these findings highlight the effectiveness of IDO1 in cancer and other diseases. Recent developments have shown that inhibition of IDO1 enzyme activity improves the efficacy of chemotherapeutic and radio therapeutic treatment of malignant tumors.[6,7,9,10]

There are a number of reported small molecule-based IDO1 inhibitors with different structural classes, including tryptophan, imidazole, triazole, *N*-hydroxyamidine, iminoquinone, and others. Natural products like norharman, β-carboline, benzomalvin, and their derivatives also showed IDO1 inhibitory potencies.[8,11−13] IDO1 inhibitors INCB024360, NLG919, and 1-methyl-L-tryptophan (L-1MT) are currently under clinical trials for the treatment of different types of cancers.[8,14,15] Successful use of ipilimumab and nivolumab and current clinical development of the inhibitors of IDO1 enzyme inspire researchers to develop IDO1 inhibitors for cancer immunotherapy.[14]

Received: September 12, 2016
Accepted: October 15, 2016
Published: October 15, 2016

DOI: 10.1021/acsmedchemlett.6b00359
ACS Med. Chem. Lett. 2016, 7, 1167−1172